PRODUCTION AND CHARACTERIZATION OF NOVEL ACTIVE POLYSACCHARIDES/ PROTEINS BLENDED BIOPLASTICS

Michela Famiglietti

Dottorato in Biotecnologie – 36° ciclo

Università di Napoli Federico II

Dottorato in Biotecnologie – 36° ciclo

Università di Napoli Federico II

PRODUCTION AND CHARACTERIZATION OF NOVEL ACTIVE POLYSACCHARIDES/ PROTEINS BLENDED BIOPLASTICS

Michela Famiglietti

Dottorando: Michela Famiglietti

Relatore: Prof. Loredana Mariniello

Coordinatore: Prof. Marco Moracci

Settore Scientifico Disciplinare: BIO/10

TABLE OF CONTENT

SUMMARY

Petroleum-based plastics have become the workhorse material of the modern economy, because of their unrivaled functional properties and their low cost. In the last century, their use has increased twenty-fold and become ubiquitous. Besides delivering many benefits, plastics of petrochemical origin are causing escalating damage to the natural environment and human health. The same properties that make plastics adapted to innumerable applications, such as durability and resistance, make these materials difficult to assimilate from the environment.

Thus, strategies to reduce plastic pollution should include the replacement of petrol-based plastics and additives known to be harmful by biobased and biodegradable materials, and by environmentally friendly components, together with the reduction of consumption and the increase of recycling.

Biopolymers are ideal candidates to replace plastics of petrochemical origin, but they also present some limitations like high manufacturing cost and low mechanical tendency.

In this scenario, the present thesis aims to contribute to developing novel bioplastics obtained from different renewable sources. The work focused on exploiting polysaccharides, like chitosan and amylose, and proteins, specifically derived from byproducts. The whole investigation works towards the improvement of such kinds of raw materials, blending them, modifying their structures, and adding active compounds and fillers to overcome their drawbacks like poor strength, water sensitivity, and low thermal stability. Moreover, the degradation of some of these novel bioplastics was investigated through the soil burial test to confirm their biodegradable nature.

The last part of the experimental work was carried out at the Department of Analytical Chemistry of the Complutense University of Madrid, where magnetic nanoparticles were produced and functionalized to be mixed as nanofillers into bioplastics and enhance their properties.

RIASSUNTO

Con il termine plastica si definiscono i polimeri derivanti dalla lavorazione del petrolio che, grazie alle loro impareggiabili proprietà funzionali e al loro basso costo, sono diventati i materiali per eccellenza dell'economia moderna. Nell'ultimo secolo, il loro uso è aumentato di circa venti volte rispetto alla metà del secolo scorso, rendendo i polimeri sintetici insostituibili nella vita dell'uomo. Oggi un mondo senza plastica sembra inimmaginabile, anche se risale solo al 1950 la diffusione della loro produzione e del loro uso in quasi tutti i settori, superando qualsiasi altra classe di materiali prodotti.
Tuttavia, le materie plastiche di origine petrolchimica stanno causando danni crescenti all'ambiente naturale e alla salute umana. Le stesse proprietà che hanno reso le plastiche adatte a innumerevoli applicazioni, come la durata e la resistenza, sono responsabili del loro difficile smaltimento.
Oggi si generano circa 400 milioni di tonnellate di rifiuti plastici all'anno in tutto il mondo e meno del 10% di essi viene riciclato. La gran parte finisce in discarica o disperso nell'ambiente, come è evidente dalla formazione del cosiddetto ottavo continente o isola di plastica, il Great Pacific Garbage Patch, presente nel mezzo dell'Oceano Pacifico.
La maggior parte dei rifiuti plastici proviene dal settore degli imballaggi, che rappresenta il più grande mercato attuale della plastica, con una crescita in accelerazione dovuta al disuso di contenitori riutilizzabili a vantaggio del packaging monouso. Esso è responsabile del 45% di tutte le plastiche non fibrose che hanno un ciclo di vita inferiore a un anno, ovvero che finiscono in discarica nello stesso anno in cui vengono prodotte.
L'unico modo sostenibile per ridurre l'inquinamento da plastica su scala globale è ridurre la plastica che entra nell'ambiente naturale. Per raggiungere questo obiettivo, è necessario considerare insieme diverse strategie: ridurre il consumo generale di plastica, soprattutto quella monouso, favorire il suo riciclo e sostituirla con materiali biodegradabili che derivano da fonti rinnovabili. Più recentemente l'attenzione è rivolta anche alla ricerca di enzimi che degradino le plastiche tradizionali, vista la scoperta nel mondo microbico di attività enzimatiche che hanno questa capacità.
In questo scenario, la presente tesi costituisce un contributo allo sviluppo delle bioplastiche, cioè di materiali biodegradabili derivati da fonti rinnovabili, come alternativa alle plastiche di origine petrolchimica. In questa tesi sono stati condotti e riportati diversi studi sulla loro

produzione a partire dalla lavorazione di biopolimeri, polisaccaridi e proteine, in presenza di additivi come plastificanti, composti attivi, agenti reticolanti e *nanofillers*. Tutti i lavori svolti hanno mostrato il potenziale dei biopolimeri di essere sfruttati nell'industria delle materie plastiche, essendo adatti a una varietà di applicazioni.
Il primo lavoro riportato si è concentrato sull'uso del chitosano come copolimero naturale, che deriva da uno dei polisaccaridi più abbondanti sulla terra, la chitina, generalmente recuperata da scarti agro-alimentari, poiché presente nell'esoscheletro di crostacei, molluschi e insetti, nonché nella parete cellulare dei funghi. I film a base di chitosano sono stati sviluppati con l'obiettivo di intrappolare al loro interno un estratto attivo derivato dalle foglie di olivo essiccate (DOLE), che sono un sottoprodotto della coltivazione e della lavorazione delle olive. Questo lavoro ha raggiunto con successo l'obiettivo di valorizzare tale sottoprodotto, trasformandolo in un prodotto ad alto valore aggiunto. Lo studio della resa in polifenoli del DOLE e della sua attività antiossidante quando incorporato in film a base di chitosano ha confermato la possibilità di utilizzarlo nella formulazione di integratori alimentari per l'apporto di composti attivi utili al supporto della dieta alimentare. Inoltre, la valutazione dell'attività antimicrobica del DOLE in combinazione con il chitosano per la produzione di bioplastiche attive ha verificato la loro applicabilità come imballaggi per migliorare la *shelf-life* degli alimenti. Ricoprendo, ad esempio, hamburger di carne in sostituzione delle plastiche tradizionali o della carta da forno normalmente usate, è stato verificato che i film edibili a base di chitosano contenenti il DOLE riuscivano a ritardarne il deterioramento dovuto ai comuni contaminanti microbici durante la conservazione. Infine, è stato dimostrato che il DOLE esercita un effetto plastificante, quindi la sua presenza potrebbe superare la necessità di un plastificante aggiuntivo, come il glicerolo, per la produzione delle bioplastiche.
Allo stesso modo è stato riportato in questa tesi che i fil ottenuti da proteine derivanti dal sottoprodotto di estrazione dell'olio di semi della *Nigella sativa,* in combinazione con composti attivi presenti nel succo d'uva, potrebbero essere utilizzati per l'imballaggio di prodotti alimentari. Il panello di *N. sativa* è un sottoprodotto dell'estrazione dell'olio di semi e di solito viene utilizzato come mangime per animali grazie al suo alto contenuto di proteine. Il lavoro riportato in questa tesi, (svolto in collaborazione con An-Najah National University a Nablus, Palestina) ha avuto l'obiettivo di valorizzare questo sottoprodotto, sfruttandolo per produrre film edibili e migliorandone le funzionalità con composti bioattivi. I risultati ottenuti hanno dimostrato che il succo d'uva

non solo agisce come plastificante ma grazie alla sua attività antiossidante e antimicrobica è in grado di ritardare il deterioramento di cibi, come dimostrato dagli esperimenti condotti con le ciliegie, i cui effetti sono stati riportati come rallentamento del cambiamento di colore, dell'acidità titolabile e dei solidi totali solubili.
Ancora nell'ambito dell'*active packaging* sono stati prodotti film edibili a base di pectine incorporando estratti di foglie di olivo e di guava (OLE e GLE) (lavoro riportato in questa tesi in collaborazione con An-Najah National University a Nablus, Palestina) per ottenere bustine solubili per l'imballaggio, dimostrando che l'attività antiossidante degli estratti aiuta a ridurre le reazioni di ossidazione degli alimenti durante la loro distribuzione e conservazione.
Nell'ottica degli obiettivi della bioeconomia, ovvero di sfruttare la biomassa per la produzione di energia e materiali e di trasformare scarti e sottoprodotti in prodotti ad alto valore aggiunto, una parte di questa tesi è stata dedicata alla produzione di nuove bioplastiche a partire da proteine di semi di argan (APs), estratte dal panello dell olio di argan, e da amilosio (AM) ottenuto da piante di orzo mediante la tecnica dell'*RNA interference* dal team guidato dal Prof. Andreas Blennow dell'Università di Copenaghen. Le matrici ottenute sono state poi modificate attraverso l'aggiunta di un agente reticolante, la transglutaminasi microbica (mTGase), capace di catalizzare la formazione di legami isopeptidici intra e intermolecolari, al fine di migliorare le funzionalità dei film in termini di proprietà meccaniche, termiche e di barriera ai gas e al vapore acqueo. Lo studio ha confermato il potenziale delle APs di migliorare le prestazioni dei film a base di AM, in particolare per quanto riguarda la loro capacità di barriera al vapore acqueo e alla CO_2, effetto ulteriormente rafforzato dall'azione dell'enzima transglutaminasi. Inoltre, i cambiamenti nell'estensibilità e nella rigidità dei film a base di AM contenenti APs potrebbero renderli adatti ad essere utilizzati come sacchetti compostabili.
Il trattamento con la mTGasi si è dimostrato efficace anche sui film a base di proteine ottenute dal panello di semi di canapa, lavoro riportato in questa tesi e svolto all'interno del gruppo Biotecnologie Biochimiche ed Enzimologia (BBE). La caratterizzazione di tali film edibili ha mostrato che la reticolazione indotta dalla transglutaminasi ha dato origine a matrici più omogenee, con una maggiore resistenza alla trazione e alla termosaldatura e una maggiore idrofobicità.
Oltre alla loro caratterizzazione in termini di proprietà fisico-chimiche necessarie allo studio della loro applicabilità, è stata valutata e riportata la capacità di degradazione di alcune delle bioplastiche preparate in

questa tesi. In particolare, i film a base di APs-AM non modificati dalla mTGasi sono stati sottoposti al test di biodegradazione nel suolo, utilizzando tre tipi di terreni con caratteristiche diverse per un periodo di 80 giorni. Come controllo sono stati usati campioni della bioplastica commerciale Mater-Bi prodotta dalla Novamont. I test hanno confermato la degradabilità dei film testati in tutti e tre i terreni nel periodo considerato. Sorprendentemente, lo stesso comportamento non è stato osservato per i campioni di Mater-Bi, suggerendo che la loro degradazione richiede un tempo maggiore in tali terreni o condizioni ambientali specifiche.

Una parte di questa tesi è stata svolta presso il Dipartimento di Chimica Analitica dell'Università Complutense di Madrid e si è concentrata sulla produzione di nanoparticelle (NPs) da utilizzare come rinforzo delle bioplastiche precedentemente prodotte. In particolare, sono state prodotte NPs a base di ossido di ferro, successivamente caratterizzate e incorporate in film a base di APs-AM. Le nanoparticelle sono state preferite alle microparticelle per il loro ampio rapporto superficie/volume che fornisce un'estesa area interfacciale matrice-riempitivo che influisce sulla mobilità molecolare della struttura e di conseguenza sulle proprietà del film. A causa della aggregazione a cui facilmente le nanoparticelle ferromagnetiche vanno incontro, si è optato per la loro funzionalizzazione e anche le NPs modificate sono testate come riempitivo nei film a base di APs-AM. I risultati hanno dimostrato che le NPs magnetiche, funzionalizzate o meno, interagiscono con le matrici dei film, come confermato dai cambiamenti delle loro proprietà termiche.

Le NPs ferromagnetiche non funzionalizzate aggiunte ai film a base di AM hanno aumentato la loro permeabilità al vapore acqueo, probabilmente perché interponendosi nella rete compatta formata dalle catene di AM hanno facilitato il passaggio delle molecole d’acqua attraverso la matrice. Questo effetto è stato osservato in maniera minore aggiungendo invece le NPs modificate, poiché la funzionalizzazione ha evitato l'aggregazione delle NPs dando origine a film con una struttura più omogenea e compatta. Un effetto simile è stato osservato quando nanocristalli (CNC) e nanofibre (CNF) di cellulosa sono stati utilizzati come *fillers* in film a base di AM, come riportato in un lavoro presente all’interno di questa tesi svolto in collaborazione con l’Università di Copenaghen. In presenza di elevate concentrazioni di CNC e CNF la permeabilità dei film al vapore acqueo presenta valori maggiori, poiché entrambi i tipi di *nanofillers* aumentando la mobilità delle catene AM facilitano il trasferimento delle molecole d'acqua attraverso la matrice del biopolimero.

L'aggiunta di NPs a film a base di APs-AM ha aumentato la loro stabilità termica nella maggior parte dei campioni analizzati. Le interazioni tra le NPs e i biopolimeri sono state suggerite dalle curve differenziali e DSC per tutti i film considerati, risultando in un effetto termoprotettivo sulla componente glicerina nei film a base di AM100 contenenti NPs ferromagnetiche funzionalizzate e non, in un aumento della stabilità termica dei film misti contenenti NPs ferromagnetiche modificate e in un più lieve ma presente miglioramento della stabilità termica nei film a base di APs contenenti NPs modificate.
In questa tesi è stato dimostrato il potenziale dell'utilizzo di polisaccaridi e proteine come biopolimeri per la produzione di bioplastiche, quando combinati con additivi non tossici ed ecologici, come riportato nei lavori sopra descritti. Si potrebbe, dunque, pianificare uno scale-up industriale per confermare la possibilità di sostituire con esse le plastiche di origine petrolchimica considerando le numerose applicazioni per le quali sono risultate essere adatte in termini di proprietà fisico-chimiche e di funzionalità aggiuntive.

1. INTRODUCTION

1.1 Plastic production and pollution

Nowadays a world without plastic seems unimaginable even if it only dates to ~1950 the widespread production and use of synthetic polymers [1]. The first truly synthetic resin was invented in 1907 by Belgian-born American scientist Leo Baekeland, by reacting phenol and formaldehyde at controlled temperatures and pressure. This discovery is considered by many as the beginning of a new era, often called the Plastics Age, even if it was only after the Second World War that the use of synthetic materials became widespread outside of the military. The plastic revolution began when PET (polyethylene terephthalate) was patented in 1941 by Rex Whinfield and James Tennant Dickinson, followed by the discovery of the catalysts to produce the isotactic polypropylene, whose paternity is by Giulio Natta and Karl Ziegler, which won the Nobel Prize in 1963 [2].
The consequent rapid growth in plastics production was extraordinary, surpassing any other class of manufactured material and becoming involved everywhere in human lives. Global production of synthetic polymer resins and fibers grew from 2 Mt to 380 Mt between 1950 and 2015, making them the workhorse materials of the modern economy thanks to the combination of their unrivaled functional properties, such as mechanical strength, lightness, flexibility, and durability with their low cost of production [3]. These properties are determined by the chemical structure of the repeating units, called monomers, forming the long, like-chains macromolecules, called polymers. Plastics are the final and commercial products deriving from the polymerization and processing of these building blocks, usually sourced from petroleum [4].
Among the most high-volume families of synthetic plastics are polyethylene (including low density (LDPE), linear low density (LLDPE) and high density (HDPE)), polypropylene (PP), polyvinylchloride (PVC), polystyrene (solid PS and expandable EPS), polyurethane (PUR) and polyethylene terephthalate (PET). They account for around 92 % of all plastics ever made. The biggest end use for plastics is represented by packaging, which took around 45% of all non-fiber plastics, predominantly composed of PE, PP, and PET. It is followed by the

building and construction sector which uses ~20% of all non-fiber plastics, particularly ~69% of all PVC. Automotive and electric and electronic sectors used ~7% and ~4% respectively of plastics resins, and finally for medical, leisure, and other applications plastics production remains at ~25% (Figure 1).

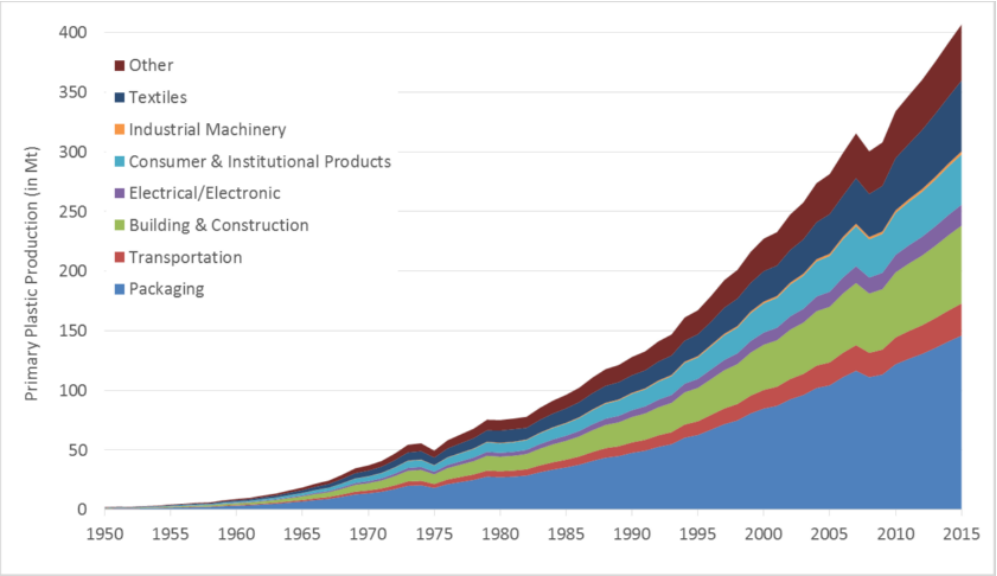

Figure 1. Global primary plastics production according to industrial use sector from 1950 to 2015: global plastics production increased with a compound annual growth rate (CAGR) of 8.4% [3].

Globally around 400 Mt of plastic are generated every year worldwide and only a low percentage of the resulting plastic wastes is managed adequately, with most of them being incinerated, disposed of into landfills, or dispersed into the natural environment [5]. Over 10 Mt of plastic are annually released into the aquatic ecosystems, causing tremendous damage to ecosystem structures and functions. Most of them exist as micro and nanoparticles that float below the sea surface, killing thousands of mammals every year and millions of fishes and birds, and entering the food chain. It was estimated that the packaging sector is responsible for producing the most amount of waste dispersed, with around 54% non-fiber plastic product-derived waste against only 5% of them deriving from the construction sector (Figure 2) [3].

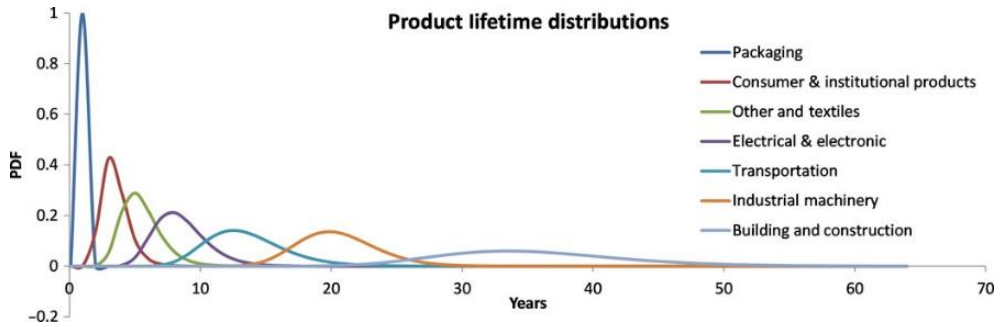

Figure 2. Production lifetime distributions for eight different industrial use sectors: plotted as log-normal probability distribution functions (PDF) [3].

Moreover, conventional plastics produced in 2015 emitted around 1.8 Giga tons (Gt) of CO_{2e} over their life cycle from production to their end-of-life (EoL), corresponding to 3.8% of the 47 $GtCO_{2e}$ globally emitted that year. The production stage is responsible for most greenhouse gases (GHGs) emitted, followed by the conversion stage. The EoL stage accounted for 9% of total life-cycle emissions and the incineration was the dominant source of GHGs emitted in this stage [1]. Dioxins generated from the incinerated waste plastic end up on the crops and in the water cycle, thus entering the food chain [6].
Thus, solving plastic pollution is one of this century's most crucial environmental challenges. This aim can be reached only if different strategies are considered and applied together, including reducing the global demand for plastic, improving the recycling rate of polymers of petrochemical origin, and substituting them with biobased and biodegradable materials.

1.2 Bioplastics as alternative to fossil-based plastics

Bioplastics is a large family of polymeric materials which are bio-based, biodegradable, or both. In this group there are plastics derived from petroleum but that have a biodegradable nature, plastics derived from renewable sources but that are not biodegradable, and finally plastics that present both the characteristics to be bio-based and biodegradable [7]. Deriving from a renewable source means that polymers are directly extracted from biomass, produced through a biological process, or that monomers are generated from a renewable source and then polymerized through a chemical process. The biodegradability property

means that these materials can be converted through the enzymatic actions of microorganisms into carbon dioxide, methane, water, biomass, humic matter, and other natural substances [8].
All these polymers, defined as bio-based, biodegradable, or both, can be classified into two main groups, agropolymers, and biopolyesters: the first one includes polymers extracted from biomass, to which belong polysaccharides (starch, chitin, cellulose, pectins), lipids and proteins of animal origin (casein, whey, gelatin) or plant-derived (gluten, zein, soya); the second group consists of polymers obtained from microorganisms, such as polyhydroxy-alkanoate (PHA) and polyhydroxy-butyrate (PHB), polymers obtained by the polymerization of bio-derived monomers such as polylactic acid, and polymers obtained from petroleum such as polycaprolactone (PCL), aliphatic and aromatic copolyesters [9].

1.3 Agropolymers

Biopolymers as polysaccharides and proteins are ideal candidates for the production of bioplastics because they are bio-based and biodegradable and involve intra and intermolecular interactions and cross-links between the macromolecules, forming a three-dimensional semi-rigid network [10]. However, they present some common characteristics like hydrophilicity, fast degradation rate, and unsatisfactory mechanical properties, especially in wet environments. Thus, modifying them to improve their performance in terms of strength, water sensitivity, and thermal stability is one of the most important challenges in this field of application [11]. Polysaccharides are polymeric carbohydrates made up of monosaccharides linked by glycosidic bonds. They are synthesized by plants, animals, and microorganisms for several biological functions such as storage of energy, cellular structure components, and cellular communication. They can be synthesized as homopolymers or heteropolymers, reaching molecular weights up to millions of Daltons, in linear or branched chains. The monomers are various sugars with or without substitute groups such as sulfate or phosphate, with anomeric configuration and ring size, that can be arranged in different kinds of secondary structures. Among the most used polysaccharides in the bioplastic industry are cellulose, which is the most widespread carbohydrate on earth because it is the main component of cell walls of

higher plants; starch, which is one of the most used to date due to its low price, as well as its film-forming property, biodegradability, and non-toxicity; chitin, which is the second abundant polysaccharide in nature after cellulose, from which chitosan is produced by deacetylation; pectin, which is a heteropolysaccharide mainly present in fruits and vegetables, used as food additives due to its gelling ability, and finally alginate and carrageenan, both obtained from algae and widely used in the food industry as thickeners and stabilizers [12][13][14][15][16]. Proteins are a group of complex organic macromolecules, consisting of combinations of 20 different amino acids linked by a peptide bond [17]. Proteins play several important biological roles within the cell and usually are classified as globular, membrane, or fibrous. They exist as extended chains of amino acid units, which fold into specific structures. Each of these repeating units contains two carbon atoms and one nitrogen atom differing only in the functional side groups. Their three-dimensional conformation is due to the formation of covalent and non-covalent interactions, such as hydrogen bonding, ionic interactions, Van der Waals forces, hydrophobic packing, and disulfide bonds. These interactions drive the primary structure (the linear chains of amino acids) into repeated secondary structures (α-helic and β-sheet), and finally into folded complex macromolecules (tertiary structure) and clusters of them (quaternary structure). The pure charge of a protein can be both positive or negative depending on the pH of the surrounding solution and the corresponding charges on the amino (-NH_2) -terminal group and the carboxyl(-COOH)-terminal group [18] [19]. Generally distributed in plants and animals, proteins have been considered for many industrial applications because of their versatile functionality and their suitable features such as dispersibility, solubility, biocompatibility, and biodegradability. They can be recovered as byproducts or wastes from the agricultural industry, thus proteins from plants such as wheat, gluten, and soy, and animals such as whey, casein, and gelatin, have been exploited to produce bioplastics [18]
Generally, polymers are classified as thermoset, thermoplastic, or rubbery: most agropolymers do not have a thermoplastic behavior without the addition of additives. Polymer processing usually involves the application of heat and pressure to mold polymeric materials into the final product with a method depending on their polymeric nature. Thermoplastic processing involves melting the polymer and cooling it into its final shape. Usually, polymer chains are linked by interactions

such as hydrogen bonding, van der Waals, and hydrophobic interactions. When energy is supplied these interactions break down and the entanglements of polymer chains are disrupted, allowing their mobility. Heating hydrophilic polymers such as starch and protein in the presence of water means processing them in the same way as conventional petrochemical-based thermoplastics [20].
Processing agropolymers for bioplastics purposes means breaking the intramolecular bonds by using chemical or physical tools and enabling the formation of new intermolecular bonds and interactions to stabilize the three-dimensional network. Therefore, a typical formulation of an agropolymer-based bioplastic includes a plasticizer or a combination of plasticizers, additives such as compounds with functional activities, preservatives, and bleaching agents, reactive additives to promote cross-link among the polymer chains, lubricants such as oil and fatty acids, and fillers such as micro and nanoparticles to reinforce the polymer-matrix [20].

1.4 Plasticizers

Agropolymers have low degradation temperatures and when subjected to processing can incur degradation because the energy necessary to disrupt the entanglement of polymer chains is close to the energy sufficient for their degradation. Plasticizers can improve the processability of the agropolymers because they can interpose themselves between the polymer chains and alter the forces between them through two mechanisms, lubrication and increasing in free volume [21].
Water is considered a natural plasticizer because it can form hydrogen bonding with polar functional groups of the agropolymers such as hydroxyl and amine groups. Some other hydrophilic compounds such as polyols, carbohydrates, and amines can interact with polar groups in agropolymer chains producing a plasticizing effect. Among them are glycerol, sorbitol, saccharose, trimethylene glycol, and polyethylene glycol. They are characterized by a polar nature, which makes them compatible with the matrix of agropolymers, and small dimensions, which allow them to penetrate the macromolecular network [20].

1.5 Bioactive compounds

Nature has a great abundance and variety of active components as different parts of plants, animals, and soils. Recently, interest in the consumption of bioactive compounds has grown due to the several benefits that have been attributed to them in terms of disease prevention [22]. Many studies focused on the extraction and characterization of bioactive compounds from different sources and their use as natural ingredients in food products. Similarly, the food packaging industry is paying attention to them to move from the traditional strategy of producing coatings and films “as inert as possible” towards active and smart packaging, able to act in prolonging food shelf-life, enhancing safety, and ensuring high-quality products [23].

Packaging is an effective means of protecting food products from external contamination. It can prevent their chemical, physical, and biological changes over all their preparation and storage. The use of active and functional packaging is one of the strategies to improve food shelf life by reducing gas exchange, respiration, and oxidative reactions of food products [24].

Various matrices can be used to incorporate compounds as antimicrobial or antioxidant agents, including proteins, lipids, polysaccharides, or composites.

Among the most studied bioactive compounds are phytochemicals, i.e. secondary metabolites of plants, such as alkaloids and phenolic compounds, for their antimicrobial and antioxidant activities [25]; antimicrobial agents produced by microorganisms such as the antimicrobial peptides bacteriocins, due to their ability to tolerate high temperatures and acidic environment; natural components founds in animals, such as lysozyme, also known as muramidase or N-acetylmuranic hydrolase, for its efficiency against several pathogenic bacteria [22].

Many studies have shown that antimicrobial and antioxidant agents when incorporated into edible films and coatings could be effective in reducing levels of pathogenic organisms and oxidative reactions [26][27].

1.6 Microbial Transglutaminase (mTGase) as reticulating agent

In the last decades, enzymes as biotechnological tools have been finding several applications. The use of chemical cross-linking reagents is discouraged because of their potential harmfulness and toxicity, even for bioplastic production. The use of transglutaminases (protein glutamine γ-glutamyltransferase, E.C.2.3.2.13, TGases) has been proposed for their capability to catalyze intra and/or intermolecular isopeptide bonds between the γ-carboxamide group of glutamines (acyl donor) and an ε-amino group of lysine residues (acyl acceptor). The reaction occurs when the acyl acceptor is either the ε-amino group of an endoprotein lysine or a low molecular mass primary amine, thus generating ε-(γ-glutamyl) lysine crosslinks in the first case, and protein-amine conjugates in the latter.

As described in the chapter titled *Enzyme assisted Food Processing* by **Michela Famiglietti**, Seyedeh Fatemeh Mirpoor, C. Valeria L. Giosafatto, and Loredana Mariniello (reported in the appendix of this thesis) TGases are multi-functional enzymes, expressed ubiquitously in living organisms since they are active in all mammalian tissues, in invertebrates, plants, yeasts as well as in bacterial cells. Special attention should be paid to a microbial TGase, first isolated in 1989 from a strain of *Streptomyces mobaraensis* (formerly classified as *Streptoverticillium mobaraense*). The enzyme is easily purified from the microbial culture medium and is a single-chain protein (molecular mass ~38 kDa, isoelectric point 8.9). Three aminoacidic residues constitute the active site of mTGase: cysteine, histidine, and aspartic acid or asparagine. mTGase does not require calcium ions for its activation. This feature is particularly advantageous for its application since the presence of calcium can lead to protein precipitation. This enzyme is used for changing the texture and several technological properties of protein-rich foods such as legumes, eggs, cereals, fish, etc. Moreover, it has various applications in biomedicine and biotechnology.

Many studies have already been performed to investigate the effect of mTGase-catalyzed glutamine-lysine isopeptide bonds on the production of protein-based bioplastics. mTGase-prepared films exhibit, in most cases, improved characteristics in terms of mechanical, barrier, and thermal properties than films prepared in the absence of the enzyme. Soy protein-based films prepared in the presence of mTGase showed higher mechanical resistance, stronger permeability to CO_2, water vapor, and O_2, and smoother film surface [28].

Biodegradable, flexible, and moisture-resistant films were obtained also by recycling wastes from fennel or grapefruit albedo and adding to their homogenates the bean globular protein phaseolin (Ph), either modified or not by the mTGase. Films were subjected to mechanical and barrier tests. The results showed that mTGase treatment of the Ph-containing fennel or albedo waste homogenates produced films comparable to the commercialized films Ecoflex and Mater-Bi® in their mechanical and barrier properties [29][30]. Recently Mirpoor et al. investigated the effect of mTGase on proteins derived from cardoon oilcake demonstrating that in the presence of mTGase, the obtained films showed improved properties than the film produced without using the enzyme as a crosslinking agent [31].

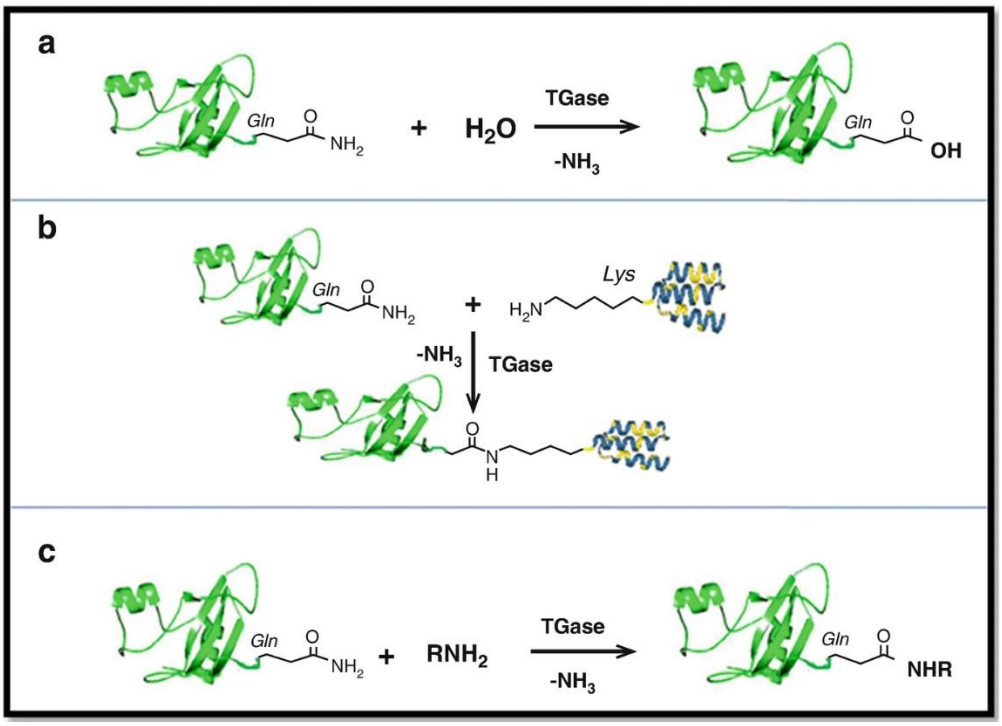

Figure 3. TGase-catalyzed reactions a) deamidation b) crosslinking c) ammine incorporation [32].

1.7 Nanoparticles as fillers

The prefix “nano” derives from the Greek νανος meaning dwarf [33]: the concept of nanotechnology was introduced in 1959 by Reichard Feynman during his pioneering lecture at American Physical Society meeting [34]. It deals with materials and structures down to one billionth of a meter (nanometer) in size and is an interdisciplinary field encompassing a whole spectrum of sciences: physics, chemistry, and biology as well as engineering [35]. Not only in academia but also in industry, the impact of nanoscience is growing as it is extremely attractive for multidimensional applications in nutrition, agriculture, cosmetics, coatings, energy production, drug delivery, diagnostics, and catalysts [36].

To date, “top-down” and “bottom-up” approaches are two strategies used in nanotechnology: in the first one nanometric structures are obtained by size reduction of bulk material, including techniques such as photolithography, nano molding, and nanofluidics; in the second one, they are fabricated in a controlled manner by thermodynamic mechanism from individual atoms or molecules capable of self-assembling, balancing attraction and repulsion forces between them to form more functional supramolecular structures [35]. Different types of functional nanostructures can be used as building blocks with new functionalities such as nanoemulsions, nanoparticles, and nanofibers destined for several applications.

Nanomaterials are designed as the combination of different constituent materials, with different physical and chemical properties in which one phase has a nanoscale morphology (a dimension of 1-100 nm) in one of their dimension [34]. Polymeric nanocomposites are produced by dispersing nanofillers into polymeric matrices: fillers are defined as solid particulate material used as reinforcement of a polymer matrix to improve its performance. They can be classified as extending or functional fillers, if they are only used to increase the bulk volume or if they can change the polymers' characteristics such as mechanical, thermal, and barrier properties. These functionalities change according to the filler composition, size, surface, concentration, shape, and affinity with the matrix. They can be categorized into two main groups according to their chemical composition: inorganic and organic fillers. Belong to the first group are calcium carbonate (Ca_2CO_3), kaolin (hydrous aluminosilicate), Silicon dioxide (SiO_2), Titanium dioxide

(TiO_2), Montmorillonite (MMT); among the second group are carbon-based nanofillers and natural fillers deriving from chitosan, chitin, lignin and cellulose [37]. A further classification of fillers concerns their three-dimensional geometry. According to their 3D structure, they are divided into 4 groups: the spherical nanostructures are considered as 0D structures also known as nano-cluster materials or nano-dispersion; the 1D structures are composites of nanoscale at one dimension, they are of tube shape with a length of 100-1000 nm and a thickness of few nanometers. The composites of 2D structures are of nano-scale at two dimensions and are also known as nano-sheet, while the 3D nanostructures are of nano-scale at three dimensions, they can form also polycrystalline systems [38]. The size of the nanophase in a nanocomposite is remarkably reduced providing a large surface-area-to-volume ratio and consequently, an extensive matrix/filler interfacial area which changes the molecular mobility, the relaxation behavior, and consequently its thermal, mechanical, and barrier properties [36][39]. Nanocomposite-starch-based films obtained with chitin nano-objects, for instance, showed superior mechanical, thermal, and barrier properties as compared to those prepared with unfilled thermoplastic starch films [40], as well as chitosan nanoparticles obtained by gelation method and incorporated into fish gelatin matrix to produce bio-nanocomposites films significantly improved the performance of the films in terms of mechanical and barrier characteristics, in particular a considerable increase of the tensile strength and elastic modulus, and a significant decrease of the water vapor permeability [41]. Silica nanoparticles ($nSiO_2$) even have been reported to improve the tensile strength of whey protein/pullulan-based films by increasing the cohesivity of the polymer matrix [42], while carbon nanotubes and carbon nanofibers have been successfully used to enhance the conductivity, thermal, mechanical and gas barrier properties of thermoplastic biopolyesters such as polyhydroxybutyrate-co-valerate (PHBV) and PCL [43].

In addition to reinforcing nanofillers, various types of nanostructures have been designed to provide active or smart properties to the system such as antimicrobial and antifungal activities, enzyme immobilization, biosensing, oxygen scavenging, and drug delivery. Some of them can even have multiple overlapping applications. The use of nanomaterials in food packaging has received attention due to the possibility of designing films with antimicrobial activity that can help control the

growth of pathogens and consequently improve the shelf-life of a food product. Nanostructures based on silver, titanium dioxide, chitosan, and carbon nanotubes (CNTs) have been investigated for their properties as growth inhibitors and killing agents against a wide range of microorganisms involved in food spoilage. Titanium dioxide (TiO_2) was studied as a photocatalytic disinfectant material since it promotes peroxidation of the polyunsaturated phospholipids of cellular membranes of microorganisms. At the same time, chitosan was proposed for its capability to interact with the negative charges of the microbial cellular membrane, modifying their permeability, and eventually causing cell lysis [35]. CNTs have been reported as antimicrobial agents for E. Coli since they can cause irreversible cell damage.

Nanocomposites were even investigated as biosensors for smart food packaging to detect microorganisms, toxic proteins, heavy metals, and degraded products in food and beverage. The nanostructures used, even called nanosensors, can reveal environmental changes, such as temperature or humidity, levels of oxygen exposure, degradation products, or microbial contamination. Due to these abilities to identify the presence of pathogens, chemical compounds, and toxins in food products, nanocomposites are promising and less time-consuming ways to control the spoilage of food, providing its real-time status of freshness. Moreover, because of their metabolism, microorganisms, that cause food spoilage, produce gases that can be detected by conducting polymer nanocomposites or metal oxides. Using gas sensors able to detect nitrogen compounds, oxygen, carbon dioxide, or even carbamate pesticides in fruits and vegetables is another way to control food deterioration [44].

1.8 Objective of the PhD project

The aim of this project was the production and characterization of novel bioplastics obtained from polysaccharides and proteins, destined for applications in the bioplastic industry, such as edible films for food packaging or new biomaterials for compostable bags. All the films were obtained in the presence of glycerol as the plasticizer. Further additives were used to produce active packaging (incorporating antimicrobial or antioxidant compounds) or to improve the properties of the films by modifying the protein structure or adding nanoparticles as fillers. Film mechanical, barrier, thermal, and hydrophilic properties were

investigated as well as their added functional activities and finally their degradation. A part of the experimental work was carried out at the Department of Analytical Chemistry of the Complutense University of Madrid, in the laboratories of Prof. Reynaldo Villalonga Santana, an expert in NPs production and characterization.

1.9 References

1. Zheng, J.; Suh, S. Strategies to Reduce the Global Carbon Footprint of Plastics. *Nat. Clim. Chang.* **2019**, *9*, 374–378, doi:10.1038/s41558-019-0459-z.
2. Porta, R. The Plastics Sunset and the Bio-Plastics Sunrise. *Coatings* **2019**, *9*, doi:10.3390/coatings9080526.
3. Geyer, R.; Jambeck, J.R.; Law, K.L. Production, Use, and Fate of All Plastics Ever Made. *Sci. Adv.* **2017**, *3*, 25–29, doi:10.1126/sciadv.1700782.
4. Finlayson, B.A.; Finlayson, B.A.; Engineering, C. Ullmann ' s Encyclopedia of Industrial Chemistry. **2016**, doi:10.1002/14356007.b01.
5. Lampitt, R.S.; Fletcher, S.; Cole, M.; Kloker, A.; Krause, S.; O'Hara, F.; Ryde, P.; Saha, M.; Voronkova, A.; Whyle, A. Stakeholder Alliances Are Essential to Reduce the Scourge of Plastic Pollution. *Nat. Commun.* **2023**, *14*, 1–3, doi:10.1038/s41467-023-38613-3.
6. Nanda, S.; Patra, B.R.; Patel, R.; Bakos, J.; Dalai, A.K. Innovations in Applications and Prospects of Bioplastics and Biopolymers: A Review. *Environ. Chem. Lett.* **2022**, *20*, 379–395, doi:10.1007/s10311-021-01334-4.
7. Faizan Muneer; Nadeem, H.; Arif, A.; Zaheer, W. Bioplastics from Biopolymers: An Eco-Friendly and Sustainable Solution of Plastic Pollution. *Polym. Sci. - Ser. C* **2021**, *63*, 47–63, doi:10.1134/S1811238221010057.
8. Rosenboom, J.G.; Langer, R.; Traverso, G. Bioplastics for a Circular Economy. *Nat. Rev. Mater.* **2022**, *7*, 117–137, doi:10.1038/s41578-021-00407-8.
9. Myasoedova, V. V. Agro-Polymers and Biopolyesters. *Russ. J. Gen. Chem.* **2017**, *87*, 1357–1363, doi:10.1134/S1070363217060378.
10. Abe, M.M.; Martins, J.R.; Sanvezzo, P.B.; Macedo, J.V.; Branciforti, M.C.; Halley, P.; Botaro, V.R.; Brienzo, M. Advantages and Disadvantages of Bioplastics Production from Starch and Lignocellulosic Components. *Polymers (Basel).* **2021**, *13*, doi:10.3390/polym13152484.
11. Aleksanyan, K. V. Polysaccharides for Biodegradable Packaging Materials: Past, Present, and Future (Brief Review). *Polymers (Basel).* **2023**, *15*, doi:10.3390/polym15020451.

12. Wang, J.; Han, X.; Zhang, C.; Liu, K.; Duan, G. Source of Nanocellulose and Its Application in Nanocomposite Packaging Material: A Review. *Nanomaterials* **2022**, *12*, doi:10.3390/nano12183158.
13. Rogovina, S.Z.; Aleksanyan, K. V.; Vladimirov, L. V.; Prut, E. V.; Berlin, A.A. New Ternary Biodegradable Compositions Based on Polyethylene and Polysaccharides. *Dokl. Phys. Chem.* **2015**, *465*, 270–272, doi:10.1134/S0012501615110056.
14. Pereira, D.G.M.; Vieira, J.M.; Vicente, A.A.; Cruz, R.M.S. Development and Characterization of Pectin Films with Salicornia Ramosissima: Biodegradation in Soil and Seawater. *Polymers (Basel).* **2021**, *13*, doi:10.3390/polym13162632.
15. Barikani, M.; Oliaei, E.; Seddiqi, H.; Honarkar, H. Preparation and Application of Chitin and Its Derivatives: A Review. *Iran. Polym. J. (English Ed.* **2014**, *23*, 307–326, doi:10.1007/s13726-014-0225-z.
16. Zhang, Y.; Man, J.; Li, J.; Xing, Z.; Zhao, B.; Ji, M.; Xia, H.; Li, J. Preparation of the Alginate/Carrageenan/Shellac Films Reinforced with Cellulose Nanocrystals Obtained from Enteromorpha for Food Packaging. *Int. J. Biol. Macromol.* **2022**, *218*, 519–532, doi:10.1016/j.ijbiomac.2022.07.145.
17. Boye, J.I.; Barbana, C. Protein Processing in Food and Bioproduct Manufacturing and Techniques for Analysis. *Food Ind. Bioprod. Bioprocess.* **2012**, 85–113, doi:10.1002/9781119946083.ch3.
18. Pratima Gupta, K.K.N. Characteristics of Protein-Based Biopolymer and Its Application. *Polym. Eng. Sci.* **2015**, 1–10, doi:10.1002/pen.
19. Yada, R.Y. Proteins in Food Processing. *Proteins Food Process.* **2004**, 1–686, doi:10.1533/9781855738379.frontmatter.
20. Verbeek, C.J.R. and J.M.B. Synthesisi and Characterization of Thermoplastic Agropolymers. *R. Soc. Chem.* **2011**, *Green Chem*.
21. Eslami, Z.; Elkoun, S.; Robert, M.; Adjallé, K. A Review of the Effect of Plasticizers on the Physical and Mechanical Properties of Alginate-Based Films. *Molecules* **2023**, *28*, doi:10.3390/molecules28186637.
22. Deshmukh, R.K.; Gaikwad, K.K. Natural Antimicrobial and Antioxidant Compounds for Active Food Packaging Applications. *Biomass Convers. Biorefinery* **2022**, doi:10.1007/s13399-022-02623-w.
23. Singh, A.K.; Kim, J.Y.; Lee, Y.S. Phenolic Compounds in Active Packaging and Edible Films/Coatings: Natural Bioactive Molecules and Novel Packaging Ingredients. *Molecules* **2022**, *27*, doi:10.3390/molecules27217513.
24. Siripatrawan, U.; Noipha, S. Active Film from Chitosan Incorporating Green Tea Extract for Shelf Life Extension of Pork Sausages. *Food Hydrocoll.* **2012**, *27*, 102–108, doi:10.1016/j.foodhyd.2011.08.011.
25. Siddiqui, S.A.; Khan, S.; Mehdizadeh, M.; Bahmid, N.A.; Adli, D.N.; Walker, T.R.; Perestrelo, R.; Câmara, J.S. Phytochemicals and Bioactive Constituents in Food Packaging - A Systematic Review. *Heliyon* **2023**, *9*, doi:10.1016/j.heliyon.2023.e21196.

26. Rocha, M.; Ferreira, F. a; Souza, M.M.; Prentice, C. Antimicrobial Films- a Review. *Microb. Pathog. Strateg. Combat. them Sci. Technol. Educ.* **2013**, 23–31.
27. Gómez-Estaca, J.; Giménez, B.; Montero, P.; Gómez-Guillén, M.C. Incorporation of Antioxidant Borage Extract into Edible Films Based on Sole Skin Gelatin or a Commercial Fish Gelatin. *J. Food Eng.* **2009**, *92*, 78–85, doi:10.1016/j.jfoodeng.2008.10.024.
28. Di Pierro P., Mariniello L., Giosafatto C.V.L., Masi P., P.R. Solubility and Permeability Properties of Edible Pectin-Soy Flour Films Obtained in the Absence or Presence of Transglutaminase. *Food Biotechnol.* **2005**, *19*, 37–49.
29. Mariniello, L.; Giosafatto, C.V.L.; Di Pierro, P.; Sorrentino, A.; Porta, R. Swelling, Mechanical, and Barrier Properties of Albedo-Based Films Prepared in the Presence of Phaseolin Cross-Linked or Not by Transglutaminase. *Biomacromolecules* **2010**, *11*, 2394–2398, doi:10.1021/bm100566j.
30. Giosafatto, C.V.L.; Mariniello, L.; Ring, S. Extraction and Characterization of Foeniculum Vulgare Pectins and Their Use for Preparing Biopolymer Films in the Presence of Phaseolin Protein. *J. Agric. Food Chem.* **2007**, *55*, 1237–1240, doi:10.1021/jf062725d.
31. Mirpoor, S.F.; Zannini, D.; Santagata, G.; Giosafatto, C.V.L. Cardoon Seed Oil Cake Proteins as Substrate for Microbial Transglutaminase: Their Application as Matrix for Bio-Based Packaging to Extend the Shelf-Life of Peanuts. *Food Hydrocoll.* **2024**, *147*, 109339, doi:10.1016/j.foodhyd.2023.109339.
32. Giosafatto C.V.L., Al-Asmar A., M.L. Transglutaminase Protein Substrates of Food Interest. In *Springer Nature*; 2018.
33. Sekhon, B.S. NSA_8677_food-Nanotechnology--an-Overview. **2022**, doi:10.2147/nsa.s12187498.
34. Şeker, Ş.; Elçin, Y.M. Bioanalytical Applications of Piezoelectric Sensors. *Nanopatterning Nanoscale Devices Biol. Appl.* **2017**, 261–287, doi:10.1201/b17161.
35. Azeredo, H.M.C. d. Nanocomposites for Food Packaging Applications. *Food Res. Int.* **2009**, *42*, 1240–1253, doi:10.1016/j.foodres.2009.03.019.
36. Basavegowda, N.; Baek, K.-H. Advances in Functional Biopolymer-Based Nanocomposites for Active Food Packaging Applications. *Polym. Rev.* **2021**, *13*, 4198.
37. Kumar M.S.T, Senthilkumar K., Chandrasekar M., Subramaniam S., Rangappa M.S., Siengchin S., R.N. Influence of Fillers on the Thermal and Mechanical Properties of Biocomposites: An Overview. *Springer Nat.* **2020**, 111–134.
38. Rahim, M.; Mas Haris, M.R.H.; Saqib, N.U. An Overview of Polymeric Nano-Biocomposites as Targeted and Controlled-Release Devices. *Biophys. Rev.* **2020**, *12*, 1223–1231, doi:10.1007/s12551-020-00750-0.

39. Othman, S.H. Bio-Nanocomposite Materials for Food Packaging Applications: Types of Biopolymer and Nano-Sized Filler. *Agric. Agric. Sci. Procedia* **2014**, *2*, 296–303, doi:10.1016/j.aaspro.2014.11.042.
40. Salaberria, A.M.; Diaz, R.H.; Labidi, J.; Fernandes, S.C.M. Role of Chitin Nanocrystals and Nanofibers on Physical, Mechanical and Functional Properties in Thermoplastic Starch Films. *Food Hydrocoll.* **2015**, *46*, 93–102, doi:10.1016/j.foodhyd.2014.12.016.
41. Hosseini, S.F.; Rezaei, M.; Zandi, M.; Farahmandghavi, F. Fabrication of Bio-Nanocomposite Films Based on Fish Gelatin Reinforced with Chitosan Nanoparticles. *Food Hydrocoll.* **2015**, *44*, 172–182, doi:10.1016/j.foodhyd.2014.09.004.
42. Hassannia-Kolaee, M.; Khodaiyan, F.; Pourahmad, R.; Shahabi-Ghahfarrokhi, I. Development of Ecofriendly Bionanocomposite: Whey Protein Isolate/Pullulan Films with Nano-SiO2. *Int. J. Biol. Macromol.* **2016**, *86*, 139–144, doi:10.1016/j.ijbiomac.2016.01.032.
43. Sanchez-Garcia, M.D.; Lagaron, J.M.; Hoa, S. V. Effect of Addition of Carbon Nanofibers and Carbon Nanotubes on Properties of Thermoplastic Biopolymers. *Compos. Sci. Technol.* **2010**, *70*, 1095–1105, doi:10.1016/j.compscitech.2010.02.015.
44. Pavase, T.R.; Lin, H.; Shaikh, Q. ul ain; Hussain, S.; Li, Z.; Ahmed, I.; Lv, L.; Sun, L.; Shah, S.B.H.; Kalhoro, M.T. Recent Advances of Conjugated Polymer (CP) Nanocomposite-Based Chemical Sensors and Their Applications in Food Spoilage Detection: A Comprehensive Review. *Sensors Actuators, B Chem.* **2018**, *273*, 1113–1138, doi:10.1016/j.snb.2018.06.118.

2. HYDROCOLLOIDS-BASED FILMS TO ENTRAP ANTIMICROBIAL AND ANTIOXIDANT COMPOUNDS

In the following paper, chitosan was exploited as a biopolymer to produce edible films with antioxidant and antimicrobial activities. Specifically, CH-based films were developed incorporating an extract derived from dried olive leaves (DOLE), obtained by Naviglio's extractor, to investigate its polyphenols yield and the antioxidant and antimicrobial properties of the active films. Olive tree cultivation produces a huge amount of byproducts that is usually simply burned. Phenolic compounds are already studied for their beneficial effects on human health. Some studies reported that phenols isolated from olive leaves have been shown to inhibit the growth of different strains of microorganisms. Thus, the antimicrobial effect of DOLE-containing films against bacterial strains (*Salmonella enterica* subsp. *enterica serovar Typhimurium* ATCC® 14028, *Salmonella enteritidis* RIVM 706, and *Enterococcus faecalis* ATCC® 29212) was tested in vitro. The DOLE component of the films is effective in inhibiting all the bacteria tested in a dose-dependent manner. Thus, it was demonstrated that these edible films can act as active bioplastics when used to wrap hamburgers in substitution of baking paper, which is normally used. Moreover, since the films are edible could be used as supplements to reinforce the human diet with polyphenols. The content of this paper is summarized in the following graphical abstract.

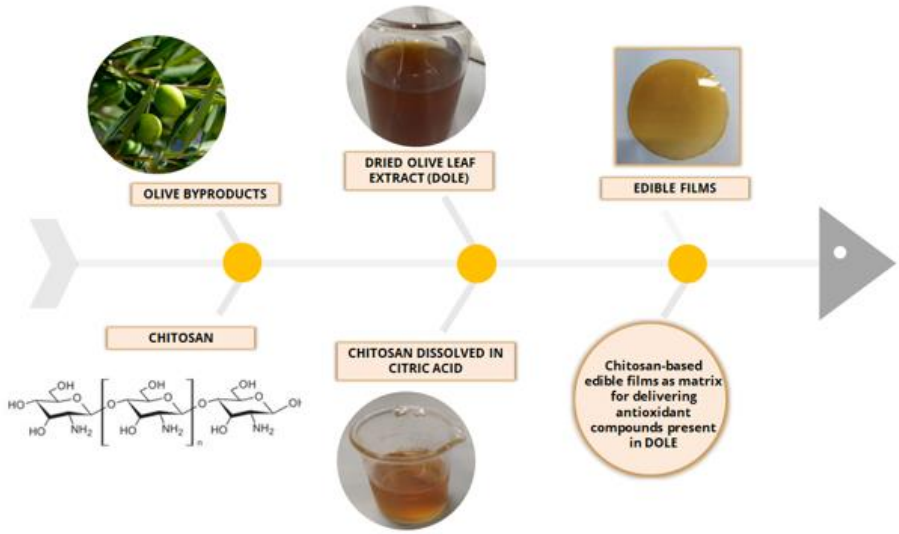

foods

MDPI

Article

Edible Films Made of Dried Olive Leaf Extract and Chitosan: Characterization and Applications

Michela Famiglietti [1], Alessandro Savastano [1], Rosa Gaglione [1], Angela Arciello [1], Daniele Naviglio [1] and Loredana Mariniello [1,2,*]

[1] Department of Chemical Sciences, University of Naples "Federico II", 80126 Naples, Italy; michela.famiglietti@unina.it (M.F.); alessandro.savastano@icloud.com (A.S.); rosa.gaglione@unina.it (R.G.); angela.arciello@unina.it (A.A.); daniele.naviglio@unina.it (D.N.)

[2] Center for Studies on Bioinspired Agro-Environmental Technology (BAT), University of Naples "Federico II", 80126 Naples, Italy

* Correspondence: loredana.mariniello@unina.it

Abstract: Nowadays a possible strategy in food preservation consists of the use of active and functional packaging to improve safety and ensure a longer shelf life of food products. Many studies refer to chitosan-based films because of the already-known chitosan (CH) antibacterial and antifungal activity. In this work, we developed CH-based films containing Dried Olive Leaf Extract (DOLE) obtained by Naviglio extractor, with the aim to investigate the polyphenols yield and the antioxidant activity of this extract entrapped in CH-based-edible films. Olive tree cultivation produces a huge amount of byproducts that are usually simply burned. Phenolic compounds are already studied for their beneficial effects on human health. Some studies reported that phenols isolated from olive leaves have been shown to inhibit the growth of different strains of microorganisms. Thus, the antimicrobial effect of DOLE-containing films against bacterial strains (*Salmonella enterica* subsp. *enterica serovar Typhimurium* ATCC® 14028, *Salmonella enteritidis* RIVM 706, and *Enterococcus faecalis* ATCC® 29212) was tested in vitro. The DOLE component of the films is effective in inhibiting all the bacteria tested in a dose-dependent manner. Thus, it was demonstrated that these edible films can act as active bioplastics when used to wrap hamburgers in substitution for baking paper, which is normally used.

Keywords: olive byproducts; chitosan; active packaging; food shelf life; antioxidants; circular economy

check for updates

Citation: Famiglietti, M.; Savastano, A.; Gaglione, R.; Arciello, A.; Naviglio, D.; Mariniello, L. Edible Films Made of Dried Olive Leaf Extract and Chitosan: Characterization and Applications. *Foods* **2022**, *11*, 2078. https://doi.org/10.3390/foods11142078

Academic Editors: Silvia Petronilho and Mario M. Martinez

Received: 10 June 2022
Accepted: 11 July 2022
Published: 13 July 2022

Publisher's Note: MDPI stays neutral with regard to jurisdictional claims in published maps and institutional affiliations.

Copyright: © 2022 by the authors. Licensee MDPI, Basel, Switzerland. This article is an open access article distributed under the terms and conditions of the Creative Commons Attribution (CC BY) license (https://creativecommons.org/licenses/by/4.0/).

1. Introduction

Chitosan (CH) is a natural linear copolymer derived from N-deacetylation of chitin and made up of units of N-acetyl-D-glucosamine and D-glucosamine (the latter exceeding 60%) [1], linked by beta-1,4 glycosidic linkage. Chitin is the second most abundant polymer on the earth, obtained from renewable sources, including exoskeletons of insects, arthropods such as shrimps, prawns, crabs, and cell walls of fungi [2].

Because of its biodegradability, biocompatibility, good film-forming capacity [3], and again because of its antibacterial and antifungal activity [4], CH is a very interesting polymer for applications in several industrial sectors.

The physical and chemical properties of CH depend on its molecular weight and degree of deacetylation. It presents one -NH_2 group and two -OH groups on each repeating unit and shows a rigid crystalline structure due to inter and intra-molecular hydrogen bonding [2]. These groups have a fundamental role in some important physicochemical characteristics including solubility and mechanical properties [3].

CH is a weak base insoluble in water and organic solvents, but amino groups make it soluble under acidic conditions below pH 6.0 [5]. It was reported that CH is effectively soluble in several organic and inorganic acids such as acetic, citric, formic, lactic, and hydrochloric [6]. The pKa value of CH strictly depends on deacetylation degree, ionic strength and the charge neutralization of -NH_2 groups [7], and the insoluble-soluble

transition occurs usually between pH 6.5 and 6.0. Below this value, the amino groups get protonated, and CH becomes a soluble polymer [5].

The known antibacterial activity of CH can be influenced by different factors such as its average molecular weight [8] and the nature of organic acid [9] used for its dissolution. Besides the different structures of the cell wall of Gram-negative and Gram-positive bacteria, these are the reasons that can explain the diverse antimicrobial behavior of CH against both bacteria, as reported in some studies. Regardless, CH has been shown to act by different mechanisms: it can behave as a barrier that changes the cell permeability, preventing oxygen transference and thereby inhibiting the respiratory activity of bacteria [8]; it can absorb on the surface of the microbe by means of electrostatic interactions and create a thick polymeric membrane that prevents the entrance of necessary nutrients in the cells influencing physiological activities that are important for the growth of microbes [10].

Inside the cells, NH_3^+ groups of CH can interact with the negatively charged phosphoryl groups on the cell membrane, causing its deformation and distortion [11]; it can also diffuse until completely disrupting the cytoplasmatic membrane and provoking the leakage of electrolytes and the cell death [12]. Finally, CH can penetrate nuclei and bind DNA, inhibiting its replication ability, and can induce the synthesis of chitinase in fruit by increasing the gene expression of this enzyme that degrades the cell walls of microbes [13].

Since CH food safety (Generally Recognized as Safe (GRAS)) was improved by the US Food and Drug Administration in 2011 [14], we investigated the solubility of CH in citric acid (CA) to use this polymer as a matrix for delivering antioxidant compounds present in DOLE. Olive tree cultivation and the olive processing industry produce every year a huge amount of byproducts and residues [15]. Olive (*Olea europaea* L.) is one of the most cultivated ancient plants in the world, with about 9 million hectares occupied worldwide [16]. Typically, it grows in the tropical and temperate regions, and it represents a fundamental cultivar of the Mediterranean region, but it is also distributed in Western Asia, Arabian Peninsula, India, Northern Africa, and Iran [17]. The byproducts from the olive processing industry are mainly made up of leaves and branches obtained from the pruning of olive trees and harvesting and cleaning of olives [18]. The amount of leaves is about 25%, while branches represent around 75% of the dried weight from the total pruning residues, and they are generally used as animal feed or simply burned [19]. The chemical composition includes a lignocellulosic fraction, proteins, and extractives, with the latter reaching up to 45% [19]. Thus, various efforts toward better olive leaf waste management were carried out to extract energy or molecules. Among them, thermochemical treatments (combustion, gasification pyrolysis), biochemical treatments (anaerobic digestion and bioethanol production), drying methods (solar drying, microwave drying, freeze-drying), extraction methods, and condensation of active components are used to produce natural additives in different applicative fields [16]. Phenolic compounds, the main high-added value fraction of extractives present in olives leaves, are already studied for their several beneficial effects on human health. It was confirmed by different researchers the high antioxidant activity of these polyphenols and their effects as antihypertensive, cholesterol-lowering, cardioprotective, anti-inflammatory, antibacterial molecules and as coadjuvants in obesity treatment [20–23]. Origin, climatic conditions, moisture content, and proportions of the branches on the tree affect the chemical composition and the amount of polyphenolic compounds in olive leaves [16]. Polyphenols mainly present in olive leaves belong to five groups: oleuropeosides (oleuropein and verbascoside), flavones (luteolin-7-glucoside, apigenin-7-glucoside, diosmetin-7-glucoside, luteolin and diosmetin), flavonols (rutin), flavan-3-ols (catechin), and substituted phenols (tyrosol, hydroxytyrosol, vanillin, vanillic acid and caffeic acid) [24]. Among these the most abundant compound in olive leaves is oleuropein, which follows hydroxytyrosol, luteolin, apigenin, and verbascoside [25]. Hydroxytyrosol is more present in processed olive fruit and olive oil, while oleuropein is predominant in unprocessed olive fruit and leaves. This fact was explained due to the enzymatic reactions that occur during the maturation and processing of olives [24]. Oleuropein can prevent the formation of free radicals thanks to its ability to chelate metal

ions such as Cu^{2+} and Fe^{3+} [26]. Moreover, both oleuropein and hydroxytyrosol have been shown to be scavengers of superoxide anions as well as of hypochlorous acid, a potent oxidant produced in vivo at the site of inflammation and a major component of chlorine-based bleaches that can often come into contact with food during manufacturing [27]. To date, different extraction methods were used to obtain high-added value from olive leaves, the traditional and most used is the solid-liquid extraction by maceration of the biomass in a solvent [28]. In the last years, new extraction methods are developed to reduce the amounts of solvent, time extraction, and sample preparation cost. Among them, supercritical fluid extraction and ultrasound-assisted extraction are more commonly used, followed by superheated liquid extraction, pressurized liquid extraction, and fractionation by solid-phase extraction. The selected extraction method, the nature of solvent, temperature, pH, and time of extraction are fundamental parameters that influence the yield and the content of polyphenolic compounds derived from olive leaves [29,30]. Obviously, the chemical characteristics of compounds make them less or more extractable by different methods: it was observed that compounds with less polarity as apigenin and luteolin are more easily obtainable by supercritical fluid extraction or pressurized liquid extraction, while maceration is more suitable to extract polar compounds such as oleuropein derivatives [31]. This work aimed to investigate the polyphenols yield of DOLE obtained by the Naviglio extractor and the antioxidant activity of this extract in chitosan-based-edible films. Our studies have also demonstrated the antioxidant activity of DOLE-containing films after in vitro oral digestion, which suggests the use of our films as a novel supplement for a diet rich in polyphenols. Moreover, we tested in vitro the antimicrobial effect of DOLE containing films against bacterial strains (*Salmonella typhimurium* ATCC® 14028, *Salmonella enteriditis* RIVM 706, and *Enterococcus faecalis* ATCC® 29212). In turn, the antimicrobial inhibitory effect of DOLE in meat samples over a time up to 20 days, in comparison to baking (parchment) paper normally used to store hamburgers, was demonstrated. We have also studied the mechanical properties of the films suggesting for DOLE a role as plasticizer. Thus, it can be assessed that multiple roles can be attributed to DOLE, nowadays a waste from olive trees pruning that can become a high-added-value product according to the principles of the circular economy.

2. Materials and Methods

2.1. Materials

CH (from shrimp shell, low molecular weight, Degree of Deacetylation $\geq$ 75%), CA (99%), urea, DPPH, NaCl were supplied by Sigma-Aldrich Company (St. Louis, MO, USA). Chemical reagents used for electrophoresis were from Bio-Rad (Segrate, Milano, Italy). Sodium hydroxide and hydrochloric acid were purchased from Sigma Aldrich Companyv (St.Louis, MO, USA). Glycerol (GLY), methanol and magnesium nitrate were from Carlo Erba S.p.A. (Milan, Italy) mTGase (Activa, WM, containing 1% of mTGase and 99% of maltodextrins) obtained from the culture of *Streptoverticillium* sp., was supplied by Prodotti Gianni (Milano, Italy). Folin–Ciocâlteu reagent was purchased by Fisher Bioreagents (Pittsburgh, PA, USA) Contact slide kit for controlling bacterial development (*Enterobacteriaceae* and *Streptococcus Faecalis*) in meat samples was purchased by Chimica Centro according to ISO 18593. Meat samples (hamburghers) were purchased from a local market. Olive leaf samples (cv "pisciottano") were collected when the pruning is traditionally done from a farm in Cilento, a seaside land of the Campania Region, Southern Italy. Olive leaves were kept in sealed bags and stored at room temperature until use.

2.2. DOLE Preparation by Naviglio's Principle

Before being submitted to the extraction process, olive leaves were dried in a static oven at 50 °C for two days. After that, 50 g of the samples were put in the filter bag (100 µm porosity), which was then inserted in the extraction chamber of the Naviglio extractor® (Lab Model 500 cm^3 capacity). Extraction was performed using 500 mL of H_2O (containing 0.15% (*w*/*v*) CA, and 0.20% (*w*/*v*) potassium sorbate, pH 4.1) at room temperature and

applying a 10-bar pressure for 2 min (static phase). After that, a remixing of liquid was applied for 2 min (dynamic phase). The pressure gradient is responsible for the extraction from the solid material (suction effect) as reported in Naviglio [32]. Liquid samples (10 mL), named DOLE, were collected after 2, 4, 6, and 24 h. DOLE samples were kept at 4 °C until they were used.

2.3. Total Polyphenols Content (TPC) Evaluation

DOLE TPC in samples obtained at different times of extraction, was determined by colorimetric in vitro assay using Folin–Ciocâlteau [33]. The calibration curve was set up with different concentrations of gallic acid (0.1–1 g/L). In particular, 0.1 mL of gallic acid solutions were mixed with 0.5 mL of 2 N Folin–Ciocâlteau reagent and 1.5 mL of freshly prepared 20% (*v*/*v*) Na_2CO_3, then the volume was adjusted to 10 mL with distilled water. Conversely, 0.1 mL of DOLE at different times of extraction (2-4-6-24 h) was mixed with the same reagents described. All the samples were incubated at room temperature in the dark for 1 h, then absorbance of the samples was measured at 765 nm using UV/visible Spectrophotometer (SmartSpec 3000 Bio-Rad, Segrate, Milan, Italy). The results were expressed as gallic acid equivalents (GAE). All determinations were carried out in triplicates.

2.4. Solubility of CH in CA

To investigate the solubility of CH in CA, different aqueous solutions of such acid were prepared (1.5–3.0% (*w*/*v*)). In each solution (50 mL) 1.5 g of CH were added under stirring. After 2 h, each solution was let stand for 1 h (without any stirring) to check the formation of precipitates. To quantify the CH dissolved, the supernatants were left to dry to obtain the dried matter. Solubility was expressed as percentage of the 1.5 g of CH added in each solution.

2.5. Preparation of Film Forming Solutions (FFSs) Containing DOLE

FFSs were prepared by using CA 3% (*w*/*v*) and chitosan 3% (*w*/*v*) at pH 2.5. DOLE was added in different volumes (10-15-20-40% (*v*/*v*)) after that its pH value was adjusted to 2.8 using CA 1 M. Finally, glycerol, used as a plasticizer, was mixed at 10% (*w*/*w*) (in respect to the weight of CH) in each type of FFS.

2.6. Zeta Potential and Particle Size Measurements

Zeta potential, average particle size, and polydispersity index of the FFSs were analyzed using the Zetasizer Nano-ZSP (Malvern®, Worcestershire, UK).

Three independent measurements were carried out on each sample of FFSs (1 mL) diluted to have a CH final concentration of 1 mg/mL.

Zetasizer Nano combines different techniques of Light Scattering to obtain a complete characterization of a colloidal system. Operating with a helium-neon laser at a fixed wavelength of 633 nm, it calculates the Zeta potential by using the Electrophoretic Light Scattering (ELS), the mean diameter of particles by using Dynamic Light Scattering (DLS) and the polydispersity index (PDI), which represents a value relative to the variance in the particle size distribution.

Three independent measurements were carried out on each sample of FFSs (1 mL) diluted to have a final concentration of 1 mg/mL.

2.7. Films Preparation

FFSs were poured in polypropylene Petri dishes (9 cm in diameter) and dried in a climatic chamber at 25 °C and 45% RH for 2 days. After that, the films were stored in a desiccator to balance the moisture content at 60% RH and room temperature during the subsequent analyses.

2.8. Antioxidant Activity

The activity to scavenge DPPH, 2,2-diphenyl-1-picrylhydrazyl, was measured for the solubilized films with all the different volumes of DOLE, for FFS 20% (*v*/*v*) and for DOLE solution (20% *v*/*v*) for one month, every 5 days.

Films were solubilized in CA 3% (*w*/*v*): 20 mg of each sample were dissolved in 500 µL of CA solution and subjected to sonication for 3 min.

For the *DPPH* assay, each sample was prepared adding to 900 µL of DPPH methanolic solution (0.005% (*w*/*v*)) 100 µL of different samples. The latter were incubated in dark for 30 min at room temperature. After that, absorbance was measured at 517 nm using a UV/visible Spectrophotometer (SmartSpec 3000 Bio-Rad, Segrate, Milan, Italy), considering methanol as blank and a sample with methanol added to DPPH solution as a control. The *DPPH scavenging activity* was calculated for each sample according to this equation:

$$\%DPPH\ scavenging\ activity = (A_{control} - A_{sample}/A_{control}) \times 100.$$

2.9. In Vitro Oral Digestion

After one month, the film containing 20% (*v*/*v*) DOLE was subjected to in vitro oral digestion, i.e., under simulated oral conditions according to Giosafatto et al. [34] with some modifications, and then the DPPH scavenging activity of this solution was measured to study the release of polyphenols entrapped in chitosan films.

For this analysis, 20 mg of each type of film was incubated in 500 µL of Simulated Salivary Fluid (SSF, (150 mM of NaCl, 3 mM of urea, pH 6.9) for 7 min at 170 rpm, according to Giosafatto et al. [34].

2.10. Film Mechanical Properties and Thickness

An Instron universal testing instrument (model no. 5543A, Instron Engineering Corp., Norwood, MA, USA) was used for mechanical properties characterization. Tensile Strength (TS), Young's Modulus (YM), and Elongation at Break (EB) were determined according to ASTM D882-18 (1997). Each film was cut into strips with a length of 40 mm and a width of 10 mm, and they were tested by using a 1 kN load cell and with a rate of grip separation of 20 mm/min. Film thickness was determined in five spots on each strip by using a digital micrometer (IP65 Alpa exacto, Alpa metrology Co., Pontoglio (BS), Italy, sensitivity 0.001 mm).

2.11. Bacterial Strains, Growth Conditions, and Antimicrobial Activity of DOLE-Based Films

Bacterial strains *Salmonella enteriditis* 706 RIVM, *Salmonella enterica* subsp. *Enterica serovar Typhimurium* (ATCC® 14028) and *Enterococcus faecalis* ATCC® 29212 were grown in Muller Hinton Broth (MHB, Becton Dickinson Difco, Franklin Lakes, NJ, USA) and on Tryptic Soy Agar (TSA; Oxoid Ltd., Hampshire, UK) as previously described [35]. In all the experiments, bacteria were inoculated and grown overnight in MHB at 37 °C.

In all the experiments to assess the antimicrobial activity of DOLE-based films, bacterial cells were inoculated and grown overnight in MHB at 37 °C. The next day, bacteria were transferred to a fresh Tryptic Soy Broth (TSB) tube and grown to mid- logarithmic phase. The antimicrobial activity of the films, containing or not containing DOLE, was tested by using a previously described experimental procedure [36]. Briefly, bacterial cells were diluted into TSB to approximately 2×10^7 CFU/mL and inoculated into TSA plates. A 1.5-cm^2 square of the edible film was placed into the center of the inoculated plate and pressed to ensure full contact with the agar surface. Plates were then incubated at 37 °C for 24 h and the bacterial growth underneath the film was evaluated.

2.12. DOLE Containing Film Capability to Contrast Bacterial Growth in Meat Samples

Hamburgers were prepared and both surfaces were covered with edible films containing DOLE at the following concentrations: 0%, 10%, 15%, and 20% (*v*/*v*). Hamburgers coated with baking paper were used as control. All samples were kept at 4 °C, but analyzed

at different times (0 days, 5 days, 10 days, and 20 days) as follows: 10 g of each hamburger (from which the edible films or baking paper were removed) were homogenized in sterile conditions in the presence of 100 mL of H_2O. Contact slides (designed for identifying *Enterobacteriaceae* and *Streptococcus Faecalis*) were dipped in these solutions for 30 s and used according to the manufacturer's instructions of Liofilchem®-Contact slide 5 kit following ISO 18593.

2.13. Statistical Analysis

SPSS19 (Version 19, SPSS Inc., Chicago, IL, USA) software was used for all statistical analyses. One-way analysis of variance (ANOVA) and Duncan's multiple range tests ($p < 0.05$) were used to determine the significant difference among the samples.

3. Results

3.1. Olive Leaf Extract Preparation and Total Polyphenol Content (TPC)

During pruning of olive trees, a huge amount of pruning wastes is produced in all countries where the olive tree cultivation is part of the local economy. It is well known that olive tree drupes can produce one of the best oils from a nutritional point of view. Olive oil is, in fact, rich with polyphenols and vitamin E, depending on the method used [36–38]. Also, the pruning waste is rich in valuable compounds, such as polyphenols. It is described that olive leaves are particularly plentiful in highly healthy molecules, such as hydroxytyrosol and oleuropein [24]. For this reason, many items can be found, especially in the online market, that are suggested as supplements and/or cosmetic purposes. In this paper we wanted to propose the use of polyphenols extracted by olive pruning wastes as antioxidants and antimicrobial components of CH-based films to be used as both supplements for an easy administration and as films to wrap hamburgers. To reach this aim we have obtained dried olive extracts (DOLE) by referring to the Naviglio methodology [32] Naviglio extractor is an innovative technology that allows to quickly extract, from solid materials, the extractable compounds in organic and inorganic solvents compared to conventional techniques. It is based on a suction effect theorized in "Naviglio's Principle" [32]. Compression of liquid in which the solid matrix occurs at a pressure of around 8–10 bar by extracting solvent for a certain time is followed by an immediate decompression at atmospheric pressure. Thereby, a rapid release of extracting liquid, caused by a pressure gradient, is transported mechanically outside from the solid matrix the extractable compounds. Each extractive cycle consists of two phases: in the first one, also called the static phase, the system is under pressure and the liquid can penetrate the solid matrix; at the beginning of the second one, a negative pressure gradient is generated between the inside and the outside of the solid matrix to provoke the suction effect necessary to the extraction [32]. The extractions were performed at different times to assess the best protocol to obtain the highest quantity of polyphenolic molecules. As shown in Table 1, the TPC increases over time. Moreover, the amount of TPC results are notable, as expected from the literature [24]. It can be assessed that Naviglio's method is very effective, as reported in Mirpoor et al. [39] In fact, these authors compared Naviglio's method with maceration-based technology for the extraction of TPC from cardon leaves. Extraction in water was assessed to be more efficient than extraction with organic solvents, also by Sabry et al. [24]. Moreover, olive leaves derived from pruning contain, after 24 h of time extraction, a higher amount of TPC (6.6 ± 0.1 g GAE/L) compared to cardon (0.15 ± 0.1 g GAE/L), suggesting the importance of recovering olive leaves wastes. It is worth to note that TPC is equal to 4.4 ± 0.2 g GAE/L after only 2 h of time extraction.

Table 1. Total phenolic content in DOLE at different times of extraction.

Hours	Polyphenols (g GAE/L)
2	4.4 ± 0.2^{a}
4	4.6 ± 0.1^{a}
6	5.5 ± 0.2^{b}
24	6.6 ± 0.4^{c}

Different small letters (a–c) indicate significant differences among the values reported in each column ($p < 0.05$).

3.2. Chitosan Solubility in Citric Acid

Because of amino groups, CH is soluble in acidic solutions among which there is CA that is food grade. However, the solubilization depends on the degree of deacetylation (DD). Thus, we have performed experiments to assess the CA concentration to achieve the maximum solubility of CH. CA was used in substitution of acetic acid normally used in our previous papers, where chitosan-based bioplastics were prepared to be proposed to wrap foods [40]. In this work we decided to recur to CA since our main aim was to use chitosan-base edible films to convey phenolic compounds present in DOLE as supplements with a pleasant taste for consumers (which is not insured using acetic acid as the solvent). The maximum solubility was achieved using 3% (w/v) CA, as shown in Figure 1. Thus, further analyses were performed using 3% (w/v) CH dissolved in 3% (w/v) CA.

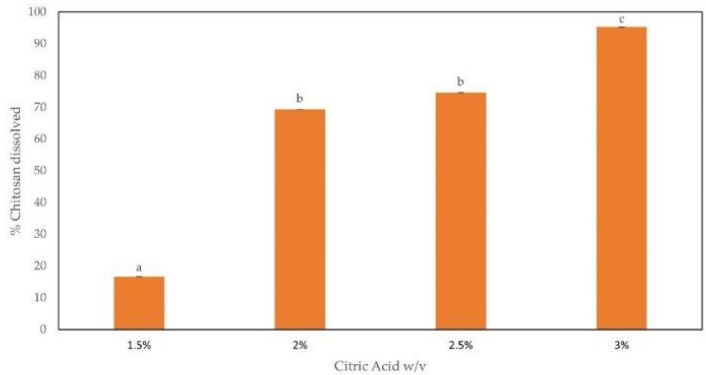

Figure 1. CH solubility, expressed in percentage, when dissolved in CA. Different small letters (a–c) indicate significant differences among the values reported in each bar ($p < 0.05$).

3.3. FFSs Characterization and Preparation of Films by Casting

FFSs prepared in absence and in presence of increasing concentrations of DOLE were analyzed via Zeta sizer to determine the Zeta potential, particle size, and PDI. Table 2 shows that all the solutions were highly stable. The addition of DOLE provoked a lowering in the Zeta potential value in respect to the control (CH-based solution in absence of DOLE), which turned out higher by increasing the amount of DOLE. The mean particle size of DOLE containing samples were lower than the one exhibited by the control and decreased by increasing the DOLE concentration. The same observation can be done regarding PDI values. The decreasing in mean particle size could be due to aggregation of CH particles provoked by polyphenolic molecules present in DOLE. These solutions were used to cast films. Obtained films are shown in Figure 2. Films appear transparent but yellowish depending on the DOLE content.

Table 2. Zeta potential, particle size, and PDI of FFSs containing DOLE (10–40% (*v*/*v*)). The control was set up in the absence of DOLE.

DOLE in FFSs % (*v*/*v*)	Z Potential (mV)	Mean Particle Size (nm)	PDI
0	55.71 ± 4.61 [a]	567.00 ± 19.33 [a]	0.67 ± 0.02 [a]
10	40.08 ± 3.20 [c]	568.96 ± 31.40 [a]	0.48 ± 0.01 [b]
15	43.59 ± 2.51 [c]	500.68 ± 28.30 [b]	0.50 ± 0.03 [b]
20	49.37 ± 5.42 [b]	426.22 ± 49.05 [c]	0.51 ± 0.05 [b]
40	53.55 ± 5.61 [a,b]	419.32 ± 73.02 [c]	0.51 ± 0.05 [b]

Different small letters (a–c) indicate significant differences among the values reported in each column ($p < 0.05$).

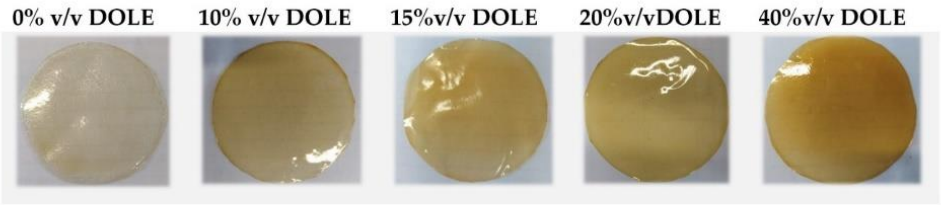

Figure 2. Chitosan-based films containing different volumes of DOLE (0–40% (*v*/*v*)).

3.4. Antioxidant Activity (AA) of DOLE-Containing Films over the Time

Figure 3 shows the AA of solubilized DOLE containing films detected from 0 time and every 5 days up to 30. Lower AA was observed in films containing 10 and 15% (*v*/*v*) DOLE even after few days of storage. Instead, the AA remained high in both kinds of films containing 20% and 40% (*v*/*v*) DOLE, respectively. The AA was also detected over the time in 20% (*v*/*v*) DOLE solutions and in 20% (*v*/*v*) DOLE FFS. It can be noticed that the AA values in solubilized films were lower than DOLE-containing solutions and FFS. In Figure 3, we report only the results obtained with 20% (*v*/*v*) DOLE containing samples, but similar results were obtained with 40% (*v*/*v*) DOLE samples. A possible explanation could be that the phenolic compounds present in DOLE exert a lower activity when entrapped in the chitosan film matrix. A reduction of AA due to cardoon leaf extracts (CLE) entrapped in cardoon protein-based films was also reported in Mirpoor et al. [39], even though for a longer time (70 days). It must be noticed that DOLE-containing films showed a high AA even after 30 days (70%) compared to CLE-containing films at time 0 (60%) [39].

3.5. In Vitro Oral Digestion

In order to ensure the release of polyphenols entrapped in CH films, samples (20% *v*/*v* DOLE) stored for 30 days were subjected to in vitro oral digestion, under simulated oral conditions, and then the DPPH scavenging activity of these solutions was measured. The results in Figure 4 showed that the release of polyphenols from 30 days storage films occurred properly after in vitro oral digestion. The AA results of such films were compared to the ones obtained from the controls represented by solubilized films stored for the same time (30 days). The AA of both groups of different samples are perfectly comparable, demonstrating that polyphenols entrapped in the films are still active after in vitro simulated oral digestion. Thus, we can affirm that DOLE containing films could be used to delivery polyphenols in a novel supplement for an effective application into the nutraceutical industry.

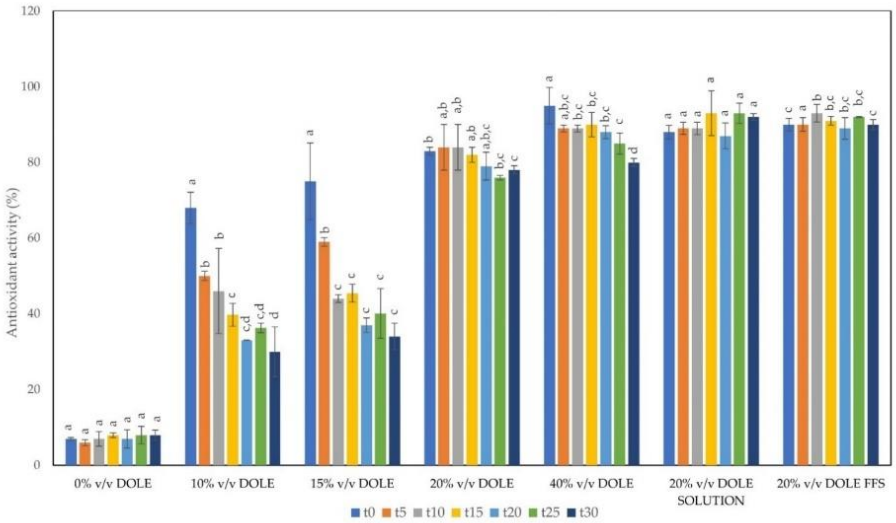

Figure 3. Antioxidant activity by DPPH assay of solubilized films (DOLE 0-10-15-20-40% (*v*/*v*)), 20% (*v*/*v*) DOLE solutions, and 20% (*v*/*v*) DOLE Film Forming Solutions (FFS) at different days of storage. Different small letters (a–d) indicate significant differences among the values reported in each bar ($p < 0.05$).

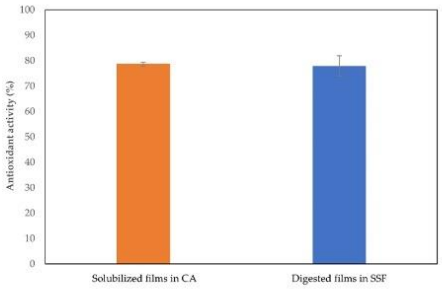

Figure 4. Antioxidant activity by DPPH assay of 20% (*v*/*v*) DOLE films subjected to in vitro oral digestion after 30 days compared to the AA of solubilized films after 30 days.

3.6. Mechanical Properties

Since DOLE visually seemed to have a plasticizer effect on chitosan-based films, we studied the mechanical properties of these films to verify the possible influence of DOLE on Tensile Strength (TS), Elongation at Break (EB), and Young's Modulus (YM). Samples thickness was also measured.

As shown in Figure 5, the medium thickness of all samples does not differ significatively from the control. Regarding mechanical properties, we note that they are influenced by the presence of DOLE. We can observe, proportionally with the increment of DOLE concentration, an increase of EB, and a decrease of TS and YM, also with respect to the control without DOLE. These results suggest a role as plasticizer for DOLE in addition to the one exerted by glycerol. Similar results were obtained by Mariniello et al., using grape juice as a plasticizer in *N. sativa* protein-based films [41].

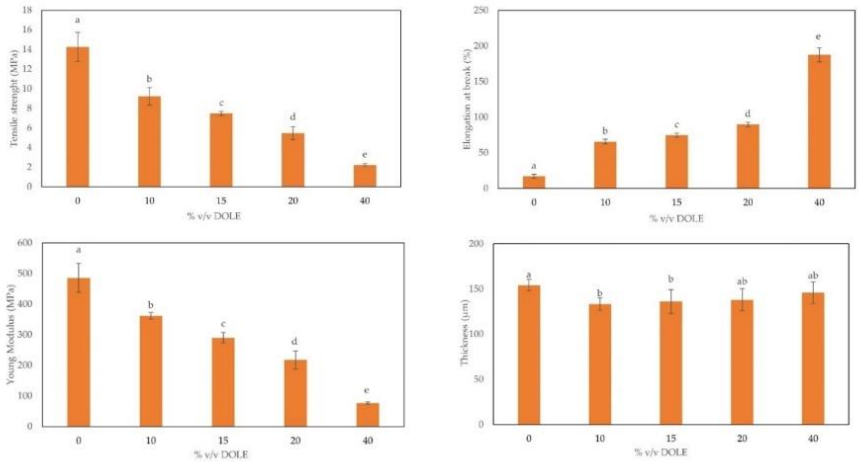

Figure 5. Properties of chitosan-based films with different % (*v*/*v*) of DOLE (0–40%). On the top: from left to right Tensile Strength and Elongation at Break. On the bottom: from left to right Young's Modulus and Thickness. Different small letters (a–e) indicate significant differences among the values reported in each bar ($p < 0.05$).

3.7. Antimicrobial Activity of Films Containing DOLE

Films prepared in the absence or in the presence of DOLE at different concentrations (10%, 20%, or 40% (*v*/*v*)) were analyzed for their antimicrobial activity towards Gram-negative bacteria (*S. enteriditis* 706 RIVM, *S. enterica* subsp. *enterica serovar* Typhimurium ATCC® 14028) and a Gram-positive bacterial strain *E. faecalis* ATCC® 29212. Usually, these strains are involved in food contamination and spoilage. In particular, the presence of *E. faecalis* suggests that a contamination by the two other pathogen strains may occur. Thus, small squares (1.5 cm × 1.5 cm) of each film were placed into the inoculated plate in full contact with the agar surface. After 24 h at 37 °C, only the films containing DOLE were found to be able to significantly inhibit bacterial growth with the strongest effects observed at the highest content of DOLE (Figure 6a,b). The DOLE component of the films is effective in inhibiting the growth of all the bacteria tested in a dose dependent manner. Other studies suggested a broad antimicrobial activity of olive leaves extract in a concentration dependent-manner [42]. Taking advantage of these results, we have tested the capability of DOLE-containing films as active bioplastics, able to control the bacterial spoilage of meat hamburgers over time. To this aim, we have used the Liofilchem® contact slide 5 kit, which allows selective detection of *Enterobacteriaceae* and enterococci. In particular, employed slides contain media to selectively identify *E. coli* ATCC® 25922 and *Enterococcus faecalis* ATCC® 19433. As samples, we have chosen meat hamburgers and covered each side with our edible films containing increasing amounts of DOLE. As controls we used hamburgers coated with baking paper, as is commonly done. We kept all samples stored at 4 °C for different times (0, 5, 10, and 20 days). Afterwards, meat samples were treated as described in materials and method in Section 2.12. As shown in Figure 7, the most effective edible films are the ones containing 15% and 20% (*v*/*v*) DOLE after 20 days storage, demonstrating that the antimicrobial activity of phenolic compounds is still valuable over time, especially against *E. coli*. Samples were also tested for the presence of *E. faecalis* bacteria, that were totally absent even in the control at time 0 (data not shown). Thus, we can assess that DOLE-containing films exhibit antimicrobial activity against all the bacteria tested both in vitro (Figure 6) and as edible films used to protect hamburgers over time (Figure 7).

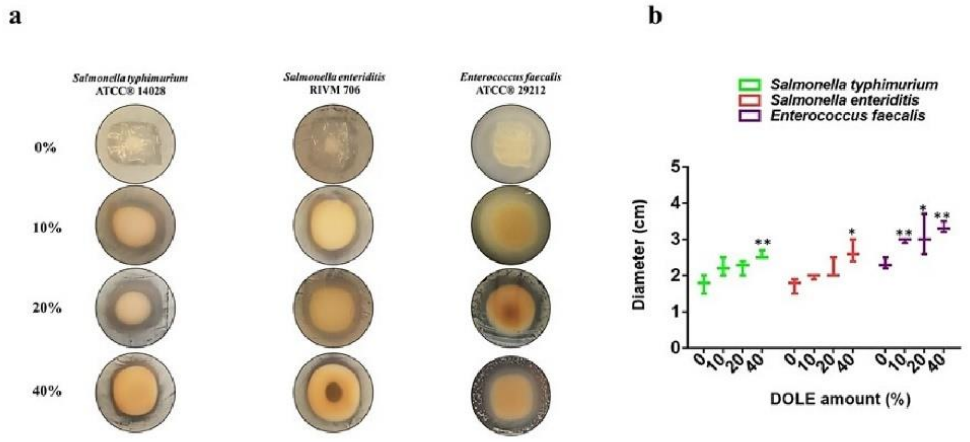

Figure 6. Antimicrobial activity of DOLE-based films. Antimicrobial effects were evaluated by analyzing the growth of the bacterial cells held in direct contact with the films (**a**). The diameter of the inhibition circle was determined for each bacterial strain in contact with the different films and shown in the graph (**b**). The experiments were carried out in triplicate. Statistical analyses were performed by using Student's *t*-test. Significant differences were indicated as * $p < 0.05$ or ** $p < 0.01$.

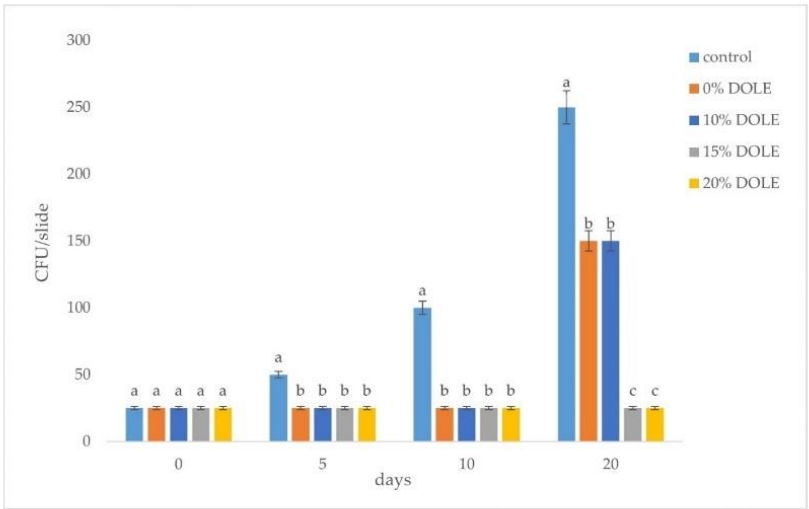

Figure 7. CFU (*Enterobacteriaceae*) in meat samples covered with DOLE-containing films. Controls represent samples covered with baking paper. Different small letters (a–c) indicate significant differences among the values reported in each bar ($p < 0.05$).

4. Conclusions

In the present paper it was demonstrated that olive byproducts can be recovered to obtain a high added-value product possibly used in the food industry. It showed the effectiveness of polyphenols contained in DOLE and entrapped in a chitosan-based matrix in acting as antimicrobials and antioxidants. Obtained films can be classified as edible

and, thus, could be used as supplements to reinforce the human diet with polyphenols. Moreover, such films can be used to wrap meat hamburgers to delay spoilage during storage due to common microbial contaminants.

Author Contributions: M.F., A.S. and L.M. planned and designed the work. D.N. and A.S. extracted polyphenol and antioxidant properties from olive leaves. R.G. and A.A. performed antimicrobial activity in vitro. All other experimental results were performed by M.F. and A.S. M.F. and L.M. wrote the article. All authors have read and agreed to the published version of the manuscript.

Funding: This research was funded by the grant PRIN: Progetti di Ricerca di Interesse Nazionale—Bando 2017—"CARDoon valorisation by InteGrAted biorefiNery (CARDIGAN)" Ministero Italiano dell'Università e della Ricerca (MUR) (COD. 2017KBTK93).

Institutional Review Board Statement: Not applicable.

Data Availability Statement: The data presented in this study are available on request from the corresponding author.

Acknowledgments: The authors would like to thank Maria Fenderico for her technical support.

Conflicts of Interest: The authors declare no conflict of interest.

References

1. Elsabee, M.Z.; Abdou, E.S. Chitosan Based Edible Films and Coatings: A Review. *Mater. Sci. Eng. C* **2013**, *33*, 1819–1841. [CrossRef]
2. Shukla, S.K.; Mishra, A.K.; Arotiba, O.A.; Mamba, B.B. Chitosan-Based Nanomaterials: A State-of-the-Art Review. *Int. J. Biol. Macromol.* **2013**, *59*, 46–58. [CrossRef]
3. Mujtaba, M.; Morsi, R.E.; Kerch, G.; Elsabee, M.Z.; Kaya, M.; Labidi, J.; Khawar, K.M. Current Advancements in Chitosan-Based Film Production for Food Technology; A Review. *Int. J. Biol. Macromol.* **2019**, *121*, 889–904. [CrossRef]
4. No, H.K.; Young Park, N.; Ho Lee, S.; Meyers, S.P. Antibacterial Activity of Chitosans and Chitosan Oligomers with Different Molecular Weights. *Int. J. Food Microbiol.* **2002**, *74*, 65–72. [CrossRef]
5. Melro, E.; Antunes, F.E.; da Silva, G.J.; Cruz, I.; Ramos, P.E.; Carvalho, F.; Alves, L. Chitosan Films in Food Applications. Tuning Film Properties by Changing Acidic Dissolution Conditions. *Polymers* **2021**, *13*, 1. [CrossRef]
6. El Knidri, H.; Belabeed, R.; Addaou, A.; Laajeb, A.; Lahsini, A. Extraction, Chemical Modification and Characterization of Chitin and Chitosan. *Int. J. Biol. Macromol.* **2018**, *120*, 1181–1189. [CrossRef]
7. Sorlier, P.; Denuzière, A.; Viton, C.; Domard, A. Relation between the Degree of Acetylation and the Electrostatic Properties of Chitin and Chitosan. *Biomacromolecules* **2001**, *2*, 765–772. [CrossRef]
8. Dotto, G.L.; Vieira, M.L.G.; Pinto, L.A.A. Use of Chitosan Solutions for the Microbiological Shelf Life Extension of Papaya Fruits during Storage at Room Temperature. *LWT Food Sci. Technol.* **2015**, *64*, 126–130. [CrossRef]
9. Vimaladevi, S.; Panda, S.K.; Xavier, K.A.M.; Bindu, J. Packaging Performance of Organic Acid Incorporated Chitosan Films on Dried Anchovy (*Stolephorus Indicus*). *Carbohydr. Polym.* **2015**, *127*, 189–194. [CrossRef]
10. Al-Naamani, L.; Dobretsov, S.; Dutta, J. Chitosan-Zinc Oxide Nanoparticle Composite Coating for Active Food Packaging Applications. *Innov. Food Sci. Emerg. Technol.* **2016**, *38*, 231–237. [CrossRef]
11. Del Hoyo-Gallego, S.; Pérez-Álvarez, L.; Gómez-Galván, F.; Lizundia, E.; Kuritka, I.; Sedlarik, V.; Laza, J.M.; Vila-Vilela, J.L. Construction of Antibacterial Poly(Ethylene Terephthalate) Films via Layer by Layer Assembly of Chitosan and Hyaluronic Acid. *Carbohydr. Polym.* **2016**, *143*, 35–43. [CrossRef]
12. Youssef, A.M.; El-Sayed, S.M.; El-Sayed, H.S.; Salama, H.H.; Dufresne, A. Enhancement of Egyptian Soft White Cheese Shelf Life Using a Novel Chitosan/Carboxymethyl Cellulose/Zinc Oxide Bionanocomposite Film. *Carbohydr. Polym.* **2016**, *151*, 9–19. [CrossRef]
13. Ochoa-Velasco, C.E.; Guerrero-Beltrán, J.Á. Postharvest Quality of Peeled Prickly Pear Fruit Treated with Acetic Acid and Chitosan. *Postharvest Biol. Technol.* **2014**, *92*, 139–145. [CrossRef]
14. Abdel-rahman, A.; Anyangwe, N.; Carlacci, L.; Casper, S.; Danam, R.P.; Enongene, E.; Erives, G.; Fabricant, D.; Gudi, R.; Hilmas, C.J.; et al. The Safety and Regulation of Natural Products Used as Foods and Food Ingredients. *Toxicol. Sci.* **2011**, *123*, 333–348. [CrossRef]
15. Kiritsakis, K.; Goula, A.M.; Adamopoulos, K.G.; Gerasopoulos, D. Valorization of Olive Leaves: Spray Drying of Olive Leaf Extract. *Waste Biomass Valoriz.* **2018**, *9*, 619–633. [CrossRef]
16. Espeso, J.; Isaza, A.; Lee, J.Y.; Sörensen, P.M.; Jurado, P.; de Avena-Bustillos, R.J.; Olaizola, M.; Arboleya, J.C. Olive Leaf Waste Management. *Front. Sustain. Food Syst.* **2021**, *5*, 1–13. [CrossRef]
17. Özcan, M.M.; Matthäus, B. A Review: Benefit and Bioactive Properties of Olive (*Olea Europaea* L.) Leaves. *Eur. Food Res. Technol.* **2017**, *243*, 89–99. [CrossRef]

18. Molina-Alcaide, E.; Yáñez-Ruiz, D.R. Potential Use of Olive By-Products in Ruminant Feeding: A Review. *Anim. Feed Sci. Technol.* **2008**, *147*, 247–264. [CrossRef]
19. Manzanares, P.; Ruiz, E.; Ballesteros, M.; Negro, M.J.; Gallego, F.J.; López-Linares, J.C.; Castro, E. Residual Biomass Potential in Olive Tree Cultivation and Olive Oil Industry in Spain: Valorization Proposal in a Biorefinery Context. *Span. J. Agric. Res.* **2017**, *15*, 1–12. [CrossRef]
20. Herrero, M.; Temirzoda, T.N.; Segura-Carretero, A.; Quirantes, R.; Plaza, M.; Ibañez, E. New Possibilities for the Valorization of Olive Oil By-Products. *J. Chromatogr. A* **2011**, *1218*, 7511–7520. [CrossRef]
21. Susalit, E.; Agus, N.; Effendi, I.; Tjandrawinata, R.R.; Nofiarny, D.; Perrinjaquet-Moccetti, T.; Verbruggen, M. Olive (*Olea Europaea*) Leaf Extract Effective in Patients with Stage-1 Hypertension: Comparison with Captopril. *Phytomedicine* **2011**, *18*, 251–258. [CrossRef]
22. Jemai, H.; Feki, A.E.L.; Sayadi, S. Antidiabetic and Antioxidant Effects of Hydroxytyrosol and Oleuropein from Olive Leaves in Alloxan-Diabetic Rats. *J. Agric. Food Chem.* **2009**, *57*, 8798–8804. [CrossRef]
23. Khalatbary, A.R.; Zarrinjoei, G.R. Anti-Inflammatory Effect of Oleuropein in Experimental Rat Spinal Cord Trauma. *Iran. Red Crescent Med. J.* **2012**, *14*, 229–234.
24. Sabry, O.M.M. Review: Beneficial Health Effects of Olive Leaves Extracts. *J. Nat. Sci. Res.* **2014**, *4*, 19.
25. Benavente-García, O.; Castillo, J.; Lorente, J.; Ortuño, A.; Del Rio, J.A. Antioxidant Activity of Phenolics Extracted from *Olea Europaea* L. Leaves. *Food Chem.* **2000**, *68*, 457–462. [CrossRef]
26. Andrikopoulos, N.; Kaliora, A.; Assimopoulou, A.; Papageorgiou, V. Inhibitory Activity of Minor Polyphenolic and Nonpolyphenolic Constituents of Olive Oil Against In Vitro Low-Density Lipoprotein Oxidation. *J. Med. Food* **2002**, *5*, 1–7. [CrossRef]
27. Visioli, F.; Poli, A.; Galli, C. Antioxidant and Other Biological Activities of Phenols from Olives and Olive Oil. *Med. Res. Rev.* **2002**, *22*, 65–75. [CrossRef]
28. Kashaninejad, M.; Sanz, M.T.; Blanco, B.; Beltrán, S.; Niknam, S.M. Freeze Dried Extract from Olive Leaves: Valorisation, Extraction Kinetics and Extract Characterization. *Food Bioprod. Process.* **2020**, *124*, 196–207. [CrossRef]
29. Ghomari, O.; Sounni, F.; Massaoudi, Y.; Ghanam, J.; Drissi Kaitouni, L.B.; Merzouki, M.; Benlemlih, M. Phenolic Profile (HPLC-UV) of Olive Leaves According to Extraction Procedure and Assessment of Antibacterial Activity. *Biotechnol. Rep.* **2019**, *23*, e00347. [CrossRef]
30. Rahmanian, N.; Jafari, S.M.; Wani, T.A. Bioactive Profile, Dehydration, Extraction and Application of the Bioactive Components of Olive Leaves. *Trends Food Sci. Technol.* **2015**, *42*, 150–172. [CrossRef]
31. Taamalli, A.; Arráez-Román, D.; Barrajón-Catalán, E.; Ruiz-Torres, V.; Pérez-Sánchez, A.; Herrero, M.; Ibañez, E.; Micol, V.; Zarrouk, M.; Segura-Carretero, A.; et al. Use of Advanced Techniques for the Extraction of Phenolic Compounds from Tunisian Olive Leaves: Phenolic Composition and Cytotoxicity against Human Breast Cancer Cells. *Food Chem. Toxicol.* **2012**, *50*, 1817–1825. [CrossRef]
32. Naviglio, D. Naviglio's Principle and Presentation of an Innovative Solid-Liquid Extraction Technology: Extractor Naviglio®. *Anal. Lett.* **2003**, *36*, 1647–1659. [CrossRef]
33. Dewanto, V.; Xianzhong, W.; Adom, K.K.; Liu, R.H. Thermal Processing Enhances the Nutritional Value of Tomatoes by Increasing Total Antioxidant Activity. *J. Agric. Food Chem.* **2002**, *50*, 3010–3014. [CrossRef]
34. Giosafatto, C.V.L.; Al-Asmar, A.; D'Angelo, A.; Roviello, V.; Esposito, M.; Mariniello, L. Preparation and Characterization of Bioplastics from Grass Pea Flour Cast in the Presence of Microbial Transglutaminase. *Coatings* **2018**, *8*, 435. [CrossRef]
35. Gaglione, R.; Cesaro, A.; Olmo, E.D.; Di Girolamo, R.; Tartaglione, L.; Pizzo, E.; Arciello, A. Cryptides Identified in Human Apolipoprotein B as New Weapons to Fight Antibiotic Resistance in Cystic Fibrosis Disease. *Int. J. Mol. Sci.* **2020**, *21*, 2049. [CrossRef]
36. Abdalrazeq, M.; Jaradat, N.; Qadi, M.; Giosafatto, C.V.L.; Dell'olmo, E.; Gaglione, R.; Arciello, A.; Porta, R. Physicochemical and Antimicrobial Properties of Whey Protein-Based Films Functionalized with Palestinian Satureja Capitata Essential Oil. *Coatings* **2021**, *11*, 1364. [CrossRef]
37. Pizarro, M.L.; Becerra, M.; Sayago, A.; Beltrán, M.; Beltrán, R. Comparison of Different Extraction Methods to Determine Phenolic Compounds in Virgin Olive Oil. *Food Anal. Methods* **2013**, *6*, 123–132. [CrossRef]
38. Gimeno, E.; Castellote, A.I.; Lamuela-Raventós, R.M.; De la Torre, M.C.; López-Sabater, M.C. The Effects of Harvest and Extraction Methods on the Antioxidant Content (Phenolics, alfa -Tocopherol, and beta-Carotene) in Virgin Olive Oil. *Food Chem.* **2002**, *78*, 207–211. [CrossRef]
39. Mirpoor, S.F.; Varriale, S.; Porta, R.; Naviglio, D.; Spennato, M.; Gardossi, L.; Giosafatto, C.V.L.; Pezzella, C. A Biorefinery Approach for the Conversion of Cynara Cardunculus Biomass to Active Films. *Food Hydrocoll.* **2022**, *122*, 107099. [CrossRef]
40. Porta, R.; Mariniello, L.; di Pierro, P.; Sorrentino, A.; Giosafatto, C.V.L. Transglutaminase Crosslinked Pectinand Chitosan-Based Edible Films: A Review. *Crit. Rev. Food Sci. Nutr.* **2011**, *51*, 223–238. [CrossRef]
41. Yaseen, D.; Sabbah, M.; Al-Asmar, A.; Altamimi, M.; Famiglietti, M.; Giosafatto, C.V.L.; Mariniello, L. Functionality of Films from Nigella Sativa Defatted Seed Cake Proteins Plasticized with Grape Juice: Use in Wrapping Sweet Cherries. *Coatings* **2021**, *11*, 1383. [CrossRef]
42. Pereira, A.P.; Ferreira, I.C.F.R.; Marcelino, F.; Valentão, P.; Andrade, P.B.; Seabra, R.; Estevinho, L.; Bento, A.; Pereira, J.A. Phenolic Compounds and Antimicrobial Activity of Olive (*Olea Europaea* L. *Cv.* Cobrançosa) Leaves. *Molecules* **2007**, *12*, 1153–1162. [CrossRef]

Other studies, reported in the appendix of this thesis demonstrated the efficiency of hydrocolloidal-based films containing antioxidant and antimicrobial compounds to improve food shelf-life when used as active packaging. In the paper *Functionality of Films from Nigella sativa Defatted Seed Cake Proteins Plasticized with Grape Juice: Use in Wrapping Sweet Cherries*, Dana Yaseen, Mohammed Sabbah, Asmaa Al-Asmar, Mohammad Altamimi, **Michela Famiglietti**, C. Valeria L. Giosafatto and Loredana Mariniello investigated the use of *Nigella sativa* defatted seed cake protein-based films, in combination with grape juice, to wrap sweet cherries.

The study revealed that the grape juice added to proteins from *Nigella sativa* positively affects the physicochemical traits of sweet cherries. Films proved to extend the shelf life of fresh sweet cherries, by delaying changes in color, titratable acidity, total soluble solids, and pH during freezing storage. Moreover, the grape juice exerts a plasticizer effect as observed for DOLE in CH-based films.

Mohammed Sabbah, Asmaa Al-Asmar; Duaa Younis, Fuad Al-Rimawi, **Michela Famiglietti** and Loredana Mariniello in the paper titled *Production and Characterization of Active Pectin Films with Olive or Guava Leaf Extract Used as Soluble Sachets for Chicken Stock Powder* successfully functionalized pectin films by incorporating Olive and Guava Leaf Extract (OLE and GLE) to produce soluble sachets to wrap chicken powder. They demonstrated that the improved antioxidant activity of the films helps to reduce the oxidation reactions of food during distribution and storage, extending its shelf-life.

3. TRANSGLUTAMINASE AS A TOOL TO RETICULATE THE PROTEIN COMPONENT OF NOVEL BIOPLASTICS

As reported previously, mTGase has been widely investigated as a reticulating agent for the protein component of hydrocolloid-based films, blended or not with polysaccharides. In this part of the thesis, argan seed proteins (APs) were demonstrated to act as mTGase substrates. Thus, engineered amylose (AM) was used to prepare APs-based composite films in the absence and the presence of the enzyme. Their characteristics were studied and published in the paper by **Famiglietti** et al. reported below and summarized in the following graphical abstract.

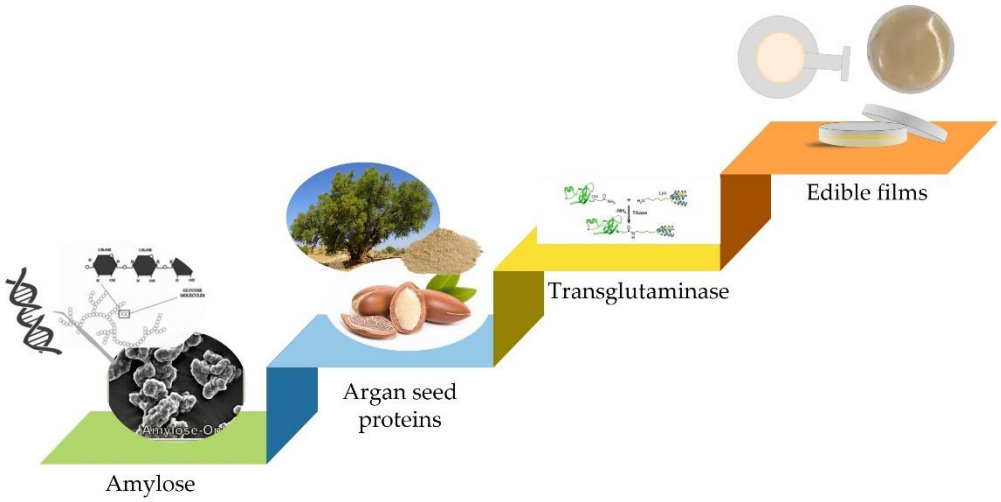

Argania spinosa is a plant widespread in arid regions of Northern Africa, where it plays a fundamental socio-ecological role. Argan seeds are used to obtain a biologically active and edible oil, producing a byproduct, the oilcake, that is rich in proteins, fibers, and fats, and is generally used as animal feed. Recently, argan oilcakes have been attracting attention as a waste to be recovered to obtain high-added-value products. In this work, APs were chosen to test the performance of blended bioplastics with AM, because they have the potential to improve the properties of the final product. High-AM-starches present attractive features for use as bioplastics, including a higher gel-forming capacity, higher thermal stability, and reduced swelling compared to normal starch. It has already been demonstrated that pure AM-based films provide more suitable properties than normal starch-based films. This study showed the performance of the novel blended bioplastics in

terms of their mechanical, barrier, and thermal properties; and the effect of the enzyme mTGase as a reticulating agent for AP's component. The obtained results contribute to the development of novel sustainable bioplastics with improved properties and confirm the possibility of valorizing the byproduct, APs, using them as a new raw material.
APs content seems to influence film elongation at break giving rise to less extensible films. In the presence of the enzyme, this property is significantly lowered, making these blended films interesting for application as bio-shoppers. The presence of APs also influences the water vapor permeability in composite films, providing a higher barrier effect which notably increases with the mTGase-induced crosslinking.

mTGase was successfully used as a reticulating agent to modify protein-based films also in the paper titled *Hemp (Cannabis sativa) seed oilcake as a promising by-product for developing protein-based films: Effect of transglutaminase-induced crosslinking* reported in the appendix of this thesis. In this work, Seyedeh Fatemeh Mirpoor, C. Valeria L. Giosafatto, Rocco Di Girolamo, **Michela Famiglietti**, and Raffaele Porta investigated protein concentrates from hemp seed oilcake as a potential waste-derived source for bioplastic production. They obtained hemp protein-based films at different protein and glycerol concentrations and different pH. Furthermore, since hemp proteins (HP) were demonstrated to act as substrates of mTGase, they have been used as raw material to obtain films after enzyme treatment. Film characterization showed that mTGase treatment was effective in producing more homogenous and smoother films, influencing positively even their resistance and their heat-sealing strength without reducing their flexibility. In addition, mTGase-induced crosslinking originated bioplastics with a higher gas permeability and a greater hydrophobicity. These results suggest the possibility of exploiting the mTGase-crosslinked hemp proteins for different applications in the bioplastic industry.

International Journal of
Molecular Sciences

MDPI

Article

Mechanical, Barrier and Thermal Properties of Amylose-Argan Proteins-Based Bioplastics in the Presence of Transglutaminase

Michela Famiglietti [1], Domenico Zannini [1,2], Rosa Turco [1,2] and Loredana Mariniello [1,3,*]

[1] Department of Chemical Sciences, Monte Sant'Angelo Campus, University of Naples "Federico II", Via Cinthia 4, 80126 Naples, Italy
[2] National Research Council, Institute of Polymers, Composites and Biomaterials, Via Campi Flegrei 34, 80078 Pozzuoli, Italy
[3] Center for Studies on Bioinspired Agro-Environmental Technology (BAT), University of Naples "Federico II", Via Cinthia 4, 80126 Naples, Italy
* Correspondence: loredana.mariniello@unina.it

Abstract: The bioeconomy aims to discover new sources for producing energy and materials and to valorize byproducts that otherwise would get wasted. In this work, we investigate the possibility of producing novel bioplastics, made up of argan seed proteins (APs), extracted from argan oilcake, and amylose (AM), obtained from barley plants through an RNA interference technique. Argan, *Argania spinosa*, is a plant widespread in arid regions of Northern Africa, where it plays a fundamental socio-ecological role. Argan seeds are used to obtain a biologically active and edible oil, producing a byproduct, the oilcake, that is rich in proteins, fibers, and fats, and is generally used as animal food. Recently, argan oilcakes have been attracting attention as a waste to be recovered to obtain high-added-value products. Here, APs were chosen to test the performance of blended bioplastics with AM, because they have the potential to improve the properties of the final product. High-AM-starches present attractive features for use as bioplastics, including a higher gel-forming capacity, a higher thermal stability, and reduced swelling compared to normal starch. It has already been demonstrated that pure AM-based films provide more suitable properties than normal starch-based films. Here, we report on the performance of these novel blended bioplastics in terms of their mechanical, barrier, and thermal properties; and the effect of the enzyme microbial transglutaminase (mTGase) as a reticulating agent for AP's components was also studied. These results contribute to the development of novel sustainable bioplastics with improved properties and confirm the possibility of valorizing the byproduct, APs, using them as a new raw material.

Keywords: amylose; argan seed proteins; transglutaminase; mechanical properties; biomaterials

check for updates

Citation: Famiglietti, M.; Zannini, D.; Turco, R.; Mariniello, L. Mechanical, Barrier and Thermal Properties of Amylose-Argan Proteins-Based Bioplastics in the Presence of Transglutaminase. *Int. J. Mol. Sci.* **2023**, *24*, 3405. https://doi.org/10.3390/ijms24043405

Academic Editors: Feng-Huei Lin and Yi Cao

Received: 30 November 2022
Revised: 23 January 2023
Accepted: 6 February 2023
Published: 8 February 2023

Copyright: © 2023 by the authors. Licensee MDPI, Basel, Switzerland. This article is an open access article distributed under the terms and conditions of the Creative Commons Attribution (CC BY) license (https://creativecommons.org/licenses/by/4.0/).

1. Introduction

One of today's most crucial environmental challenges is solving plastic pollution. With a compound annual growth rate (CAGR) of 8.4%, since the 1950s plastic production has been increasing faster than any other class of manufactured materials [1]. It is estimated that plastic synthesis is going to require half of the global oil demand by 2050, with emissions of over 56 billion Mt of carbon dioxide equivalent (CO_{2e}), around 10–13% of the remaining carbon budget [2]. Plastics are derived from fossil fuels, and each stage of their life, from extraction up to their end-of-life, produces emissions of greenhouse gases (GHGs). Moreover, their molecular structures exhibit strong resistance to environmental degradation, producing materials that persist for decades or longer if not destroyed by incineration [3]. Some of the strategies to reduce the global carbon footprint of plastics are replacing fossil fuel-based plastics with biobased plastics, increasing their recycling rate, and reducing their growth in demand [4]. Biobased plastics are derived from renewable plant feedstocks, and in their overall life cycle produce lower GHG emissions than conventional plastics [5]. However, this is dependent on their composition, their end-of-life management, and the

carbon storage potential lost because of the lands needed to cultivate the biomass, with damage to biodiversity and a loss of soil dedicated to food production [4]. Other challenges to be overcome are their poor performances, variability of feedstock properties, and high production costs [6].

Starch is one of the most attractive biopolymers to produce bioplastics because of its abundance (it is the predominant carbohydrate reserve in plants), cheapness, and its well-defined chemical features [7]. Starch consists of two glucose-based polymers, amylose (AM) and amylopectin. In the native starch granule, AM is mainly amorphous and comprises predominantly linear chains of α-1,4-linked glucose residues, with a molecular weight (M_w) of 10^5 g/mol, whereas amylopectin exists as a semicrystalline highly branched α-1,4: α-1,6 glucan polymer with a M_w of 10^6–10^7 g/mol [8]. Normally, starch is made up of about 20–30% AM and 70–80% amylopectin, but the AM content varies from less than 5% in waxy starches up to 70% in high-AM starches [9,10]. The amylopectin molecule contains regions with low and high levels of branching. In the highly branched regions, side-chain branches intertwine to form double helices, whose association gives rise to the crystalline zones. Three types of crystalline structure have been identified as A-type, B-type, and C-type, with the latter consisting of a mixture of A and B types. In native starch, AM is mainly amorphous, but if starch granules are subjected to gelatinization in aqueous media, the AM adopts a single left-handed helical conformation, called Vh-type, with a pitch of 8 Å, where ligands like hydrophobic molecules or hydrophobic side chains of molecules can arrange. AM-lipid complexes can be endogenously present in starch or formed after gelatinization in the presence of added lipids, as during starch-processing techniques [11].

The structure of starch granules present an amorphous bulk core area surrounded by concentric semicrystalline growth rings alternating with amorphous growth rings. Starch granules can be examined on at least five levels of structure. At the largest scale are the intact granules, with sizes from 1 to 100 μm. Next come the alternating semicrystalline and amorphous growth rings. Then come the block structural elements that are made up of the left-handed superhelices, and finally there are the structural elements of superhelices that are crystalline and amorphous lamellae [12]. During high-temperature processing, starch granules undergo structural changes that determine some functional properties such as water uptake, swelling of the granule, formation of a viscoelastic paste, reassociation of starch chains, and formation of a gel. When starch is heated in water, the granules become hydrated and swollen, transforming into a paste. This is caused by the breaking of hydrogen bonds and the unwinding of the double helix, resulting in the final collapse of the granule. During the cooling, starch chains go to meet a phenomenon called retrogradation, in which they return to a partially ordered structure that, nevertheless, differs from the original structure. This induces some further physical changes in viscosity, gel formation, and degree of crystallinity. Starch retrogradation occurs because of intermolecular hydrogen-bond formation between residues of AM molecules and residues of sidechains of amylopectin molecules, and between different molecules of amylopectin. This process of reassociation and recrystallization can vary for different types of starch because it depends on the AM and amylopectin contents. For bioplastic purposes, these phenomena have a crucial relevance: the formation of crystallites affects the mechanical properties, causing a decrease of elongation at break and an increase in tensile strength. The films become stiffer, less flexible, and more difficult to handle [12]. Even if AM retrogradation was found to be a fast event relative to amylopectin retrogradation, it is worth noting that AM chains longer than approximately 1000 glucose units form a gel consisting of crosslinked AM chains [13]. Thus, high AM starches present interesting features for bioplastics production, including a high gel-forming capacity, enhanced mechanical properties, a high thermal stability, and reduced swelling. These improvements are attributed to the entanglement of long linear AM chains and the partial retention of granular structures, which act as self-reinforcement [14].

Thus, modifying the ratio of AM/amylopectin leads to changes in functionalities of the starch. Until now the separation of AM from amylopectin has not been performed on a

significant production scale because of the high process cost. Innovative systems to provide added-value functionalities directly in the crop, also known as molecular farming, can be used to improve the yields and reduce the costs of production [7]. Classical breeding, random mutagenesis, and site-directed mutagenesis technology have already provided many important special starch qualities [15]. The present work utilizes AM derived from a transgenic barley line that synthesizes starch with 99% of AM. This line was obtained by the RNA interference technique, silencing genes coding for starch branching enzymes (SBE I, SBE IIa, and SBE IIb) [16]. AM derived from this crop line has already been used to produce biomaterials: Sagnelli et al. tested a crosslinked AM in the presence of glycerol, and Xu et al. verified the performance of an AM blended with cellulose nanofibers using glycerol as a plasticizer [13,15].

The aim of this work is to contribute to overcoming the challenges to new biobased plastics in terms of the performance of materials, the cost of feedstocks, and the sustainability of the entire process of production. The choice to develop a blended biomaterial derives from the effort to reduce the cost of production, avoid the loss of carbon storage potential, utilize an inexpensive byproduct as a resource that otherwise would be destined for disposal, and improve the bioplastic properties. Recent research has focused on the recovery of waste material from oil seed processing of plants such as hemp, cardoon, cottonseed, sunflower, and argan [17–19]. These crops are grown all over the world, mainly for oil extraction, which produces a waste around 50% of the original seed weight. This byproduct, called oil seed cake, is made up of a high percentage of proteins besides fibers, remaining fats, and different bioactive compounds, such as antioxidants, vitamins, and minerals [20].

Argan, *Argania spinosa,* is an endemic species of Morocco and the southwest Algeria region belonging to the *Sapotaceae* family [20]. It can be cultivated in arid and semi-arid regions and protects soils from desertification, erosion, and sand encroachment thanks to its long and deep roots; its wood is used as fuel by the local population and its leaves are usually exploited as forage [21]. Argan fruits are a source of biologically active and edible oil that finds applications in cosmetic and pharmaceutical products or is consumed as food. It is rich in monounsaturated and polyunsaturated fatty acids, and in minor compounds such as tocopherols, polyphenols, and carotenoids [22]. The byproduct derived from the argan oil extraction process, referred to as argan press cake (APC), has traditionally been used for animal feeding because of its high levels of dry matter, that includes proteins (48.4%). APC is also rich in fibers (17.6%) and fats (18.9%), and contains significant levels of calcium, potassium, and phosphorous [23]. Recently, Mirpoor et al. used argan seed proteins (APs) derived from APC to produce protein-based bioplastics by the casting method and using glycerol as a plasticizer. They showed satisfying mechanical, barrier, and hydrophilicity features, and they were successfully tested as wound dressings [19]. Here, APs were chosen to test the performance of a blended bioplastic with AM, because they represent a waste to be recovered, that does not subtract soil from food cultivations, and that has the potential to improve the properties of the final product. Moreover, it was demonstrated that APs act as a substrate in microbial transglutaminase (mTGase, E.C.2.3.2.13)-mediated polymerization. In recent years, the use of enzymes as a biotechnological tool for strengthening the film polymer matrix has increased [24]. Using chemical crosslinking reagents is becoming less acceptable because of their potential harmfulness and toxicity, especially in the production of edible films. The use of mTGase has been proposed for its capability to catalyze intra and/or intermolecular isopeptide bonds between the γ-carboxamide group of glutamine (acyl donor) and the ε-amino group of lysine residues (acyl acceptor). Proteins modified with mTGase showed changes in their functional characteristics, influencing the properties of film matrices [25].

2. Results and Discussion

2.1. Transglutaminase Assay

The use of mTGase has been proposed for its capability to act as a biotechnological tool for strengthening the film polymer matrix, catalyzing intra and/or intermolecular isopeptide bonds between the γ-carboxamide group of glutamine residues (acyl-donor) and the ε-amino group of lysine residues (acyl-acceptor).

To verify the effect of mTGase on APs in the presence of AM, the SDS-PAGE profile following protein incubation with mTGase (40 U/g) was carried out. Figure 1 shows that APs act as both acyl donor and acyl acceptor substrates of the enzyme. APs samples incubated in the absence of mTGase exhibited three main bands and two less intense bands (Figure 1 (1,2)). A decrease in the intensity of the low molecular protein bands and the formation of high molecular weight polymers (Figure 1 (3,4)), that are not able to enter the stacking gel and appear at the entrance of the wells, demonstrate the effect of the enzyme.

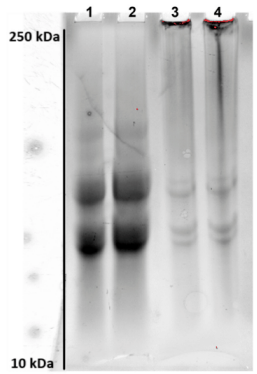

Figure 1. SDS-PAGE analysis of APs mixed with AM (50% (*w/w*) APs and 50% (*w/w*) AM) incubated for 2 h in the absence (1–2: 30 and 60 µg of the sample, respectively), or the presence of mTGase (40 U/g) (3–4: 30 and 60 µg of the sample, respectively).

2.2. Two-Dimensional Polyacrylamide Gel Electrophoresis (2-D PAGE)

The APs analysis was carried out using 2-D PAGE in the absence and presence of mTGase (40 U/g). As shown in Figure 2 panel A, four main groups were observed in the absence of the enzyme with pI nearby neutral or alkaline values and Mw in the range 15–75 kDa. The effect of the enzyme is evident in panel B, since the intensity of spots has decreased for all the groups identified, confirming the role of APs as a substrate for mTGase. APs subjected to the crosslinking reaction present a higher Mw, that does not allow them to penetrate the gel: a less severe spot is visible to the interface of the wells.

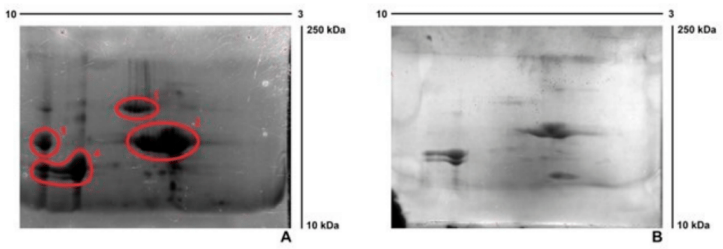

Figure 2. 2D-PAGE of APs: samples were separated using IPG strips (3–10). (**A**) in the absence of mTGase. (**B**) in the presence of mTGase (40 U/g).

2.3. Zeta Potential Analysis of Film Forming Solutions (FFSs) Prepared Blending AM and APs in the Absence and the Presence of mTGase

Different FFSs were prepared, with different ratios APs-AM (0/100–15/85–30/70–50/50–100/0% (*w/w*)), and their stability was investigated using the Zeta Potential analysis (Table 1). The first sample (containing 100% AM) exhibits a Zeta Potential value of -10.85 ± 1.39 mV, indicating a low stability of FFSs. This result can be explained by taking into account that, during the experiment, the sample goes through a recrystallization process due to FFSs cooling. At 50 °C (our casting T) water evaporates quickly, promoting hydrogen bond formation among AM chains, which results in a well-structured matrix. Increased Zeta Potential values can be observed in all the other samples, increasing the protein content because the presence of proteins influences the interactions among AM chains, preferring interactions between proteins and AM. Lower values of Zeta Potential in the presence of the enzyme could be due to increased interparticle interactions (Van der Waals, hydrophobic interactions together with hydrogen bonding) among proteins modified using the enzyme.

Table 1. Zeta Potential analysis of FFSs at different ratios APs-AM (0–100, 15–85, 30–70, 50–50, 100–0% (*w/w*)). Different small letters (a–d) indicate significant differences among the values reported in the columns ($p < 0.05$). The analysis was carried out in triplicate.

APs-AM Ratio	Zeta Potential (mV)	APs-AM Ratio–mTGase	Zeta Potential (mV)
0–100	-10.85 ± 1.39^{a}	-	-
15–85	-37.60 ± 0.45^{b}	15–85	-37.58 ± 1.17^{b}
30–70	-46.20 ± 1.20^{d}	30–70	-39.32 ± 0.64^{b}
50–50	$-46.24 \pm 1.28^{c,d}$	50–50	-42.80 ± 0.71^{c}
100–0	-52.87 ± 1.033^{d}	100–0	-43.23 ± 1.65^{c}

2.4. Opacity, Density, Thickness, and Morphology

Values of opacity, density, and thickness of the films with an increasing amount of Aps, incubated in the absence and the presence of mTGase, are shown in Table 2. The optical properties are crucial to developing products, such as for food packaging, able to attract the interest of consumers. As reported, AM100-based films possess an opacity value of 1.84 ± 0.34 A_{600nm}/mm, similar to the commercial petrol-based plastic LDPE (low-density polyethylene) (opacity value = 1.44 ± 0.04 A_{600nm}/mm) [19]. The addition of APs notably increases the opacity of the films already, with a content of 15% (*w/w*). The film color becomes darker proportionally with the increase of APs content (Figure 3). It reaches the highest value, for APs100-based films, of 5.55 ± 0.18 A_{600nm}/mm that, nevertheless, is lower than the opacity value of commercial MaterBi® (61.92 ± 3.55 A_{600nm}/mm) [19]. The presence of mTGase reduces film opacity: probably, crosslinking reactions induce the formation of a more ordered structure of film matrices, increasing light transmission and changing the refractive index. Indeed, the opacity value was significantly lower in APs100-based films treated with mTGase (4.79 ± 0.04) than in APs100-based films cast without the enzyme, even if the latter were significantly thicker than the first. Thickness increases with the increasing of APs content, and further in the presence of mTGase when the amount of APs reaches 50% (*w/w*). Density values are not significantly different among the samples treated or not with the enzyme.

Table 2. Opacity, density, and thickness of films prepared at different ratios APs-AM treated or not with mTGase (40 U/g). Different small letters (a–h) indicate significant differences among the values reported in the columns ($p < 0.05$). Analyses of opacity and density were carried out in triplicate. Thickness values are reported as the average of five values.

APs-AM Ratio	Opacity (A_{600nm}/mm)	Density (g/cm^3)	Thickness (μm)
0–100	1.84 ± 0.34 ^{a}	1.15 ± 0.002 ^{a}	102.6 ± 5.86 ^{a}
15–85	3.87 ± 0.02 ^{d}	1.17 ± 0.05 ^{a}	111.8 ± 7.01 ^{a,b}
30–70	4.45 ± 0.09 ^{e}	1.18 ± 0.09 ^{a}	115 ± 16.4 ^{a,b}
50–50	5.28 ± 0.16 ^{g}	1.20 ± 0.10 ^{a}	125.6 ± 12.05 ^{b}
100–0	5.55 ± 0.18 ^{h}	1.25 ± 0.04 ^{a}	189.4 ± 25.2 ^{d}
APs-AM Ratio—mTGase	**Opacity (A_{600nm}/mm)**	**Density (g/cm^3)**	**Thickness (μm)**
15–85	2.86 ± 0.11 ^{b}	1.17 ± 0.02 ^{a}	114.4 ± 5.98 ^{a,b}
30–70	3.04 ± 0.07 ^{b}	1.20 ± 0.17 ^{a}	117.5 ± 12.23 ^{a,b}
50–50	3.57 ± 0.01 ^{c}	1.24 ± 0.14 ^{a}	149.4 ± 1.34 ^{c}
100–0	4.79 ± 0.04 ^{f}	1.29 ± 0.02 ^{a}	225.6 ± 22.34 ^{e}

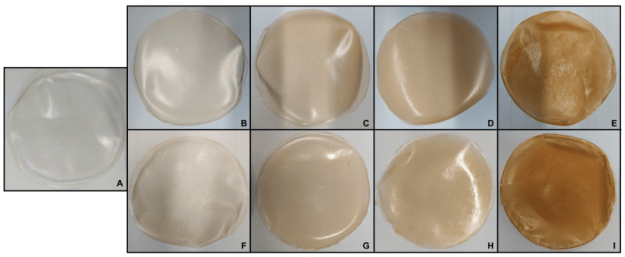

Figure 3. Film obtained with different ratios of APs-AM and incubated in the absence or the presence of mTGase: APs-AM(0–100) (**A**), APs-AM(15–85) in the absence of mTGase (**B**), APs-AM(15–85) in the presence of mTGase (**F**), APs-AM(30–70) in the absence of mTGase (**C**), APs-AM(30–70) in the presence of mTGase (**G**), APs-AM(50–50) in the absence of mTGase (**D**), APs-AM(50–50) in the presence of mTGase (**H**), APs-AM(100–0) in the absence of mTGase (**E**), APs-AM(100–0) in the presence of mTGase (**I**).

Film microstructure was determined by SEM-analysis: film surface and cross-section images are reported in Figure 4. The microstructure of the films depends on the interactions among the films' components that directly affect their physical, mechanical, and barrier properties. SEM surface analysis of AM100-based films, blended films (APs50-AM50), and APs100-based films, incubated in the absence and the presence of mTGase, showed that the topography changed significantly. The AM100-based film surface was smooth (Figure 4A), compared to the surface of a pure AM-based film prepared by Xu et al., in the absence of glycerol, which showed pleated structures [13]. The plasticizer used to prepare the AM-based films, creating new hydrogen bonds, filled the free volume among the polysaccharide molecules making the surface homogenous. The blended films showed a less smooth and less homogeneous surface, probably due to the presence of the oil fraction in APs, as reported also by Mirpoor et al. [19], both in the presence and absence of mTGase (Figure 4B,C). The cross-sections of blended films (Figure 4B,C) showed irregularities and cracks that visibly increased in APs100-based films (Figure 4D,E). Formation of a phase separate from the aqueous phase resulted in oil droplets after drying that made the surface heterogeneous and discontinuous, both for films treated or not with the enzyme (Figure 4D,E).

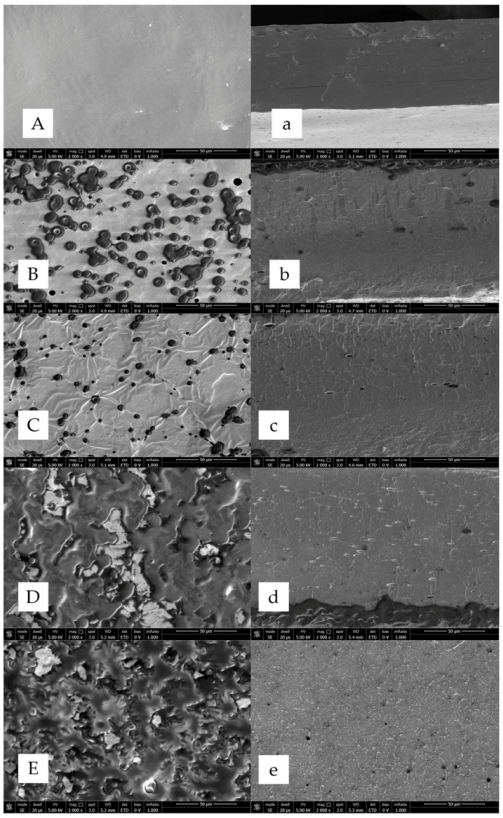

Figure 4. SEM micrographs (surface in uppercase and cross-section in lowercase) of AM100-based films (**A**,**a**), blended films (APs50-AM50) in the absence (**B**,**b**) and the presence of mTGase (**C**,**c**), APs100-based films in the absence (**D**,**d**) and the presence of mTGase (**E**,**e**). SEM analyses were performed at a magnification of 2000×. Further experimental details are given in the text.

2.5. Film Mechanical Properties

As already reported, AM can improve film performance in terms of mechanical properties, relative to normal starch, because it influences the degree of crystallinity and the entanglement of AM chains [13,15]. This results in an increase in the Tensile Strength (TS) and a decrease in the Elongation at Break (EB). This latter direct effect can be overcome using a plasticizer such as glycerol [14].

In this work, the same content of glycerol was used for all the produced films. AM100-based films show the highest EB (~70%), with respect to both blended films and APs100-based films, a value of TS similar to APs100-based films (~4.6 and ~5 MPa respectively) and higher than blended films, and a value of Young's Modulus (YM) lower than APs100-based films (~100 MPa and ~310 MPa respectively) and similar to blended films. As reported in Figure 5, AM100-based films show preferable mechanical characteristics since they are extensible, not stiff, and at the same time resistant. Blended films exhibit a TS value lower than both AM100-based films and APs100-based films, an EB value lower than AM100-based films but higher than APs100-based films, and a YM value lower than APs100-based

films and similar to that of AM100-based films. The AM component seems to keep the extensibility and the lower stiffness in blended films, but the entanglement of AM chains is probably interrupted by the presence of Aps, resulting in reduced values of TS, EB, and YM with respect to the AM100-based films. The presence of mTGase reduces the TS and the YM of APs100-based films, increasing their EB, this effect has already been noted for other protein-based films modified by mTGase [26].

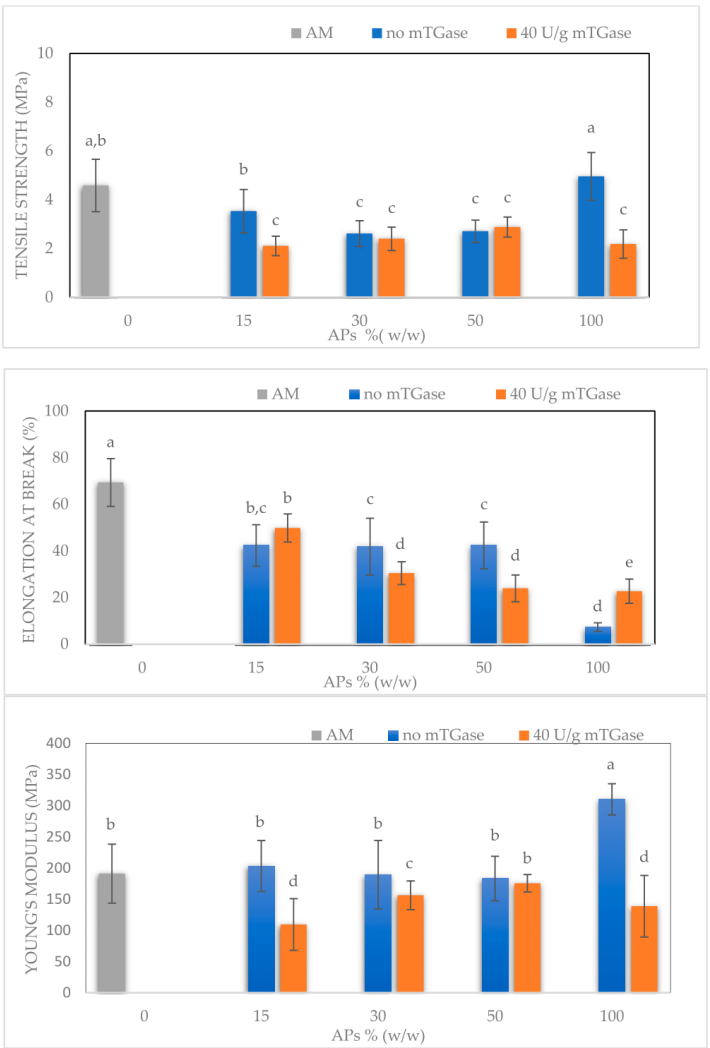

Figure 5. Mechanical properties of films containing 50% (*w*/*w*) glycerol, prepared at different ratios of APs-AM and treated or not by mTGase (40 U/g). Different small letters (a–d) indicate significant differences among the values reported in each bar ($p < 0.05$). For each sample six specimens were evaluated.

2.6. Moisture Content, Water Solubility, Swelling Ratio

Figure 6 shows further results for the moisture content, water solubility, and swelling ratio of AM100-based films, APs100-based films in the absence and presence of mTGase, and blended films (APs50-AM50) treated or not with the enzyme. The moisture content of the AM100-based films was significantly higher than the blended films and the APs100-based films, as confirmed also by FT-IR analysis, by which the presence of free water molecules is detected. Moreover, the moisture content slightly decreases in the presence of mTGase: probably this effect is due to the reduction of the free ε-amino groups of lysine residues after the formation of the isopeptide bond catalyzed by mTGase [17]. Conversely, the film water solubility increases with the addition of APs: blended films and APs100-based films show similar water solubility values, higher than the value of AM100-based films. Similarly, the swelling ratio is higher for blended films and further increases for APs100-based films relative to AM100-based films. The entanglement of AM chains can explain this effect, because the hydroxyl groups are not available to bond with free water molecules resulting in reduced swelling ratio and solubility. In contrast, the hydrophilic nature of APs probably promotes the absorption of free water molecules, promoting the swelling of the films and making them more soluble.

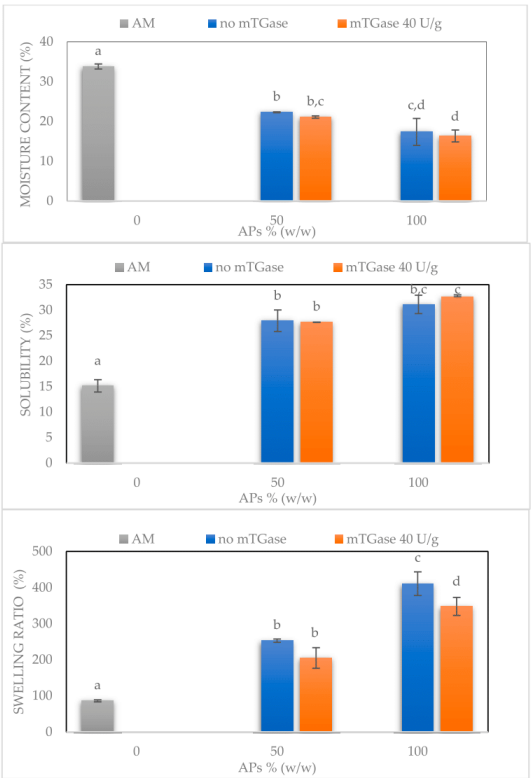

Figure 6. Moisture content, water solubility, and swelling ratio of AM100-based films, blended films (APs50-AM50) in the absence and the presence of mTGase, and APs100-based films treated or not by the enzyme. Different small letters (a–d) indicate significant differences among the values reported in each bar ($p < 0.05$). The analysis was carried out in triplicate.

2.7. Water Vapor Permeability (WVP) and CO_2 Permeability (CO_2P)

Water vapor and CO_2 permeabilities were investigated because of their crucial importance for film applications such as food packaging (Table 3). Film barrier properties influence the shelf life of food products and can improve food quality during storage.

Table 3. Water vapor permeability and CO_2 permeability of films with different ratios of APs-AM treated or not with mTGase. Different small letters (a–d) indicate significant differences among the values reported in each column ($p < 0.05$). The analysis was carried out in duplicate.

APs-AM Ratio	WVP ($g*mm*m^{-2}*d^{-1}*kPa^{-1}$)	CO_2P ($cm^3*mm*m^{-2}*d^{-1}*kPa^{-1}$)
0–100	8.68 ± 0.36^{a}	0.42 ± 0.04^{a}
15–85	6.16 ± 0.10^{b}	0.42 ± 0.06^{a}
30–70	3.56 ± 0.57^{c}	$0.25 \pm 0.02^{a,b,c}$
50–50	3.27 ± 0.31^{c}	$0.24 \pm 0.06^{a,b}$
100–0	2.89 ± 0.13^{c}	$0.30 \pm 0.09^{a,b,c}$
APs-AM Ratio—mTGase	**WVP ($g*mm*m^{-2}*d^{-1}*kPa^{-1}$)**	**CO_2P ($cm^3*mm*m^{-2}*d^{-1}*kPa^{-1}$)**
15–85	3.010 ± 0.03^{c}	$0.35 \pm 0.02^{a,b}$
30–70	2.74 ± 0.42^{c}	0.12 ± 0.02^{c}
50–50	$2.35 \pm 0.97^{c,d}$	0.16 ± 0.04^{c}
100–0	1.87 ± 0.28^{d}	0.45 ± 0.07^{a}

To evaluate the permeability function of hydrocolloid-based films, some parameters have to be taken into account: thickness, crystallinity, porosity, plasticizer content, and water activity. Usually, plasticized-starch-based films show poor water vapor barrier properties because of their hydrophilic nature. Here, AM100-based films showed a WVP of 8.7 g mm/m^2 d kPa, similar to that exhibited by high-AM-based films reported by Colussi et al. [27] and by the commercial starch-based bioplastics Mater Bi (9.8 g mm/m^2 d kPa) [17]. Addition of APs reduced proportionally the WVP, probably because of the decreasing of the mass transfer rate through the film of water vapor molecules that bind the hydrophilic groups of APs, as demonstrated using the investigation of the swelling ratio. Nevertheless, the WVP value for APs100-based films is still far from that exhibited by commercial conventional plastics such as LDPE (0.075 g mm/m^2 d kPa). The effect of mTGase confirmed the results already reported in different papers regarding the improved film barrier capability, probably due to the decrease of the available free polar groups of APs following the formation of isopeptide bonds catalyzed by the enzyme [17].

AM100-based films show stronger CO_2 barrier capability, equal to 0.42 ± 0.04 $cm^3*mm*m^{-2}*d^{-1}*kPa^{-1}$, than the commercialized bioplastics MaterBi® and LDPE (5.19 ± 0.60 and 13.99 ± 1.08 $cm^3*mm*m^{-2}*d^{-1}*kPa^{-1}$, respectively). Furthermore, blended films exhibit improved barrier capability relative to both AM100-based films and APs100-based films. In the presence of mTGase, this effect seems to be conserved: blended films show a lower value of CO_2 permeability than pure films of AM and APs treated by the enzyme.

2.8. Fourier Transform Infrared Spectra (FT-IR)

The AM100-based film's spectrum (Figure 7) shows a wide absorption band at 3000–3600 cm^{-1}, attributed to the stretching vibration of O-H bonds, which are the dominant functional group and are involved in intra- and inter-molecular hydrogen bonds with other hydroxyl groups [28]. The peak at 3272 cm^{-1} is due to the strong hydrogen bond formation between the hydroxyl groups in the AM chains and the hydroxyl groups in the glycerol molecules. This new and strong hydrogen bond formation between AM and glycerol replaces the original interactions in the AM chains, shifting to lower wavenumbers compared to the peak detected for AM in the absence of glycerol, as reported in Muscat D. et al. [28]. The AM100-based film's spectrum exhibited a peak at 1647 cm^{-1}

corresponding to the presence of free water molecules (water molecule bending) [29]. The peak at 1337 cm^{-1} in the AM100-based film's spectrum is associated with the O-H bending of primary or secondary alcohols [28]. Finally, the area between 1200 and 950 cm^{-1} is the fingerprinting region: peaks at 920, 996, and 1075 cm^{-1} are associated with the C-O stretching in the anhydro-glucose ring, while a peak at 1149 cm^{-1} is assigned to C-O-C asymmetric bending [30,31]. The characteristic C-C and C-O vibration bands of glycerol, normally occurring in the range 850–1100 cm^{-1}, are probably overlapped by signals of AM and APs, and not easily detected, as reported also by Simona J. et al. [30].

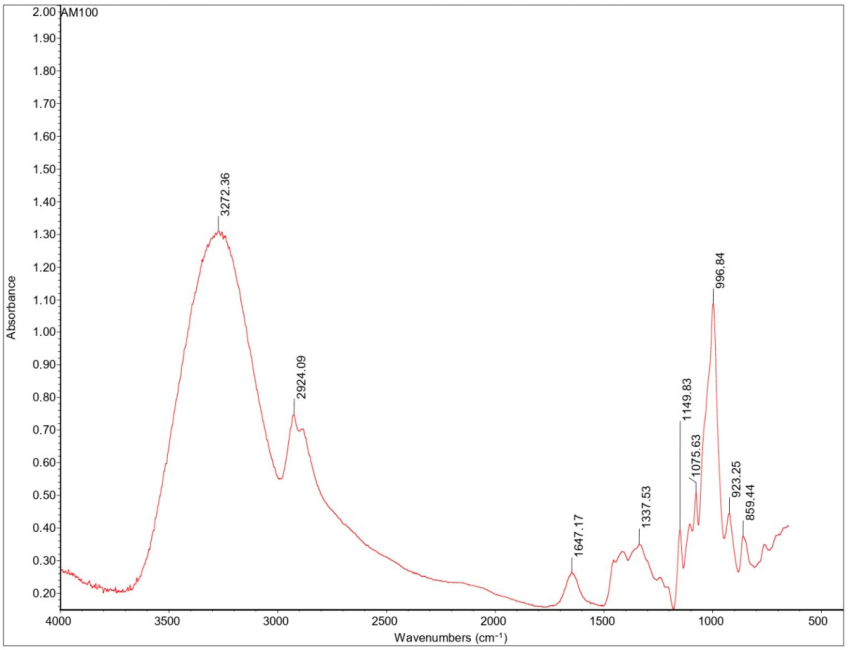

Figure 7. FT-IR spectra of AM100-based films.

The broad band 3600–3000 cm^{-1} peak for the APs100-based film in the presence or absence of mTGase (Figure 8) was attributed to stretching vibrations of –OH and –NH groups, but its intensity decreases as compared to the AM100-based film's spectrum because of the lower presence of -OH groups. Asymmetric and symmetric stretches of CH_2 groups were identified around 2920 and 2850 cm^{-1}. These peaks are related to the fats present in APs: in fact, because of the oil remaining in the argan oilcake, this area of the spectrum is higher in absorbance in APs100-based films. The sharp peak at 2924 cm^{-1} was observed also in AM100-based films, followed by a shoulder peak at around 2850 cm^{-1} due to the presence of lipids/AM complexes [15].

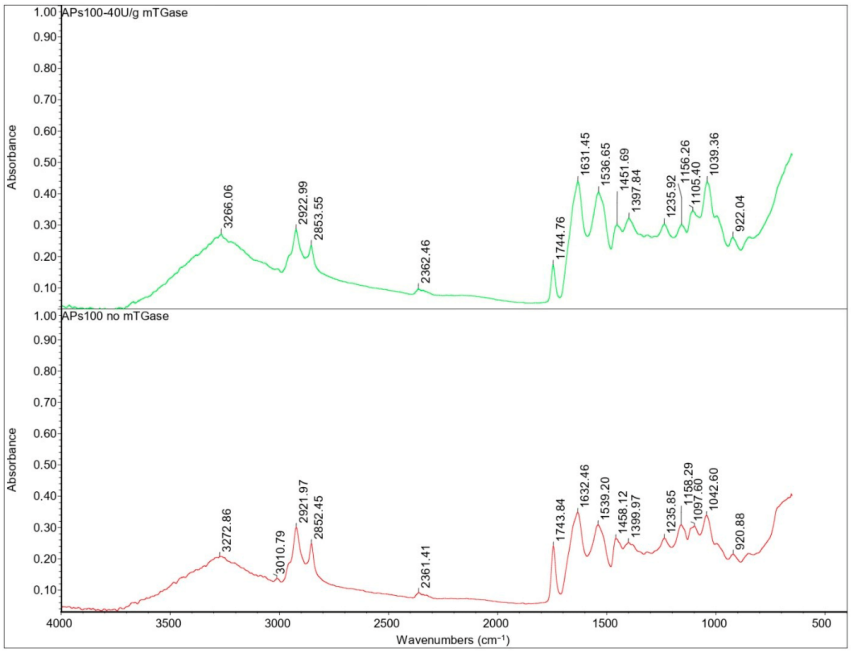

Figure 8. FT-IR spectra of APs100-based films in the presence and the absence of mTGase.

The peak at 1745 cm^{-1} is attributed to the stretching vibration of ester carbonyl C=O functional groups of the triglycerides present in APs. The area of the spectrum between 1480–1200 cm^{-1} is the fingerprint area of proteins, which was attributed to single bond (C-H and N-H) vibration and tautomerism of the amide structure [32].

The absorption bands at 1630 and 1540 cm^{-1} represent amides I and II, respectively. The presence of a peptide bond is usually indicated by a C-O vibration at the amide I band (1700–1600 cm^{-1}) and N-H bending vibration and C-N stretching vibration at the amide II band (1600–1500 cm^{-1}). Generally, the amide I band indicates the secondary structure of the protein, in particular, absorption at 1610–1640 cm^{-1} can be assigned to the β-sheet, while the amide II band represents the environment for hydrogen bonding [33].

Despite the presence of AM, in the blended film spectra there was no significant shift in the absorption peaks of the amides I and II (Figure 9). This shows that the addition of AM had no significant influence on the secondary structure of the proteins, as reported also by Xu X. et al. [31]. The blended film's spectrum shows the characteristic peaks of AM and APs without significant shifts, indicating that interactions, if any, cannot be detected this way.

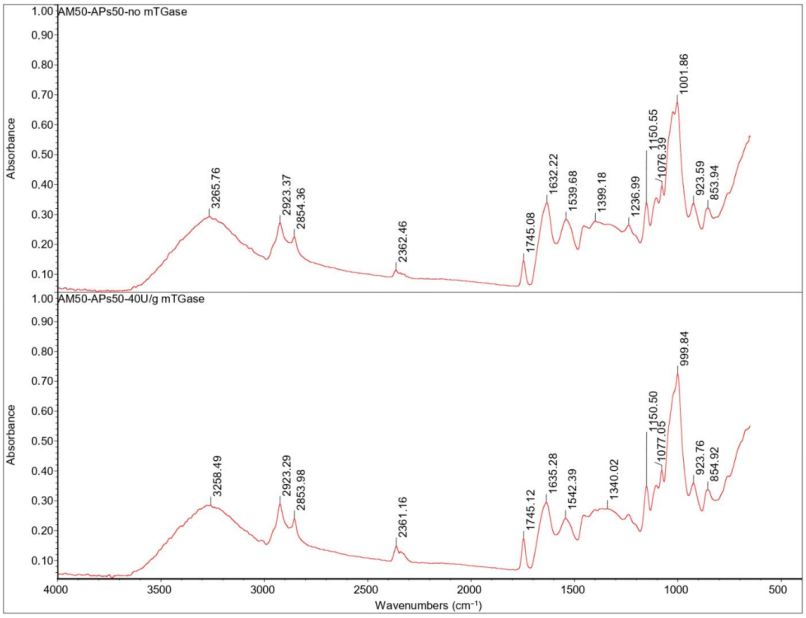

Figure 9. FT-IR spectra of blended films (APs50-AM50) in the absence and presence of mTGase.

In the same way, mTGase does not seem to cause changes in the structure of the proteins detectable by FT-IR analysis.

2.9. Thermogravimetric Analysis (TGA)

The TGA and the differential thermogravimetric (DTG) curves obtained are reported in Figure 10. All the curves were normalized with respect to the starting sample size. From the AM100-based film's thermogram three different regions of weight loss can be detected (Figure 10a). In the first one, from 30 °C up to 100 °C, the sample lost about 10–15% of its weight, which was attributed to the free and bound water molecules in the films. The second mass loss process was observed in the range of 100–200 °C, which is the characteristic event of polysaccharides and is also associated with the thermal degradation of glycerol [34]. The third stage, between 300 and 350 °C, was possibly associated with the main degradation of starch crystallites containing AM/lipid complexes [35]. The DTG thermogram (Figure 10b) for APs100-based films in the absence of mTGase showed, besides the mass loss associated with the release of moisture, three main regions of weight loss. The first one, between 180 and 200 °C, was probably due to the depolymerization of low molecular weight proteins [31]. The second one, from 200 °C to 260 °C, could be due to the decomposition of hemicellulose, possibly present in APs, and the third peak, which appears as a pronounced shoulder, includes the thermal degradation of cellulose and lignin present in APs in the range between 320 and 350 °C [36]. APs100-based films treated with mTGase showed some differences: it seems that the enzyme improves the thermal stability of the protein component of APs-based films, shifting their maximum degradation temperature to ~240 °C. This value may be attributed to the crosslinked polymerization reaction catalyzed by the enzyme that results in a stiffer network with a higher thermal stability. Still, in this film sample, only a second region of weight loss can be detected (between 270 and 350 °C), which probably represents the degradation of the lignocellulose fraction in the presence of the mTGase-modified proteins [37]. Differently, blended films

(AM50-APs50) treated with mTGase showed a clear decrease in the maximum degradation temperature at around 170 °C, a value lower than the one registered in the sample prepared in the absence of the enzyme (200 °C), as reported in Figure 10b. This could be due to the polymerization reaction (isopeptide bonds) mediated by mTGase, that results in the formation of high molecular weight proteins that interrupt the entanglement of AM chains and create discontinuous domains, making films more susceptible to thermal degradation.

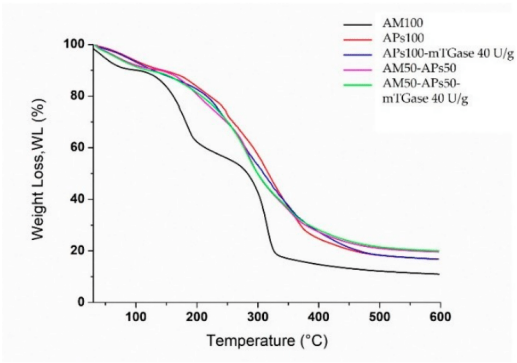

(**a**)

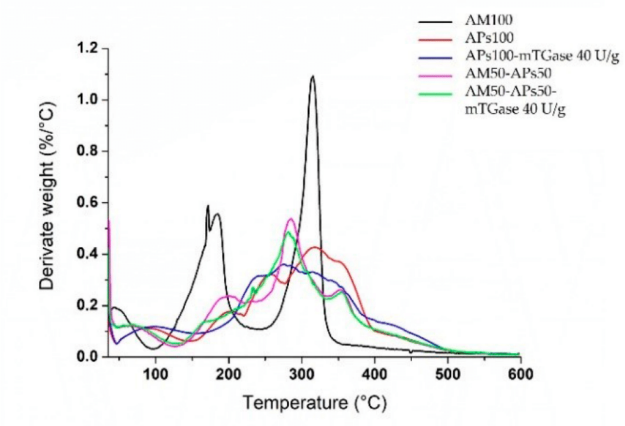

(**b**)

Figure 10. TGA (**a**) and DTG (**b**) curves of AM100-based films, blended films (APs50-AM50) treated or not by mTGase, APs100-based films in the absence and the presence of the enzyme.

For the same reason probably, in both blended films, treated or not by mTGase, the peaks related to AM were observed at lower temperatures (280–285 °C) than the AM pure single peak of AM100-based films. Moreover, the reduction of the thermal stabilities could be caused by the presence of APs oil that, as a plasticizer, increases the macromolecular mobility, encouraging AM chains' thermal degradation, as widely reported in the literature [38].

Finally, even in the blended films, it is possible to observe a clear and small peak in the range of 300–400 °C, caused by the thermal degradation of the cellulose fraction.

2.10. Differential Scanning Calorimetry (DSC)

In the DSC thermograms reported in Figure 11, only the melting temperature can be observed. There is no glass transition temperature, indicating that amylose, like starch, undergoes degradation. AM100-based films show an endothermic peak around 127 °C, which is the melting temperature of AM/lipid complexes and is slightly higher than the melting temperature of LDPE (105–123 °C) [39]. The endothermic profile of AM transition was in accordance with the one reported by Sagnelli et al. [40]. DSC results indicated a higher melting temperature for APs100 (endothermic peak at 150 °C), related to the denaturation of APs. For blended films treated with the enzyme, a second transition was found in the temperature range of 90–105 °C. This probably corresponds to the denaturation of low molecular weight proteins because, as reported in the literature, mTGase-mediated polymerization destabilizes non-covalent interactions within the proteins [41].

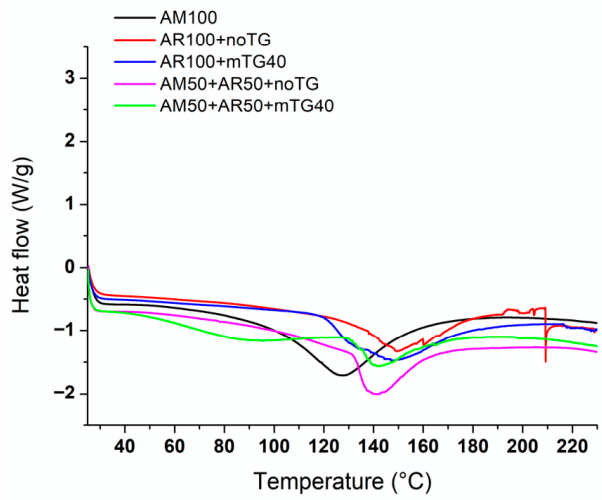

Figure 11. DSC curves of AM100-based films, blended films (APs50-AM50) in the absence and the presence of mTGase, APs100-based films treated or not by the enzyme.

3. Materials and Methods

3.1. Materials

Argan seeds were purchased from a local market in Marrakech (Morocco). AM was produced by Professor Andreas Blennow's team at the University of Copenhagen. Chemical reagents used for electrophoresis were purchased from Bio-Rad (Segrate, Milano, Italy).

mTGase (Activa) was supplied by Prodotti Gianni (Milano, Italy).

Sodium hydroxide, hydrochloric acid, and n-hexane (99%) were purchased from Sigma Aldrich Company (St. Louis, MO, USA). Glycerol and magnesium nitrate were purchased from Carlo Erba S.p.A. (Milan, Italy).

3.2. Preparation of APs Concentrate

APs were extracted according to the method described by Mirpoor et al. [19]: argan seeds were ground in a miller (Retsh GH200) for 3 min and the oil was extracted by means of the Soxhlet apparatus using n-hexane as solvent. The sample was then kept in an oven at 45 °C to let the solvent evaporate. After that 100 g of the sample was dissolved in 1 L of distilled H_2O and the pH was adjusted to 11 by NaOH 1 M, then stirring the mixture for 1 h. The supernatant was collected after centrifugation at 10,000× *g* for 30 min and the pH was adjusted to 5.4, to allow the precipitation of proteins. Centrifugation at 10,000× *g*

for 30 min followed; the pellet was collected and dried at 25 °C and 45% RH for 2 days to obtain the APs concentrate. Finally, the latter was ground in a mortar and the protein content was determined by Kijeldhal's method, using a nitrogen conversion factor of 6.25.

3.3. Transglutaminase Assay

SDS-PAGE was used to verify the action of mTGase on APs, also in the presence of AM. Film-forming solutions with the same amount of APs and AM (50% (*w/w*) APs and 50% (*w/w*) AM) were prepared, as described below, and incubated at 37 °C in the presence of 40 U/g of proteins. 50 µL of sample buffer (15.5 mM Tris-HCl, pH 6.8, 0.5% (*w/v*) SDS, 2.5% (*v/v*) glycerol, 200 mM β-mercaptoethanol and 0.003% (*w/v*) bromophenol blue) were added to the reaction mixtures at the end of the incubation. Samples containing 30 and 60 µg of proteins were heated for 5 min in a boiling water bath and analysed by SDS-PAGE (Precast SDS-PAGE gel 12% Mini-Protein gels, Bio-Rad, Segrate (MI), Italy)) at 80 mA for 2 h. Bio-Rad Precision Protein Standards were run as molecular weight markers.

3.4. Two-Dimensional Polyacrylamide Gel Electrophoresis (2-D PAGE)

2-D PAGE was used for the detection and analysis of APs. In the first dimension (IEF isoelectric-focusing PAGE), proteins were separated by the pI value, and in the second dimension (SDS-PAGE) by the relative molecular weight. IEF was carried out using 7 cm IPG strips (pH 3–10) (Bio-Rad ReadyStrip IPG) and analyzing 100 µg of APs previously dissolved in 125 µL of rehydration sample buffer (Bio-Rad ReadyPrep 2-D Starter Kit Rehydratation/Sample Buffer). The sample was loaded in an IEF cell and 2 mL of mineral oil were added to the strip to avoid evaporation during the 24 h protein separation in a Bio-Rad PROTEAN IEF CELL, with a potential difference of 50 V. Before the SDS-PAGE step, oil was removed and the strip was treated with DTT and iodoacetamide. Precast SDS-PAGE gel (12%, Mini-Protein gels, Bio-Rad, Segrate (MI), Italy) was used to carry out the SDS-PAGE at 80 mA for 40 min. The gel was finally stained with Coomassie Brilliant Blue R250 (Bio-Rad).

3.5. Preparation of FFSs

Different FFSs were prepared with different ratios of APs-AM (0/100–15/85–30/70–50/50–100/0 (%*w/w*)) using H_2O as a solvent to have a final concentration of 10 mg/mL, and glycerol as plasticizer with a concentration of 50% (*w/w*) (in respect to the total mass). AM was gelatinized by leaving it to hydrate overnight at 4 °C and then heating it in an oil bath at 140 °C for 1 h using a hydrothermal autoclave reactor. APs were solubilized in H_2O adjusting the pH to 12 with NaOH 1M and stirring the solution for 1 h. FFSs were obtained by mixing AM after gelatinization and APs after solubilization in the correct ratios.

3.6. Zeta Potential

The Zeta Potential of the FFSs prepared with different ratios of APs-AM (0/100–15/85–30/70–50/50–100/0 (%*w/w*)) were analyzed using the Zetasizer Nano-ZSP (Malvern®, Worcestershire, UK).

The Zetasizer Nano combines different techniques of light scattering to obtain a complete characterization of a colloidal system. Operating with a helium-neon laser at a fixed wavelength of 633 nm, it determines the Zeta Potential by using the Electrophoretic Light Scattering (ELS).

Three independent measurements were carried out on each sample, diluted to have a final concentration of 1 mg/mL.

3.7. Films Preparation

FFSs were poured into polypropylene Petri dishes (9 cm in diameter) and dried in an oven at 50 °C for ~28 h. After that, the films were stored in a desiccator at room temperature to balance the moisture content at ~50% RH for 4 days before the subsequent analyses. The appearance of the films is shown in Figure 3.

3.8. Film Characterization

3.8.1. Film Transparency

The opacity of the films was determined according to Jahed et al. [42]. The method involved the measurement of the absorbance of the films at a wavelength of 600 nm. Each film was cut into 1 cm × 4 cm strips, placed in a quartz cuvette, and forced to adhere to its wall, to measure the absorbance by using a UV-Vis spectrophotometer (SmartSpec 3000 Bio-Rad, Segrate, Milan, Italy). The opacity value was then obtained by calculating:

$$\text{Opacity} = A_{(600\text{nm})}/X_{(\text{mm})}$$

where $A_{(600\ \text{nm})}$ is the absorbance and $X_{(\text{mm})}$ is the film thickness, determined as the average in five spots on each specimen by means of a digital micrometer (IP65 Alpa Exacto, Alpa metrology Co., Pontoglio (BS), Italy) with a precision of 0.001 mm. Three randomly chosen specimens of each sample were examined.

3.8.2. Film Density

To determine the density (g/cm^3) of the films, each sample was cut into 2 × 2 cm^2 pieces and weighed after conditioning. The film density value was calculated according to the following equation reported by Cruz-Diaz [43]:

$$\rho = m_{(g)}/A_{(cm^2)}\ X_{(cm)}$$

where m is the dry mass of the film, A is the film area, and X is the film thickness, determined as described above. Three specimens of each sample were randomly examined.

3.8.3. Morphology

The morphology of the films was examined using field emission scanning electron microscopy (SEM) (Nova NanoSem 450-FEI-Thermo Fisher, Scientific, Waltham, MA, USA). The films were cryo-fractured in liquid nitrogen and then the samples were coated with a thin layer of Au-Pd using a vacuum sputter coater. They were finally observed at a magnification of 2000× with an accelerating voltage of 5 kV by using an ETD detector.

3.8.4. Film Mechanical Properties

The Tensile Strength, Young's Modulus, and Elongation at Break were determined by using a dynamometer (Instron universal testing instrument model no. 5543A, Instron Engineering Corp., Norwood, MA, USA) according to ASTM D882-18 (1997). Each film was cut into strips with a length of 40 mm and a width of 10 mm, and they were tested by using a 1 kN load cell with a rate of grip separation of 10 mm/min. The film thickness was determined in five spots on each specimen by means of a digital micrometer (IP65 Alpa Exacto, Alpa metrology Co., Pontoglio (BS), Italy) with a precision of 0.001 mm.

3.8.5. CO_2 and Water Vapor Permeability

Film barrier permeabilities to CO_2 and water vapor were analyzed using a MultiPerm apparatus (ExtraSolution s.r.l, Pisa, Italy) according to the Standard Methods (ASTM D3985-05, 2010; ASTM F-2476-13, 2013). Each sample is loaded within the instrument, where it constitutes a separate septum between two semi-chambers. A stream of the permeant gas is made to flow through the upper chamber and permeate through the sample, then it is picked up by the carrier gas and detected by a sensor. This process is carried out while maintaining the chamber at a fixed temperature (25 °C) and monitoring continuously the relative humidity (50%), the flow, and other variables that can alter the permeation of the sample. Aluminum masks were used to reduce the film test area to 2 cm^2, and the analyses were performed in duplicate.

3.8.6. Moisture Content and Solubility

Film moisture content and solubility were determined according to the method described by Zahedi et al., with some modifications [44]. The analysis was performed in triplicate on samples of 2 cm^2.

Each sample was initially weighed (W_i), dried at 105 °C in an oven for 24 h, and after drying weighed again (W_d). The moisture content was determined by calculating the difference between the initial and the final weight of the samples using the following equation:

$$\text{Moisture content (\%)} = [(W_i - W_d)/W_i] \times 100$$

To determine film solubility, the dried samples were then immersed in 30 mL of distilled H_2O and stirred at 25 °C for 24 h in a shaker incubator. After that, the undissolved films were carefully collected and dried in an oven at 105 °C for 24 h. The final weight (W_f) of the dried samples was measured, and the solubility value was calculated as follows:

$$\text{Water solubility (\%)} = [(W_i - W_f)/W_i] \times 100$$

3.8.7. Swelling Ratio

The swelling ratio of the films was determined by weighing the film samples (2 cm^2) (W_i) before immersing them in 30 mL of distilled H_2O at 25 °C for 1 h. The films were then collected, dried with absorbent paper, and weighed again (W_s). The film swelling ratio was calculated using the following equation as reported by Roy S. et al. [45]:

$$\text{Swelling ratio (\%)} = [(W_s - W_i)/W_i] \times 100$$

The analysis was carried out in triplicate.

3.8.8. Fourier Transform Infrared Spectra (FT-IR)

FT-IR analysis was performed at room temperature by using an FT-IR Nicolet 5700 spectrophotometer (Thermo Fisher Scientific, Waltham, MA, USA). The FT-IR spectrum of each sample was recorded in the range of 4000–500 cm^{-1} (spectral resolution of 2 cm^{-1}, 64 average scans) and processed using the Omnic software.

3.8.9. Thermogravimetric Analyses (TGA)

Thermogravimetric analyses were carried out with a Perkin-Elmer Pyris Diamond thermogravimetric analyzer (TGA/DTA), equipped with a gas station. An amount of 3–4 mg of each sample was placed in an open ceramic crucible and heated from 30 °C up to 600 °C at a rate of 10 °C/min, under nitrogen at 30 mL/min.

3.8.10. Differential Scanning Calorimetry (DSC)

The melting temperature of the samples was determined by Differential Scanning Calorimetry (DSC) using a Q2000 T zero DSC, TA Instrument (New Castle, DE, USA), equipped with a liquid nitrogen accessory for fast cooling. The calorimeter was calibrated for temperature and energy using indium. Dry nitrogen was used as the purge gas. A single scan was run at 10 °C/min from 25 to 250 °C. The melting temperature was defined from the endotherm peak value.

3.9. Statistical Analysis

The SPSS19 (Version 19, SPSS Inc., Chicago, IL, USA) software was used for all statistical analyses. One-way analysis of variance (ANOVA) and Duncan's multiple range tests ($p < 0.05$) were used to determine the significant difference among the samples.

4. Conclusions

Engineered amylose (AM) was used to prepare argan protein-based (APs) composite films. Their characteristics were studied with respect to different protein concentrations

and compared to AM-based and APs-based films. The protein content seems to influence Elongation at Break giving rise to less extensible films. In the presence of the enzyme, this property is significantly lowered, making these blended films interesting for application as bio-shoppers. The presence of proteins also influences the water vapor permeability in composite films, providing a higher barrier effect which notably increases when TGase is used as a reticulating agent. Even though thermal analysis results suggest that the thermal properties are not greatly influenced by film composition, all samples analyzed show good thermal stabilities.

Author Contributions: M.F.: Investigation; Methodology; Formal analysis; Writing-original draft. D.Z.: Investigation; Methodology; writing part of the original draft. R.T.: Conceptualization; L.M.: Investigation, Supervision; Conceptualization; Writing review and editing. All authors have read and agreed to the published version of the manuscript.

Funding: This study was carried out within the Agritech National Research Center and received funding from the European Union Next-Generation EU (PIANO NAZIONALE DI RIPRESA E RESILIENZA (PNRR) MISSIONE 4 COMPONENTE 2, INVESTIMENTO 1.4 D.D. 1032 17/06/2022, CN00000022). This manuscript reflects only the authors' views and opinions, neither the European Union nor the European Commission can be considered responsible for them.

Institutional Review Board Statement: This study did not require ethical approval because it used leftover samples after routine analysis.

Informed Consent Statement: Informed consent was obtained from all subjects involved in the study.

Data Availability Statement: The data presented in this study are available on request from the corresponding author.

Acknowledgments: We thank Rocco Di Girolamo for performing the SEM analysis and Domenico Sagnelli for his advice on amylose-based film preparation.

Conflicts of Interest: The authors declare no conflict of interest.

Abbreviations

APs	Argan Proteins
AM	Amylose
APC	Argan Press Cake
mTGase	Microbial transglutaminase
FFSs	Film-Forming Solutions
TS	Tensile Strength
EB	Elongation at Break
YM	Young's Modulus
WVP	Water Vapor Permeability
CO_2P	CO_2 Permeability
FT-IR	Fourier Transform Infrared Spectra
TGA	Thermogravimetric Analysis
DSC	Differential Scanning Calorimetry

References

1. Geyer, R.; Jambeck, J.R.; Law, K.L. Production, Use, and Fate of All Plastics Ever Made. *Sci. Adv.* **2017**, *3*, 25–29. [CrossRef] [PubMed]
2. Ford, H.V.; Jones, N.H.; Davies, A.J.; Godley, B.J.; Jambeck, J.R.; Napper, I.E.; Suckling, C.C.; Williams, G.J.; Woodall, L.C.; Koldewey, H.J. The Fundamental Links between Climate Change and Marine Plastic Pollution. *Sci. Total Environ.* **2022**, *806*, 150392. [CrossRef] [PubMed]
3. Law, K.L.; Narayan, R. Reducing Environmental Plastic Pollution by Designing Polymer Materials for Managed End-of-Life. *Nat. Rev. Mater.* **2022**, *7*, 104–116. [CrossRef]
4. Zheng, J.; Suh, S. Strategies to Reduce the Global Carbon Footprint of Plastics. *Nat. Clim. Chang.* **2019**, *9*, 374–378. [CrossRef]
5. Hottle, T.A.; Bilec, M.M.; Landis, A.E. Biopolymer Production and End of Life Comparisons Using Life Cycle Assessment. *Resour. Conserv. Recycl.* **2017**, *122*, 295–306. [CrossRef]

6. Abe, M.M.; Martins, J.R.; Sanvezzo, P.B.; Macedo, J.V.; Branciforti, M.C.; Halley, P.; Botaro, V.R.; Brienzo, M. Advantages and Disadvantages of Bioplastics Production from Starch and Lignocellulosic Components. *Polymers* **2021**, *13*, 2484. [CrossRef] [PubMed]
7. Blennow, A. *Starch Bioengineering*; Elsevier Ltd.: Amsterdam, The Netherlands, 2018; ISBN 9780081008966.
8. Domene-López, D.; García-Quesada, J.C.; Martin-Gullon, I.; Montalbán, M.G. Influence of Starch Composition and Molecular Weight on Physicochemical Properties of Biodegradable Films. *Polymers* **2019**, *11*, 1084. [CrossRef]
9. Seung, D. Amylose in Starch: Towards an Understanding of Biosynthesis, Structure and Function. *New Phytol.* **2020**, *228*, 1490–1504. [CrossRef]
10. Li, H.; Gidley, M.J.; Dhital, S. High-Amylose Starches to Bridge the "Fiber Gap": Development, Structure, and Nutritional Functionality. *Compr. Rev. Food Sci. Food Saf.* **2019**, *18*, 362–379. [CrossRef]
11. Goderis, B.; Putseys, J.A.; Gommes, C.J.; Bosmans, G.M.; Delcour, J.A. The Structure and Thermal Stability of Amylose-Lipid Complexes: A Case Study on Amylose-Glycerol Monostearate. *Cryst. Growth Des.* **2014**, *14*, 3221–3233. [CrossRef]
12. Wang, S.; Li, C.; Copeland, L.; Niu, Q.; Wang, S. Starch Retrogradation: A Comprehensive Review. *Compr. Rev. Food Sci. Food Saf.* **2015**, *14*, 568–585. [CrossRef]
13. Xu, J.; Sagnelli, D.; Faisal, M.; Perzon, A.; Taresco, V.; Mais, M.; Giosafatto, C.V.L.; Hebelstrup, K.H.; Ulvskov, P.; Jørgensen, B.; et al. Amylose/Cellulose Nanofiber Composites for All-Natural, Fully Biodegradable and Flexible Bioplastics. *Carbohydr. Polym.* **2021**, *253*, 117277. [CrossRef] [PubMed]
14. Faisal, M.; Kou, T.; Zhong, Y.; Blennow, A. High Amylose-Based Bio Composites: Structures, Functions and Applications. *Polymers* **2022**, *14*, 1235. [CrossRef] [PubMed]
15. Sagnelli, D.; Hooshmand, K.; Kemmer, G.C.; Kirkensgaard, J.J.K.; Mortensen, K.; Giosafatto, C.V.L.; Holse, M.; Hebelstrup, K.H.; Bao, J.; Stelte, W.; et al. Cross-Linked Amylose Bio-Plastic: A Transgenic-Based Compostable Plastic Alternative. *Int. J. Mol. Sci.* **2017**, *18*, 2075. [CrossRef] [PubMed]
16. Carciofi, M.; Blennow, A.; Jensen, S.L.; Shaik, S.S.; Henriksen, A.; Buléon, A.; Holm, P.B.; Hebelstrup, K.H. Concerted Suppression of All Starch Branching Enzyme Genes in Barley Produces Amylose-Only Starch Granules. *BMC Plant Biol.* **2012**, *12*, 223. [CrossRef] [PubMed]
17. Mirpoor, S.F.; Giosafatto, C.V.L.; Di Girolamo, R.; Famiglietti, M.; Porta, R. Hemp (*Cannabis Sativa*) Seed Oilcake as a Promising by-Product for Developing Protein-Based Films: Effect of Transglutaminase-Induced Crosslinking. *Food Packag. Shelf Life* **2022**, *31*, 100779. [CrossRef]
18. Mirpoor, S.F.; Varriale, S.; Porta, R.; Naviglio, D.; Spennato, M.; Gardossi, L.; Giosafatto, C.V.L.; Pezzella, C. A Biorefinery Approach for the Conversion of Cynara Cardunculus Biomass to Active Films. *Food Hydrocoll.* **2022**, *122*, 107099. [CrossRef]
19. Mirpoor, S.F.; Giosafatto, C.V.L.; Mariniello, L.; D'Agostino, A.; D'Agostino, M.; Cammarota, M.; Schiraldi, C.; Porta, R. Argan (*Argania spinosa* L.) Seed Oil Cake as a Potential Source of Protein-Based Film Matrix for Pharmaco-Cosmetic Spplications. *Int. J. Mol. Sci.* **2022**, *23*, 8478. [CrossRef]
20. Mirpoor, S.F.; Giosafatto, C.V.L.; Porta, R. Biorefining of Seed Oil Cakes as Industrial Co-Streams for Production of Innovative Bioplastics. A Review. *Trends Food Sci. Technol.* **2021**, *109*, 259–270. [CrossRef]
21. Taarji, N.; Rabelo da Silva, C.A.; Khalid, N.; Gadhi, C.; Hafidi, A.; Kobayashi, I.; Neves, M.A.; Isoda, H.; Nakajima, M. Formulation and Stabilization of Oil-in-Water Nanoemulsions Using a Saponins-Rich Extract from Argan Oil Press-Cake. *Food Chem.* **2018**, *246*, 457–463. [CrossRef]
22. Rahib, Y.; Sarh, B.; Chaoufi, J.; Bonnamy, S.; Elorf, A. Physicochemical and Thermal Analysis of Argan Fruit Residues (AFRs) as a New Local Biomass for Bioenergy Production. *J. Therm. Anal. Calorim.* **2021**, *145*, 2405–2416. [CrossRef]
23. Lakram, N.; Moutik, S.; Mercha, I.; El Maadoudi, E.H.; Kabbour, R.; Douaik, A.; Zouahri, A.; El Housni, A.; Naciri, M. Effects of the Inclusion of Detoxified Argan Press Cake in the Diet of Dairy Goats on Milk Production and Milk Quality. *Turkish J. Vet. Anim. Sci.* **2019**, *43*, 323–333. [CrossRef]
24. Al-Asmar, A.; Giosafatto, C.V.L.; Sabbah, M.; Mariniello, L. Hydrocolloid-Based Coatings with Nanoparticles and Transglutaminase Crosslinker as Innovative Strategy to Produce Healthier Fried Kobbah. *Foods* **2020**, *9*, 698. [CrossRef] [PubMed]
25. Al-Asmar, A.; Giosafatto, C.V.L.; Panzella, L.; Mariniello, L. The Effect of Transglutaminase to Improve the Quality of Either Traditional or Pectin-Coated Falafel (Fried Middle Eastern Food). *Coatings* **2019**, *9*, 331. [CrossRef]
26. Giosafatto, C.V.L.; Al-Asmar, A.; D'Angelo, A.; Roviello, V.; Esposito, M.; Mariniello, L. Preparation and Characterization of Bioplastics from Grass Pea Flour Cast in the Presence of Microbial Transglutaminase. *Coatings* **2018**, *8*, 435. [CrossRef]
27. Colussi, R.; Pinto, V.Z.; El Halal, S.L.M.; Biduski, B.; Prietto, L.; Castilhos, D.D.; da Rosa Zavareze, E.; Dias, A.R.G. Acetylated Rice Starches Films with Different Levels of Amylose: Mechanical, Water Vapor Barrier, Thermal, and Biodegradability Properties. *Food Chem.* **2017**, *221*, 1614–1620. [CrossRef]
28. Muscat, D.; Adhikari, B.; Adhikari, R.; Chaudhary, D.S. Comparative Study of Film Forming Behaviour of Low and High Amylose Starches Using Glycerol and Xylitol as Plasticizers. *J. Food Eng.* **2012**, *109*, 189–201. [CrossRef]
29. Seki, T.; Chiang, K.; Yu, C.; Yu, X.; Okuno, M.; Hunger, J.; Nagata, Y.; Bonn, M. The Bending Mode of Water: A Powerful Probe for Hydrogen Bond Structure of Aqueous Systems. *J. Phys. Chem. Lett.* **2020**, *11*, 8459–8469. [CrossRef]
30. Simona, J.; Dani, D.; Petr, S.; Marcela, N.; Jakub, T.; Bohuslava, T. Edible Films from Carrageenan/Orange Essential Oil/Trehalose—Structure, Optical Properties, and Antimicrobial Activity. *Polymers* **2021**, *13*, 332. [CrossRef]

31. Xu, X.; Liu, H.; Duan, S.; Liu, X.; Zhang, K.; Tu, J. A Novel Pumpkin Seeds Protein-Pea Starch Edible Film: Mechanical, Moisture Distribution, Surface Hydrophobicity, UV-Barrier Properties and Potential Application. *Mater. Res. Express* **2019**, *6*, 125355. [CrossRef]
32. Zhang, B.; Luo, Y.; Wang, Q. Effect of Acid and Base Treatments on Structural, Rheological, and Antioxidant Properties of a -Zein. *Food Chem.* **2011**, *124*, 210–220. [CrossRef]
33. Dong, S.; Guo, P.; Chen, Y.; Chen, G.; Ji, H.; Ran, Y.; Li, S.; Chen, Y. Industrial Crops & Products Surface Modi Fi Cation via Atmospheric Cold Plasma (ACP): Improved Functional Properties and Characterization of Zein Fi Lm. *Ind. Crops Prod.* **2018**, *115*, 124–133. [CrossRef]
34. Zou, Y.; Yuan, C.; Cui, B.; Sha, H.; Liu, P.; Lu, L.; Wu, Z. High-Amylose Corn Starch/Konjac Glucomannan Composite Film: Reinforced by Incorporating β-Cyclodextrin. *J. Agric. Food Chem.* **2021**, *69*, 2493–2500. [CrossRef]
35. Thakur, R.; Pristijono, P.; Golding, J.B.; Stathopoulos, C.E.; Scarlett, C.J.; Bowyer, M.; Singh, S.P.; Vuong, Q.V. Amylose-Lipid Complex as a Measure of Variations in Physical, Mechanical and Barrier Attributes of Rice Starch- ι -Carrageenan Biodegradable Edible Film. *Food Packag. Shelf Life* **2017**, *14*, 108–115. [CrossRef]
36. Ifguis, O.; Bouhdadi, R.; Ziat, Y.; George, B.; Mbarki, M. Characterization and Analysis of Argania Spinosa Shells from Souss-Massa Area: Application in the Adsorption of Methylene Blue in Aqueous Solution. *J. Nanomater.* **2022**, *2022*, 6403838. [CrossRef]
37. Zannini, D.; Dal Poggetto, G.; Malinconico, M.; Santagata, G.; Immirzi, B. Citrus Pomace Biomass as a Source of Pectin and Lignocellulose Fibers: From Waste to Upgraded Biocomposites for Mulching Applications. *Polymers* **2021**, *13*, 1280. [CrossRef]
38. Turco, R.; Tesser, R.; Cucciolito, M.E.; Fagnano, M.; Ottaiano, L.; Mallardo, S.; Malinconico, M.; Santagata, G.; Di Serio, M. Cynara Cardunculus Biomass Recovery: An Eco-Sustainable, Nonedible Resource of Vegetable Oil for the Production of Poly(Lactic Acid) Bioplasticizers. *ACS Sustain. Chem. Eng.* **2019**, *7*, 4069–4077. [CrossRef]
39. LDPE (Low Density Polyethylene). Available online: https://polymerdatabase.com (accessed on 30 November 2022).
40. Sagnelli, D.; Hebelstrup, K.H.; Leroy, E.; Rolland-Sabaté, A.; Guilois, S.; Kirkensgaard, J.J.K.; Mortensen, K.; Lourdin, D.; Blennow, A. Plant-Crafted Starches for Bioplastics Production. *Carbohydr. Polym.* **2016**, *152*, 398–408, *Corrigendum in Carbohydr. Polym.* **2017**, *157*, 903. [CrossRef]
41. Damodaran, S.; Agyare, K.K. Effect of Microbial Transglutaminase Treatment on Thermal Stability and PH-Solubility of Heat-Shocked Whey Protein Isolate. *Food Hydrocoll.* **2013**, *30*, 12–18. [CrossRef]
42. Jahed, E.; Khaledabad, M.A.; Bari, M.R.; Almasi, H. Effect of Cellulose and Lignocellulose Nanofibers on the Properties of Origanum Vulgare Ssp. Gracile Essential Oil-Loaded Chitosan Films. *React. Funct. Polym.* **2017**, *117*, 70–80. [CrossRef]
43. Cruz-Diaz, K.; Cobos, Á.; Fernández-Valle, M.E.; Díaz, O.; Cambero, M.I. Characterization of Edible Films from Whey Proteins Treated with Heat, Ultrasounds and/or Transglutaminase. Application in Cheese Slices Packaging. *Food Packag. Shelf Life* **2019**, *22*, 100397. [CrossRef]
44. Zahedi, Y.; Fathi-Achachlouei, B.; Yousefi, A.R. Physical and Mechanical Properties of Hybrid Montmorillonite/Zinc Oxide Reinforced Carboxymethyl Cellulose Nanocomposites. *Int. J. Biol. Macromol.* **2018**, *108*, 863–873. [CrossRef] [PubMed]
45. Roy, S.; Rhim, J.W.; Jaiswal, L. Bioactive Agar-Based Functional Composite Film Incorporated with Copper Sulfide Nanoparticles. *Food Hydrocoll.* **2019**, *93*, 156–166. [CrossRef]

Disclaimer/Publisher's Note: The statements, opinions and data contained in all publications are solely those of the individual author(s) and contributor(s) and not of MDPI and/or the editor(s). MDPI and/or the editor(s) disclaim responsibility for any injury to people or property resulting from any ideas, methods, instructions or products referred to in the content.

4. EVALUATION OF THE DEGRADATION OF ARGAN SEEDS PROTEINS-AMYLOSE-BASED FILMS IN SOIL

4.1 Degradation of bioplastics

Bioplastics can be considered biodegradable if microorganisms like bacteria and fungi can absorb and metabolize them as a source of energy. This results in a significant change in the chemical structure of the materials leading to the formation of carbon dioxide, water, inorganic compounds, methane, and biomass. This process consists, firstly, of the degradation of long polymeric chains into oligomers, dimers, and monomers because of the action of water, temperature, and sunlight. Subsequently, these small units can pass through the cell walls of microorganisms and be used as substrates for their biochemical processes [1]. Extracellular and intracellular depolymerase are responsible for the microbial degradation of bioplastics. Extracellular enzymes break down the longer chains into shorter molecules that are then completely transformed inside the cell by intracellular enzymes. The degradation can occur aerobically or anaerobically: more than 90 microorganisms responsible for the catabolism of bioplastics are already known including aerobes, anaerobes, photosynthetic bacteria, and archaebacteria present in different environments. The degradation of bioplastics depends on numerous conditions, the most important being their chemical structure and the environment in which they are disposed of. Factors influencing the degradation of biopolymer chains can be divided into biotic and abiotic and include microbiota (it depends on the specific environment), UV radiation, temperature, oxidation, humidity, and mechanical forces [2].

Factors enabling the degradation of bioplastics related to their chemical structures are chemical bonds, crystallinity, and the surface-to-volume ratio. Polymer chains are made up of monomers linked by chemical reactions forming covalent bonds, which can consist of carbon-carbon-bonds only or carbon-heteroatoms like nitrogen, oxygen, or phosphorous besides hydrogen atoms. Carbon-carbon bonds are strong and not easy to be broken. For this reason, polymers with a high content of carbon-carbon bonds undergo a slower breakdown process than polymers that contain heteroatoms. Therefore, polymers with higher amorphous fractions are more accessible to degradation than polymers highly crystalline because the polymer chains are less entangled in the amorphous region. Also, a high surface-to-volume ratio

promotes degradation because the enzymatic processes take place only at the surface of the polymer and therefore the fragmentation into micro and nanoparticles increases the surface-to-volume ratio potentially enhancing the enzymatic breakdown [3].

The degradation of bioplastics varies in different environments such as soil, water, and compost. Soil contains a wide variety of microorganisms, which makes the degradation of bioplastic more feasible than in other environments such as water and air. The main species in the soil that can use bioplastics as carbon sources are *Actinobacteria* species, including mainly *Streptomyces* and *Amycolatopsis*.

Even *Bacillus* sp., *Pseudomonas* sp., and *Burkholderia* sp. have been also identified as soil-isolated species capable of degrading bioplastics along with some species of fungi such as *Aspergillus*, *Fusarium*, and *Penicillium*. Besides the microbiota, environmental factors such as temperature, moisture, and acidic nature affect the degradation of bioplastic. A study reported the field tests for some biodegradable plastic films burying them into soil to demonstrate degradation rate by measuring the changes in weights and other physical properties. Starch-based bioplastics blended with PCL were found to reduce weight faster than the PHB, PLA, and polybutylene-succinate-co-adipate (PBSA). Starch-based plastic films lost weight within one week, whereas PLA maintained its weight the longest (about 12 weeks) [4].

Some studies reported that bioplastic-composted soil enhances the soil's fertility and potent crop yield. Generally, the soil microbiota is enriched after the decomposition of biopolymers, it was reported that PHA films increase the soil bacterial population more than PLA-based films. Normally, proteins-based films are more suitable for bacteria growth due to their high content both in carbon and nitrogen.

Bioplastics degradation in aquatic environments seems to be slower compared to soil degradation. Probably factors such as low temperature, nutrient levels, and microbe population density negatively affect the process. Bacteria responsible for the catabolism of bioplastics in aquatic environments, such as river water and seawater include *Bacillus* sp., *Pseudomonas* sp., *Enterobacter* sp. The aquatic microbial population, however, does not have the same composition in all aquatic environments and this changes the degradation rate of bioplastics. Moreover, differences were also found in the same habitats: sea sediments may have a favorable effect on biodegradation, but the highest biodegradation rate was found at the water-sediment interface [2][3].

In this chapter, hydrocolloid-based bioplastics made up of argan seeds proteins and amylose (prepared as explained in the previous chapter) were subjected to the burial test to evaluate their degradation in soil as described in the following paragraph.

4.2 Degradability of APs-AM-based films and Mater-bi by soil burial test

Soil burial degradation tests[5] were carried out sandwiching the films between two layers of three different soils, collected at a depth of 10-30 cm, from i) soil A: forest soil under mature holm oak trees (*Quercus ilex* L.), at the Royal Park of Portici (Naples, Campania, Italy); ii) soil B: from an agricultural area located at Castel Volturno (60 km north of Naples, Campania, Italy; iii) soil C: from the agricultural area of Piana del Sele, an area of 700 km^2 crossed by the river Sele in the province of Salerno, Campania, Italy. These three different tested soils have been found characterized by different physicochemical properties (Table 7).
Soil A was a loamy textured, sub-neutral, and poorly calcareous soil of volcanic origin, with a good content of organic C and available P and optimal C/N ratio. Soil B was a poorly calcareous flood soil with a sandy clay loam texture and alkaline pH (8.7), showing the highest CEC (due to the high clay content) and the lowest P availability (due to its alkalinity). Soil C was a loamy and alkaline (pH=8.5) flood soil, with a great occurrence of carbonates and the highest contents of total N and available P [6] [7].

Soil Properties	Soil A	Soil B	Soil C
Sand g kg^{-1}	466±27	513±21	390±15
Silt g kg^{-1}	349±21	244±15	388±18
Clay g kg^{-1}	185±12	243±9	222±13
pH (in H_2O)	7.2±0.1	8.7±0.1	8.5±0.2
Carbonates g kg^{-1}	35.9±1.6	24.1±1.1	75.0±2.8
Organic carbon g kg^{-1}	21.0±0.6	10.5±0.4	12.5±0.5

Total N g kg^{-1}	1.9±0.1	1.3±0.1	2.4±0.3
C/N ratio	11.3	8.0	8.9
Available P mg kg^{-1}	28.5±0.9	12.0±0.6	57.0±1.2
CEC cmol (+) kg^{-1}	19.7±0.5	24.1±0.7	21.6±0.8

Table 1. Physicochemical properties of three different soils used for the degradation test: soil A from the Parco Gussone of Portici (Naples), soil B from the agricultural area of Castel Volturno (Naples), and soil C from the agricultural area of Piana del Sele (Salerno). CEC, Cation Exchange Capacity; cmol: centimole. (Data from [6],[7] for Soil A and Soil B, unpublished data by Adamo P. for Soil C).

4.2.1 Methods

According to Mantia et al. [5] tests were conducted at room temperature and RH. Film portions of 2 cm x 2 cm were cut. Specimens of the film were weighted and sandwiched between two layers of soil to have the film at 4 cm of depth and moistened every day with 100 mL of water. Film samples were removed after regular intervals, brushed softly, and weighed. The degree of degradation was evaluated by weight loss using the following equation:

$$WL\ (\%) = (W_i - W_t) / W_i \times 100$$

Where W_i is the initial weight of the sample and W_t is the weight after the established time.
SEM analyses of APs-AM-based films before and after degradation under soil conditions were performed using field emission scanning electron microscopy (SEM) (Nova NanoSem 450-FEI-Thermo Fisher, Scientific, Waltham, MA, USA).
The films were cryo-fractured in liquid nitrogen and then the samples were coated with a thin layer of Au-Pd using a vacuum sputter coater. They were observed at a magnification of 10000x with an accelerating voltage of 3 kV by using an ETD detector.

4.2.2 Results

Degradation of AM100-based films, APs100-based films, blended films, and commercial Mater-Bi was studied in these soils over a period of 80 days (Figures 1-2). From the visual images of all the samples, it can be

observed that AM100-based films, APs100-based films, and blended films lost their integrity, highlighting the degradation process. This result was confirmed by the microscopic morphology of the films observed by SEM (Figures 4-5-6-7), revealing rough and eroded surfaces, with porous pits visible in their cross-sections. The degradation process does not seem to affect Mater-Bi samples during the time considered, as confirmed by the weight loss analysis reported in Figure 3. The obtained results during the time of degradation showed a weight loss of the films of ~30% for AM100-based films, ~25% for APs100-based films, and ~20% for blended films (APs50-AM50) (Figure 3). No significant differences were observed among the weight losses of the same sample in the different soils. Sample degradation depends on different factors such as soil microbiota, organic matter, and water availability. Probably the higher content of organic matter in soil A and its overall better fertility balances the lower content in available water with respect to soils B and C, which showed a higher occurrence of clay minerals, in the degradation of bioplastics. Further investigation will be carried out to clarify the differences among the microbiota of the three soils and clarify their role in the degradation process.

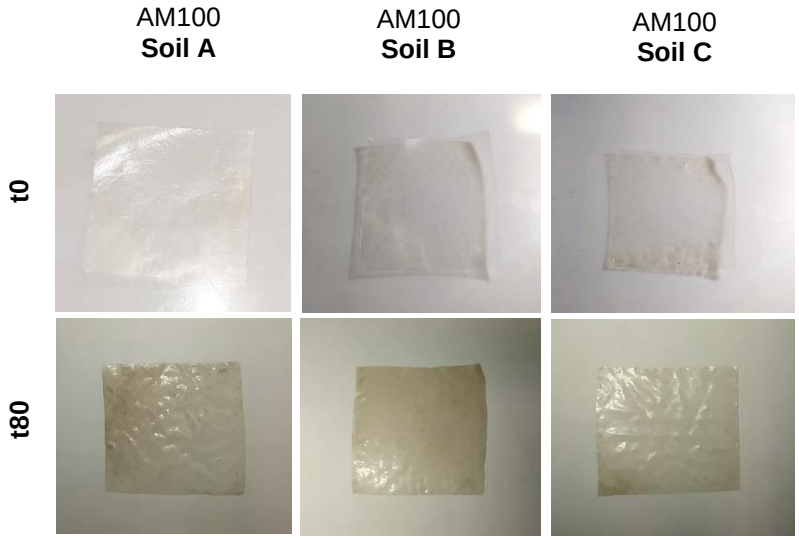

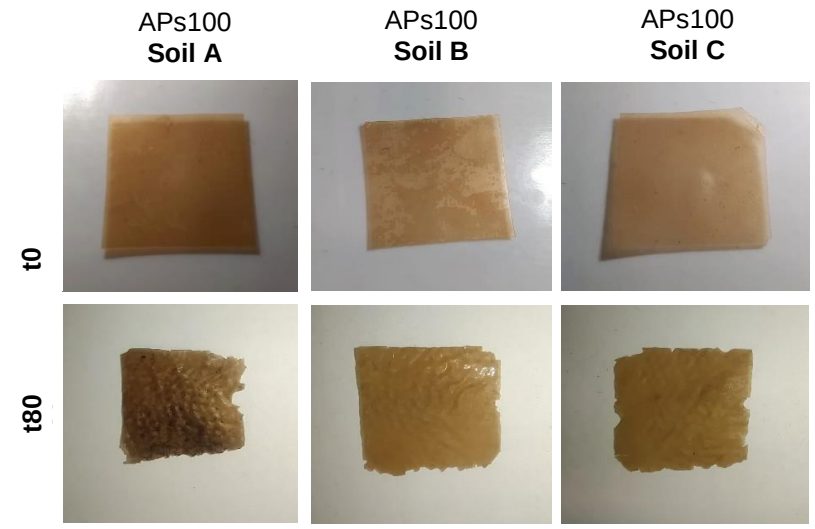

Figure 1. The appearance of AM100-based films and APs100-based films before degradation (t0) and after 80 days (t80) in Soils A, B, and C.

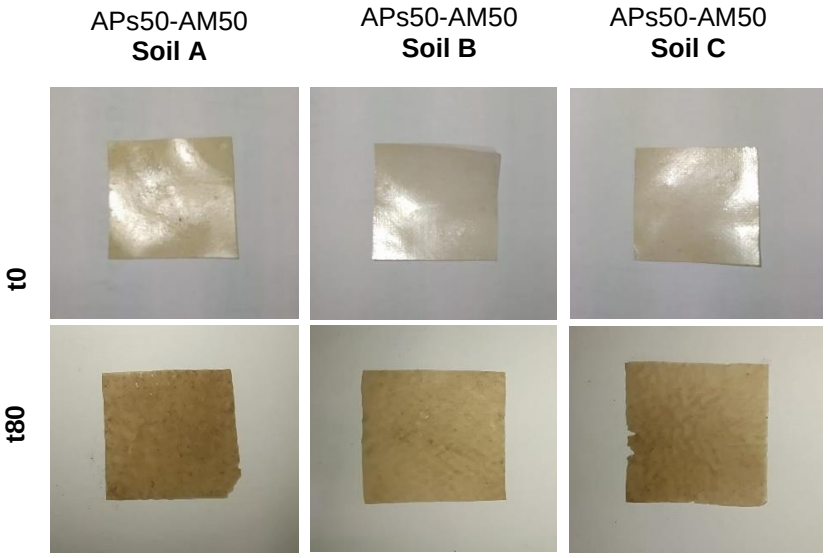

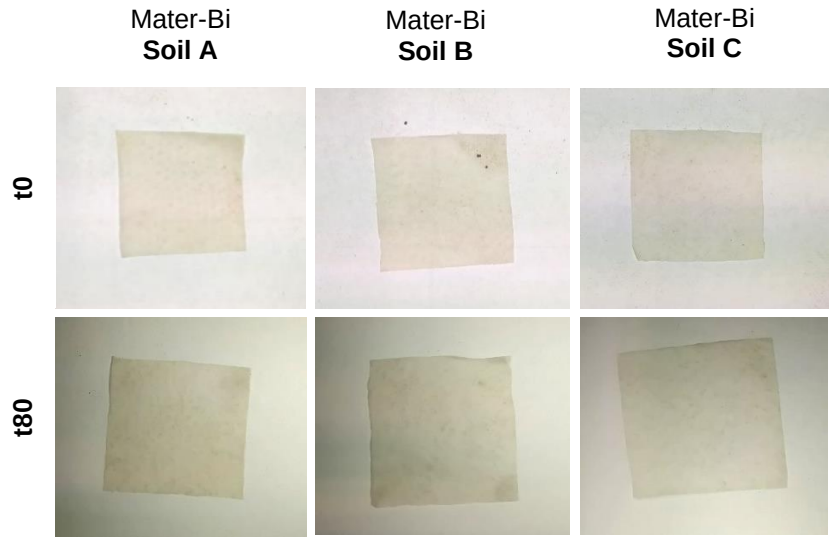

Figure 2. The appearance of APs50-AM50-based films and Mater-Bi films before degradation (t0) and after 80 days (t80) in Soils A, B and C.

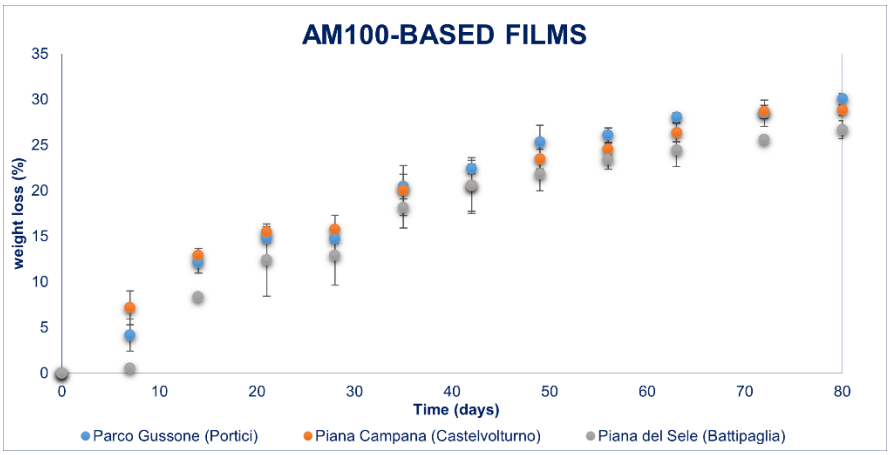

(a)

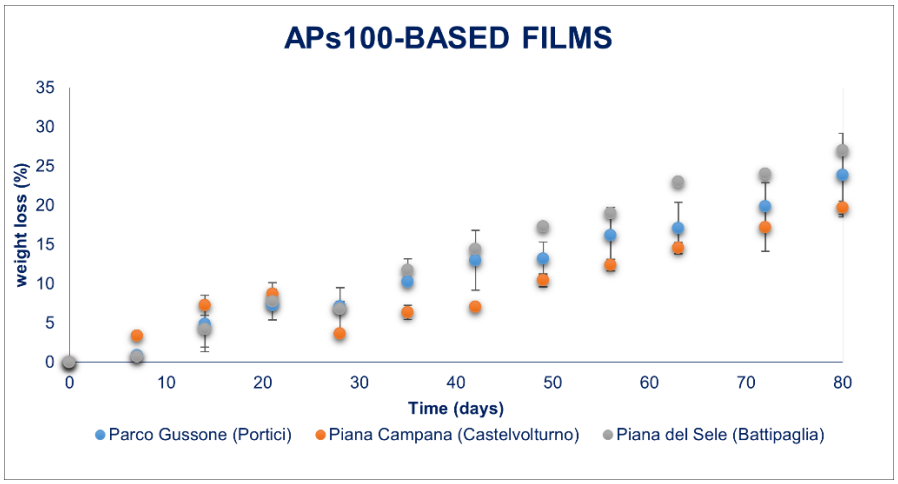
APs100-BASED FILMS
weight loss (%)
Time (days)
Parco Gussone (Portici)
Piana Campana (Castelvolturno)
Piana del Sele (Battipaglia)

(b)

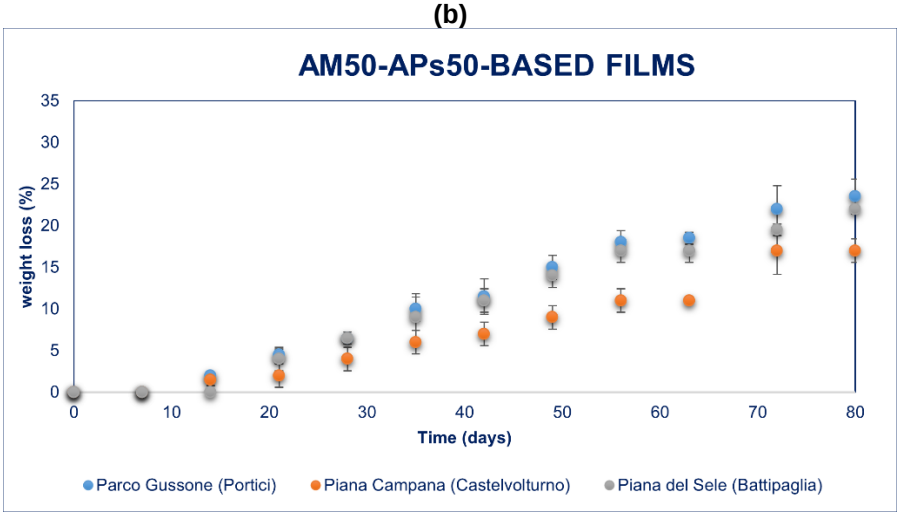
AM50-APs50-BASED FILMS
weight loss (%)
Time (days)
Parco Gussone (Portici)
Piana Campana (Castelvolturno)
Piana del Sele (Battipaglia)

(c)

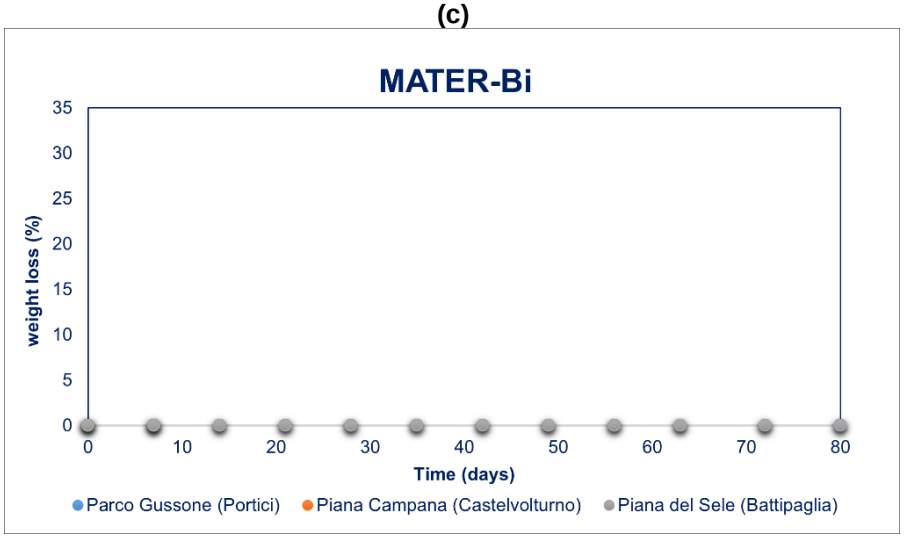
MATER-Bi
weight loss (%)
Time (days)
Parco Gussone (Portici)
Piana Campana (Castelvolturno)
Piana del Sele (Battipaglia)

(d)

Figure 3. Average weight loss values (%) over 80 days for AM100-based films (**a**), APs100-based films (**b**), APs50-AM50-based films (**c**), and Mater-Bi (**d**).

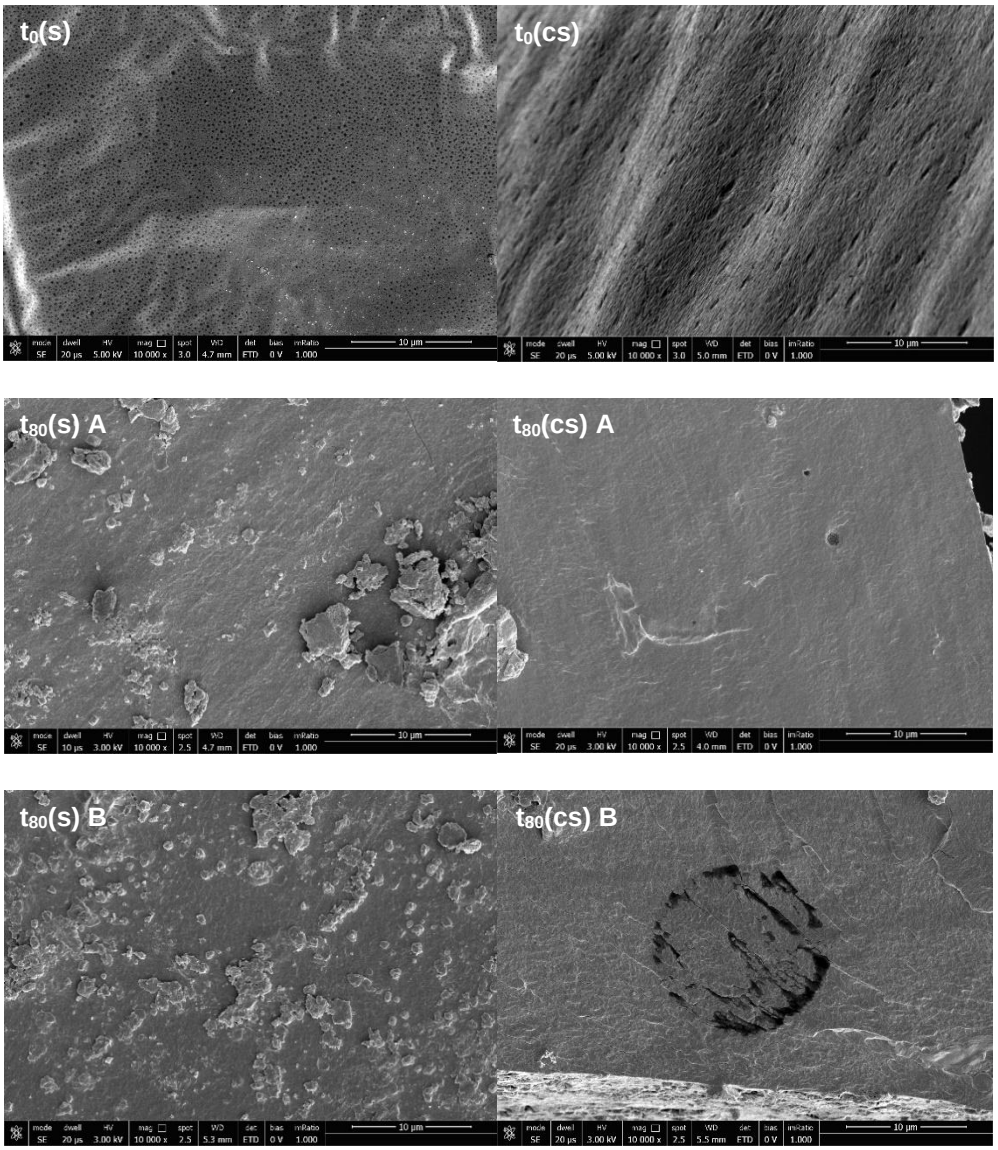

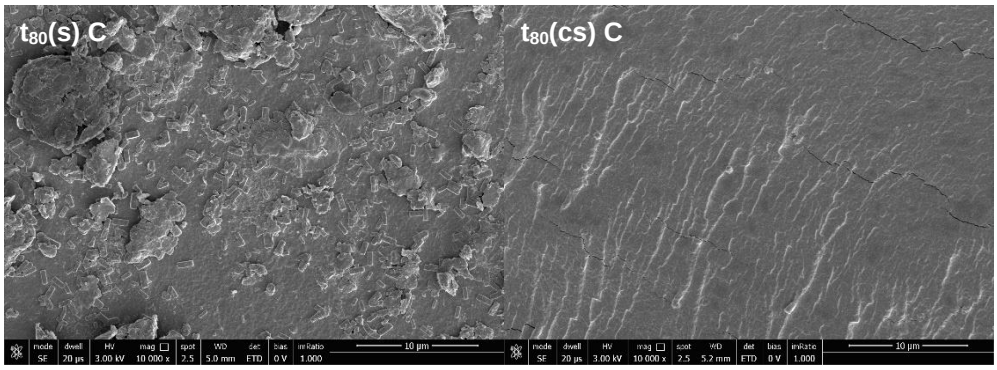

Figure 4. SEM micrographs of AM100-based film surfaces (s) and cross-sections (cs) before degradation (t_0) and in Soils A, B, and C, after 80 days (t_{80}).

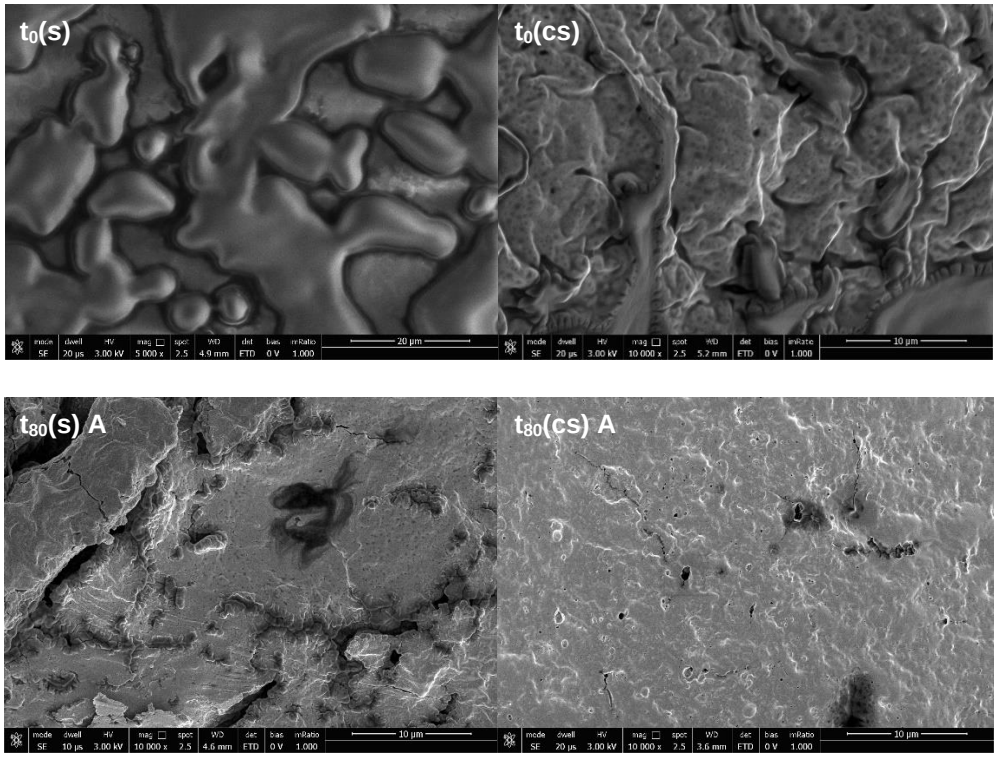

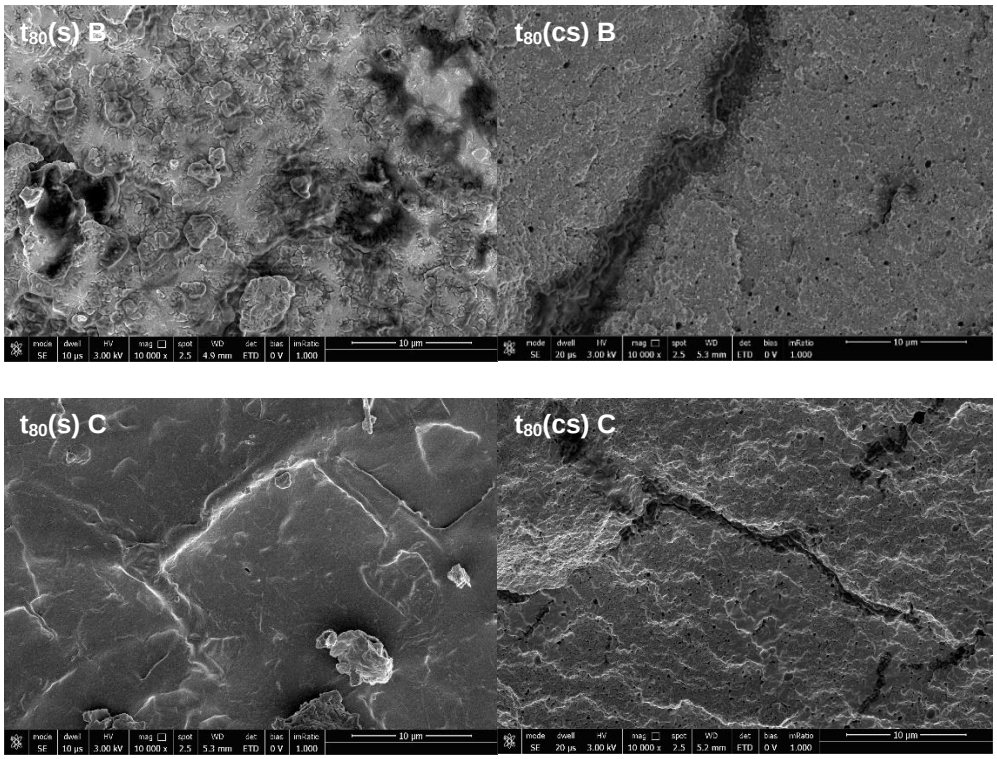

Figure 5. SEM micrographs of APs100-based film surfaces (s) and cross-sections (cs) before degradation (t_0) and in Soils A, B, and C, after 80 days (t_{80}).

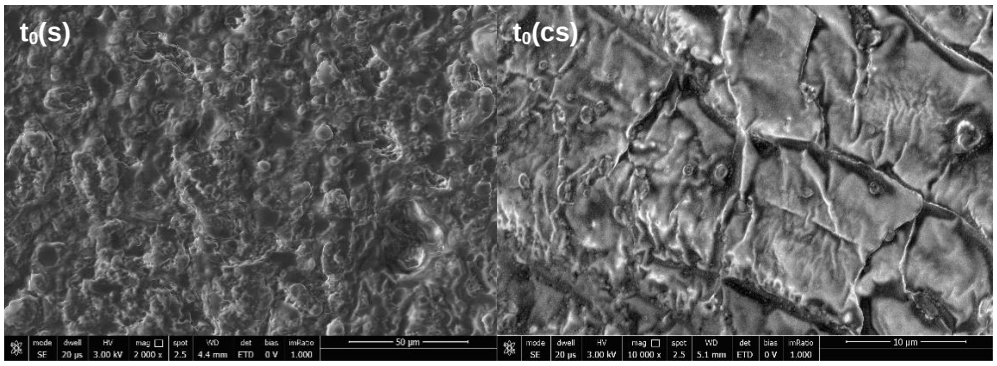

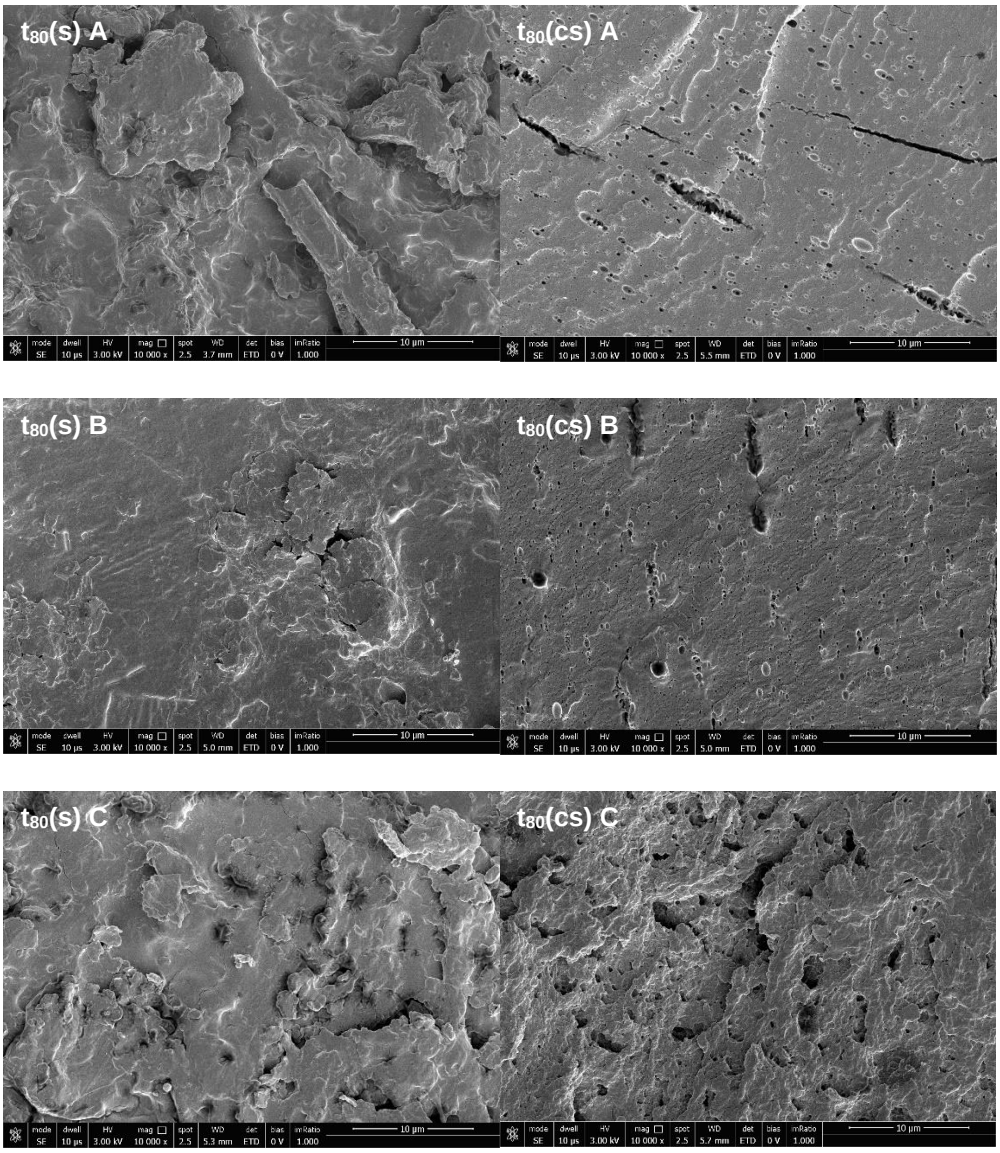

Figure 6. SEM micrographs of APs50-AM50-based films surface (s) cross-section (cs) before degradation (t_0) and in Soils A, B, and C after 80 days (t_{80}).

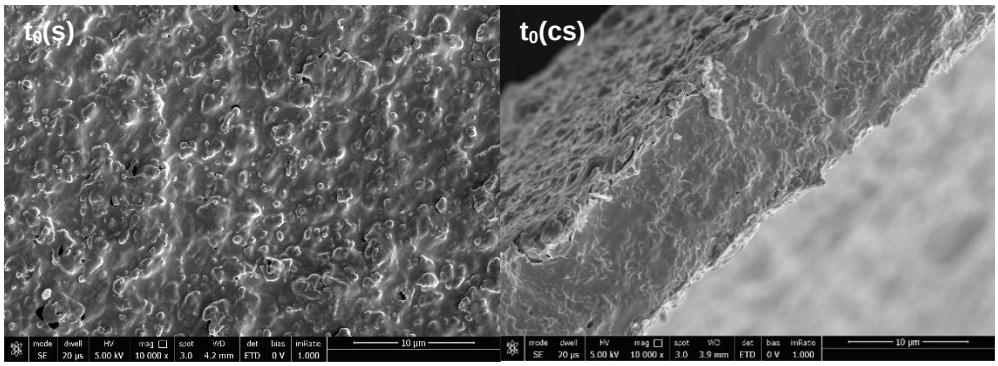
t_0(s)
t_0(cs)

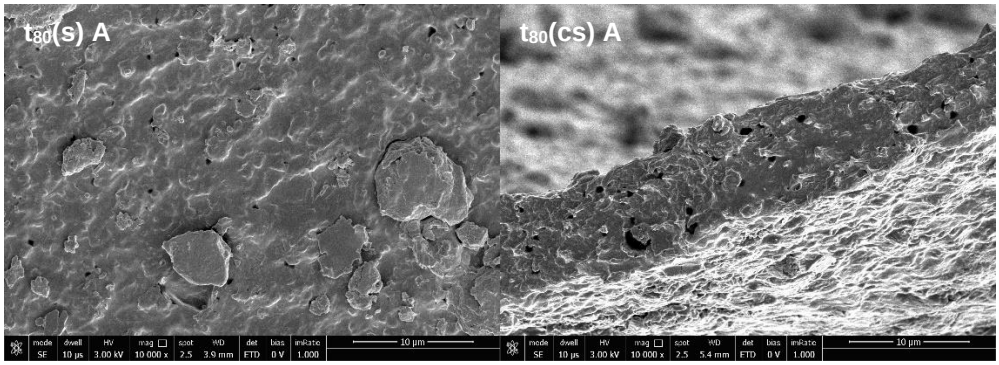
t_{80}(s) A
t_{80}(cs) A

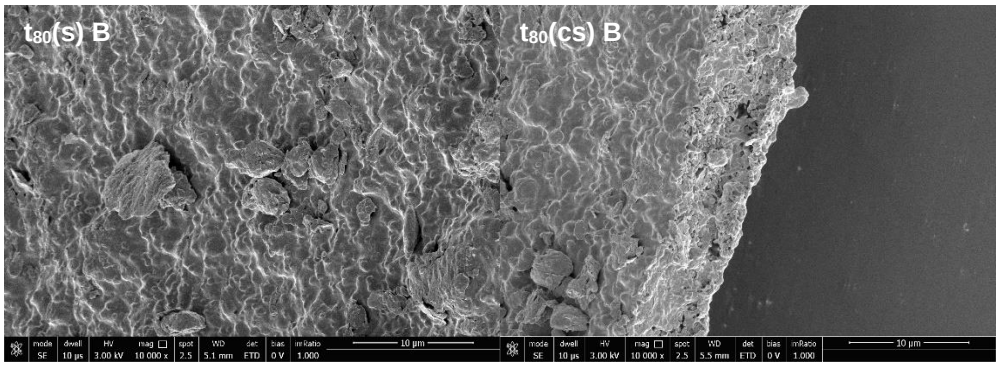
t_{80}(s) B
t_{80}(cs) B

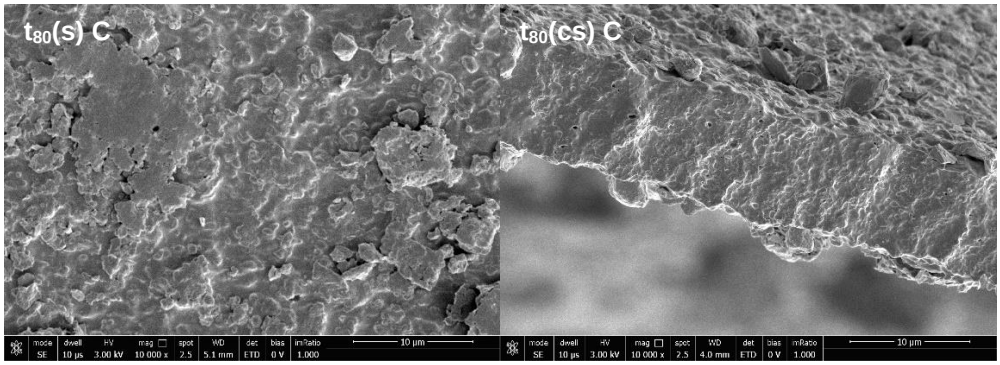
t_{80}(s) C
t_{80}(cs) C

Figure 7. SEM micrographs of Mater-Bi surfaces (s) and cross-section (cs) before degradation (t_0) and in Soils A, B, and C after 80 days (t_{80}).

4.2.3 Conclusions

The performed tests have underlined that the novel bioplastics can degrade easily in the soils used. On the contrary, Mater-Bi was shown to follow a slower degradation process. SEM images confirmed what was evaluated by the burial test. It could be assessed that the novel bioplastics can be defined as compostable since obeys the definition described by the European label EN13432.

4.3 References

1. Ahsan, W.A.; Hussain, A.; Lin, C.; Nguyen, M.K. Biodegradation of Different Types of Bioplastics through Composting—A Recent Trend in Green Recycling. *Catalysts* **2023**, *13*, 1–14, doi:10.3390/catal13020294.
2. Emadian, S.M.; Onay, T.T.; Demirel, B. Biodegradation of Bioplastics in Natural Environments. *Waste Manag.* **2017**, *59*, 526–536, doi:10.1016/j.wasman.2016.10.006.
3. European Commission *Biodegradability of Plastics in the Open Environment*; **2021**; ISBN 9789276237853.
4. Polman, E.M.N.; Gruter, G.J.M.; Parsons, J.R.; Tietema, A. Comparison of the Aerobic Biodegradation of Biopolymers and the Corresponding Bioplastics: A Review. *Sci. Total Environ.* **2021**, *753*, 141953, doi:10.1016/j.scitotenv.2020.141953.
5. Mantia, F.P.L.; Ascione, L.; Mistretta, M.C.; Rapisarda, M.; Rizzarelli, P. Comparative Investigation on the Soil Burial Degradation Behaviour of Polymer Films for Agriculture before and after Photo-Oxidation. *Polymers (Basel).* **2020**, *12*, doi:10.3390/POLYM12040753.
6. Caporale, A.G.; Vitaglione, P.; Troise, A.D.; Pigna, M.; Ruocco, M. Influence of Three Different Soil Types on the Interaction of Two Strains of *Trichoderma Harzianum* with *Brassica Rapa* Subsp. *Sylvestris Cv. Esculenta*, under Soil Mineral Fertilization. *Geoderma* **2019**, *350*, 11–18, doi:10.1016/j.geoderma.2019.05.003.
7. Cozzolino, V.; Di Meo, V.; Piccolo, A. Impact of Arbuscular Mycorrhizal Fungi Applications on Maize Production and Soil Phosphorus Availability. *J. Geochemical Explor.* **2013**, *129*, 40–44, doi:10.1016/j.gexplo.2013.02.006.

5. IRON OXIDE-BASED MAGNETIC NANOPARTICLES (NPs) TO REINFORCE ARGAN SEEDS PROTEINS-AMYLOSE-BASED FILMS

5.1 Iron oxide-based magnetic NPs

Among the different types of nano and microparticles, iron oxide particles (IOs) have been attracting attention for their ease of synthesis, low cost, high reactivity, biocompatibility, low toxicity, and sustainability. Recently, they are playing an important role in different applicative fields such as electrochemical and gas sensing, energy storage, catalysis, wastewater treatment, cancer therapy, and other biomedical treatments, as well as for applications such as coatings, sorbents, and semiconductors [1][2]. Iron is the most widespread metal on Earth and is characterized by high reactivity, easy oxidation, and naturally magnetic properties. Several crystalline forms of iron oxide (IO) are known such as hematite (Fe_2O_3) (with 70mass% of iron), magnetite (Fe_3O_4) (with 72mass% of iron), and wüsite (FeO) (with 78 mass% of iron). Each one of these has different crystallographic phases as a result of their synthesis processes, and depending on this their particles find application in different fields. Iron ores can be identified by their color: hematite is reddish-brown, magnetite is black and maghemite presents a light brown color. Magnetite and maghemite are widespread in the environment, but they are thermodynamically less stable than hematite, considered as the more stable, in the presence of oxygen: at near room temperature magnetite very slowly oxidizes to maghemite and at higher temperatures transforms into hematite [3].

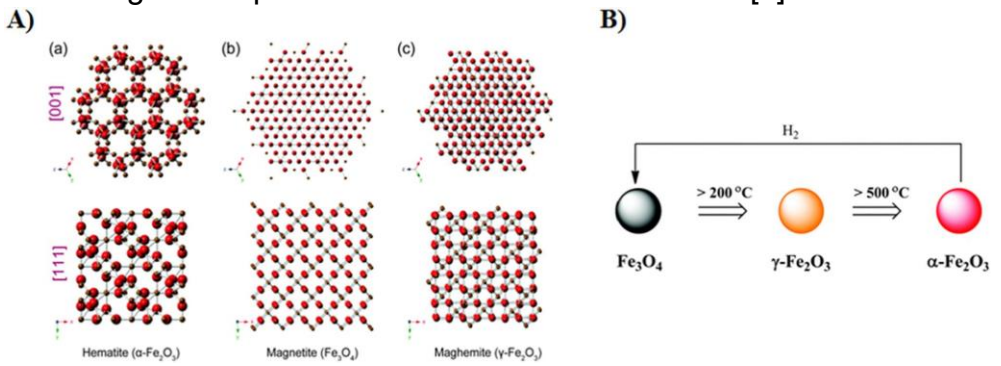

Figure 1. **A**) Crystal structure of (**a**) α-Fe_2O_3, (**b**) Fe_3O_4, and (**c**) γ-Fe_2O_3. **B**) Scheme of the phase transformation of magnetite, maghemite, and hematite [3].

Among the methods of preparation of IOs are co-precipitation, thermal decomposition, sol-gel method, hydrothermal/solvothermal method, microwave assisted-method, electron spinning, electron beam lithography, and pulsed laser ablation. Depending on the synthesis method and synthesis parameters different characteristics such as high phase purity, good stability, size and morphology, ferromagnetic properties, and absorption of toxic pollution can be obtained [4][5][6][7]. The high ratio of surface area to volume and the magnetic dipole-dipole attraction between particles lead to the agglomeration of pure IOs, negatively affecting their application. Different strategies have been developed to prevent this effect such as enclosing NPs in a matrix or support material, encapsulating them in macromolecules like starch, chitosan, or inorganic coatings like silver, silica, or carbon, or modifying their surface with reactive functional ligands such as small organic and inorganic particles, polymers, and graphene structures [3].
Coatings IOs with inorganic materials not only solve the problem of agglomeration but also improve their stability. Silanes have been used to modify many surfaces, for their excellent reactivity towards silicon and oxide surfaces, and for their ability to react with several functional groups. The surface modification of IOs through the grafting of aminopropylsilane groups $(–O)_3Si–CH_2–CH_2–CH_2–NH_2$, for instance, because of the active groups of -NH_2, can easily connect to bioligands such as proteins and enzymes [8].

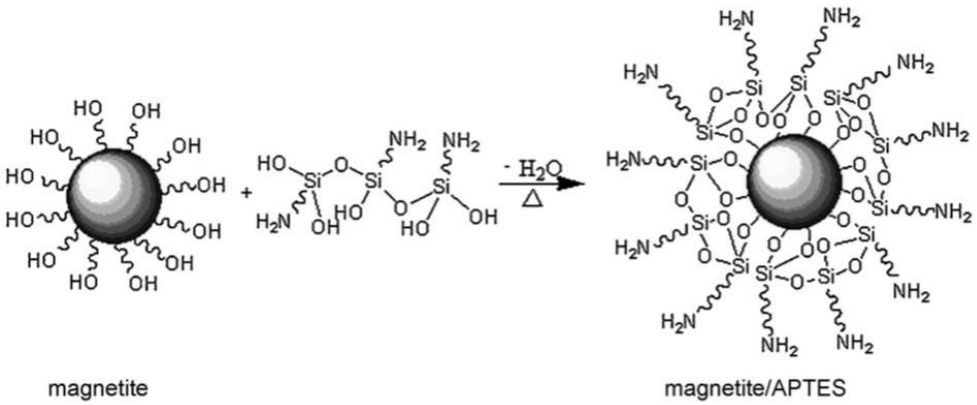

Figure 2. Scheme of the simplified silanization reaction of APTES on the magnetite surface [8].

5.2 Methods

5.2.1 Solvothermal method to synthesize iron oxide-based NPs

The solvothermal method refers to a method in which water or organic solvents are used as a reaction environment in a specially sealed reactor within elevated pressure and high-temperature reaction conditions. This method has many advantages: first, the magnetic properties of magnetic particles can be improved in a high-temperature environment; the components' volatilization is reduced, and the purity of the final product is improved; it has simple operation and cheap raw materials and finally it has low toxicity [9][10].
In this project magnetic NPs based on Fe_3O_4 were prepared using $FeCl_3$ $6H_2O$ as the source of iron ions, CH_3COONa as an alkali source and a structure-directive agent, and ethylene glycol as a high-boiling-point solvent and as reducing agent.
Ethylene glycol is first oxidized under heating to generate glycolaldehyde; $Fe[Ac]_3$ and $Fe[Ac]_2$ are formed by the reaction of Ac^- and Fe^{3+} (Fe^{2+}); $Fe(OH)_3$ and $Fe(OH)_2$ are formed by the hydrolytic and alcoholysis process of $Fe[Ac]_3$ and $Fe[Ac]_2$; finally, Fe_3O_4 primary IOs are generated via the dehydration of these products.
All the reagents used were purchased by Sigma-Aldrich Company (St.Louis, MO, USA).
2.7 g of $FeCl_3$ $6H_2O$ and 7.2 g of CH_3COONa were dissolved in 100 mL of ethylene glycol and stirred for 1 h. Then the solution was poured into a hydrothermal autoclave reactor in a muffle furnace at 200°C for 8 h. Using a magnet IOs were separated from the supernatant and washed several times with water and EtOH. Finally, IOs were dried at 60°C.

5.2.2 Ferrofluid preparation

To avoid their aggregation IOs were suspended in Trisodium citrate (0.3 M) in the hydrothermal autoclave reactor at 90°C for 30 min under stirring. Then the IOs were separated again from the supernatant using a magnet and were washed 2-3 times with H_2O. Finally, they were suspended in 20 mL of H_2O to have a final concentration of 2 % (*w/v*).

5.2.3 Functionalization of IOs with APTES ((3-aminopropyl) triethoxysilane)

10 mL of ferrofluid were added to a solution of CH_3OH and APTES and stirred for 3 h. Then particles were separated and washed three times with H_2O and finally suspended again in 10 mL of H_2O to have a final concentration of 20 mg/mL.

5.2.4 NPs characterization: SEM Microscopy and ATR - FT-IR

The NPs electron microscope images were obtained with a JEOL JSM 7600F instrument. Samples were observed at a magnification of 5000x and 50000x with an accelerating voltage of 15 kV.
Fourier Transform Infrared (FT-IR) spectra of the samples were obtained using a Bruker Alpha FT-IR spectrometer with a Diamond Crystal ATR (Attenuated Total Reflection) accessory. The spectrometer runs Opus 7.8 software.
The ATR - FT-IR spectrum of each sample was recorded in the range of 4000–400 cm^{-1} with at least 20 scans and a resolution of 4 cm^{-1} and processed using the OPUS software.

5.2.5 Preparation of APs-AM FFSs with magnetic NPs

Different FFSs were prepared with different ratios of AM-APs (100/0–50/50–0/100 % (*w/w*)) using H_2O as a solvent to have a final concentration of 10 mg/mL and glycerol as plasticizer with a concentration of 50% (*w/w*). Fe_3O_4 NPs and Fe_3O_4-APTES NPs were added with a concentration of 1 % (*w/w*) (with respect to the total mass). AM was gelatinized by heating it in a graphite-bath at 150°C for 1 h using a hydrothermal autoclave reactor. APs were solubilized in H_2O adjusting the pH to 12 with NaOH 1M and stirring the solution for 1 h. FFSs were obtained by mixing AM after gelatinization and APs after solubilization in the correct ratios.

5.2.6 Preparation of APs-AM-based films with magnetic NPs

Film preparation was carried out as described by Famiglietti et al. and reported above (Chapter 3). FFSs were poured into polypropylene Petri dishes (9 cm in diameter) and dried in an oven at 50°C for ~28 h. After that, the films were stored in a desiccator at room temperature to balance the moisture content before the subsequent analyses.

5.2.7 Film moisture content and solubility

Film moisture content and solubility were determined according to the method described by Famiglietti et al. and reported above (Chapter 3). The analysis was performed in duplicate on samples of 2 cm^2. The moisture content was determined by calculating the difference between the initial and the final weight of the samples using the following equation:

$$\text{Moisture content (\%)} = [(W_i - W_d)/W_i] \times 100$$

5.2.8 Film swelling ratio

Film swelling ratio were determined as described by Famiglietti et al. and reported above (Chapter 3). The analysis was carried out in duplicate. Film swelling ratio was calculated using the following equation:

$$\text{Swelling ratio (\%)} = [(W_s - W_i)/W_i] \times 100$$

5.2.9 Film Water Vapor Permeability

Film barrier permeability to water vapor was analyzed using a MultiPerm apparatus (ExtraSolution s.r.l, Pisa, Italy) according to the Standard Methods (ASTM F1249-13 (2013)). Each sample is loaded within the instrument, where it constitutes a separate septum between two semi-chambers. The process is carried out while maintaining the chamber at a fixed temperature (25 °C) and monitoring continuously the relative humidity (50%), the flow, and other variables that can alter the permeation of the sample. Aluminum masks were used to reduce the film test area to 2 cm^2, and the analyses were performed in duplicate.

5.2.10 Film Thermogravimetric analysis (TGA) and Differential Scanning Calorimetry (DSC)

Thermogravimetric analyses (TGA/DSC) were performed with the TA instruments DSC SDT Q600 Thermogravimetric Analyzer (TGA) and Differential Scanning Calorimeter (DSC), which provides simultaneous measurement of weight change (TGA) and true differential heat flow (DSC) on the same sample.
Each sample was heated from 25°C to 1000 °C at a rate of 10°C/min.

5.2.11 Statistical analysis

SPSS19 (Version 19, SPSS Inc., Chicago, IL, USA) software was used for all statistical analyses. One-way analysis of variance (ANOVA) and Duncan's multiple range tests ($p < 0.05$) were used to determine the significant difference among the samples.

5.3 Results

5.3.1 SEM microscopy and ATR - FT-IR of magnetic NPs

SEM analyses were performed at different magnifications (5000x, 50000x) for both Fe_3O_4 NPs and Fe_3O_4 NPs functionalized with APTES.

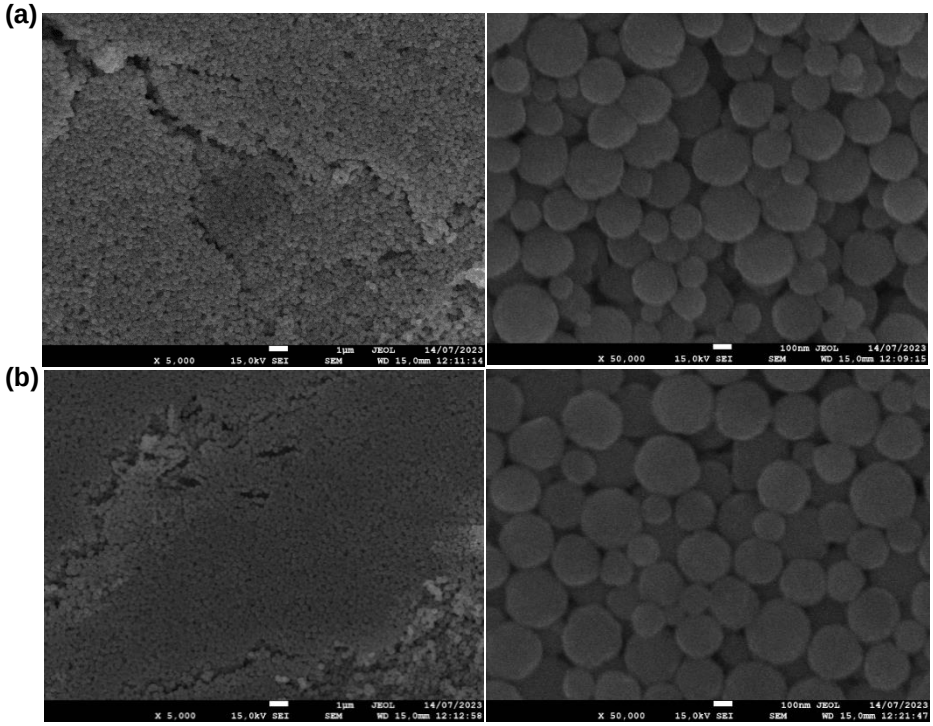

Figure 3. (a) Fe_3O_4 NPs, **(b)** Fe_3O_4-APTES NPs at magnification of 5000x and 50000x.

IR spectra of Fe_3O_4 NPs: the peak at 536 cm^{-1} corresponds to the vibration of Fe-O bonds. The peaks at 3422 cm^{-1} and 3399 cm^{-1} can be attributed to the stretching vibration of O-H bonds of the hydroxyl groups on the surface of the magnetic NPs, that overlap the N-H bonds

in Fe_3O_4-APTES NPs spectra. The peaks at 1636 cm^{-1} and 1620 cm^{-1} are possibly associated with the bending vibration of O-H bonds [11].

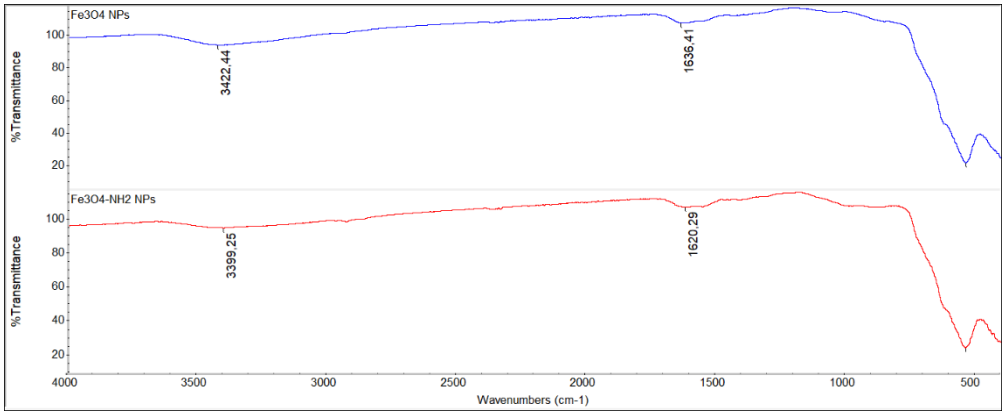

Figure 4. IR spectra of Fe_3O_4 NPs and Fe_3O_4-APTES NPs.

5.3.2 Characterization of AM-APs-based films reinforced with ferromagnetic NPs

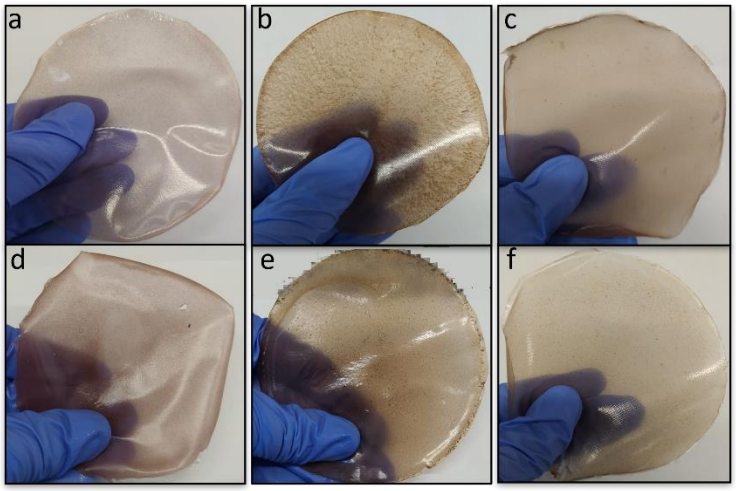

Figure 5. The appearance of APs-AM-based films reinforced with Iron oxide-based NPs: **a**) AM100-based film - Fe_3O_4 NPs **b**) APs100-based films - Fe_3O_4 NPs **c**) APs50-AM50-based film - Fe_3O_4 NPs **d**) AM100-based film - Fe_3O_4-APTES NPs **e**) APs100-based film - Fe_3O_4-APTES NPs **f**) APs50-AM50-based film - Fe_3O_4-APTES NPs.

5.3.3 Film moisture content, water solubility, and swelling ratio

Moisture content values observed were not significantly different among AM-APs-based films reinforced or not with magnetic NPs for both Fe_3O_4 NPs and Fe_3O_4-APTES NPs. The differences noted were related to the different concentrations of AM and APs as described by Famiglietti et al. and reported above (Chapter 3). Water solubility values and swelling ratio were not reported as significantly different for AM-based films reinforced with NPs compared to the films without them. The presence of NPs seems to affect them in APs-based films, as reported in Figure 6: specifically, APs-based films reinforced with Fe_3O_4 NPs showed values of solubility and swelling ratio significantly higher than both APs-based films without NPs and with Fe_3O_4-APTES NPs.

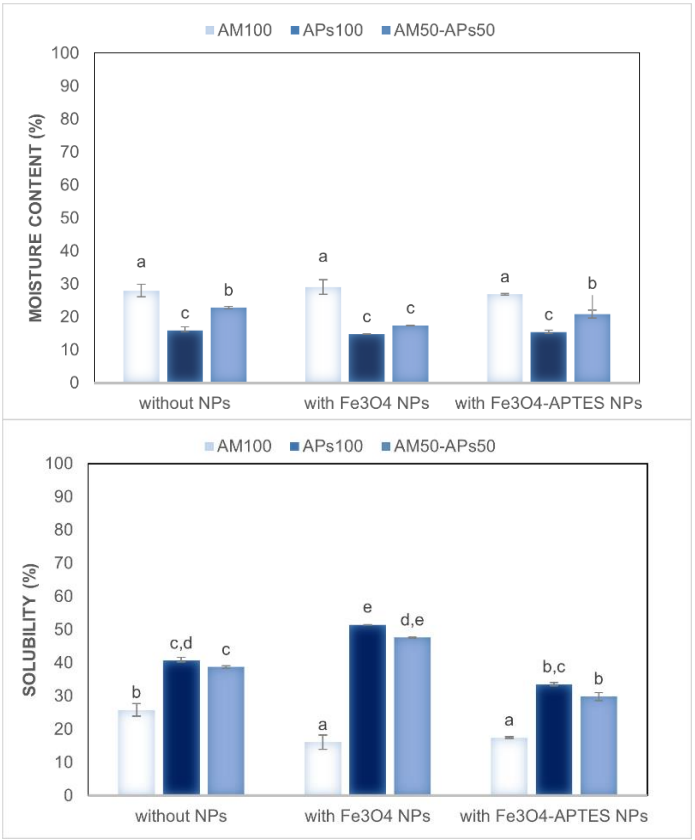

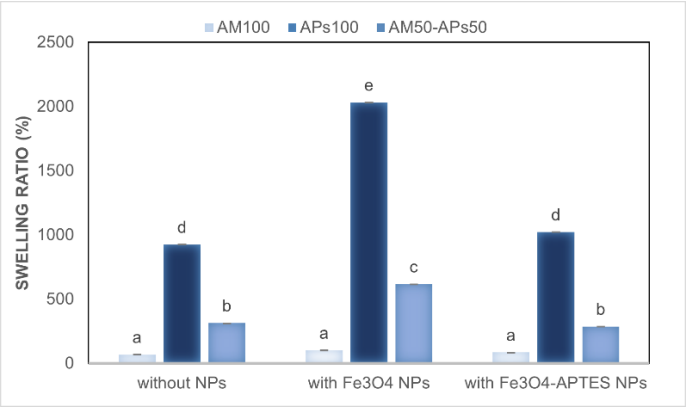

Figure 6. Moisture content, water solubility, and swelling ratio of AM100-based films, APs100-based films, and blended films (APs50-AM50) mixed with Fe_3O_4 NPs and Fe_3O_4-APTES NPs or without NPs. Different small letters (a–e) indicate significant differences among the values reported in each bar ($p < 0.05$). The analysis was carried out in triplicate.

5.3.4 Film Water Vapor Permeability (WVP)

Film WVP depends on crystallinity, hydrophilic groups, intricate pathways formed within the films, and the compactness of the matrix. Tortuosity is a vital parameter that affects film WVP. For these reasons some authors found that mixing NPs into the film matrices could have different effects on WVP depending on their concentrations, their homogenous dispersion, and the interactions between them and the film matrices. When NPs concentrations are higher the structures can be less compact due to the NPs aggregation and water molecules may easily pass through the films [12].

This result was observed adding cellulose nanocrystals (CNC) and nanofibers (CNF) as reinforcement to AM-based composite bioplastics [13], in which elevation of both CNC and CNF concentrations led to diminished barrier performance against WV as observed in the study reported in the appendix of this thesis *A Comparison of Cellulose Nanocrystals and Nanofibers as Reinforcements to Amylose-Based Composite Bioplastics* by Marwa Faisal, Marija Žmiri´c, Ngoc Quynh Nhu Kim, Sander Bruun, Loredana Mariniello, **Michela Famiglietti**, Heloisa N. Bordallo, Jacob Judas Kain Kirkensgaard, Bodil Jørgensen, Peter Ulvskov, Kim Henrik Hebelstrup and Andreas Blennow.

The same effect was observed by adding Fe_3O_4 NPs at a concentration of 1% (*w/w*) in AM-based films, probably due to the break of the entanglement of AM-chains caused by NPs aggregation. When Fe_3O_4 NPs are functionalized with APTES, the film WV barrier results higher

probably because the functionalization avoids their aggregation. APs-based films and blended films obtained by adding both unfunctionalized Fe_3O_4 NPs and functionalized Fe_3O_4-APTES were not affected by this effect, since they showed values of WVP similar to the films obtained without NPs, indicating that the interaction between NPs and film matrix does not create inhomogeneity in the film structures.

APs-AM ratio	WVP (g mm/m^{2}d kPa)
0-100	8.68±0.36^{c}
50-50	3.27±0.31^{d,e}
100-0	2.89±0.13^{d,e}
0-100 - Fe_3O_4	23.86±1.08^{a}
50-50 - Fe_3O_4	2.63±1.78^{d,e}
100-0 - Fe_3O_4	2.99±1.29^{d,e}
0-100 - Fe_3O_4-APTES	16.41±0.92^{b}
50-50 - Fe_3O_4-APTES	4.96±0.54^{d}
100-0 - Fe_3O_4-APTES	1.13±0.005^{e}

Table 1. Water vapor permeability of AM100-based films, APs100-based films, and blended films (APs50-AM50) mixed with Fe_3O_4 NPs and Fe_3O_4-APTES NPs or without NPs. Different small letters (a–e) indicate significant differences among the values reported in each column ($p < 0.05$). The analysis was carried out in duplicate.

5.3.5 Thermogravimetric analyses (TGA/DSC)

The TGA, the differential thermogravimetric (DTG), and the DSC curves obtained are reported in Figure 7-8-9. AM100-based films (Figure 7a): from 30 °C up to 100 °C, the sample lost about 10–15% of its weight, which was attributed to the free and bound water molecules in the films. The second mass loss process was observed in the range of 100 ºC – 200 °C with a maximum rate of thermal transformation at 157 ºC (curve blue). This process should be mainly associated with the thermal degradation of glycerol [4]. The third thermal transformation was

observed between 250 ºC and 400 °C, with a maximum rate of thermal transformation at 317 ºC, probably associated with the pyrolysis of AM. This last thermal transformation was confirmed by DSC, where a clear endothermal peak centered at 317 ºC was observed, which is ascribed to the decomposition of AM. The shoulder endothermal peak at 283 ºC in DSC could be associated with the gelatinization of AM [15].

AM100-based film with Fe_3O_4 NPs (Figure 7b): this composite material showed a similar thermogravimetric pattern to those without Fe_3O_4 NPs because a primary loss of adsorbed water was observed at temperatures below 100 °C, while a second mass loss with a maximum rate of thermal transformation at 174 ºC corresponding to pyrolysis of glycerol was revealed, suggesting a thermoprotective effect of NPs on this component. The composite material showed a third thermal transformation with a maximum rate at 313 ºC associated with the pyrolysis of AM. Interestingly, the maximum gelatinization rate of AM was observed at a higher temperature of 302 ºC, suggesting interaction with NPs affected the intermolecular interaction of polysaccharide chains.

AM100-based film with Fe_3O_4-APTES NPs (Figure 7c): the film prepared with APTES-modified magnetic NPs also showed a first thermal desorption of water at temperatures below 100 °C, and a second mass loss with a maximum rate at 182 ºC corresponding to the thermal transformation of glycerol. This increase in the thermal stability of glycerol could be associated with a higher interaction with the magnetic NPs through the formation of hydrogen bonds between the pedant primary amino groups in the nanomaterial and the hydroxyl groups in the polyalcohol. Amino-modified NPs seem to interact more efficiently with AM chains, as can be assumed by the higher temperature for the maximum rate of pyrolysis (318 ºC) and the absence of the gelatinization phase transition previously observed in DSC for the other films.

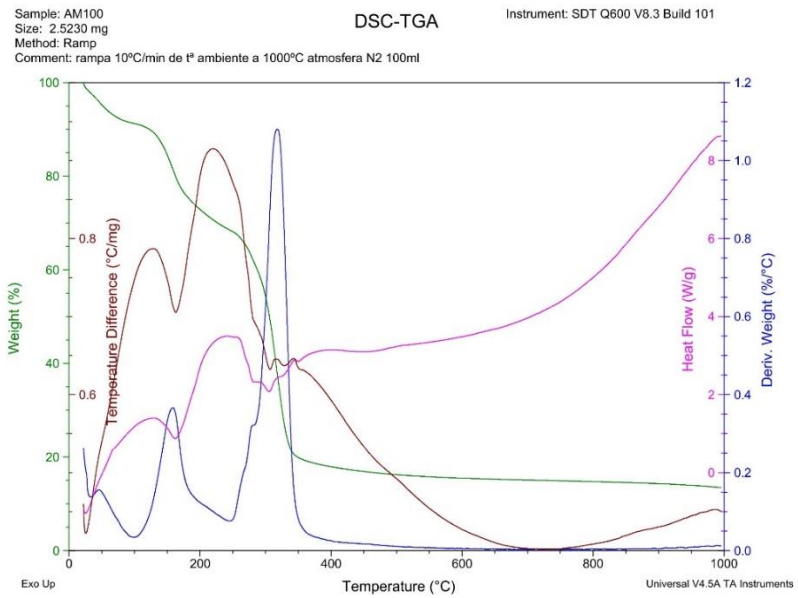
Sample: AM100
Size: 2.5230 mg
Method: Ramp
Comment: rampa 10ºC/min de tª ambiente a 1000ºC atmosfera N2 100ml
DSC-TGA
Instrument: SDT Q600 V8.3 Build 101
Weight (%)
Temperature Difference (°C/mg)
Heat Flow (W/g)
Deriv. Weight (%/°C)
Exo Up
Temperature (°C)
Universal V4.5A TA Instruments

(a)

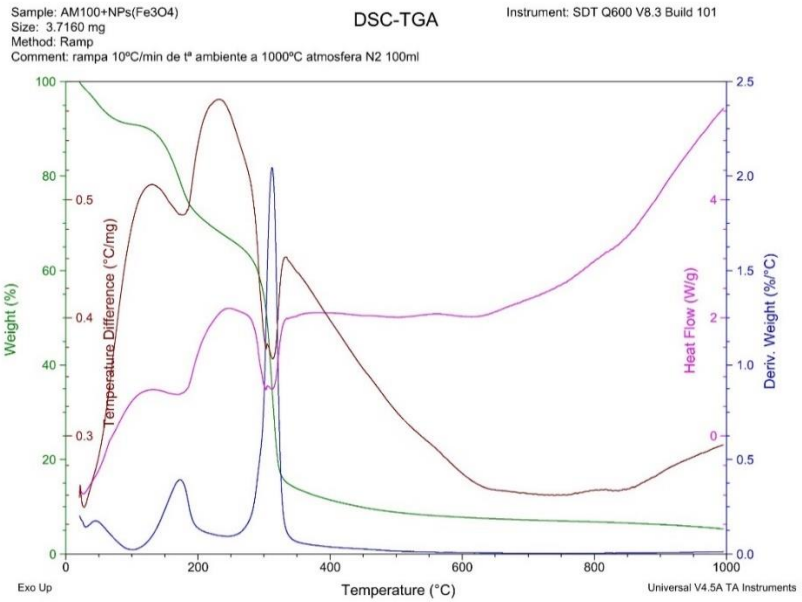
Sample: AM100+NPs(Fe3O4)
Size: 3.7160 mg
Method: Ramp
Comment: rampa 10ºC/min de tª ambiente a 1000ºC atmosfera N2 100ml
DSC-TGA
Instrument: SDT Q600 V8.3 Build 101
Weight (%)
Temperature Difference (°C/mg)
Heat Flow (W/g)
Deriv. Weight (%/°C)
Exo Up
Temperature (°C)
Universal V4.5A TA Instruments

(b)

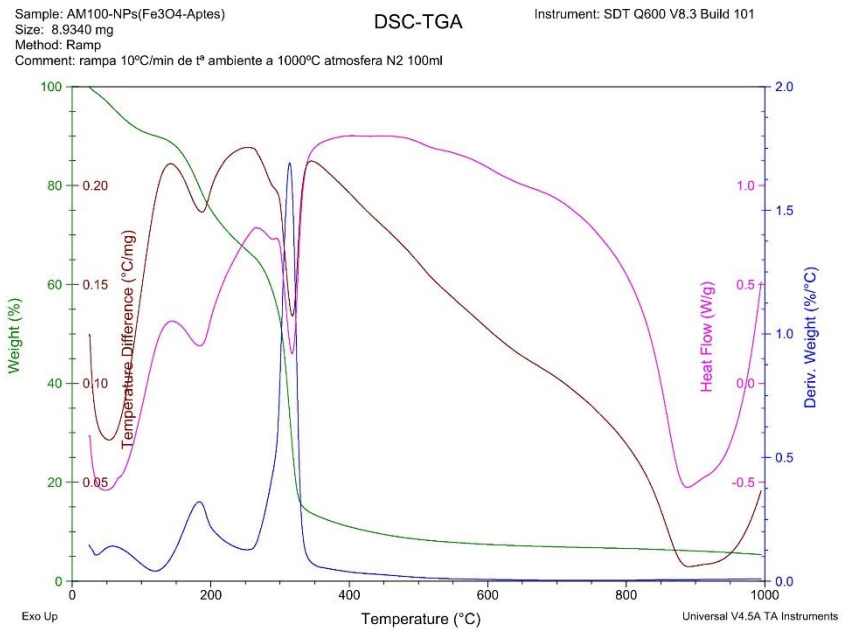

(c)

Figure 7. TGA-DSC curves of (a) AM100-based films, b) AM100-based films reinforced with Fe_3O_4 NPs, and c) AM100-based films reinforced with Fe_3O_4-APTES NPs.

APs100-based film (Figure 8a): the first thermal transformation observed between 50 ºC and 100 °C is ascribed to the heat-induced desorption of adsorbed water molecules. Secondly, depolymerization and decomposition of low molecular weight proteins, as well as pyrolysis of glycerol was observed between 171 ºC and 243 ºC, with a maximum rate of thermal transformation at 196 ºC. Progressive pyrolysis of hemicellulose and lignin [16] was further observed between 243 ºC and 482 ºC, through different, consecutive, and overlapped thermal processes, as revealed by the multiple peaks in the differential curve as well as in the DSC pattern. Complete incineration of the residual material was observed at temperatures higher than 800 ºC, which could be associated with the decomposition of inorganic components in the raw material, as reported by Mirpoor et al [17].
APs100-based films with Fe_3O_4 NPs and Fe_3O_4-APTES NPs (Figure 8b and c): no significant difference in the thermogravimetric pattern of APs100-based films was observed after mixing with raw and APTES-modified NPs. However, changes in the patterns of the differential curves and shifting of the peaks associated with the maximum rates for thermal transformations, as well as variations in the DSC curve

revealed that the interaction of APs with the nanomaterials affected its thermal stability. In special, thermal stability seems to be slightly increased in the presence of APTES-modified NPs.

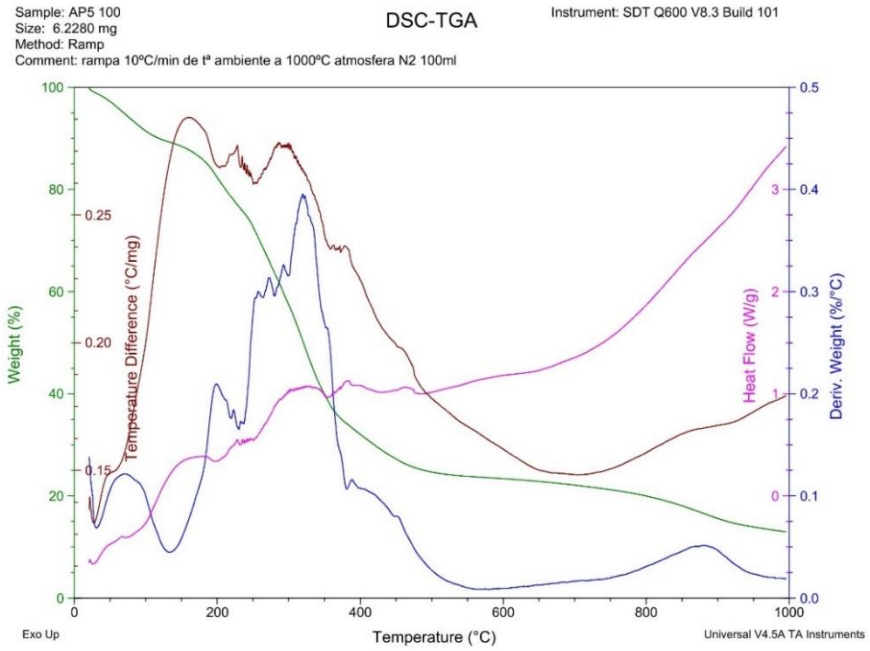

(a)

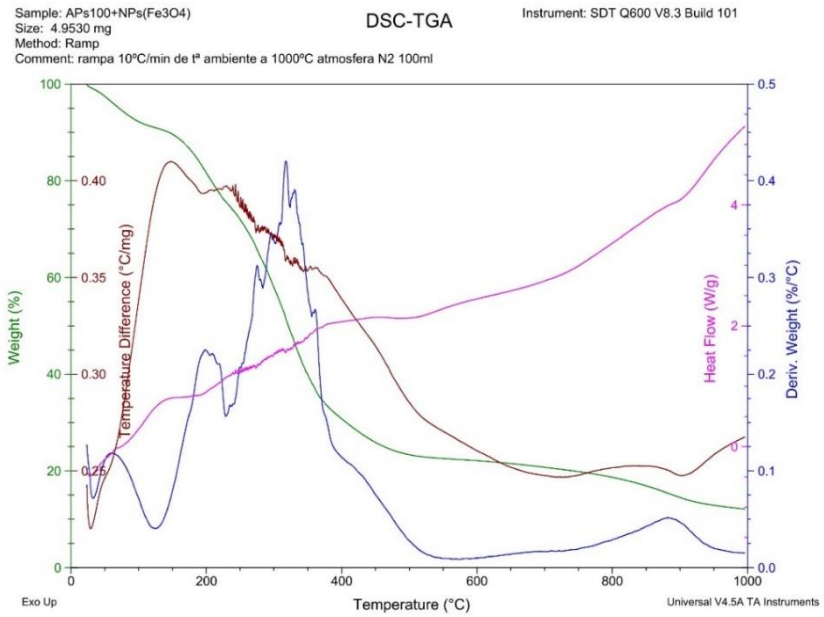

(b)

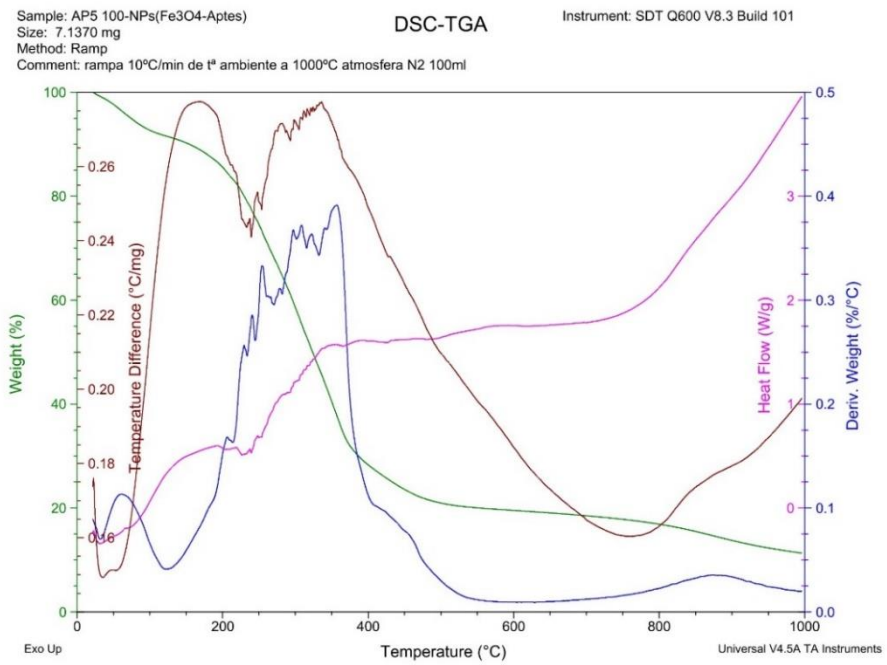

(c)

Figure 8. TGA-DSC curves of (a) APs100-based films, (b) APs100-based films reinforced with Fe_3O_4, NPs, and (c) APs100-based films reinforced with Fe_3O_4-APTES NPs.

AM50-APs50-based films (Figure 9a): films prepared by mixing AM and APs showed the initial thermal desorption of water molecules up to 100 °C. From 142 ºC to 512 ºC several overlapped thermal transformations are observed, associated with pyrolysis of glycerol and the polymeric components of the natural materials, as previously commented.
APs50-AM50-based films reinforced with Fe_3O_4 NPs and Fe_3O_4-APTES NPs (Figure 9b and c): although these composite materials showed a similar thermogravimetric pattern to those without NPs, the complexity of the differential and DSC curved suggested strong interactions between the nanomaterials and the natural polymers contained in the raw materials. Such interactions seem to slightly increase the thermal stability of the film containing APTES-modified NPs.

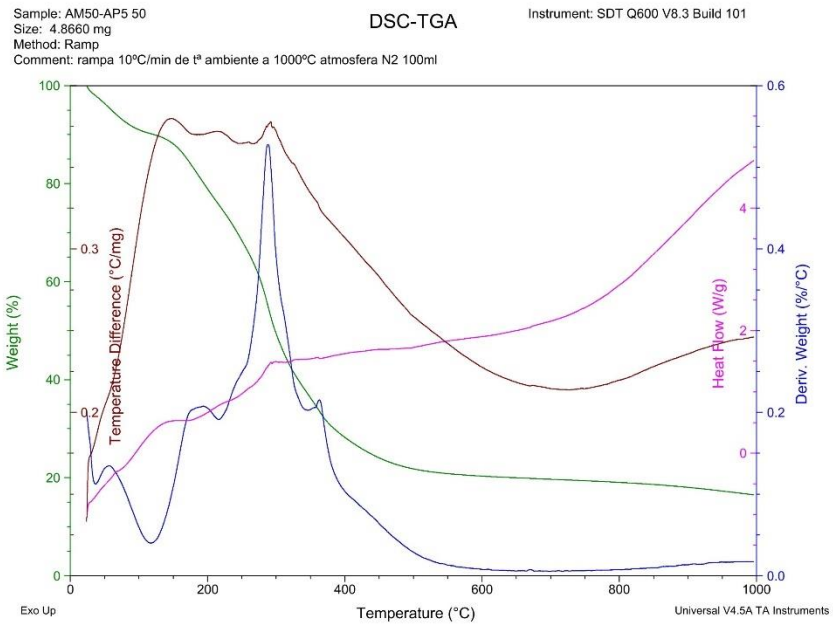
Sample: AM50-AP5 50
Size: 4.8660 mg
Method: Ramp
Comment: rampa 10ºC/min de tª ambiente a 1000ºC atmosfera N2 100ml
DSC-TGA
Instrument: SDT Q600 V8.3 Build 101
Weight (%)
Temperature Difference (°C/mg)
Heat Flow (W/g)
Deriv. Weight (%/°C)
Temperature (°C)
Exo Up
Universal V4.5A TA Instruments

(a)

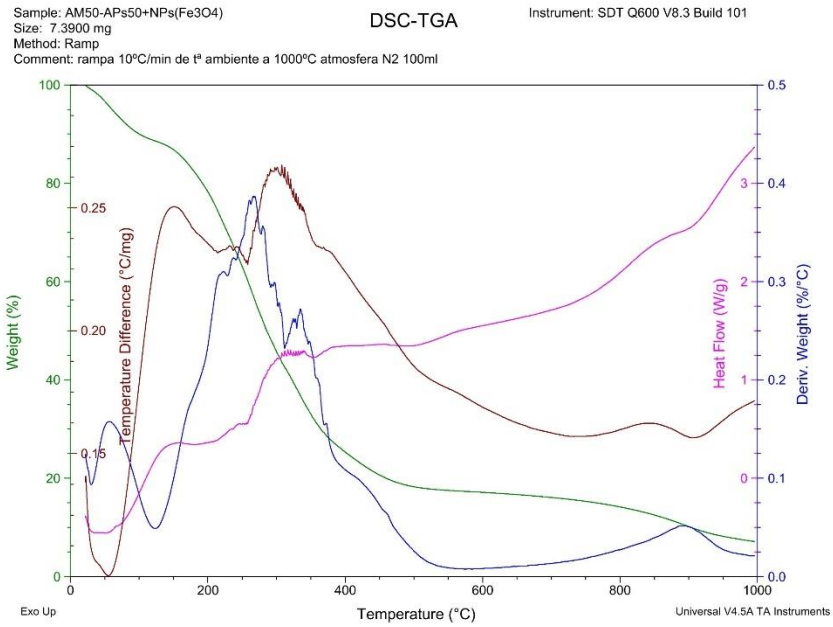
Sample: AM50-APs50+NPs(Fe3O4)
Size: 7.3900 mg
Method: Ramp
Comment: rampa 10ºC/min de tª ambiente a 1000ºC atmosfera N2 100ml
DSC-TGA
Instrument: SDT Q600 V8.3 Build 101
Weight (%)
Temperature Difference (°C/mg)
Heat Flow (W/g)
Deriv. Weight (%/°C)
Temperature (°C)
Exo Up
Universal V4.5A TA Instruments

(b)

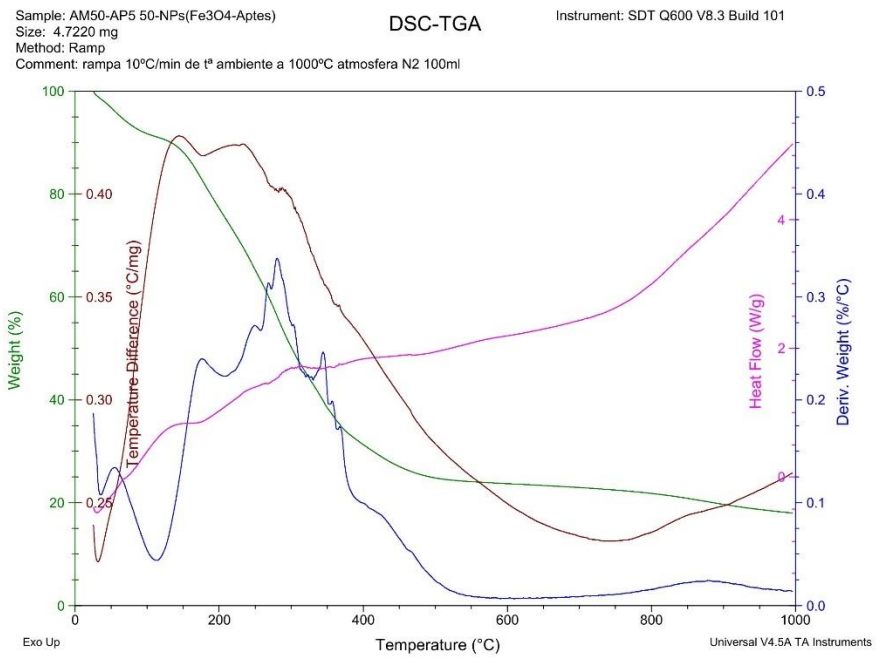

(c)

Figure 9. TGA-DSC curves of (a) APs50-AM50-based films, (b) APs50-AM50-based films reinforced with Fe_3O_4 NPs, and (c) APs50-AM50-based films reinforced with Fe_3O_4-APTES NPs.

5.4 Conclusions

Iron-oxide-based NPs were produced, characterized, and then used as nanofillers in APs-AM-based films to boost their functionalities. Thermal and hydrophilic properties were investigated as well as water vapor barrier capability. Further studies will be carried out to study NPs effect on film mechanical and gas barrier (CO_2-O_2) properties. Magnetic NPs were chosen for their ease of synthesis, low cost, low toxicity, and environmental compatibility.

Once produced, Fe_3O_4 NPs were functionalized to improve their stability and avoid their aggregation, and both types of NPs were mixed with the APs-AM-based FFSs. The presence of NPs in AM-based films increased the WVP probably because NPs broke the entanglement of AM-chains. Thermal analyses showed that both Fe_3O_4 NPs and APTES-modified NPs exert a thermoprotective effect on glycerol in AM100-based films. Specifically, the formation of hydrogen bonds between the pedant primary amino groups of functionalized NPs and

the hydroxyl groups in the polyalcohol could explain the increase in the thermal stability of glycerol. Moreover, changes in the temperature of the maximum gelatinization rate of AM for both Fe_3O_4 NPs containing films and APTES-modified NPs containing films suggested the formation of interactions with NPs that affected the intermolecular network of AM.

Even in the case of blended films strong interactions between NPs and polymer matrices were observed, potentially increasing the stability of Fe_3O_4-APTES-containing films. Finally, thermal stability seems to be slightly increased in the presence of APTES-modified NPs in APs100-based films.

5.5 References

1. Rajput, S.; Pittman, C.U.; Mohan, D. Magnetic Magnetite (Fe3O4) Nanoparticle Synthesis and Applications for Lead (Pb2+) and Chromium (Cr6+) Removal from Water. *J. Colloid Interface Sci.* **2016**, *468*, 334–346, doi:10.1016/j.jcis.2015.12.008.
2. Sangaiya, P.; Jayaprakash, R. A Review on Iron Oxide Nanoparticles and Their Biomedical Applications. *J. Supercond. Nov. Magn.* **2018**, *31*, 3397–3413, doi:10.1007/s10948-018-4841-2.
3. Kobyliukh, A.; Olszowska, K.; Szeluga, U.; Pusz, S. Iron Oxides / Graphene Hybrid Structures – Preparation , Modi Fi Cation , and Application as Fi Llers of Polymer Composites. *Adv. Colloid Interface Sci.* **2020**, *285*, 102285, doi:10.1016/j.cis.2020.102285.
4. Qiao, K.; Tian, W.; Bai, J.; Wang, L.; Zhao, J.; Du, Z.; Gong, X. Application of Magnetic Adsorbents Based on Iron Oxide Nanoparticles for Oil Spill Remediation: A Review. *J. Taiwan Inst. Chem. Eng.* **2019**, *97*, 227–236, doi:10.1016/j.jtice.2019.01.029.
5. Lassoued, A.; Lassoued, M.S.; Dkhil, B.; Ammar, S.; Gadri, A. Synthesis, Structural, Morphological, Optical and Magnetic Characterization of Iron Oxide (α-Fe2O3) Nanoparticles by Precipitation Method: Effect of Varying the Nature of Precursor. *Phys. E Low-Dimensional Syst. Nanostructures* **2018**, *97*, 328–334, doi:10.1016/j.physe.2017.12.004.
6. Zia, M.; Phull, A.R.; Ali, J.S. Challenges of Iron Oxide Nanoparticles. *Powder Technol.* **2016**, *7*, 49–67.
7. Katikaneani, P.; Vaddepally, A.K.; Reddy Tippana, N.; Banavath, R.; Kommu, S. Phase Transformation of Iron Oxide Nanoparticles from Hematite to Maghemite in Presence of Polyethylene Glycol: Application as Corrosion Resistant Nanoparticle Paints. *J. Nanosci.* **2016**, *2016*, 1–6, doi:10.1155/2016/1328463.

8. Feng, B.; Hong, R.Y.; Wang, L.S.; Guo, L.; Li, H.Z.; Ding, J.; Zheng, Y.; Wei, D.G. Synthesis of Fe3O4/APTES/PEG Diacid Functionalized Magnetic Nanoparticles for MR Imaging. *Colloids Surfaces A Physicochem. Eng. Asp.* **2008**, *328*, 52–59, doi:10.1016/j.colsurfa.2008.06.024.
9. Liu, S.; Yu, B.; Wang, S.; Shen, Y.; Cong, H. Preparation, Surface Functionalization and Application of Fe3O4 Magnetic Nanoparticles. *Adv. Colloid Interface Sci.* **2020**, *281*, 102165, doi:10.1016/j.cis.2020.102165.
10. Ge, S.; Shi, X.; Sun, K.; Li, C.; Uher, C.; Baker, J.R.; Banaszak Holl, M.M.; Orr, B.G. Facile Hydrothermal Synthesis of Iron Oxide Nanoparticles with Tunable Magnetic Properties. *J. Phys. Chem. C* **2009**, *113*, 13593–13599, doi:10.1021/jp902953t.
11. Yingjun L.; Hua C.; Jie W.; Qin H.; Yintao L.; Wenbin Y.; Yuanlin Z.; Preparation and characterization of APTES modified magnetic MMT capable of using as anisotropic nanoparticles; Applied Surface Science 447 (2018) 393–400 https://doi.org/10.1016/j.apsusc.2018.03.230.
12. Navaf, M.; Sunooj, K.V.; Aaliya, B.; Akhila, P.P.; Sudheesh, C.; Mir, S.A.; George, J. Impact of Metal and Metal Oxide Nanoparticles on Functional and Antimicrobial Activity of Starch Nanocomposite Film; A Review. *Meas. Food* **2023**, *11*, doi:10.1016/j.meafoo.2023.100099.
13. Faisal, M.; Žmirić, M.; Kim, N.Q.N.; Bruun, S.; Mariniello, L.; Famiglietti, M.; Bordallo, H.N.; Kirkensgaard, J.J.K.; Jørgensen, B.; Ulvskov, P.; et al. A Comparison of Cellulose Nanocrystals and Nanofibers as Reinforcements to Amylose-Based Composite Bioplastics. *Coatings* **2023**, *13*, doi:10.3390/coatings13091573.
14. Almazrouei, M.; Samad, T. El; Janajreh, I. Thermogravimetric Kinetics and High Fidelity Analysis of Crude Glycerol. *Energy Procedia* **2017**, *142*, 1699–1705, doi:10.1016/j.egypro.2017.12.552.
15. Liu, H.; Xie, F.; Chen, L.; Yu, L.; Dean, K.; Bateman, S. Thermal Behaviour of High Amylose Cornstarch Studied by DSC. *Int. J. Food Eng.* **2005**, *1*, doi:10.2202/1556-3758.1004.
16. Faleeva, Y.M.; Lavrenov, V.A.; Zaichenko, V.M. Investigation of Plant Biomass Two-Stage Pyrolysis Based on Three Major Components: Cellulose, Hemicellulose, and Lignin. *Biomass Convers. Biorefinery* **2022**, doi:10.1007/s13399-022-03385-1.
17. Mirpoor, S.F.; Giosafatto, C.V.L.; Mariniello, L.; D'Agostino, A.; D'Agostino, M.; Cammarota, M.; Schiraldi, C.; Porta, R. Argan *(Argania Spinosa L.*) Seed Oil Cake as a Potential Source of Protein-Based Film Matrix for Pharmaco-Cosmetic Spplications. *Int. J. Mol. Sci.* **2022**, *23*, doi:10.3390/ijms23158478.

6. CONCLUSIONS

Nowadays about 400 Mt of plastic waste are generated every year, and this amount is expected to grow dramatically over decades. Most of the attention has been focused on the effects of plastic pollution on marine ecosystems but also the tremendous impacts of plastics in terrestrial and freshwater ecosystems are now evident, increasing concern for human health. The only sustainable way to reduce plastic pollution at a global scale is to reduce plastic entering the natural environment. To reach this aim, different strategies should be considered together: reduce the consumption of plastic, especially single-use plastic, improve their recycling, and substitute them with bio-based and biodegradable materials. In this scenario, the present thesis constitutes a contribution to the development of bioplastics, i.e. biodegradable materials derived from renewable sources, as an alternative to petroleum-based plastics. Different studies were carried out and reported in this thesis about their production from the manipulation and the processing of different biopolymers, polysaccharides, and proteins, in the presence of several additives like plasticizers, active compounds, reticulating agents, and nanofillers. All the performed works showed the potential for the manipulated biopolymers to be exploited in the bioplastic industry, being suitable for a variety of applications. Specifically, chitosan was considered as a natural copolymer derived from one of the most abundant polysaccharides on earth, chitin, hence obtained from renewable sources. CH-based films were developed to incorporate an active extract derived from dried olive leaves (DOLE), a byproduct of olive cultivation and processing. This work successfully achieved the aim of valorizing this byproduct, transforming it into a high-added value product. Investigating the polyphenols' yield of DOLE and its antioxidant activity when incorporated into CH-based films verified the possibility of using it as a supplement for the delivery of active compounds useful to boost the human diet. Moreover, the evaluation of the antimicrobial activity of DOLE in combination with CH made CH-based films containing DOLE suitable for active packaging to improve food shelf-life and wrapping, for instance, meat hamburgers to delay their spoilage due to common microbial contaminants during storage. Finally, it was demonstrated that DOLE exerts a plasticizer effect, hence its presence could overcome the necessity of an additional plasticizer, such as glycerol, for bioplastic production. In the same way, it was reported in this thesis that films obtained from mixed grape juice to *Nigella sativa* defatted seed cake-protein-based films could be used

as active packaging to wrap sweet cherries and prolong their shelf life. *N. sativa* defatted cake is a byproduct of seed oil extraction and usually is used as animal feed due to its high content of proteins. This work aimed to valorize this byproduct exploiting it to produce edible films and improving their functionality by using grape juice. The obtained results showed that grape juice acts as a plasticizer and adds very promising functionalities to the films thanks to its antioxidant and antimicrobial activity. Thus, the films were used successfully to wrap sweet cherries, delaying their spoilage as confirmed by the slowing down of their change in color, titratable acidity, and total soluble solids. Similarly, pectin-based films were obtained incorporating Olive and Guava Leaf Extract (OLE and GLE) (work reported in this thesis in collaboration with the An-Najah National University of Nablus) to produce soluble sachets to wrap chicken powder demonstrating that the antioxidant activity of the extracts helps to reduce the oxidation reactions of food during its distribution and storage.

Still with a view to the aims of bioeconomy, i.e. discovering new sources to produce energy and materials and to transform wastes into high-added value products a part of this thesis was dedicated to the production of novel bioplastics, made up of argan seed proteins (APs), extracted from argan oil cake, and amylose (AM) obtained from barley plants. Moreover, the addition of a reticulating agent such as microbial transglutaminase (mTGase) was tested to verify its contribution to the development of the films. The study confirmed the potential of APs to improve the performance of AM-based films in terms of some properties, specifically their barrier capability to water vapor and CO_2, results strengthened by the presence of mTGase. Furthermore, changes in the extensibility and rigidity of the AM-based films containing APs could make them suitable for application as compostable bags.

mTGase treatment was demonstrated to be effective even on protein-based films obtained from hemp seed oilcake. Film characterization showed that mTGase-induced crosslinking originated more homogenous and smoother films, with higher resistance and heat-sealing strength as well as greater hydrophobicity.

Besides the useful properties of the obtained bioplastics in applications, even their degradation was evaluated to confirm their biodegradable nature. Specifically, APs-AM-based films not modified by mTGase were subjected to the burial test method in three soils having different characteristics over 80 days and the commercial Mater-Bi was used as control. The tests confirmed the biodegradability of the tested films for all the samples in all three soils over the period considered. Surprisingly

this behaviour was not observed for Mater-Bi samples suggesting that their degradation takes more time or needs specific conditions.
The last part of this thesis was in part performed at the Department of Analytical Chemistry of the Complutense University of Madrid and focused on the production of nanofillers to use as reinforcement of the obtained bioplastics. Specifically, iron oxide-based NPs were produced, characterized, and incorporated into APs-AM-based films. Nanofillers were preferable to microfillers thanks to their large surface-area-to-volume ratio that provides an extensive matrix-filler interfacial area affecting the molecular mobility of the structure and consequently film properties. The work showed that magnetic NPs functionalized or did not interact with the film matrices as confirmed by changes in their thermal properties.
Fe_3O_4 NPs mixed with AM-based films increased their WVP, probably because they broke the entanglement of AM-chains, but this effect was reduced by adding Fe_3O_4-APTES NPs since the functionalization avoided NPs aggregation originating more homogeneous and compact film structures. A similar effect was observed when cellulose nanocrystals (CNC) and nanofibers (CNF) were used as nanofillers in AM-based films as reported in a work in this thesis. High concentrations of both CNC and CNF increased film WVP since they increased AM-chains mobility easing the transition of water molecules through the matrices.
The addition of NPs to APs-AM-based films increased their thermal stability in most of the analyzed samples as observed by thermal analyses. Interactions between NPs and polymer matrices were suggested from the differential and DSC curves for all the films considered, resulting in a thermoprotective effect on glycerol component in AM100-based films containing Fe_3O_4 NPs and APTES-modified NPs, in an increasing of the thermal stability for blended films containing Fe_3O_4-APTES NPs and in its more slightly improvement in APs100-based films containing APTES-modified NPs.
All these works demonstrated the great potential of using polysaccharides and proteins as biopolymers for bioplastics production, mixing them with eco-friendly additives and thus exploiting them in several applications. Now an industrial scale-up could be planned to confirm the possibility of substituting plastics of petrochemical origin with them.

7. APPENDIX

7.1 PAPERS PUBLISHED IN COLLABORATION

- *Enzyme Assisted Food Processing*
  Michela Famiglietti, Seyedeh Fatemeh Mirpoor, C. Valeria L. Giosafatto, and Loredana Mariniello
  DOI:10.1016/B978-0-12-823960-5.00030-5

- *Functionality of Films from Nigella sativa Defatted Seed Cake Proteins Plasticized with Grape Juice: Use in Wrapping Sweet Cherries*
  Dana Yaseen, Mohammed Sabbah, Asmaa Al-Asmar, Mohammad Altamimi, **Michela Famiglietti**, C. Valeria L. Giosafatto and Loredana Mariniello
  DOI:10.3390/coatings11111383

- *Production and Characterization of Active Pectin Films with Olive or Guava Leaf Extract Used as Soluble Sachets for Chicken Stock Powder*
  Mohammed Sabbah, Asmaa Al-Asmar; Duaa Younis, Fuad Al-Rimawi, **Michela Famiglietti** and Loredana Mariniello
  DOI:10.3390/coatings13071253

- *Hemp (Cannabis sativa) seed oilcake as a promising by-product for developing protein-based films: Effect of transglutaminase-induced crosslinking*
  Seyedeh Fatemeh Mirpoor, C. Valeria L. Giosafatto, Rocco Di Girolamo, **Michela Famiglietti**, Raffaele Porta
  DOI: 10.1016/j.fpsl.2021.100779

- *A Comparison of Cellulose Nanocrystals and Nanofibers as Reinforcements to Amylose-Based Composite Bioplastics*
  Marwa Faisal, Marija Žmiri´c, Ngoc Quynh Nhu Kim, Sander Bruun, Loredana Mariniello, **Michela Famiglietti**, Heloisa N. Bordallo, Jacob Judas Kain Kirkensgaard, Bodil Jørgensen, Peter Ulvskov, Kim Henrik Hebelstrup and Andreas Blennow
  DOI: 10.3390/coatings13091573

Enzyme Assisted Food Processing

Michela Famiglietti[#], Seyedeh Fatemeh Mirpoor[#], C. Valeria L. Giosafatto[*], and Loredana Mariniello, Department of Chemical Sciences, University of Naples Federico II, Naples, Italy

© 2023 Elsevier Inc. All rights reserved.

Key Points

- Many enzymes of different origin are exploited for food processing
- Enzymes are used for influencing food organoleptic and technological properties
- Enzymes may improve food safety
- Some of food enzymes have been so far investigated only at laboratory level

Abstract

Enzymes are biological catalysts able to accelerate chemical reactions in living organisms. Their characteristics to act at low concentrations together with specificity, are important features that make them suitable industrial tools. The present paper deals with the main enzymes exploited in food sector. These enzymes may be easily purified from plants, animal tissues, and microorganisms. They are currently used in bread, wine, beer, juice, dairy and meat processing for improving the food safety, i.e., immunogenicity and allergenicity and enhancing the technological and organoleptic properties of the food products in which they are involved. However, although some of them have already been used for centuries in the food industry, like the milk coagulating chymosin for cheese manufacturing, there are many others only still investigated at laboratory level, for which it would be worth an industrial scale up. Nevertheless, that would be possible following advises from food authorities.

[#]Equally contributing authors.
[*]Corresponding author

Introduction

Enzymes are proteins that enhance biochemical reactions and are normally used to speed up and/or target specific chemical reactions. They can be purified from different sources, from plants to animals, and they can be obtained also by fermentation from microorganisms, including genetically modified microorganisms (Fig. 1). The enzymes are used and exploited in the food sector to improve the quality of foods as well as to enhance the safety and the efficiency of the production process (Fernandes, 2010). Their employ in different industrial sectors is considered sustainable as they can reduce the need of harsh chemical-based processing, thus, leading to a benefit for the environment together with a less potential toxicity. In addition, the enzymes normally operate under mild conditions, like low temperatures, neutral pH and normal atmospheric pressure, which consequently results in low energy consumption.

Food enzymes (Table 1) are included in the EU list of authorized food enzymes when they are not harmful for consumers; there is a technological need for their use, and their use does not mislead consumers. The inclusion of food enzymes in the EU list will be carried out in accordance with the procedures laid down in Regulation (EC) No. 1331/2008 (https://eur-lex.europa.eu/legal-content/EN/TXT/?uri=celex%3A32011R0234) and with the implementing rules set out in Regulation (EU) No. 234/2011 (https://eur-lex.europa.eu/legal-content/EN/TXT/?uri=celex%3A32011R0234), which specifies the general provisions on data required for risk assessment and risk management of food enzymes. Enzymes are able to modify and improve the functional, nutritional and sensory properties of ingredients and products, and, hence, they have found widespread applications in processing and

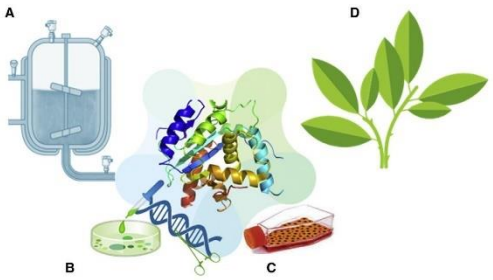

Fig. 1 Different sources of food enzymes (A) bioreactor for microorganism fermentation, (B) genetically modified organisms, (C) animal tissues, (D) plants.

Table 1 Enzyme classification

EC	*Enzyme common name*	*Examples of enzymes*[a]
1	Oxidoreductases	Catalase
		Peroxidase
		Laccase
		Glucose oxidase
2	Transferases	Transglutaminase
		Transaminase
3	Hydrolases	Asparaginase
		Naringinase
		Esterase
		Lipase
		Cellulase
		Amylase
		Pectinase
		Xylanase
		Protease
		Lactase
4	Lyases	A-acetolactate decarboxylase
5	Isomerases	Glucose isomerase
		Triosephosphate isomerase
6	Ligases	DNA ligase
		Argininosuccinate synthase

[a]In red enzymes exploited in food processing.

production of all kinds of food products. The enzymes exploited in the food sectors are several and there are many researchers that investigate their application for different kinds of foods, such as juices, meat, fish, beer. The breakdown of plant cells to help extraction of the vegetable oil, the removal of pectins from fruit juice in order to produce clear fruit juices by pectinase (Nighojkar et al., 2019), the acceleration of beer fermentation, conversion of starch to sugar for alcohol production by amylase (Toksoy Oner et al., 2005), the curdling of milk in order to produce cheese by chymosin (Kumar et al., 2010) and also the reduction of acrylamide in cooked products (Jiao et al., 2020) by asparaginase are only few examples of activities mediated by food enzymes currently exploited by the scientists (**Fig. 2**). However, the utilization of free enzymes in industrial operations is often limited by their high cost, low stability under extreme industrial settings, and high amount requirements (Xie et al., 2022). Potential applications of enzymes in the food industry include assisted extraction processes for nutritional compounds and for increasing the concentration/production, stability, efficient recovery, etc.

Enzyme immobilization is one of the strategies developed to tailor and enhance the enzymological characteristics, including catalytic activity, selectivity, specificity and stability toward wider range of pH, temperatures and solvents, as well as reusability, and so on (Bilal et al., 2019; Taheri-Kafrani et al., 2021) (**Fig. 1**). An immobilized enzyme is defined as one that is attached to an inert and insoluble support material while still maintaining enzymatic activity (Xie et al., 2022). In this chapter the main enzymes used for food processing are reported ranging from different points of view regarding the type of food product and also the type of modification produced. Special attention is paid to the crosslinking enzyme microbial transglutaminase for its known ability to modify the structure and the biological properties of proteins and peptides founds in foods. For example, it is demonstrated that this enzyme is able to influence the structure (Al-Asmar et al., 2019), the digestion (Giosafatto et al., 2012; Romano et al., 2016, 2019; Mariniello et al., 2007; Xing et al., 2019, 2020, 2021) and allergenic potential (Porta et al., 2013) of many food proteins as well as also to change the structure of the prion protein, the main agent of transmissible spongiform encephalopathies affecting humans and animals, by leading to the formation of intra-molecular crosslinks making the protein more prone in amyloid formation compared to the unmodified one (Sorrentino et al., 2012).

Microbial Transglutaminase

Transglutaminases (TGs) (EC 2.3.2.13), i.e., protein-glutamine γ-glutamyltransferase, are multi-functional, pleiotropic enzymes, expressed ubiquitously and extensively in living organisms being active in all mammalian tissues, in invertebrates, plants, yeasts as well as in bacterial cells (Mirpoor et al., 2022; Giosafatto et al., 2020). For industrial purposes, special attention should be given to a microbial TG, isolated for the first time in 1989 from a strain of *Streptomyces mobaraensis* (formerly classified as *Streptoverticillium mobaraense*). This isoform (mTG) is widely used as a biological glue in biomedicine, biotechnology, and food sector. The enzyme, easily purified from the culture medium of *S. mobaraense* (Yokoyama et al., 2004), is a single-chain protein with a low molecular weight of approximately 38 kDa and isoelectric point of 8.9 (Yokoyama et al., 2004). The active site of mTG is constituted by the residue of cysteine, histidine, and aspartic acid or asparagine. mTG possesses peculiar features that make it different from the other isoforms. Contrary to TGs of animal origin, mTG does not need calcium ions for its activation. This characteristic is particularly desirable in the applicative sector since the presence of calcium may let to precipitation of the proteins.

This enzyme is used for changing the texture and several technological properties of protein rich foods like legumes, eggs, cereals, fish etc. In the following paragraph an overview of the most popular food products recently modified by such enzyme is reported.

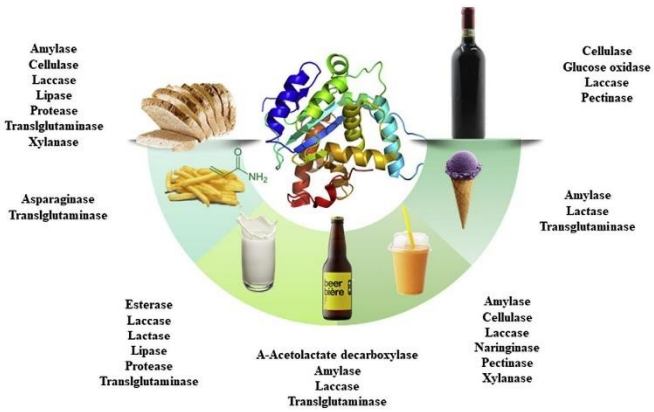

Fig. 2 Common items in which the food enzymes are mainly exploited.

Gluten-Based Products

Gluten is found in cereals such as wheat, barley and rye. Some people are genetically predisposed to gluten intolerance, so there is a growing demand for gluten-free bakery products with high quality proteins. Replacing gluten represents a technological challenge, as it requires the use of additives, primarily hydrocolloids or enzymes, to improve the mechanical properties of dough. Castillejos et al. (2018), evaluated the effect of mTG on the chemical properties of sorghum bread enriched with quinoa. Bread was prepared by mixing, fermenting and baking sorghum flour (80%) and quinoa flour (20%), with the addition of 0.5% mTG. Control bread with no added enzyme was prepared too. The results showed that the content of protein (14.61%), fiber (16.04%), minerals (2.45%) and carbohydrates were higher in the mTG-containing bread, while the fat content was higher in the bread without the enzyme (14.14%). The analysis of textural parameters such as chewiness, gumminess and cohesiveness showed a significant difference in the mTG bread. These results suggest that adding mTG to sorghum-quinoa bread improves its nutritional properties by increasing its content of protein and fiber, resulting in a gluten-free product of high nutritional value. Some studies found out that the use of sourdough together with mTG improved the viscoelastic properties of bread (Scarnato et al., 2017). It is worth to say that mTG protein crosslinking did not affect antibody-binding capacity, in fact, no immunological changes of gliadin extract from pasta dough treated with mTG using the sera of patients affected by celiac disease was detected (Ruh et al., 2014). Moreover, transamidation of wheat flour with a food-grade enzyme and an appropriate amine donor can be used to block T cell-mediated gliadin activity and to prevent cereal toxicity (Rizzello et al., 2007).

Legume-Based Products

As far as legumes many efforts have been carried out to use the proteins contained in them as substrate of mTG. One of the most recent objectives is to prepare novel foods by mixing different kind of sources, such as legumes and wheat to prepare novel foods. For example, some efforts have been done to prepare free gluten pasta. In this regard Ertaş et al. (2022) used three different ingredients (lentil flour (LF), egg white powder (EWP) and whey powder (WP)) and three different additives (hydroxypropyl methylcellulose (HPMC), xanthan gum (XG) and (mTG)) in gluten-free pasta and their effects on different properties were analyzed. They found out that mTG was effective on modifying the pasta products in which EWP was treated my means of mTG producing a kind of product quite acceptable by panelists.

Soybean (*Glycine max*) is one of the most prevalently grown and used oilseed crop. It is utilized especially in the Eastern countries as human and animal food, ingredients as well as precursor materials. The main proteins found in soybean comprise glycinin, beta-conglycinin, soybean vacuolar protein, and Kunitz trypsin inhibitor, all, except the latter, acting as mTG substrate. This aspect led many scientists to prepare different products, from edible films to novel foods, by using mTG-modified soy proteins. In fact, way back in 2003 Mariniello et al. found out that the modification by means of mTG of the proteins present in soy flour gave rise to edible materials, prepared by casting, with improved technological attitude. On the other hand, quite recently, the same authors published some papers on the preparation of a bio-tofu made of a mixture of soymilk and cow milk. The mixture was made by using two kinds of coagulants, lactic acid bacteria and mTG. It seemed that the presence of lactic acid bacteria improved the mTG-mediated modification of the proteins creating a dense and fine gel network with an increased storage modulus (G') (Xing et al., 2020). Subsequently the same authors (Xing et al., 2021) also demonstrated that the treatment with both the enzyme and lactic acid bacteria also affected the allergenicity of soy proteins by reducing their antibody reactivity. Therefore, the authors speculated that mTG added together with lactic acid bacteria might be useful to create hypoallergenic soy protein-based products (Xing et al., 2021).

Egg-Based Products

In 2012 Giosafatto et al. studied the effect of mTG on the rheological and digestion properties of ovalbumin, the main protein in the albumen, when the latter were modified by the microbial enzyme. They have demonstrated that mTG was able to extensively modify the protein by intra-and inter-molecular crosslinking when the protein was heat denatured leading to the formation of macroscopically strong gels. The derived gels were characterized by a well-developed viscoelastic gel network with higher modulus and lower phase angle values. The biopolymers obtained after mTG treatment were more resistant to both gastric and duodenal digestion carried out under physiological conditions (Giosafatto et al., 2012). These results were quite similar to those obtained by Alavi et al. (2020), who investigated the impact of mTG-mediated crosslinking on the thermally denatured egg white proteins produced under alkaline pH in relation to their gelling properties. Unlike native proteins that did not act as a good substrate for mTG due to their compact structure, SDS-PAGE and gel solubility data showed that the denatured ones were sufficiently crosslinked by mTG. As matter of fact, mTG significantly increased the gel strength, fracture stress, fracture strain, as well as the texture profile parameters and decreased the frequency dependence of elastic modulus and stress dependence of creep compliance of the denatured protein-based gel. However, the authors speculated that the enhanced mechanical properties of the thermally denatured gelled samples treated with mTG may be suitable for delivering sensitive compounds as well as in fabricating tailored scaffolds, rather than in food sector, in tissue engineering and biomedical products (Alavi et al., 2020). In 2013 Porta et al. demonstrated that the only glutamine residue present on ovomucoid chain, another protein of the albumen, was able to act as an acyl donor substrate for the enzyme mTG and, as a consequence, to give rise to a covalent monodansylcadaverine conjugate of the protein in the presence of both enzyme and the diamine dansylated derivative. It is worthy to point out that this protein is a trypsin

inhibitor, and it is considered one of the most allergenic proteins of the albumen. It was demonstrated that the obtained structural modification following mTG treatment of ovomucoid significantly reduced the capability of the protein to inhibit trypsin activity, also having impact on its *anti*-ovomucoid serum-binding properties (Porta et al., 2013).

Wheat-Based Products

Shahsavani Mojarrad et al. (2017) investigated textural and microstructural properties of composite prepared by mixing wheat flour and high amylose corn starch (Hylon VII) with mTG at different concentrations and temperatures. The results showed that by increasing the starch content, the firmness increased, and adhesiveness decreased. Indeed, high level of amylose and crosslinking induced by mTG enhanced the gel elasticity and reduced adhesiveness (Shahsavani Mojarrad et al., 2017).

On the other hand, Gharibzahedi et al. (2019) discovered that mTG had a great influence on developing noodles and pasta by modifying the crystallinity or molecular structure via covalent crosslinks between protein molecules and, hence, by strengthening the dough stability and the textural characteristics of final products. Compared with the control samples, the mTG-supplemented products indicate slower digestion rates and better sensory and cooking properties without any remarkable color instability.

Fish-Based Products

There are plenty of papers about the manufacture of fish-based products prepared in the presence of mTG, the fish proteins acting as effective substrate of mTG (Chen et al., 2021). In particular, many studies focused on surimi, a concentrated myofibrillar protein made from fish flesh prepared by mincing, washing and other processes. Surimi-based products are formed by a gelation process, in which myofibrillar proteins undergo denaturation, followed by association, resulting in a unique textural property. Recently An et al. (2021) demonstrated that the mTG-induced crosslinking reaction can enhance the textural properties of surimi gels. However, when the crosslinking degree exceeds a certain range, surimi gels become brittle, giving the gel a special mouthfeel.

In addition, Chen et al. (2021) have prepared strong fish gelatin hydrogels by double crosslinking gelatin with mTG and κ-carrageenan. They found out that both the mechanical and thermal properties of gelatin hydrogels were greatly enhanced. The obtained results indicated that the gel strength, compression fracture stress and storage modulus of the double crosslinked gelatin hydrogels all reached the largest value when the concentration of mTG was 20 U/g gelatin. These data are of a great significance for expanding the application of natural polymer-based products. Another study (Tokay et al., 2021) underlines the possibility to increase the consumption of seafood by using mTG for optimizing the quality, in terms of shelf life and hardness, of restructured fish products from the meat of European seabass (*Dicentrarchus labrax*). In this study the authors have also found out, besides the concentration of mTG, the best conditions regarding the pressure weight and setting time in order to obtain a ready to eat seafood product. In particular, they have demonstrated that 0.32% mTG, 17.5 h of setting time and 3.56 gf/cm^2 of pressure weight were the optimal processing parameters (Tokay et al., 2021).

Meat-Based Products

Myofibrillar proteins (MP) such as myosin, actin, tropomyosin and troponin muscle contribute to the physicochemical properties of final meat products. mTG has been used so far specially for increasing the textural features and gel strength of the meat-based products (Bourneow et al., 2012).

In fact, meat contains high levels of proteins such as actin and myosin that constitute the majority of myofibrillar proteins able to be polymerized by mTG and this leads to an improvement the textural properties of gel structured meat products (Tseng et al., 2002). In particular, mTG plays an important role in heat stability, gel-formation capability, water-holding capacity, emulsification and nutritional properties of meat foods. Uran and Yilmaz (2017) investigated the influence of mTG on the quality characteristics of chicken burgers. The enzyme was added at 5 different concentrations (0.2%, 0.4%, 0.6%, 0.8% and 1%). The enzyme addition did not cause changes in the nutritional aspects (ash, fat, protein) of the products nor in their sensory properties. However, there was a significant decrease in the cooking loss and a significant increase in the texture values supported by means of Scanning Electron Microscopy (SEM) images, thank to which it was possible to see a more strengthened microstructure in the presence of mTG. Very recently some scientists investigated the possibility to use mTG and fibrinogen/thrombin protein isolate (FB) on the oxidative stability and the residual nitrite level in thermally processed ground beef during cold (4 °C) storage (0, 1, 7, 15, 30 days). They found out that the treatment of the cold set ground beef with 10% FB or 1% mTG was able to reduce the cooking loss and lipid oxidation and at the same time to enhance the meat textural properties. Nevertheless, the best result they obtained was the decrease of residual nitrite levels that are formed when sodium nitrite is added to the meat. Such result seems quite interesting as it may lead to a reduction of the use of sodium nitrite, normally used by food industries as an additive for meat, that may react with secondary amines in the product or in acidic conditions in the stomach to form nitrosamines, which are carcinogenic (Masuda et al., 2000).

Milk-Based Products

Caseins represent about 80% of the bovine milk proteins and, together with calcium phosphate, constitute the so-called casein micelles. Caseins can be classified in four different types: αS1-casein, αS2-casein, β-casein, and k-casein. They are known as proteins poor in tertiary structure that do not have a well-defined secondary structure as well. These characteristics are responsible for their

flexibility that makes them excellent substrates for mTG. On the other hand, whey proteins (β-lactoglobulin and α-lactalbumin) present a very compact and globular structure that make them poor substrate of mTG. In fact, enzymatic crosslinking can take place after denaturation promoted by heating, reducing agents, increasing pH, or recurring to high hydrostatic pressure as these treatments expose internal aminoacid residues and reduce disulphide bonds rendering the proteins susceptible to the enzyme-mediated modification.

Romeih and Walker (2017) have recently published a list of patents where mTG has been used to prepare dairy products. The interest, both at research and applied levels, is due to the importance of dairy products at commercial level, since in the Western countries, there is a high demand of this kind of foods. Recurring to the use of mTG results in higher cheese yield and improves texture and water-holding capacity of soft cheeses. In addition, Belén García-Gómez et al. (2020) reported that cheeses obtained using mTG were less grainy, more soluble, creamier and showed a greater milk intensity and fresh cheese aroma. Furthermore, the authors demonstrated that mTG was able to modify sensory properties of cheese traditionally coagulated with animal rennet. In ice creams, mTG was shown to improve aeration and foam stability. The consistency, a rheological measurement of a fluid viscosity, is influenced by protein polymerization, and, since ice cream displays a pseudoplastic behavior, a limited amount of cross-links are required to reach the desired consistency (Gharibzahedi et al., 2018). mTG has been also extensively used in yoghurt production, mainly to prevent syneresis since the enzyme has a positive impact on water-holding capacity of the milk gel (Motoki and Seguro, 1998; Yokoyama et al., 2004; Bönisch et al., 2007). In this respect, García-Gómez et al. (2019) underlined the effect of the microbial enzyme in improving the texture properties of yogurt with the advantage to avoid the addition of milk protein or other additives into the product, decreasing production cost with the same overall acceptability by consumers. It is worth to report a paper from Fotschki et al. (2020) who use mTG to crosslink the proteins from horse milk (HM) and cow milk (CM). HM could be considered a substitute for CM especially for people who suffer from CM allergy. They demonstrated that following the treatment with mTG which leads conformational changes in proteins, modulates the exposure of CM and HM protein epitopes and their recognition by elements of the immune system. In fact, by utilizing the highest amount of enzyme they were able to increase the immunoreactivity of α-CN and to decrease the immunoreactivity of β-lactoglobulin, in both HM and CM. However, after digestion carried out under physiological conditions (Giosafatto et al., 2012), HM was characterized by 2.4-fold lower average IgE and 4.8-fold lower IgG reactivity than CM with patients' sera. The authors envisaged the application of crosslinking with mTG to reduce the allergenicity of some milk proteins and might be useful in producing "allergoids" for desensitization immunotherapy during individualized designed treatment (Fotschki et al., 2020). In another paper from Xing et al. (2021) the allergenic potential of β-lactoglobulin was reduced in a system formed of cow milk and soymilk-cow milk mixture to which mTG and lactic acid bacteria were added. LAB combined with mTG enhanced the polymerization of the cow milk protein. Besides the authors' results demonstrated that the microbial enzyme was able to reduce the antigenicity of β-lactoglobulin envisaging the possibility to use lactic acid bacteria and mTG as coagulant for preparing new food products (Xing et al., 2021).

Catalase and Peroxidase

Catalases and peroxidases are ubiquitous heme enzymes that catalyze the removal of hydrogen peroxide (H_2O_2). Both enzymes use one molecule of hydrogen peroxide to form a high valent iron intermediate called "Compound I" (Cpd I). However, whereas catalase Cpd I oxidizes a second H_2O_2 molecule to oxygen, peroxidases use this intermediate to oxidize other substrates rather than H_2O_2. The importance of these two enzymes in the industry, especially in the food sector, resides in the fact that H_2O_2 is dangerous for the cells. Catalase (E.C.1.11.1.6), that is the first antioxidant discovered enzyme, is a bleaching, or sterilizing agent (Mhamdi et al., 2010). The enzyme normally utilized is from bovine liver or microbial sources (Mir Khan and Selamoglu, 2020). Currently, there are at least eight strains that can produce catalases (Liu and Kokare, 2017): *Penicillium variabile, A. niger, S. cerevisiae, Staphylococcus, Micrococcus lysodeikticus, Thermoascus aurantiacus, Bacillus subtilis, and Rhizobium radiobacter*. It is employed in the food industry, especially for egg processing, along with other enzymes. For example, quite recently EFSA (2021) reported the production of catalase enzyme from a genetically modifies *Aspergillus strain* and its potential use for treating eggs (fresh whole egg, egg white and yolk). The food enzyme remains in the final pasteurized egg products that will be further used for production of different foods including bakery products and mayonnaize. With their data and the results about margin of exposure (MoE) the panels were able to conclude that the food enzyme catalase produced by use a transgenic *Aspergillus* strain does not give rise to safety concerns under the intended conditions of use. The enzyme can be used in a limited amount also in cheese production. In fact, in some cases it is used for eliminating the H_2O_2 residues normally utilized for cheese bleaching or sterilization (Kang et al., 2012). As hydrogen peroxidase may obstacle the bacterial growth necessary for cheese processing, it is eliminated by using catalase enzyme (Mir Khan and Selamoglu, 2020). EFSA (2017) took into consideration the one obtained from hulls of soybeans (*Glycine max*) utilized for baking processes. As far as peroxidase (EC 1.11.1.7) Revanappa et al. (2014) investigated the influence of the horseradish peroxidase on arabinoxylans isolated from whole wheat flour and textural parameters of whole wheat flour dough were studied. By treating the dough with the enzyme an enhancement in dough hardness was observed, besides the arabinoxylans isolated from peroxidase treated dough were shown to possess higher molecular weight, viscosity, arabinose to xylose ratio, ferulic acid, and protein contents as compared to that of untreated dough. EFSA (2017) took into consideration the one obtained from hulls of soybeans (*Glycine max*) utilized for baking processes. As soybean- and soybean hull contain different allergens, the panels investigated the allergen potential of this food enzyme and following biochemical investigations such peroxidase may contain allergenic soybean proteins that may create adverse reactions to individuals susceptible to this legume.

α-Acetolactate Decarboxylase

The use of the enzyme α-acetolactate decarboxylase (EC 4.1.1.5) allows the acceleration of beer fermentation/maturation because it avoids the diacetyl formation. In fact, during beer production process, diacetyl is formed by spontaneous but slow oxidative decarboxylation of α-acetolactate, a product of yeast metabolism. Diacetyl at very low level confers a strong off-flavor to beer. Godtfredsen and Ottesen proposed to use α-acetolactate decarboxylase to accelerate the brewing process (1982) as it leads straight to the formation of acetoin (Dulieu and Poncelet, 1999). Dulieu (Dulieu et al., 2000) proposed to both immobilize and encapsulate this enzyme in small spheres of polyelectrolyte complexes. The authors demonstrated, with the help of simulation studies conducted via mathematical modeling approach, that in this way it was possible to accelerate the beer fermentation more efficiently than by using the free α-acetolactate decarboxylase. The advantage of the immobilized enzyme is that it is recoverable and reusable, leading to the reduction of the process costs (Dulieu et al., 2000)

Naringinase

Naringinase (E.C. 3.2.1.40) is a hydrolytic enzyme with the activity of both α-L-rhamnosidase (E.C. 3.2.1.40) and β-D-glucosidase (E.C. 3.2.1.21). It has numerous important applications in the food industries (Singh et al., 2019a,b,c). One of the most important uses of naringinase has been in enzymatic debittering of citrus fruit juices. Among those bitter compounds, naringin, which is a flavanoid-7-O-glycoside, is considered the most responsible for the bitter taste. To mask or control the bitterness on these fruit juices, the food industry has used naringin physical absorption by passing the juice through a food grade synthetic or natural polymers. For example, Housseiny and Aboelmagd (2019) have encapsulated the enzyme in chitosan and alginate polymers. The authors proved that the nano-encapsulated enzyme was much more stable at high temperature than the free one, the latter losing about 92% of its weight at approximately 110 °C as shown by thermogravimetric analyses. The authors concluded that the nano-capsulation process improves the kinetics and operational stability so could be useful as a debittering agent for different thermal processing applications in citrus juices industries (Housseiny and Aboelmagd, 2019). On the other hand Busto et al. (2007) immobilize naringinase from *Aspergillus niger* into a polymeric matrix consisting of poly(vinyl alcohol) hydrogel, cryostructured in liquid nitrogen. They were able to obtain bio-catalytically active beads so that they can re-use the enzyme for six cycles retaining 36% efficacy naringin-mediated hydrolysis in simulated juice (Busto et al., 2007).

Asparaginase

L-asparaginase (E.C.3.5.1.1) hydrolyzes L-asparagine to L-aspartic acid and ammonia, which has been widely applied in the pharmaceutical and food industries. The main field in which the enzyme is exploited is for acrylamide reduction. In 2002, researchers from Sweden discovered high contents of acrylamide in carbohydrate-rich foods subjected to elevated temperatures, highlighting the significant sources of dietary acrylamide intakes (Tareke et al., 2002; Svensson et al., 2003). Acrylamide is formed between reducing sugars such as glucose and L-asparagine due to frying, baking, or grilling starchy foods at over 120 °C in low humidity conditions through a non-enzymatic process called the Maillard reaction (Jia et al., 2021). Acrylamide has adverse effects on human health and has been proven to be neurotoxic, genotoxic, carcinogenic, and toxic to the reproductive system (Corrêa et al., 2021). According to EFSA, foods much more involved in acrylamide production are primarily fried potato products, bakery products, and coffee, and the intake of acrylamide in diets is estimated to be between 0.3 and 1.9 μg/kg body weight (da Cunha et al., 2019). Al-Asmar et al. (2018) proposed the use of hydrocolloid-based coatings such as those formed of grass pea flour prepared in the presence of mTG to control the formation of acrylamide, water retention as well as on oil content of French fries. Zyzak et al. (2003) first reported the application of L-asparaginase for acrylamide reduction in a potato matrix. In addition, Jiao et al. (2020) used recombinant type-I actinobacterial L-asparaginase expressed by *E. coli* to reduce acrylamide in potato chips, whereas L-asparaginase can penetrate through the cell wall weakened by ultrasonic energy according to the patent (Ehrik et al., 2004) which involved its application in fried potato products. It is worthy to mention that Alam et al. (2018) used magnetic nanoparticle-immobilized L-asparaginase to reduce acrylamide in a starch–asparagine food model. L-asparaginase from *Bacillus aryabhattai* was immobilized on magnetic nanoparticles modified with aminopropyl triethoxysilane (APTES) using a crosslinking agent, glutaraldehyde. The immobilized enzyme showed more than a three-fold increase in thermal stability and retained 90% activity after the fifth cycle. Also, coffee significantly contributes to the total acrylamide content in the diet (Mesías and Morales, 2016). The roasting process is the exclusive cause of high acrylamide content in roasted coffee beans. In this respect, Khalil et al. (2021) used fungal L-asparaginase from *Penicillium crustosum* NMKA 511 (PcAsnase) to reduce acrylamide in roasted coffee beans. Green Arabica coffee beans (5 g) were steamed at 100 °C for 45 min and then incubated in PcAsnase (2 U/g of beans) solution at 35 °C at 20 rpm for 1 h, which enabled good access of L-asparaginase to the free L-asparagine inside the beans instead of just on the surface. Compared with the control, the acrylamide content of roasted beans incubated with the enzyme were reduced to 80.7% and 75.8%, respectively. Furthermore, the amount of L-asparaginase used to reduce acrylamide in roasted coffee beans was considered safe based on the result of a cytotoxicity assay (Khalil et al., 2021).

Esterases

Esterases (EC 3.1.1.X), belonging to hydrolase group of enzymes, can be obtained from different sources such as animals, microorganisms and plants (Sharma et al., 2017). Among the different sources of enzyme isolation, the ones isolated from microbes possess favorable functional properties due to the microbe's diversity. It has been reported that microorganisms with esterase activity are spread in oily substances or surfaces such as cheese surface or surfaces that have been exposed to the oil (Lai et al., 2019). *Bacillus pumilis* (Sharma et al., 2016), *Bacillus subtilis* (Kaiser et al., 2006), *Vibrio fischeri* (Ranjitha et al., 2009), *Geodermatophilus obscurus* (Jaouani et al., 2012), *Geobacillus* sp. (Özbek et al., 2014) etc. are examples of microbial species with esterase activity (Torres et al., 2009). Esterase that acts on water soluble substrate, is significantly active and stable at pH around 6 and is responsible for hydrolyzing ester bonds of short-chain acyl residues (<8 carbons) by interesterification, intraesterification and transesterification reactions as well as non-ester bonds such as thiols, amides, and carbamates (Lai et al., 2019; Sharma et al., 2017). Esterases are biodegradable and do not need co-factors, moreover, they have a wide range of substrate and high stereoselectivity that make them a fruitful enzyme for industrial application (López-Iglesias and Gotor-Fernández, 2015; Littlechild, 2015). Esterases have been widely used in several industrial sectors such as pharmaceuticals, food (including dairy products), paper, detergents, animal food, cosmetics and leather (Coughlan et al., 2015). More specifically, esterase plays an important role in food industry, for producing fragrances and flavors as well as modifying the oil and fat content in several fruit juices (Kaur and Gill, 2019; Raveendran et al., 2018). Plant sterols present in vegetable oil are responsible for LDL cholesterol-reducing and possess antioxidant activity (Zheng et al., 2012), hence, they are considered as a functional additive for foods such as dairy products, margarine and mayonnaize. However, microbial sterol esterases (cholesterol esterases) are utilized to develop phytosterol esters in order to overcome the limits of phytosterols such as its low solubility, stability and absorption rate (Villeneuve et al., 2005; Vaquero et al., 2016). To produce an emulsifier with strong hydrophilicity (lysolecithin) that can stabilize the oil in water emulsions like mayonnaize, phospholipases A (aliphatic esterases) it is used to hydrolyze the lecithin of egg yolk (Borrelli and Trono, 2015). Another application of esterase in food industry is flavor development and it is reported that *Starmerella bombicola* lactone acetyl esterase (Ciesielska et al., 2016) can develop macrocyclic lactones that possess musky aroma and considered as a precious aromatic substance. Esterase isolated from *Lactobacillus casei* had been used to increase the flavor and aroma in cheese products by hydrolyzing the milk fat (Choi and Lee, 2001).

Liang et al. (2020) reported that hydrolyzing the ester bond of rosmarinic acid, that crosslinked caffeic acid with 3,4-dihydroxyphenyllactic acid, by feruloyl esterase (FAEs, EC3.1.1.73) isolated from *Bacillus pumilus* leads to the better bioavailability of this polyphenolic acid in human body and higher potential of its application in food industry as a supplement. Moreover, feruloyl esterase isolated from *Lactobacillus acidophilus* has been used to produce ferulic acid from agricultural residues, that can be utilized in food industry due to its antioxidant and anticancer activity (Liu et al., 2021).

Lipase

Another enzyme belonging to hydrolases family is lipase (triacylglycerol acylhydrolases; EC 3.1.1.3) that breaks the ester bonds at a water/oil interface in triglycerides and produce glycerol, fatty acids and partial glycerides (mono- and diglycerides) (Javed et al., 2018; Sanrom'an and Deive, 2017). The most common source of isolating lipase is microbial sources since the cost of microbial lipases production is low at industrial level and it possess high stability and availability comparing to those isolated from plant and animal sources (Borrelli and Trono, 2015; Javed et al., 2018). Industrial application of lipases produced from yeasts and fungi (mainly *Candida*, *Yarrowia*, *Aspergillus*, *Penicillium*, *Rhizopus*, *Rhizomucor*, and *Thermomyces*) are more than those achieved from bacteria (Kocabaş et al., 2021). Lipase activity is dependent on the substrate area rather than its concentration and due to this peculiarity, it can hydrolyze the ester bonds of the insoluble or aggregated long chain fatty acid. The final products of the reactions catalyzed by lipase are affected by the presence or absence of water. Free fatty acid and partial acylglycerols are produced from hydrolysis, alcoholysis, and aminolysis of triacylglycerol ester bonds and triacylglycerol (TAG), diacylglycerol (DAG) or monoacylglycerol (MAG) are formed from esterification reaction of fatty acid and glycerol (GLY) in the presence and absence of water, respectively (Lai et al., 2019). Lipase has several applications in different industries such as pharmaceuticals and cosmetics, food, leather, textile, detergents and paper (Loli et al., 2015; Mouad et al., 2016; García-Silvera et al., 2018; Tomke et al., 2017). In addition, it can be applied in food industries such as dairy, fat and oil, cocoa butter, tea processing, biosensor and flavor and fragrances synthesizing in beverages, bakery foods as well as meat and fish products (Chandra et al., 2020; Mehta et al., 2021). In dairy industry, lipase is used for hydrolyzing the milk fat, modifying the length of fatty acid chain in butter fats and ripening the cheese in order to promote the flavor (Ray, 2012; Karaca and Güven, 2018). In fat and oil industry lipase is utilized to alter the location of fatty acid chains in the glycerides to improve the characteristic of lipids and to obtain value-added products (Titus et al., 2018). It has been reported that microbial lipase is able to develop cocoa butter-type triacylglycerols that possess a melting point around 37 °C by inducing a favorable cooling sensation in the mouth (Ray, 2015). The tea leaves underwent two different type of process that are called orthodox or the Cut-Tear-Curl (CTC) process that leads to the production of high quality and aromatic tea and a tea with less aroma, respectively. Production of tea by CTC process is more economic and enhancing the aroma and flavor in these types of teas can be achieved by means of *Rhizomucor miehei* lipase that breaks the membrane lipids in tea leaves (Chandra et al., 2020). *Candida utilis*, possessing beefy/blue cheese like flavor, produced in the presence of lipase and beef extract/butter oil (Hasan et al., 2006), can be utilized to

produce flavor and aroma in alcoholic beverages (Mehta et al., 2021). The lipase isolated from *A. niger*, *R. oryzae*, *C. cylindracea* is applied in bakery to enhance and control the non-enzymatic browning reactions, prolong its shelf life and improve the flavor, softness and volume of the bread as well (Moayedallaie et al., 2010; Ray, 2012). Isoamyl acetate and methyl salicylate are utilized in confectionery sector such as chewing gums due to their flavor enhancing properties. It is worthy to mention that they are synthesized from the lipases isolated from *Bacillus aerius* and *Geobacillus* sp., respectively (Narwal et al., 2016). In meat and fish industry lipases are applied to eliminate the surplus fat for producing lean meat as well as to develop flavor (Xiao et al., 2018).

Phospholipase can be classified in two groups of acyl hydrolases and phosphodiesterases based on their site of action within the phospholipid molecules. In this regard, phospholipase A1 (PLA1), phospholipase A2 (PLA2), phospholipase B (PLB) and lysophospholipase A1/2 (lysoPLA1/2) belong to acyl hydrolases group and phospholipase C (PLC) and phospholipase D (PLD) are allocated to the phosphodiesterases group (Richmond and Smith, 2011; Song et al., 2005). Phospholipase A1 (EC 3.1.1.32) has been applied in dairy industry to increase the yield in cheese processing due to presence of lysophospholipids that is a surface-active agent that stabilize the emulsion of lipid and water as well as fat and protein retention in cheese processing. This phospholipase hydrolyzes the ester bond of phospholipids into lysophospholipids, free fatty acids and diacylglycerols since they possess high specificity and little or no activity toward di- or triglycerides that results in preventing the flavor defects that caused by releasing the short-chain fatty acids (Lilbaek et al., 2006; Karahan and Akin, 2017; Monsalve-Atencio et al., 2022; Kocabaş et al., 2021). Phospholipase C (EC 3.1.4.3) has attracted a lot of attention in oil degumming by catalyzing the hydrolysis of phospholipids into 1,2-diacylglycerol (DAG) and organic phosphate that results in incrementing the extra oil production (Cerminati et al., 2017; Wang et al., 2021). Furthermore, phospholipase can develop emulsifying lipids trough wheat lipids degradation as well as enhancing the flavor of bakery products through esterification reaction (Mehta et al., 2021). Phospholipases A produces lysolecithin that is considered as a surface-active emulsifier, by hydrolyzing the egg yolk lecithin that can stabilize oil-in-water (O/W) type emulsions, such as dressings and mayonnaise-like products (Borrelli and Trono, 2015). As a consequence of the improved emulsifying properties of egg yolk, the rate of the application of the latter in foods decreases (Chandra et al., 2020; Mehta et al., 2021).

Cellulase

Cellulase can break the β-1,4-glucosidic of cellulose via acid hydrolysis mechanism. However, it is worth to mention that the complete system of cellulase comprised of *endo*-1,4-β-D-glucanase (EC-3.2.1.4), exo-1,4-β-glucanase (exocellobiohydrolase, EC-3.2.1.91), and β-D-glucosidase (β-D-glucoside glucanohydrolase, EC-3.2.1.21). In order to convert cellulose into its monomer reducing sugars a combined action of these enzymes is vital (Kuhad et al., 2011; Sukumaran et al., 2005; Juturu and Wu, 2014). In this regard, during the enzyme hydrolysis, synergistic action of endoglucanase and exoglucanase leads to the formation of small cello-oligosaccharides hydrolyzed by β-glucosidase into simple sugar or glucoses (Sindhu et al., 2016). Cellulase can be originated from several sources and microorganisms (bacteria and fungi) are considered as potential candidates. It is reported that the cellulase obtained from fungi possesses higher ability to penetrate and to utilize the substrate than that obtained from bacteria (Srivastava et al., 2018). The source of cellulase isolation affects on their features such as their optimum pH, solubility, substrate specificity and thermal stability (Bhat, 2000; Parry et al., 2001). Among all the enzymes, cellulases are the third group of enzymes after amylases and proteases that are utilized widely in industries (Sajith et al., 2016). Major cellulase applications are in starch processing, textile, paper and pulp, food industry, extraction of fruit and vegetable juices, animal feed production malting and brewing, waste, management, pharmaceutical industry, protoplast fusion, and genetic engineering (Sulyman et al., 2020). Cellulase is applied in several sectors of food industry including beverage, wine production, bakery and olive oil extraction. Endoglucanases are able to catalyze the hydrolysis of pentosans in wheat flour and as a consequence they enhance the number of soluble pentosans, that play a crucial role in improvement of the elasticity of the dough and quality of the bread according to their high-water holding capacity (Ramesh et al., 2020). Moreover, in the production of the fermented beverages such as beer, cellulase hydrolyzes the glycosidic bonds between β-glucans and produces smaller chains of polymers with lower viscosity in order to prevent the gelatinous precipitate and to improve the malt extraction that leads to the easier filterability and drainage of wort as well as a higher fermentation rate (Singh et al., 2021). Furthermore, the low quality of barley crops due to the seasonal variations can be controlled by using cellulase during malting process (Singh et al., 2021; de Souza and Kawaguti, 2021). In the production of red wine, a combination of cellulase, hemicellulases and pectinases that are called maceration enzymes are applied to improve the extraction of phenolic compounds and color from the cell wall of the grape, filterability and clarification as well as the stability and the overall quality of the wine (Ramesh et al., 2020; Sharma et al., 2017; Toushik et al., 2017). Moreover, cellulase plays a key role in fruit juice processing industry by reducing the viscosity, improving the texture, aroma and flavor, facilitating the extraction and clarification process, reducing and controlling of extreme bitterness in fruit juice especially of citrus fruit as well as releasing the antioxidant compound from fruits and vegetables (Bilal and Iqbal, 2020; Singh et al., 2021). Application of cellulase alone or in combination with pectinase in olive oil extraction has been studied extensively. It is reported that the synergistic effect of cellulase and pectinase can improve the yield of oil extraction by depolymerizing and solubilizing the cell wall of the olives as well as reducing the viscosity of olive paste that leads to interactions among the oil droplets and coalesced them to into larger droplets (Huang et al., 2022). Moreover, cellulase utilization in olive oil industry results in better quality and higher amount of antioxidants in the oil possessing a lower chance of rancidity (Singh et al., 2021). Al-Rousan et al. (2019) reported that the yield of olive oil extraction enhanced 5.25% in the presence of the mixture of cellulase and pectinase (1:1), however this increasing rate was 4.38% and 3.29% in the presence of cellulase and pectinase, respectively.

Pectinases

Pectinases (EC 3.2.1.15) are responsible for catalyzing the degradation of glycosidic bonds in pectic polymers. Pectinases can be grouped based on their substrate preferences, action on pectinaceous substances and mode of action (de Souza and Kawaguti, 2021). Pectinases can be categorized in four different groups based on their preferences of acting on pectin, pectic acid, protopectin, or oligo-D-galacturonate as different substrates. In the other classification of pectinases, according to the cleavage mechanism, they are classified in depolymerases and esterases that possess catalytic action on pectin, polygalacturonic acid, rhamnogalacturonan, respectively (Zhang et al., 2021). Furthermore, they can be sorted in endoenzymes, that cleave randomly leading to depolymerization and liquefaction, and exoenzymes which degrade the terminal ends (Bhardwaj et al., 2017; Ramadan, 2019). The pectinolytic enzymes obtained from fungi, bacteria, and yeast possess a huge diversity, however bacterial pectinase is more preferred among the others. The potential bacteria from which pectinases can be isolated are *Bacillus*, *Pseudomonas*, *Chryseobacterium*, and *Erwinia* (Oumer and Abate, 2018; Roy et al., 2018; Abdollahzadeh et al., 2020). The major and principal applications of pectinases in food industry are especially in the fruit and vegetable juice industry (Raveendran et al., 2018; Prajapati et al., 2021). However, they have multitude applications in the extraction, washing, degumming and retting of plant fibers, extraction of vegetable oil (e.g., olive oil); enhancing the fermentation speed of tea/coffee; and producing alcoholic beverages and other food products of plant origin (Garg et al., 2016; Haile and Kang, 2019; Ramadan, 2019; Ruiz et al., 2017; Sharma et al., 2017; Singh et al., 2019c; Tapre and Jain, 2014).

Pectinase has been applied in juice industry and it is able to reduce the turbidity, viscosity, and consistency by hydrolyzing the structural polysaccharides of fruit or vegetable pulp (Dey et al., 2014; Lu et al., 2016). Furthermore, pectinase can improve the press ability of the pulp, that leads to the enhancement of juice yields through extraction, as well as splintering the jelly structure and stability of the juice (Benucci et al., 2019; Dal Magro et al., 2021). Enzymatic juice clarification is more advantageous comparing to the conventional method due to their high degree of specificity, high catalytic efficiency and slight energy utilization (Lu et al., 2016). It is reported that the application of pectinase to the pulp of the fruits possessing a high amount of soluble pectin, including bananas and papayas, can produce a juice with lower viscosity and facilitate the extraction process by breaking down the pectin (Singh et al., 2019a,b; Tapre and Jain, 2014). In wine production pectinase plays an important role by breaking down the polysaccharides present in the grape cell wall making the clarification and filtration easier, enhancing the quality and stability of the wines and leading to the increment in the extraction of the grape skin pigments as well as polymeric anthocyanins and tannins, that influence the taste and color in wines (Chaudhri and Suneetha, 2012; Jayani et al., 2005; Kawaguti and Koblitz, 2019; Uenojo and Pastore, 2007). In the oil industry, as mentioned above, a combination of pectinase and cellulases simplifies the oil extraction through hydrolyzing the cell wall structural component and consequently enhances the yield of oil extraction and the quality of the obtained oil (Bhardwaj et al., 2017; Kashyap et al., 2001; Kawaguti and Koblitz, 2019; Kohli et al., 2015). It is reported that the pectinases in citrus oil extraction were able to break the pectin–protein complexes and remove the emulsifying properties of the pectin (de Souza and Kawaguti, 2021). For the coffee fermentation the polysaccharidic layer consisting of pectin, starch and cellulose should be removed to prevent the growth of fungi due to the prolonging the time needed for coffee to be dried. In this regard, pectinases are applied to remove the mucilage layer and to prevent the development of astringent flavor in the final product (Bhardwaj et al., 2017; Kashyap et al., 2001; Koshy and De, 2019).

Xylanases

Xylanases (EC 3.2.1.8) that are allocated in the hydrolytic group of enzymes are responsible for cleaving the β-1,4- glycosidic backbone of xylans that are present extensively in hemicellulose (Kaushal et al., 2021). It is worthy to mention that three different subclasses of endoxylanases, exoxylanases and β-xylosidases constitute the xylanase, however, *endo*-xylanases are considered as a major group among these hydrolytic enzymes that randomly breakdown xylan into xylooligomers (Motta et al., 2013). Different sources of xylanases in nature include bacteria, fungus, actinomycetes, protozoans, marine algae, snails, crustaceans, insects, plants and germinating seeds (Sharma et al., 2020). *Streptomyces* sp., *Bacillus* sp. and *Pseudomonas* sp. are the most prominent actinomycete and bacterial species that produce xylanase (Sharma and Chand, 2012). It worthy to say that xylanases from actinomycete and bacterial sources are active in a broader range of pH (5.0–9.0) possessing the optimum activity at temperature between 35 and 60 °C. Fungi are considered as the main source of xylanase extraction according to the high amount of the obtained enzyme as well as extracellular release (Nair and Shashidhar, 2008). *Aspergillus* sp., *Fusarium* sp. and *Penicillium* sp. are the main fungi sources of xylanases extraction possessing a greater activity comparing with those obtained from yeast or bacterial sources (Mandal, 2015). Xylanases were applied extensively in several industries including food, feed, pulp and paper, textiles and bio-fuel due to their hydrolysis potential (Kumar et al., 2017). Moreover, xylanases have multiple application in food industry such as bread and biscuits making as well as juice industry. In bakery industry, xylanase is applied in order to cleave the hemicelluloses such as arabinoxylan and makes them water extractable and solvable that leads to the homogeneous distribution of water in dough matrix and amends the gluten network of the dough. Therefore, xylanase application can enhance loaf volume by delaying the crumb formation as well as the rheological properties quality of the bread (Mandal, 2015; Bajaj and Manhas, 2012). Moreover, xylanase plays an important role in improving the taste, aroma and texture of the biscuits (Raveendran et al., 2018). Xylanase is used in juice industry to improve the extraction, clarification and stabilization process (Camacho and Aguilar, 2003). Juices with high amount of hemicellulose are clarified by means of xylanases that cause the liquefaction and enhancement in the yield of extraction as well as the quality of the obtained juice (Kaushal et al., 2021). In addition, xylanase improves the recovery of aromas, essential oils mineral salts, pigments and vitamins (Raveendran et al., 2018).

Amylases

Amylases are hydrolases that break down glycosidic bonds present in starch molecules producing glucose, dextrins and oligosaccharides (Farooq et al., 2021). They are among the most studied enzymes because of their wide distribution in living systems, from bacteria to plants to humans, and one of the main classes of enzymes exploited for different industrial applications, occupying around 25%–30% of the enzyme market (Sindhu et al., 2017; Elumalai et al., 2019).

According to the way the glycosidic bond is attacked, different types of amylases were identified: exo-amylases and *endo*-amylases. Exo-amylases can hydrolyze exclusively the non-reducing α-1,4 glycosidic linkages of glucose chain or cleave both α-1,4 glycosidic bonds at the non-reducing end and α-1,6 glycosidic bonds; *endo*-amylases hydrolyze randomly the α-1,4 glycosidic bonds present within amylose and amylopectin chains causing the formation of linear and branched chains of different size (Van Der Maarel et al., 2002; Gopinath et al., 2017).

Amylases are mainly classified into three groups: α-amylase (EC 3.2.1.1), a well-known *endo*-amylase that keeps the α-anomeric configuration in the final product (Raveendran et al., 2018); β-amylase (EC 3.2.1.2), an exo-amylase that releases maltose as the final product of its catalytic activity on a linear chain of glucose (Husain and Ullah, 2019) converting the anomeric configuration from α to β (Tiwari et al., 2015); γ-amylase (EC 3.2.1.3) that can cleave the α-1,6 glycosidic linkages on the branched chains and the α-1,4 glycosidic bonds at the non-reducing end of linear chains producing glucose molecules as final products (Tiwari et al., 2015).

In industrial processes, predominantly, α-amylases were obtained by bacteria, fungi and yeasts (Gopinath et al., 2017) because of some important advantages such as high yield, cost-effectiveness, stability, ease of process optimization (Elumalai et al., 2019; Gupta et al., 2003).

Among the most used bacteria, *Bacillus* sp. is predominant (Farooq et al., 2021; Tiwari et al., 2015; Burhan et al., 2003; Razdan and Kocher, 2018) especially for the possibility to produce a thermostable amylase, followed by *Aspergillus* sp. for the fungi kingdom (Souza, 2010; Srivastava, 2019).

β-amylase used for industrial applications was purified from higher plants such as soybean, barley, and wheat (Koide et al., 2011) or from bacterial sources, including thermophiles and halophiles. DNA recombinant technology is being used to optimize the production improving the yield of the enzyme (Duan et al., 2019).

Amylases were involved in the conversion of starch to produce glucose and fructose syrup: after gelatinization α-amylase is responsible for liquefaction of starch into short-chain dextrins while saccharification is carried out by γ-amylase that catalyzes the hydrolysis of α-1,4 glycosidic linkages at the non-reducing end, producing glucose. This process can be improved by the enzyme pullulanase to produce high glucose syrup; finally, a glucose isomerase can convert glucose into fructose obtaining high fructose syrup, used as a sweetener in the beverage industry (Sundarram and Murthy, 2014). Recently, recombinant amylases are also of great interest because of their success in improving yield and accelerating the production processes. An example is the production of a recombinant α-amylase cloned from the thermophilic fungus *Thermomyces dupontii* and successfully overexpressed in *Pichia pastoris* to improve the production of maltose syrup (Wang et al., 2019).

Amylases are also abundantly used in the baking industry: α-amylase hydrolyzes the starch of the flour into small dextrins. The yeast can work continuously during dough fermentation reducing the viscosity and increasing the fermentation rate. In this way, the texture and the volume of the product are also improved (Farooq et al., 2021).

Amylases can improve the shelf life of baked goods: they can retard bread staling, using the hydrolysis of glycosidic bonds, avoiding the recrystallization of amylopectin and the rapid formation of a partly crystalline network of amylose in fresh bread (Haghighat-Kharazi et al., 2018). Anyway, amylases concentration must be kept under control because an excess can have the undesired effect of gumminess (Farooq et al., 2021). Some authors have studied new strategies to improve the stability of these enzymes during preparation, fermentation, baking, and storage of bread, for example, with innovative techniques of microencapsulation to improve the shelf life of gluten-free bread, much more susceptible to staling (Haghighat-Kharazi et al., 2018).

Amylases are also used for clarification of beer and fruit juice: light beer is produced mainly by adding glucoamylase to the wort before or during fermentation. This enzyme can transform dextrins into fermentable sugars and reduce the alcohol content and calorific value. In the last years, genetically engineered yeast strains with amylolytic genes were used to metabolize these carbohydrate residues and have a better fermentability (Blanco et al., 2014).

Proteases

Ubiquitously distributed in all living systems and involved in many aspects of cell and organism functions, proteases (E.C.3.4.X.X) represent a large group of hydrolytic enzymes (Ward, 2011).

They are classified by their site active structure and by the mechanism of their catalytic activity into eight groups: aspartate, cysteine, glutamate, metal, mixed, serine, threonine, and unknown (Contesini et al., 2018). Proteases break down proteins by hydrolysis of the peptide bonds: in serine, threonine and cysteine proteases, the enzyme forms a complex with the substrate followed by the release of carboxylate and amine products; aspartic, glutamic and metalloproteases catalyze the nucleophile attack by an activated water molecule that allows the hydrolysis of the peptide bond (Agbowuro et al., 2018). The production of proteases from microorganisms is preferred in industrial applications for the ease and the velocity of the process in respect to mammalian and plant cells. Microorganisms can produce extracellular enzymes making easier the downstream processing and reducing the costs (Contesini et al., 2018). The most prominent group of protease bacteria producers is the genus *Bacillus* (Contesini et al., 2018;

Razzaq et al., 2019), followed by many other organisms as the fungal genera *Aspergillus, Humicola, Penicillium, Rhizopus* (Razzaq et al., 2019; Singh et al., 2016). Microbial proteases are used in the food industry for a vast range of applications. They can modify some properties of food proteins improving important characteristics of the final products as digestibility, nutritional value, flavor, and allergenic compounds presence. They are also used to check coagulation, foaming, emulsification of food proteins (Pardo et al., 2000).

In the bakery industry, proteases are used to impact on gluten network: with the addition of proteases the reduction of the mixing time, the decreasing of dough shrinkage, and the increasing of dough uniformity during the preparation of some products were obtained (Goesaert et al., 2005).

Moreover, it was shown that proteases can degrade gluten and other proline peptides into small fragments reducing to an acceptable level their immunogenicity (Rizzello et al., 2007). Anyway, the quality of these products is lower relative to the rheological characteristics of the final products and should be improved with other additives (Heredia-Sandoval et al., 2016).

The main application of proteases in the dairy industry is in the manufacture of cheese. Although conventionally animal rennet is being used as a milk-clotting agent for the hydrolysis of specific peptide bonds to obtain para-k-casein and macro peptides, the increasing demand pushed to look for other effective alternatives, such as microbial rennet. Nowadays microbial rennet occupies 70% of the cheese production in the dairy industry in the USA and 33% worldwide (Ismail et al., 2019).

Proteases are also used to improve the quality of fermented milk products, for example, to enhance their flavor because by means their activity single amino acidic residues are secreted from oligopeptides. Moreover, because of the potential immunogenicity of many proteins presents in milk products some studies focused on the possibility to produce hydrolyzate proteins milk using endopeptidases, thus reducing the immunologic response in a person predisposed to that (Osborn et al., 2018).

The fermented dairy products and other kinds of by-products deriving from food processing can be used to produce bioactive peptides by microbial proteases-mediated hydrolysis. These small protein molecules with less than 20 aminoacidic units exhibit a lot of health benefits such as antihypertensive, immunostimulant, antimicrobial and antioxidant activities and can find applications in the different industrial fields, from the nutraceutical to food industry (Chew et al., 2019).

Proteases are usually used for meat tenderization as a method to improve meat quality. The proteolytic enzymes can break down the proteins in muscle and hydrolyze collagen and elastin when they are mixed with meat. For this application, among the most used proteases papain, bromelain, actinidin, cucumisin, and ficin derive from plants while aspartic protease and subtilisin are enzymes produced from *Aspergillus oryzae* and *Bacillus subtilis*, respectively. The last presents less efficient hydrolytic activity in myofibrillar proteins with respect to plant enzyme while in the hydrolysis of collagen their activity seems to be intermediate with respect to that of papain and bromelain (Arshad et al., 2016).

Laccases

Laccase (benzenediol: oxygen oxidoreductase, EC 1.10.3.2) is considered a green tool because it can perform the catalysis process using molecular oxygen as the only co-substrate and releasing water as a by-product (Mayolo-Deloisa et al., 2020). Laccase belongs to the blue multicopper oxidases and it is characterized by the presence of at least four copper ions, distributed in three cupper centers Type 1 (T1), Type 2 (T2) and binuclear Type 3 (T3α-T3β) in its active site (Sitarz et al., 2016). It can catalyze the oxidation of an array of different substrates, such as phenols, polyphenols, benzenethiols, polyamines, hydroxyindoles and aryldiamines (Sitarz et al., 2016), performing the four electrons reduction of molecular oxygen to water (Jones and Solomon, 2015). Laccase has been found in plants, fungi, some insects and a few bacteria but most biotechnologically used laccases derive from fungi (Nunes and Kunamneni, 2018). Until now more than 150 laccases have been fully characterized: the most studied derive from white-rot fungi as *Agaricus bisporus, Trametes versicolor, Pleurotus pulmonarius*, while plant laccase is less studied (Nunes and Kunamneni, 2018).

Naturally, laccase is an extracellular enzyme secreted by fungi to degrade the lignin in the wood and access to cellulose and hemicellulose. The enzyme is, generally, produced during fungi secondary metabolism (Brijwani et al., 2010).

In the food industry, laccases can improve the functionality of food processing including baking, juice manufacturing, wine, and beer stabilization, improving fermented milks.

Thanks to the oxidizing effect on the constituents of dough, laccases are used in bread manufacturing to improve the strength of gluten structure and the dough consistency, increase volume, stability, and softness of the goods baked and reduce stickiness. The effect of dough strengthening was suggested to be due to the ability of the laccase to crosslink the esterified ferulic acid on the arabinoxylan fraction of dough that results in a strong arabinoxylan network (Selinheimo et al., 2006).

In wine production, laccase finds an important application because it is used to remove the undesirable effects of polyphenols on the organoleptic characteristics of wine. Polyphenols are responsible for discoloration, haze, and flavor changes of wine which is referred to as maderization. Polyphenols removal by chemical methods, such as the addition of polyvinylpolypyrrolidone (PVPP) and high doses of sulfur dioxide, is normally carried out to prevent this phenomenon. Laccase treatment is selective, feasible, and ecological, anyway, the enzyme cannot be used as a food additive but its immobilization is a suitable alternative to the improvement of must and wine preparation, to increase their storability and reduce processing costs (Blue et al., 2021). Also, for the storage of beer, factors such as haze formation should be under control together with oxygen content and temperature. In this case, the presence of small quantities of polyphenolic compounds as proanthocyanidins can cause the precipitation of proteins that promotes haze formation (Brijwani et al., 2010). Laccase treatment can improve the storability of beer using the oxidation of polyphenols. It has also been used for the removal of oxygen at the end of the beer production process (Dhillon et al., 2012).

Laccase has been also used to improve the viscoelastic properties of skimmed milk yogurt by crosslinking of milk proteins: one of the main aims of the dairy industry is enhancing the consistency of fermented milks, such as yogurt, and reduced structural losses in post-processing steps (Struch et al., 2015).

The crosslinking activity of a laccase mediator system (LMS) was even suggested to be suitable in curd manufacture with improvements in yield and even antioxidant properties: a recombinant system made up from a purified laccase from the fungus *Pleurotus eyngii* expressed in *Saccharomyces cerevisiae* with three polyphenolic mediators was investigated to verify the effect of milk protein crosslink induced by an LMS on curd preparation and its antioxidant properties with satisfying results (Loi et al., 2018).

Lactases

Lactase or β-D-galactosidase (EC 3.2.1.23) catalyzes the hydrolysis of β-1,4-D-galactosidic linkages. This enzyme has wide applications in food-processing industries mainly for the hydrolysis of lactose, a disaccharide sugar present in milk, into two monosaccharides, galactose and glucose. In mammals, intestinal cells normally produce β-galactosidase: the condition of insufficient or absent production of β-galactosidase leads to intestinal symptomatic lactose intolerance. The primary lactase deficiency can develop during childhood, in adults, this condition is known as adult-type hypolactasia or lactase non persistence (Xavier et al., 2018). Around 70% of the population of the world, comprising different age groups, are lactose intolerant (Corgneau et al., 2017). Therefore, new technologies for lactose hydrolysis or separation have been already developed and continue to be of great interest. β-galactosidase has also transgalactosylation activity that allows the synthesis of transgalactosylated oligosaccharides, such as galacto-oligosaccharides (GOS), used as prebiotics because of their several health benefits (Husain, 2010). When lactose concentration is high the transgalactosylation activity prevails on the hydrolytic activity that then becomes predominant when the reaction proceeds, producing glucose and galactose (Guerrero et al., 2015). β-galactosidase is mainly obtained from microbial sources like bacteria, yeasts, and fungi thanks to the high yield obtained and low cost of processes. The most used sources of β-galactosidase are the genera *Aspergillus, Bacillus*, and *Kluyveromyces*, the latter with higher hydrolytic activity with respect to the first two that exhibited instead higher transgalactosylation activity (Xavier et al., 2018; Saqib et al., 2017; Guerrero et al., 2015). Recently, the production of this enzyme from psychrophiles, mesophiles, thermophiles, and hyperthermophilic bacteria has become predominant. Anyway, on an industrial scale, the choice of sources depends also on the final applications: in the case of acidic whey hydrolysis for example fungal β-galactosidase with pH of 3.0–5.0 is normally used while β-galactosidase obtained from yeast *Kluyveromyces* requires ions such as Mn2+, Na+, K+, or Mg2+ (Anisha, 2016). Besides using lactase to reduce lactose intolerance, the hydrolytic activity of β-galactosidase is suited for producing concentrated syrup from whey lactose containing glucose and galactose that can be used as a sweetener in ice creams, bakery, and confectionery products preparation (Xavier et al., 2018). Another application is lactose hydrolysis in dairy whey. It is a highly polluting by-product, rich in proteins, minerals, and lactose with high biological oxygen demand (BOD) and chemical oxygen demand (COD). After hydrolysis of lactose, it can be used as a cheap and suitable source for many other applications. Whey proteins can be recovered to produce pharmaceutical intermediates (Saqib et al., 2017); moreover, they have been proposed successfully as a polymer source to produce biodegradable materials (Abdalrazeq et al., 2019). For the enzymatic hydrolysis of lactose in milk and milk products, the simplest but more expensive method is the addition of the enzyme to the product and the deactivation of the enzyme by heat treatment after that reaction occurred. The alternative process involves immobilized β-galactosidase on the skimmed milk; compared to the free enzyme method it has the advantage of enzyme recycling and even of a final product without additional components which could be potential allergens (López-Gallego et al., 2020).

Glucose Oxidase

Glucose oxidase (GOD) (β-D-glucose: oxygen 1-oxidoreductase, EC 1.1.3.4) is a well-known enzyme made up of two identical subunits (80 kDa) at the active site and containing the cofactor flavin adenine dinucleotide (FAD). It catalyzes the oxidation of β-D-glucose to D-glucono-δ-lactone with the production of hydrogen peroxide (H_2O_2) by using molecular oxygen as an electron acceptor. In the first step, GOD catalyzes the oxidation of β-D-glucose to D-glucono-δ-lactone, which subsequently is hydrolyzed to gluconic acid by the enzyme lactonase. This reductive half-reaction causes the reduction of cofactor FAD to $FADH_2$. In the second step, the oxidative half-reaction, FAD is re-oxidized by oxygen with the production of H_2O_2. This is then broken down by catalase (CAT) to O_2 and H_2O (Dubey et al., 2017; Bankar et al., 2009; Kona et al., 2001; Wong et al., 2008). GOD naturally is present in some fungi and insects: because of its catalytic activity, its main function is the antibacterial and *anti*-fungal effect through the production of hydrogen peroxide (Wong et al., 2008). The most common forms of this enzyme are produced by fungi, especially from the spp. *Aspergillus* and *Penicillium*. The first one produces an intracellular enzyme at the level of peroxisomes, while the *Penicillium* GOD is secreted extracellularly. Both *Aspergillus* and *Penicillium* glucose GOD have the optimal range of pH between 4.5 and 7.5 (Buchert et al., 2007). GOD can oxidize monosaccharides, nitroalkanes, and hydroxyl compounds recruiting an electron acceptor to complete the reaction and it has been recognized as Generally Regarded As Safe (GRAS) under FDA classification. Therefore, it finds many applications in the food industry, as glucose and oxygen removal in foods and beverages to prolong their shelf life (Wong et al., 2008). In the production of dried egg powder, the Maillard reaction causes undesirable browning and the development of unwanted flavor. By adding GOD before dehydration, glucose is removed in liquid egg, improving the shelf-life of the product both reducing glucose and oxygen available for microorganisms and inhibiting their growth by formation of hydrogen

peroxide (Sisak et al., 2006). The removal of glucose in the must, the juice used for wine fermentation, can be useful for reducing the alcohol content. Adding GOD to the must before fermentation is among the strategies to reduce the presence of glucose and make it unavailable for microorganisms to produce alcohol. Even in this case, the formation of hydrogen peroxide improves the preservation of the product. Another approach is to modify genetically the yeasts used: by modifying a strain of *Saccharomyces cerevisiae* with the introduction of a GOD gene from *Aspergillus niger*, some authors obtained wine that contained 2% less ethanol (Malherbe et al., 2003). GOD usually is then used in combination with catalase to stabilize color and flavor in some different foods and beverages such as beer, fish meat, and tinned foods. In high-fat foods lipid oxidation causes deterioration and rancid taste: the antioxidant effect of the enzymatic system GOD/catalase can retard this process in mayonnaize stored at 5 °C and 25 °C by decreasing the oxygen available for lipid metabolism (Isaksen and Adler-Nissen, 1997).

Conclusions

The present article provided a comprehensive overview on the main enzymes exploited for the food processing. They are used extensively for improving the food products from different points of view: e.g., for changing the food structure and technological aspects, for improving food safety as well as for enhancing the organoleptic properties. These enzymes can be obtained from plant and animal tissues even though most of them are of microbial origin. As matter of the fact, the bioreactor for microorganism fermentation is considered a powerful, sustainable and economical process to produce enzymes on industrial level. In order to enhance the enzyme features a very important role is played by enzyme immobilization. In general, the applied biocatalysis through the use of enzymes allows the implementation of different processes for a rational and cost-effective approach aimed to improve the food product features.

References

Abdalrazeq, M., Giosafatto, C.V.L., Esposito, M., Fenderico, M., Di Pierro, P., Porta, R., 2019. Glycerol-plasticized films obtained from whey proteins denatured at alkaline pH. Coatings 9 (5), 322.

Abdollahzadeh, R., Pazhang, M., Najavand, S., Fallahzadeh-Mamaghani, V., Amani-Ghadim, A.R., 2020. Screening of pectinase-producing bacteria from farmlands and optimization of enzyme production from selected strain by RSM. Folia Microbiol. 65 (4), 705–719.

Agbowuro, A.A., Huston, W.M., Gamble, A.B., Tyndall, J.D., 2018. Proteases and protease inhibitors in infectious diseases. Med. Res. Rev. 38 (4), 1295–1331.

Alam, S., Ahmad, R., Pranaw, K., Mishra, P., Khare, S.K., 2018. Asparaginase conjugated magnetic nanoparticles used for reducing acrylamide formation in food model system. Bioresour. Technol. 269, 121–126.

Al-Asmar, A., Naviglio, D., Giosafatto, C.V.L., Mariniello, L., 2018. Hydrocolloid-based coatings are effective at reducing acrylamide and oil content of French fries. Coatings 8 (4), 147.

Al-Asmar, A., Giosafatto, C.V.L., Panzella, L., Mariniello, L., 2019. The effect of transglutaminase to improve the quality of either traditional or pectin-coated falafel (Fried Middle Eastern Food). Coatings 9 (5), 331.

Alavi, F., Emam-Djomeh, Z., Salami, M., Mohammadian, M., 2020. Effect of microbial transglutaminase on the mechanical properties and microstructure of acid-induced gels and emulsion gels produced from thermal denatured egg white proteins. Int. J. Biol. Macromol. 153, 523–532.

Al-Rousan, W.M., Al-Marazeeq, K.A., Abdullah, M., Khalaileh, N., Ajo, R.Y., 2019. Use enzymatic preparations to enhance olive oil extraction and their quality. J. Food Nutr. Res. 7 (4), 311–318.

An, Y., Xiong, S., Liu, R., You, J., Yin, T., Hu, Y., 2021. The effect of cross-linking degree on physicochemical properties of surimi gel as affected by MTGase. J. Sci. Food Agric. https://doi.org/10.1002/jsfa.11274.

Anisha, G.S., 2016. β-galactosidases. In: Current Developments in Biotechnology and Bioengineering: Production, Isolation and Purification of Industrial Products. Elsevier B.V.

Arshad, M.S., Kwon, J.H., Imran, M., Sohaib, M., Aslam, A., Nawaz, I., Amjad, Z., Khan, U., Javed, M., 2016. Plant and bacterial proteases: a key towards improving meat tenderization, a mini review. Cogent Food Agric. 2 (1), 1261780.

Bajaj, B.K., Manhas, K., 2012. Production and characterization of xylanase from *Bacillus licheniformis* P11 (C) with potential for fruit juice and bakery industry. Biocatal. Agric. Biotechnol. 1 (4), 330–337.

Bankar, S.B., Bule, M.V., Singhal, R.S., Ananthanarayan, L., 2009. Glucose oxidase—an overview. Biotechnol. Adv. 27 (4), 489–501.

Benucci, I., Mazzocchi, C., Lombardelli, C., Cacciotti, I., Esti, M., 2019. Multi-enzymatic systems immobilized on chitosan beads for pomegranate juice treatment in fluidized bed reactor: effect on haze-active molecules and chromatic properties. Food Bioprocess Technol. 12 (9), 1559–1572.

Bhardwaj, V., Degrassi, G., Bhardwaj, R.K., 2017. Microbial pectinases and their applications in industries: a review. Polymer 4 (08).

Bhat, M., 2000. Cellulases and related enzymes in biotechnology. Biotechnol. Adv. 18 (5), 355–383.

Bilal, M., Iqbal, H.M., 2020. State-of-the-art strategies and applied perspectives of enzyme biocatalysis in food sector—current status and future trends. Crit. Rev. Food Sci. Nutr. 60 (12), 2052–2066.

Bilal, M., Asgher, M., Cheng, H., Yan, Y., Iqbal, H.M., 2019. Multi-point enzyme immobilization, surface chemistry, and novel platforms: a paradigm shift in biocatalyst design. Crit. Rev. Biotechnol. 39 (2), 202–219.

Blanco, C.A., Caballero, I., Barrios, R., Rojas, A., 2014. Innovations in the brewing industry: light beer. Int. J. Food Sci. Nutr. 65 (6), 655–660.

Blue, T., Oxidase, C., Thomas, D., Gangawane, A.K., 2021. Laccase what is laccase. Distrib. Laccases 41–49.

Bönisch, M.P., Huss, M., Weitl, K., Kulozik, U., 2007. Transglutaminase cross-linking of milk proteins and impact on yoghurt gel properties. Int. Dairy J. 17 (11), 1360–1371.

Borrelli, G.M., Trono, D., 2015. Recombinant lipases and phospholipases and their use as biocatalysts for industrial applications. Int. J. Mol. Sci. 16 (9), 20774–20840.

Bourneow, C., Benjakul, S., Sumpavapol, P., Aran, H., 2012. Isolation and cultivation of transglutaminase-producing bacteria from seafood processing factories. Innovat. Rom. Food Biotechnol. 10, 28.

Brijwani, K., Rigdon, A., Vadlani, P.V., 2010. Fungal Laccases: Production, Function, and Applications in Food Processing, vol. 2010. Enzyme Research.

Buchert, J., Selinheimo, E., Kruus, K., Mattinen, M.L., Lantto, R., Autio, K., 2007. Cross-linking enzymes in food processing. In: Novel Enzyme Technology for Food Applications, p. 336.

Burhan, A., Nisa, U., Gökhan, C., Ömer, C., Ashabil, A., Osman, G., 2003. Enzymatic properties of a novel thermostable, thermophilic, alkaline and chelator resistant amylase from an alkaliphilic *Bacillus* sp. isolate ANT-6. Process Biochem. 38 (10), 1397–1403.

Busto, M.D., Meza, V., Ortega, N., Perez-Mateos, M., 2007. Immobilization of naringinase from *Aspergillus niger* CECT 2088 in poly (vinyl alcohol) cryogels for the debittering of juices. Food Chem. 104 (3), 1177–1182.
Camacho, N.A., Aguilar, G., 2003. Production, purification, and characterization of a low-molecular-mass xylanase from *Aspergillus* sp. and its application in baking. Appl. Biochem. Biotechnol. 104 (3), 159–171.
Castillejos, G.R., Lizarazo, C., Ortega, A.G.P., García, N.M., Salazar, R.R., 2018. Effects of transglutaminase on the proximal and textural properties of gluten-free bread of sorghum and quinoa. Rev. Fac. Agron. 35 (2), 188–201.
Cerminati, S., Eberhardt, F., Elena, C.E., Peirú, S., Castelli, M.E., Menzella, H.G., 2017. Development of a highly efficient oil degumming process using a novel phosphatidylinositol-specific phospholipase C enzyme. Appl. Microbiol. Biotechnol. 101 (11), 4471–4479.
Chandra, P., Singh, R., Arora, P.K., 2020. Microbial lipases and their industrial applications: a comprehensive review. Microb. Cell Factories 19 (1), 1–42.
Chaudhri, A., Suneetha, V., 2012. Microbially derived pectinases: a review. IOSR J. Pharm. Biol. Sci. 2 (2), 1–5.
Chen, H., Wu, D., Ma, W., Wu, C., Liu, J., Du, M., 2021. Strong fish gelatin hydrogels double crosslinked by transglutaminase and carrageenan. Food Chem. 131873.
Chew, L.Y., Toh, G.T., Ismail, A., 2019. Application of proteases for the production of bioactive peptides. In: Enzymes in Food Biotechnology.
Choi, Y.J., Lee, B., 2001. Culture conditions for the production of esterase from *Lactobacillus casei* CL96. Bioproc. Biosyst. Eng. 24 (1), 59–63.
Ciesielska, K., Roelants, S.L., Van Bogaert, I.N., De Waele, S., Vandenberghe, I., Groeneboer, S., Soetaert, W., Devreese, B., 2016. Characterization of a novel enzyme—*Starmerella bombicola* lactone esterase (SBLE)—responsible for sophorolipid lactonization. Appl. Microbiol. Biotechnol. 100 (22), 9529–9541.
Contesini, F.J., Melo, R.R.D., Sato, H.H., 2018. An overview of *Bacillus proteases*: from production to application. Crit. Rev. Biotechnol. 38 (3), 321–334.
Corgneau, M., Scher, J., Ritie-Pertusa, L., Le, D.T., Petit, J., Nikolova, Y., Banon, S., Gaiani, C., 2017. Recent advances on lactose intolerance: tolerance thresholds and currently available answers. Crit. Rev. Food Sci. Nutr. 57 (15), 3344–3356.
Corrêa, C.L.O., das Merces Penha, E., Dos Anjos, M.R., Pacheco, S., Freitas-Silva, O., Luna, A.S., Gottschalk, L.M.F., 2021. Use of asparaginase for acrylamide mitigation in coffee and its influence on the content of caffeine, chlorogenic acid, and caffeic acid. Food Chem. 338, 128045.
Coughlan, L.M., Cotter, P.D., Hill, C., Alvarez-Ordóñez, A., 2015. Biotechnological applications of functional metagenomics in the food and pharmaceutical industries. Front. Microbiol. 6, 672.
da Cunha, M.C., dos Santos Aguilar, J.G., de Melo, R.R., Nagamatsu, S.T., Ali, F., de Castro, R.J.S., Sato, H.H., 2019. Fungal L-asparaginase: strategies for production and food applications. Food Res. Int. 126, 108658.
Dal Magro, L., Pessoa, J.P.S., Klein, M.P., Fernandez-Lafuente, R., Rodrigues, R.C., 2021. Enzymatic clarification of orange juice in continuous bed reactors: fluidized-bed versus packed-bed reactor. Catal. Today 362, 184–191.
de Souza, T.S., Kawaguti, H.Y., 2021. Cellulases, hemicellulases, and pectinases: applications in the food and beverage industry. In: Food and Bioprocess Technology, pp. 1–32.
Dey, T.B., Adak, S., Bhattacharya, P., Banerjee, R., 2014. Purification of polygalacturonase from *Aspergillus awamori* Nakazawa MTCC 6652 and its application in apple juice clarification. LWT-Food Sci. Technol. 59 (1), 591–595.
Dhillon, G.S., Kaur, S., Brar, S.K., Verma, M., 2012. Flocculation and haze removal from crude beer using in-house produced laccase from *Trametes versicolor* cultured on brewer's spent grain. J. Agric. Food Chem. 60 (32), 7895–7904.
Duan, X., Shen, Z., Zhang, X., Wang, Y., Huang, Y., 2019. Production of recombinant beta-amylase of *Bacillus aryabhattai*. Prep. Biochem. Biotechnol. 49 (1), 88–94.
Dubey, M.K., Zehra, A., Aamir, M., Meena, M., Ahirwal, L., Singh, S., Shukla, S., Upadhyay, R.S., Bueno-Mari, R., Bajpai, V.K., 2017. Improvement strategies, cost effective production, and potential applications of fungal Glucose Oxidase (GOD): current updates. Front. Microbiol. 8, 1032.
Dulieu, C., Poncelet, D., 1999. Spectrophotometric assay of α-acetolactate decarboxylase. Enzyme Microb. Technol. 25 (6), 537–542.
Dulieu, C., Moll, M., Boudrant, J., Poncelet, D., 2000. Improved performances and control of beer fermentation using encapsulated α-acetolactate decarboxylase and modeling. Biotechnol. Prog. 16 (6), 958–965.
EFSA Panel on Food Contact Materials, Enzymes, Flavourings and Processing Aids (CEF), Silano, V., Bolognesi, C., Castle, L., Chipman, K., Cravedi, J.P., Fowler, P., Franz, R., Grob, K., Gürtler, R., Husøy, T., 2017. Safety evaluation of the food enzyme peroxidase obtained from soybean (Glycine max) hulls. EFSA J. 15 (12), e05119.
EFSA Panel on Food Contact Materials, Enzymes and Processing Aids (CEP), Lambré, C., Barat Baviera, J.M., Bolognesi, C., Cocconcelli, P.S., Crebelli, R., Gott, D.M., Grob, K., Lampi, E., Mengelers, M., Mortensen, A., 2021. Safety evaluation of the food enzyme catalase from the genetically modified *Aspergillus niger* strain DP-Azw58. EFSA J. 19 (8), e06787.
Ehrik, B., Maganlal, D.P., Allen, E.V., Gregori, F.D., Kin-Khang, L.G., Vu, L., Grant, T.M., 2004. Method for Reducing Acrylamide Formation. U.S. Patent RU2423876C2.
Elumalai, P., Lim, J.M., Park, Y.J., Cho, M., Shea, P.J., Oh, B.T., 2019. Enhanced amylase production by a *Bacillus subtilis* strain under blue light-emitting diodes. Prep. Biochem. Biotechnol. 49 (2), 143–150.
Ertaş, N., Aslan, M., Çevik, A., 2022. Improvement of structural and nutritional quality of gluten free pasta. J. Culin. Sci. Technol. 1–19.
Farooq, M.A., Ali, S., Hassan, A., Tahir, H.M., Mumtaz, S., Mumtaz, S., 2021. Biosynthesis and industrial applications of α-amylase: a review. Arch. Microbiol. 203 (4), 1281–1292.
Fernandes, P, 2010. Enzymes in food processing: a condensed overview on strategies for better biocatalysts. Enzyme Res. https://doi.org/10.4061/2010/862537.
Fotschki, J., Wróblewska, B., Fotschki, B., Kalicki, B., Rigby, N., Mackie, A., 2020. Microbial transglutaminase alters the immunogenic potential and cross-reactivity of horse and cow milk proteins. J. Dairy Sci. 103 (3), 2153–2166.
García-Gómez, B., Romero-Rodríguez, Á., Vázquez-Odériz, L., Muñoz-Ferreiro, N., Vázquez, M., 2019. Skim yoghurt with microbial transglutaminase: evaluation of consumer acceptance. CyTA-J. Food 17 (1), 280–287.
García-Gómez, B., Vázquez-Odériz, L., Muñoz-Ferreiro, N., Romero-Rodríguez, Á., Vázquez, M., 2020. Rennet type and microbial transglutaminase in cheese: effect on sensory properties. Eur. Food Res. Technol. 246 (3), 513–526.
García-Silvera, E.E., Martínez-Morales, F., Bertrand, B., Morales-Guzmán, D., Rosas-Galván, N.S., León-Rodríguez, R., Trejo-Hernández, M.R., 2018. Production and application of a thermostable lipase from *Serratia marcescens* in detergent formulation and biodiesel production. Biotechnol. Appl. Biochem. 65 (2), 156–172.
Garg, G., Singh, A., Kaur, A., Singh, R., Kaur, J., Mahajan, R., 2016. Microbial pectinases: an ecofriendly tool of nature for industries. 3 Biotech 6 (1), 1–13.
Gharibzahedi, S.M.T., Koubaa, M., Barba, F.J., Greiner, R., George, S., Roohinejad, S., 2018. Recent advances in the application of microbial transglutaminase crosslinking in cheese and ice cream products: a review. Int. J. Biol. Macromol. 107, 2364–2374.
Gharibzahedi, S.M.T., Yousefi, S., Chronakis, I.S., 2019. Microbial transglutaminase in noodle and pasta processing. Crit. Rev. Food Sci. Nutr. 59 (2), 313–327.
Giosafatto, C.V.L., Rigby, N.M., Wellner, N., Ridout, M., Husband, F., Mackie, A.R., 2012. Microbial transglutaminase-mediated modification of ovalbumin. Food Hydrocoll. 26 (1), 261–267.
Giosafatto, C.V.L., Fusco, A., Al-Asmar, A., Mariniello, L., 2020. Microbial transglutaminase as a tool to improve the features of hydrocolloid-based bioplastics. Int. J. Mol. Sci. 21 (10), 3656.
Godtfredsen, S.E., Ottesen, M., 1982. Maturation of beer with α-acetolactate decarboxylase. Carlsberg Res. Commun. 47 (2), 93–102.
Goesaert, H., Brijs, K., Veraverbeke, W.S., Courtin, C.M., Gebruers, K., Delcour, J.A., 2005. Wheat flour constituents: how they impact bread quality, and how to impact their functionality. Trends Food Sci. Technol. 16 (1–3), 12–30.
Gopinath, S.C., Anbu, P., Arshad, M.M., Lakshmipriya, T., Voon, C.H., Hashim, U., Chinni, S.V., 2017. Biotechnological processes in microbial amylase production. BioMed Res. Int. 2017.
Guerrero, C., Vera, C., Conejeros, R., Illanes, A., 2015. Transgalactosylation and hydrolytic activities of commercial preparations of β-galactosidase for the synthesis of prebiotic carbohydrates. Enzyme Microb. Technol. 70, 9–17.
Gupta, R., Gigras, P., Mohapatra, H., Goswami, V.K., Chauhan, B., 2003. Microbial α-amylases: a biotechnological perspective. Process Biochem. 38 (11), 1599–1616.
Haghighat-Kharazi, S., Milani, J.M., Kasaai, M.R., Khajeh, K., 2018. Microencapsulation of α-amylase in beeswax and its application in gluten-free bread as an *anti*-staling agent. LWT 92, 73–79.

Haile, M., Kang, W.H., 2019. Isolation, identification, and characterization of pectinolytic yeasts for starter culture in coffee fermentation. Microorganisms 7 (10), 401.
Hasan, F., Shah, A.A., Hameed, A., 2006. Industrial applications of microbial lipases. Enzyme Microb. Technol. 39 (2), 235–251.
Heredia-Sandoval, N.G., Valencia-Tapia, M.Y., Calderón de la Barca, A.M., Islas-Rubio, A.R., 2016. Microbial proteases in baked goods: modification of gluten and effects on immunogenicity and product quality. Foods 5 (3), 59.
Housseiny, M.M., Aboelmagd, H.I., 2019. Nano-encapsulation of naringinase produced by *Trichoderma longibrachiatum* ATCC18648 on thermally stable biopolymers for citrus juice debittering. J. Microbiol. 57 (6), 521–531. https://eur-lex.europa.eu/legal-content/en/ALL/?uri=CELEX:32008R1331. (Accessed 1 February 2022). https://eur-lex.europa.eu/legal-content/EN/TXT/?uri=celex%3A32011R0234.
Huang, M., Huang, S., Wang, Q., Hayat, K., Ahmad, M., Ying, R., Hussain, S., 2022. Mixed pretreatment based on pectinase and cellulase accelerates the oil droplet coalescence and oil yield from olive paste. Food Chem. 369, 130915.
Husain, Q., Ullah, M.F., 2019. Biocatalysis. Springer, Cham. https://doi.org/10.1007/978-3-030-25023-2_2, 978–3.
Husain, Q., 2010. β Galactosidases and their potential applications: a review. Crit. Rev. Biotechnol. 30 (1), 41–62.
Isaksen, A., Adler-Nissen, J., 1997. Antioxidative effect of glucose oxidase and catalase in mayonnaises of different oxidative susceptibility. II. Mathematical modelling. LWT-Food Sci. Technol. 30 (8), 847–852.
Ismail, B., Mohammed, H., Nair, A.J., 2019. Influence of proteases on functional properties of food. In: Green Bio-processes. Springer, Singapore, pp. 31–53.
Jaouani, A., Neifar, M., Hamza, A., Chaabouni, S., Martinez, M.J., Gtari, M., 2012. Purification and characterization of a highly thermostable esterase from the actinobacterium *Geodermatophilus obscurus* strain G20. J. Basic Microbiol. 52 (6), 653–660.
Javed, S., Azeem, F., Hussain, S., Rasul, I., Siddique, M.H., Riaz, M., Afzal, M., Kouser, A., Nadeem, H., 2018. Bacterial lipases: a review on purification and characterization. Prog. Biophys. Mol. Biol. 132, 23–34.
Jayani, R.S., Saxena, S., Gupta, R., 2005. Microbial pectinolytic enzymes: a review. Process Biochem. 40 (9), 2931–2944.
Jia, R., Wan, X., Geng, X., Xue, D., Xie, Z., Chen, C., 2021. Microbial L-asparaginase for application in acrylamide mitigation from food: current research status and future perspectives. Microorganisms 9 (8), 1659.
Jiao, L., Chi, H., Lu, Z., Zhang, C., Chia, S.R., Show, P.L., Tao, Y., Lu, F., 2020. Characterization of a novel type I L-asparaginase from *Acinetobacter soli* and its ability to inhibit acrylamide formation in potato chips. J. Biosci. Bioeng. 129 (6), 672–678.
Jones, S.M., Solomon, E.I., 2015. Electron transfer and reaction mechanism of laccases. Cell. Mol. Life Sci. 72 (5), 869–883.
Juturu, V., Wu, J.C., 2014. Microbial cellulases: engineering, production and applications. Renew. Sustain. Energy Rev. 33, 188–203.
Kaiser, P., Raina, C., Parshad, R., Johri, S., Verma, V., Andrabi, K.I., Qazi, G.N., 2006. A novel esterase from *Bacillus subtilis* (RRL 1789): purification and characterization of the enzyme. Protein Expr. Purif. 45 (2), 262–268.
Kang, E.J., Smith, T.J., Drake, M.A., 2012. Alternative bleaching methods for Cheddar cheese whey. J. Food Sci. 77 (7), C818–C823.
Karaca, O.B., Güven, M., 2018. Effects of proteolytic and lipolytic enzyme supplementations on lipolysis and proteolysis characteristics of white cheeses. Foods 7 (8), 125.
Karahan, L.E., Akin, M.S., 2017. Phospholipase applications in cheese production. J. Food Sci. Eng. 7, 312–315.
Kashyap, D.R., Vohra, P.K., Chopra, S., Tewari, R., 2001. Applications of pectinases in the commercial sector: a review. Bioresour. Technol. 77 (3), 215–227.
Kaur, H., Gill, P.K., 2019. Microbial enzymes in food and beverages processing. In: Engineering Tools in the Beverage Industry. Woodhead Publishing, pp. 255–282.
Kaushal, J., Khatri, M., Singh, G., Arya, S.K., 2021. A multifaceted enzyme conspicuous in fruit juice clarification: an elaborate review on xylanase. Int. J. Biol. Macromol. 193, 1350–1361.
Kawaguti, H.Y., Koblitz, M.G.B., 2019. Carboidrases. In: Koblitz, M.G.B. (Ed.), Bioquímica de Alimentos—Teoria e Aplicações Práticas, second ed. Guanabara Koogan, pp. 21–93.
Khalil, N.M., Rodríguez-Couto, S., El-Ghany, M.N.A., 2021. Characterization of *Penicillium crustosum* L-asparaginase and its acrylamide alleviation efficiency in roasted coffee beans at non-cytotoxic levels. Arch. Microbiol. 203 (5), 2625–2637.
Kocabaş, D.S., Lyne, J., Ustunol, Z., 2021. Hydrolytic enzymes in the dairy industry: applications, market and future perspectives. Trends Food Sci. Technol. https://doi.org/10.1016/j.tifs.2021.12.013.
Kohli, P., Kalia, M., Gupta, R., 2015. Pectin methylesterases: a review. J. Bioprocess. Biotech. 5 (5), 1.
Koide, T., Ohnishi, Y., Horinouchi, S., 2011. Characterization of recombinant β-amylases from *Oryza sativa*. Biosci. Biotechnol. Biochem. 75 (4), 793–796.
Kona, R.P., Qureshi, N., Pai, J.S., 2001. Production of glucose oxidase using *Aspergillus niger* and corn steep liquor. Bioresour. Technol. 78 (2), 123–126.
Koshy, M., De, S., 2019. Effect of *Bacillus tequilensis* SALBT crude extract with pectinase activity on demucilation of coffee beans and juice clarification. J. Basic Microbiol. 59 (12), 1185–1194.
Kuhad, R.C., Gupta, R., Singh, A., 2011. Microbial Cellulases and Their Industrial Applications. Enzyme Research.
Kumar, A., Grover, S., Sharma, J., Batish, V.K., 2010. Chymosin and other milk coagulants: sources and biotechnological interventions. Crit. Rev. Biotechnol. 30 (4), 243–258.
Kumar, D., Kumar, S.S., Kumar, J., Kumar, O., Mishra, S.V., Kumar, R., Malyan, S.K., 2017. Xylanases and their industrial applications: a review. Biochem. Cell. Arch. 17 (1), 353–360.
Lai, O.M., Lee, Y.Y., Phuah, E.T., Akoh, C.C., 2019. Lipase/esterase: properties and industrial applications. In: Encyclopedia of Food Chemistry. Elsevier, Amsterdam, pp. 158–167.
Liang, W., Xiong, T., Wang, X., Deng, H., Bai, Y., Fan, T.P., Zheng, X., Cai, Y., 2020. A novel feruloyl esterase with high rosmarinic acid hydrolysis activity from *Bacillus pumilus* W3. Int. J. Biol. Macromol. 161, 525–530.
Lilbaek, H.M., Broe, M.L., Høier, E., Fatum, T.M., Ipsen, R., Sørensen, N.K., 2006. Improving the yield of mozzarella cheese by phospholipase treatment of milk. J. Dairy Sci. 89 (11), 4114–4125.
Littlechild, J.A., 2015. Enzymes from extreme environments and their industrial applications. Front. Bioeng. Biotechnol. 3, 161.
Liu, X., Kokare, C., 2017. Microbial Enzymes of Use in Industry. Biotechnology of Microbial Enzymes. Academic Press, pp. 267–298.
Liu, S., Soomro, L., Wei, X., Yuan, X., Gu, T., Li, Z., Wang, Y., Bao, Y., Wang, F., Wen, B., Xin, F., 2021. Directed evolution of feruloyl esterase from *Lactobacillus acidophilus* and its application for ferulic acid production. Bioresour. Technol. 332, 124967.
Loi, M., Quintieri, L., Fanelli, F., Caputo, L., Mulè, G., 2018. Application of a recombinant laccase-chlorogenic acid system in protein crosslink and antioxidant properties of the curd. Food Res. Int. 106, 763–770.
Loli, H., Kumar Narwal, S., Kumar Saun, N., Gupta, R., 2015. Lipases in medicine: an overview. Mini Rev. Med. Chem. 15 (14), 1209–1216.
López-Gallego, F., Guisan, J.M., Betancor, L., 2020. Immobilization of enzymes on supports activated with glutaraldehyde: a very simple immobilization protocol. In: Immobilization of Enzymes and Cells. Humana, New York, NY, pp. 119–127.
López-Iglesias, M., Gotor-Fernández, V., 2015. Recent advances in biocatalytic promiscuity: hydrolase-catalyzed reactions for nonconventional transformations. Chem. Rec. 15 (4), 743–759.
Lu, X., Lin, J., Wang, C., Du, X., Cai, J., 2016. Purification and characterization of exo-polygalacturonase from *Zygoascus hellenicus* V25 and its potential application in fruit juice clarification. Food Sci. Biotechnol. 25 (5), 1379–1385.
Malherbe, D.F., Du Toit, M., Cordero Otero, R.R., Van Rensburg, P., Pretorius, I.S., 2003. Expression of the *Aspergillus niger* glucose oxidase gene in *Saccharomyces cerevisiae* and its potential applications in wine production. Appl. Microbiol. Biotechnol. 61 (5), 502–511.
Mandal, A., 2015. Review on microbial xylanases and their applications. Appl. Microbiol. Biotechnol. 42, 45–42.
Mariniello, L., Giosafatto, C.V.L., Di Pierro, P., Sorrentino, A., Porta, R., 2007. Synthesis and resistance to in vitro proteolysis of transglutaminase cross-linked phaseolin, the major storage protein from *Phaseolus vulgaris*. J. Agric. Food Chem. 55 (12), 4717–4721.
Masuda, M., Mower, H.F., Pignatelli, B., Celan, I., Friesen, M.D., Nishino, H., Ohshima, H., 2000. Formation of N-nitrosamines and N-nitramines by the reaction of secondary amines with peroxynitrite and other reactive nitrogen species: comparison with nitrotyrosine formation. Chem. Res. Toxicol. 13 (4), 301–308.

Mayolo-Deloisa, K., González-González, M., Rito-Palomares, M., 2020. Laccases in food industry: bioprocessing, potential industrial and biotechnological applications. Front. Bioeng. Biotechnol. 8, 222.
Mehta, A., Guleria, S., Sharma, R., Gupta, R., 2021. The lipases and their applications with emphasis on food industry. In: Microbial Biotechnology in Food and Health. Academic Press, pp. 143–164.
Mesías, M., Morales, F.J., 2016. Acrylamide in coffee: estimation of exposure from vending machines. J. Food Compos. Anal. 48, 8–12.
Mhamdi, A., Queva, G., Chaouch, S., Vanderauwera, S., Breusegem, F.V., Nocto, G., 2010. Catalase function in plants: a focus on Arabidopsis mutants as stress-mimic models. J. Exp. Bot. 61, 4197–4220.
Mir Khan, U., Selamoglu, Z., 2020. Use of enzymes in dairy industry: a review of current progress. Arch. Razi Inst. 75 (1), 131.
Mirpoor, S.F., Giosafatto, C.V.L., Di Girolamo, R., Famiglietti, M., Porta, R., 2022. Hemp (*Cannabis sativa*) seed oilcake as a promising by-product for developing protein-based films: effect of transglutaminase-induced crosslinking. Food Packag. Shelf Life 31, 100779.
Moayedallaie, S., Mirzaei, M., Paterson, J., 2010. Bread improvers: comparison of a range of lipases with a traditional emulsifier. Food Chem. 122 (3), 495–499.
Monsalve-Atencio, R., Sanchez-Soto, K., Chica, J., Echavarría, J.A.C., Vega-Castro, O., 2022. Interaction between phospholipase and transglutaminase in the production of semi-soft fresh cheese and its effect on the yield, composition, microstructure and textural properties. LWT 154, 112722.
Motoki, M., Seguro, K., 1998. Transglutaminase and its use for food processing. Trends Food Sci. Technol. 9 (5), 204–210.
Motta, F.L., Andrade, C.C.P., Santana, M.H.A., 2013. A review of xylanase production by the fermentation of xylan: classification, characterization and applications. In: Sustainable Degradation of Lignocellulosic Biomass-Techniques, Applications and Commercialization, p. 1.
Mouad, A.M., Taupin, D., Lehr, L., Yvergnaux, F., Porto, A.L.M., 2016. Aminolysis of linoleic and salicylic acid derivatives with *Candida antarctica* lipase B: a solvent-free process to obtain amphiphilic amides for cosmetic application. J. Mol. Catal. B Enzyme 126, 64–68.
Nair, S.G., Shashidhar, S., 2008. Fungal xylanase production under solid state and submerged fermentation conditions. Afr. J. Microbiol. Res. 2 (4), 82–86.
Narwal, S.K., Saun, N.K., Dogra, P., Gupta, R., 2016. Green synthesis of isoamyl acetate via silica immobilized novel thermophilic lipase from *Bacillus aerius*. Russ. J. Bioorg. Chem. 42 (1), 69–73.
Nighojkar, A., Patidar, M.K., Nighojkar, S., 2019. Pectinases: production and applications for fruit juice beverages. In: Processing and Sustainability of Beverages. Woodhead Publishing, pp. 235–273.
Nunes, C.S., Kunamneni, A., 2018. Laccases—properties and applications. In: Enzymes in Human and Animal Nutrition. Academic Press, pp. 133–161.
Osborn, D.A., Sinn, J.K.H., Jones, L.J., 2018. Infant formulas containing hydrolysed protein for prevention of allergic disease. Cochrane Database Syst. Rev. 10 (10).
Oumer, O.J., Abate, D., 2018. Screening and molecular identification of pectinase producing microbes from coffee pulp. BioMed Res. Int. 2018.
Özbek, E., Kolcuoglu, Y., Konak, L., Colak, A., ÖZ, F., 2014. Partial purification and biochemical characterization of an extremely thermo-and pH-stable esterase with great substrate affinity. Turk. J. Chem. 38 (4), 538–546.
Pardo, M.F., et al., 2000. Purification of balansain I, an endopeptidase unripe fruits of *Bromelia balansae* Mez (Bromeliaceae). J. Agric. Food Chem. 48, 3795–3800.
Parry, N.J., Beever, D.E., Owen, E., Vandenberghe, I., Beeumen, J.V., Bhat, M.K., 2001. Biochemical characterization and mechanism of action of a thermostable β-glucosidase purified from *Thermoascus aurantiacus*. Biochem. J. 353 (1), 117–127.
Porta, R., Giosafatto, C.V.L., di Pierro, P., Sorrentino, A., Mariniello, L., 2013. Transglutaminase-mediated modification of ovomucoid: effects on its trypsin inhibitory activity and antigenic properties. Amino Acids 44 (1), 285–292.
Prajapati, J., Dudhagara, P., Patel, K., 2021. Production of thermal and acid-stable pectinase from *Bacillus subtilis* strain BK-3: optimization, characterization, and application for fruit juice clarification. Biocatal. Agric. Biotechnol. 102063.
Ramadan, M.F., 2019. Enzymes in fruit juice processing. In: Enzymes in Food Biotechnology. Academic Press, pp. 45–59.
Ramesh, A., Harani Devi, P., Chattopadhyay, S., Kavitha, M., 2020. Commercial applications of microbial enzymes. Microb. Enzymes 11, 137–184.
Ranjitha, P., Karthy, E.S., Mohankumar, A., 2009. Purification and partial characterization of esterase from marine *Vibrio fischeri*. Mod. Appl. Sci. 3 (6).
Raveendran, S., Parameswaran, B., Ummalyma, S.B., Abraham, A., Mathew, A.K., Madhavan, A., Rebello, S., Pandey, A., 2018. Applications of microbial enzymes in food industry. Food Technol. Biotechnol. 56 (1), 16.
Ray, A., 2012. Application of lipase in industry. Asian J. Pharm. Technol 2 (2), 33–37.
Ray, S., 2015. A review: applications of extracellular microbial lipase. Int. J. Biotechnol. Biochem. 5, 6–12.
Razdan, N., Kocher, G.S., 2018. Utilization of damaged and spoiled wheat grains for bioethanol production. Biosci. Biotechnol. Res. Commun. 11, 658–673.
Razzaq, A., Shamsi, S., Ali, A., Ali, Q., Sajjad, M., Malik, A., Ashraf, M., 2019. Microbial proteases applications. Front. Bioeng. Biotechnol. 7, 110.
Revanappa, S.B., Salimath, P.V., Prasada Rao, U.J.S., 2014. Effect of peroxidase on textural quality of dough and arabinoxylan characteristics isolated from whole wheat flour dough. Int. J. Food Prop. 17 (10), 2131–2141.
Richmond, G.S., Smith, T.K., 2011. Phospholipases A 1. Int. J. Mol. Sci. 12, 588–612.
Rizzello, C.G., De Angelis, M., Di Cagno, R., Camarca, A., Silano, M., Losito, I., De Vincenzi, M., De Bari, M.D., Palmisano, F., Maurano, F., Gianfrani, C., 2007. Highly efficient gluten degradation by lactobacilli and fungal proteases during food processing: new perspectives for celiac disease. Appl. Environ. Microbiol. 73 (14), 4499–4507.
Romano, A., Giosafatto, C.V.L., Di Pierro, P., Romano, R., Masi, P., Mariniello, L., 2016. Impact of transglutaminase treatment on properties and in vitro digestibility of white bean (*Phaseolus vulgaris* L.) flour. Food Res. Int. 88, 239–246.
Romano, A., Giosafatto, C.V.L., Al-Asmar, A., Masi, P., Romano, R., Mariniello, L., 2019. Structure and in vitro digestibility of grass pea (*Lathyrus sativus* L.) flour following transglutaminase treatment. Eur. Food Res. Technol. 245 (9), 1899–1905.
Romeih, E., Walker, G., 2017. Recent advances on microbial transglutaminase and dairy application. Trends Food Sci. Technol. 62, 133–140.
Roy, K., Dey, S., Uddin, M., Barua, R., Hossain, M., 2018. Extracellular pectinase from a novel bacterium *Chryseobacterium indologenes* strain SD and its application in fruit juice clarification. Enzyme Res. 2018.
Ruh, T., Ohsam, J., Pasternack, R., Yokoyama, K., Kumazawa, Y., Hils, M., 2014. Microbial Transglutaminase Treatment in Pasta-Production Does Not Affect the Immunoreactivity of Gliadin with Celiac Disease Patients' Sera. J. Agric. Food Chem. 62, 7604–7611.
Ruiz, H.A., Rodriguez-Jasso, R.M., Hernandez-Almanza, A., Contreras-Esquivel, J.C., Aguilar, C.N., 2017. Pectinolytic enzymes. In: Pandey, A., Negi, S., Soccol, C.R. (Eds.), Current Developments in Biotechnology and Bioengineering-Production, Isolation and Purification of Industrial Products. Elsevier, pp. 47–71.
Sajith, S., Priji, P., Sreedevi, S., Benjamin, S., 2016. An overview on fungal cellulases with an industrial perspective. J. Nutr. Food Sci. 6 (1).
Sanromàn, M.A., Deive, F.J., 2017. Food enzymes. In: Current Developments in Biotechnology and Bioengineering: Food and Beverages Industry. Elsevier, pp. 119–142.
Saqib, S., Akram, A., Halim, S.A., Tassaduq, R., 2017. Sources of β-galactosidase and its applications in food industry. 3 Biotech 7 (1), 1–7.
Scarnato, L., Montanari, C., Serrazanetti, D.I., Aloisi, I., Balestra, F., Lanciotti, R., 2017. New bread formulation with improved rheological properties and longer shelf-life by the combined use of transglutaminase and sourdough. LWT - Food Sci. Technol. 81, 101–110.
Selinheimo, E., Kruus, K., Buchert, J., Hopia, A., Autio, K., 2006. Effects of laccase, xylanase and their combination on the rheological properties of wheat doughs. J. Cereal. Sci. 43 (2), 152–159.
Shahsavani Mojarrad, L., Rafe, A., Sadeghian, A., Niazmand, R., 2017. Effects of high amylose corn starch and microbial transglutaminase on the textural and microstructural properties of wheat flour composite gels at high temperatures. J. Texture Stud. 48 (6), 624–632.
Sharma, P.K., Chand, D., 2012. Production of cellulase free thermostable xylanase from *Pseudomonas* sp. XPB-6. Int. Res. J. Biol. Sci. 1 (5), 31–41.
Sharma, T., Sharma, A., Kanwar, S.S., 2016. Purification and characterization of an extracellular high molecular mass esterase from *Bacillus pumilus*. J. Adv. Biotechnol. Bioeng. 4 (1), 9–16.
Sharma, H.P., Patel, H., Sugandha, 2017. Enzymatic added extraction and clarification of fruit juices–a review. Crit. Rev. Food Sci. Nutr. 57 (6), 1215–1227.

Sharma, T., Sharma, A., Sharma, S., Kanwar, S.S., 2017. An overview on esterases: structure, classificaon, sources and their applicaon. In: Recent Advances in Biotechnology. Shree Publishers & Distributors, New Delhi, p. 216.
Sharma, D., Chaudhary, R., Kaur, J., Arya, S.K., 2020. Greener approach for pulp and paper industry by xylanase and laccase. Biocatal. Agric. Biotechnol. 25, 101604.
Sindhu, R., Binod, P., Pandey, A., 2016. Biological pretreatment of lignocellulosic biomass–an overview. Bioresour. Technol. 199, 76–82.
Sindhu, R., Binod, P., Pandey, A., 2017. α-amylases. In: Current Developments in Biotechnology and Bioengineering. Elsevier, pp. 3–24.
Singh, R., Mittal, A., Kumar, M., Mehta, P.K., 2016. Microbial proteases in commercial applications. J. Pharm. Chem. Biol. Sci. 4 (3), 365–374.
Singh, J., Kundu, D., Das, M., Banerjee, R., 2019a. Enzymatic processing of juice from fruits/vegetables: an emerging trend and cutting edge research in food biotechnology. In: Enzymes in Food Biotechnology. Academic Press, pp. 419–432.
Singh, J., Kundu, D., Das, M., Banerjee, R., 2019b. Enzymatic processing of juice from fruits/vegetables: an emerging trend and cutting edge research in food biotechnology. In: Kuddus, M. (Ed.), Enzymes in Food Biotechnology. Elsevier, pp. 419–432.
Singh, R.S., Singh, T., Pandey, A., 2019c. Microbial enzymes—an overview. In: Singh, R.S., Singhania, R.R., Pandey, A., Larroche, C. (Eds.), Advances in Enzyme Technology. Elsevier, pp. 1–40.
Singh, A., Bajar, S., Devi, A., Pant, D., 2021. An overview on the recent developments in fungal cellulase production and their industrial applications. Bioresour. Technol. Rep. 14, 100652.
Sisak, C., Csanádi, Z., Ronay, E., Szajáni, B., 2006. Elimination of glucose in egg white using immobilized glucose oxidase. Enzyme Microb. Technol. 39 (5), 1002–1007.
Sitarz, A.K., Mikkelsen, J.D., Meyer, A.S., 2016. Structure, functionality and tuning up of laccases for lignocellulose and other industrial applications. Crit. Rev. Biotechnol. 36 (1), 70–86.
Song, J.K., Han, J.J., Rhee, J.S., 2005. Phospholipases: occurrence and production in microorganisms, assay for high-throughput screening, and gene discovery from natural and man-made diversity. J. Am. Oil Chem. Soc. 82 (10), 691–705.
Sorrentino, A., Giosafatto, C.V.L., Sirangelo, I., De Simone, C., Di Pierro, P., Porta, R., Mariniello, L., 2012. Higher susceptibility to amyloid fibril formation of the recombinant ovine prion protein modified by transglutaminase. Biochim. Biophys. Acta 1822 (10), 1509–1515.
Souza, P.M.D., 2010. Application of microbial α-amylase in industry-a review. Braz. J. Microbiol. 41 (4), 850–861.
Srivastava, N., Srivastava, M., Mishra, P.K., Gupta, V.K., Molina, G., Rodriguez-Couto, S., Manikanta, A., Ramteke, P.W., 2018. Applications of fungal cellulases in biofuel production: advances and limitations. Renew. Sustain. Energy Rev. 82, 2379–2386.
Srivastava, N., 2019. Production of food-processing enzymes from recombinant microorganisms. In: Kuddus, M. (Ed.), Enzymes in Food Biotechnology.
Struch, M., Linke, D., Mokoonlall, A., Hinrichs, J., Berger, R.G., 2015. Laccase-catalysed cross-linking of a yoghurt-like model system made from skimmed milk with added food-grade mediators. Int. Dairy J. 49, 89–94.
Sukumaran, R.K., Singhania, R.R., Pandey, A., 2005. Microbial cellulases-production, applications and challenges. J. Sci. Ind. Res. 64, 832–844.
Sulyman, A.O., Igunnu, A., Malomo, S.O., 2020. Isolation, purification and characterization of cellulase produced by *Aspergillus niger* cultured on *Arachis hypogaea* shells. Heliyon 6 (12), e05668.
Sundarram, A., Murthy, T.P.K., 2014. α-amylase production and applications: a review. J. Appl. Environ. Microbiol. 2 (4), 166–175.
Svensson, K., Abramsson, L., Becker, W., Glynn, A., Hellenäs, K.E., Lind, Y., Rosen, J., 2003. Dietary intake of acrylamide in Sweden. Food Chem. Toxicol. 41 (11), 1581–1586.
Taheri-Kafrani, A., Kharazmi, S., Nasrollahzadeh, M., Soozanipour, A., Ejeian, F., Etedali, P., Mansouri-Tehrani, H.A., Razmjou, A., Yek, S.M.G., Varma, R.S., 2021. Recent developments in enzyme immobilization technology for high-throughput processing in food industries. Crit. Rev. Food Sci. Nutr. 61 (19), 3160–3196.
Tapre, A.R., Jain, R.K., 2014. Pectinases: enzymes for fruit processing industry. Int. Food Res. J. 21 (2).
Tareke, E., Rydberg, P., Karlsson, P., Eriksson, S., Törnqvist, M., 2002. Analysis of acrylamide, a carcinogen formed in heated foodstuffs. J. Agric. Food Chem. 50 (17), 4998–5006.
Titus, D., Samuel, E.J.J., Roopan, S.M., 2018. Importance of food science and technology-way to future. In: Bioorganic Phase in Natural Food: An Overview. Springer, Cham, pp. 11–23.
Tiwari, S.P., Srivastava, R., Singh, C.S., Shukla, K., Singh, R.K., Singh, P., Singh, R., Singh, N.L., Sharma, R., 2015. Amylases: an overview with special reference to alpha amylase. J. Glob. Biosci. 4 (1), 1886–1901.
Tokay, F.G., Alp, A.C., Yerlikaya, P., 2021. Production and shelf life of restructured fish meat binded by microbial transglutaminase. LWT 152, 112369.
Toksoy Oner, E., Oliver, S.G., Kırdar, B., 2005. Production of ethanol from starch by respiration-deficient recombinant *Saccharomyces cerevisiae*. Appl. Environ. Microbiol. 71 (10), 6443–6445.
Tomke, P.D., Zhao, X., Chiplunkar, P.P., Xu, B., Wang, H., Silva, C., Rathod, V.K., Cavaco-Paulo, A., 2017. Lipase-ultrasound assisted synthesis of polyesters. Ultrason. Sonochem. 38, 496–502.
Torres, S., Baigorí, M.D., Swathy, S.L., Pandey, A., Castro, G.R., 2009. Enzymatic synthesis of banana flavour (isoamyl acetate) by *Bacillus licheniformis* S-86 esterase. Food Res. Int. 42 (4), 454–460.
Toushik, S.H., Lee, K.T., Lee, J.S., Kim, K.S., 2017. Functional applications of lignocellulolytic enzymes in the fruit and vegetable processing industries. J. Food Sci. 82 (3), 585–593.
Tseng, T.F., Chen, M.T., Liu, D.C., 2002. Purification of transglutaminase and its effects on myosin heavy chain and actin of spent hens. Meat Sci. 60 (3), 267–270.
Uenojo, M., Pastore, G.M., 2007. Pectinases: industrial applications and future perspectives. Quím. Nova 30, 388–394.
Uran, H., Yilmaz, I., 2017. A research on determination of quality characteristics of chicken burgers produced with transglutaminase supplementation. Food Sci. Technol. 38, 19–25.
Van Der Maarel, M.J., Van der Veen, B., Uitdehaag, J.C., Leemhuis, H., Dijkhuizen, L., 2002. Properties and applications of starch-converting enzymes of the α-amylase family. J. Biotechnol. 94 (2), 137–155.
Vaquero, M.E., Barriuso, J., Martínez, M.J., Prieto, A., 2016. Properties, structure, and applications of microbial sterol esterases. Appl. Microbiol. Biotechnol. 100 (5), 2047–2061.
Villeneuve, P., Turon, F., Caro, Y., Escoffier, R., Baréa, B., Barouh, B., Lago, R., Piombo, G., Pina, M., 2005. Lipase-catalyzed synthesis of canola phytosterols oleate esters as cholesterol lowering agents. Enzyme Microb. Technol. 37 (1), 150–155.
Wang, Y.C., Zhao, N., Ma, J.W., Liu, J., Yan, Q.J., Jiang, Z.Q., 2019. High-level expression of a novel α-amylase from *Thermomyces dupontii* in *Pichia pastoris* and its application in maltose syrup production. Int. J. Biol. Macromol. 127, 683–692.
Wang, L., Hu, T., Jiang, Z., Yan, Q., Yang, S., 2021. Efficient production of a novel alkaline cold-active phospholipase C from *Aspergillus oryzae* by molecular chaperon co-expression for crude oil degumming. Food Chem. 350, 129212.
Ward, O.P., 2011. Proteases. In: Comprehensive Biotechnology, p. 571.
Wong, C.M., Wong, K.H., Chen, X.D., 2008. Glucose oxidase: natural occurrence, function, properties and industrial applications. Appl. Microbiol. Biotechnol. 78 (6), 927–938.
Xavier, J.R., Ramana, K.V., Sharma, R.K., 2018. β-galactosidase: biotechnological applications in food processing. J. Food Biochem. 42 (5), e12564.
Xiao, F., Li, Z., Pan, L., 2018. Application of microbial lipase and its research progress. Prog. Appl. Microbiol. 1 (1).
Xie, J., Zhang, Y., Simpson, B., 2022. Food enzymes immobilization: novel carriers, techniques and applications. Curr. Opin. Food Sci. 43, 27–35.
Xing, G., Giosafatto, C.V.L., Rui, X., Dong, M., Mariniello, L., 2019. Microbial transglutaminase-mediated polymerization in the presence of lactic acid bacteria affects antigenicity of soy protein component present in bio-tofu. J. Funct. Foods 53, 292–298.
Xing, G., Giosafatto, C.V.L., Carpentieri, A., Pasquino, R., Dong, M., Mariniello, L., 2020. Gelling behavior of bio-tofu coagulated by microbial transglutaminase combined with lactic acid bacteria. Food Res. Int. 134, 109200.

Xing, G., Giosafatto, C.V.L., Fusco, A., Dong, M., Mariniello, L., 2021. Combined lactic fermentation and enzymatic treatments affect the antigenicity of β-lactoglobulin in cow milk and soymilk-cow milk mixture. LWT 143, 111178.

Yokoyama, K., Nio, N., Kikuchi, Y., 2004. Properties and applications of microbial transglutaminase. Appl. Microbiol. Biotechnol. 64 (4), 447–454.

Zhang, S., Bilal, M., Zdarta, J., Cui, J., Kumar, A., Franco, M., Ferreira, L.F.R., Iqbal, H.M., 2021. Biopolymers and nanostructured materials to develop pectinases-based immobilized nano-biocatalytic systems for biotechnological applications. Food Res. Int. 140, 109979.

Zheng, M.M., Wang, L., Huang, F.H., Dong, L., Guo, P.M., Deng, Q.C., Li, W.L., Zheng, C., 2012. Ultrasonic pretreatment for lipase-catalyed synthesis of phytosterol esters with different acyl donors. Ultrason. Sonochem. 19 (5), 1015–1020.

Zyzak, D.V., Sanders, R.A., Stojanovic, M., Tallmadge, D.H., Eberhart, B.L., Ewald, D.K., Gruber, D.C., Morsch, T.R., Strothers, M.A., Rizzi, G.P., Villagran, M.D., 2003. Acrylamide formation mechanism in heated foods. J. Agric. Food Chem. 51 (16), 4782–4787.

coatings

MDPI

Article

Functionality of Films from *Nigella sativa* Defatted Seed Cake Proteins Plasticized with Grape Juice: Use in Wrapping Sweet Cherries

Dana Yaseen [1], Mohammed Sabbah [1,*], Asmaa Al-Asmar [2], Mohammad Altamimi [1], Michela Famiglietti [3], C. Valeria L. Giosafatto [3,4] and Loredana Mariniello [3,4]

[1] Department of Nutrition and Food Technology, An-Najah National University, P.O. Box 7, Nablus P400, Palestine; danayaseen1@gmail.com (D.Y.); m.altamimi@najah.edu (M.A.)
[2] An-Najah BioSciences Unit (NBU), An-Najah National University, P.O. Box 7, Nablus P400, Palestine; a.alasmar@najah.edu
[3] Department of Chemical Sciences, University of Naples "Federico II", 80126 Naples, Italy; michela.famiglietti@unina.it (M.F.); giosafat@unina.it (C.V.L.G.); loredana.mariniello@unina.it (L.M.)
[4] Center for Studies on Bioinspired Agro-Environmental Technology (BAT), University of Naples "Federico II", 80126 Naples, Italy
* Correspondence: m.sabbah@najah.edu; Tel.: +790-92345115

Abstract: The main aim of this work is to improve the functionality of *Nigella sativa* protein concentrate (*NS*PC) films by using grape juice (GJ). The film's mechanical, antioxidant, and antimicrobial activities were evaluated. The obtained results showed, for the first time, that GJ at concentrations of 2%–10% (*v*/*v*) are able to act as plasticizer for the *NS*PC films with promising film properties. The results showed that the tensile strength and Young's modulus of *NS*PC films were reduced significantly when the GJ increased. However, the *NS*PC films prepared with 6% GJ observed a higher elongation at break compared with other films. Moreover, the obtained films showed very interesting and promising results for their antioxidant and antimicrobial properties compared with the control films. The sweet cherries wrapped with *NS*PC film showed that the TSS (Brix) was significantly lower compared to the control, after 10 days of storage. However, the titratable acidity, pH value, and L^* of all cherries, either wrapped or not, was not significantly different in all storage times. On the other hand, hue angle was significantly lower after 10 days of storage at −18 °C compared with control films. GJ has a multi-functional effect for protein-based films as plasticizer, antioxidant, and antimicrobial function.

Keywords: edible film; *Nigella sativa*; sweet cherry; grape juice; functional edible films

check for updates

Citation: Yaseen, D.; Sabbah, M.; Al-Asmar, A.; Altamimi, M.; Famiglietti, M.; Giosafatto, C.V.L.; Mariniello, L. Functionality of Films from *Nigella sativa* Defatted Seed Cake Proteins Plasticized with Grape Juice: Use in Wrapping Sweet Cherries. *Coatings* **2021**, *11*, 1383. https://doi.org/10.3390/coatings11111383

Received: 20 October 2021
Accepted: 9 November 2021
Published: 12 November 2021

Publisher's Note: MDPI stays neutral with regard to jurisdictional claims in published maps and institutional affiliations.

Copyright: © 2021 by the authors. Licensee MDPI, Basel, Switzerland. This article is an open access article distributed under the terms and conditions of the Creative Commons Attribution (CC BY) license (https://creativecommons.org/licenses/by/4.0/).

1. Introduction

Today we are living in an era called a "plastic age", in which plastic pollution has become one of the most urgent environmental issues, with plastic production increasing exponentially, from 2.3 million tons in 1950 to 448 million tons in 2015. Production is expected to double by 2050. Approximately 1 million plastic bottles are sold every minute worldwide, according to National Geographic, and the oceans contain 18 billion pounds of plastic every year [1,2]. The ubiquitous presence of plastic has some strong and valid reasons such as its durability, flexibility, and cheapness, due to some additives that make it stronger, more flexible, and durable, so plastic products may take hundreds of years to degrade. However, it is now not hidden that the overuse and disposal of plastic are becoming a major threat to Earth's environment. Unnecessary use of plastic, improper dumping, excessive use of single-use plastics, and lack of awareness are some of the factors responsible for the current condition of the world's ecosystems.

In recent decades, concerns surrounding conventional plastics have stimulated a focus of attention on environmentally friendly, non-toxic, and biodegradable materials

derived from natural ingredients such as polysaccharides, lipids, and proteins due to their sustainable supply and biodegradable potential [3,4].

Biodegradation refers to the ability of materials to degrade and return to nature within a short period of time after they are disposed of—typically a year or less [5]. Natural polymers derived from agricultural products (such as polysaccharides, proteins, and plant oils) are the main resource for the development of renewable and biodegradable or edible films polymer materials. The edible films can be integral part of foods and can be consumed with products, so there is no packaging and no disposed material [6,7]. It may also be incorporated with some different bioactive compounds such as virgin coconut oil [8], oregano essential oil [9,10], thyme essential oil [10], cloves [11], lacto peroxidase enzyme [12], pomegranate peel extract [13], and others, which act as an antimicrobial and antioxidant agent in edible coatings or films to maintain food safety and quality and enhance the shelf life of food products. The mechanical and barrier properties of edible films depend on many factors, such as the biopolymer sources, concentration, and viscosity [14]. For example, films based on proteins or polysaccharides have very efficient oxygen and carbon dioxide barriers; whereas, their resistance to water vapor transmission is limited. Multicomponent films have also been manufactured in an attempt to combine the advantages of individual materials with film forming.

Seeds are classified as the main source of protein and other important nutrients for supporting health and well-being. Seeds are not only used for nutrition but can also be used in traditional medicine or herbal medicine for their pharmacological properties. Many pharmacological applications derive from these bioactive components [15]. Physicians always endeavor to find drugs with fewer side effects. Nigella sativa (*N. sativa*) belongs to the Ranunculaceae family and has a spiritual and historical background that makes it one of the most promising therapeutic plants. It is cultivated in many countries but is native to Southern Europe, Southeast Asia, and Southwest Asia, and is grown as a spice or for its medicinal value [16,17]. The flowers may be white, pale blue, or dark blue, and the plant is self-branching [18]. Its seeds are mainly used as a condiment and as a relieving agent for different ailments [19–21].

Black seed can be used as directed or active ingredients in herbal medicines or as herbal tea. *N. sativa* seed is extracted, and its extracted oil may be exploited in traditional medicine to treat a wide range of ailments such as diabetes, hypertension, oxidative stress, epilepsies, ulcers, asthma, inflammatory disorders, and cancers in model organisms, as well as in human beings [22–29]. Some of the bioactive compounds obtained from *N. sativa* have been identified and studies have shown that the biological activity of *N. sativa* seeds is mainly attributed to its essential oil component, thymoquinone [30,31], which is a major phytochemical in *N. sativa*, and widely considered to be most important for the broad-spectrum medicinal properties of this valuable plant. Other phytochemicals from different varieties of *N. sativa* include sterols, saponins, phenolic compounds, various alkaloids, as well as volatile oils of different compositions [32,33].

Huge quantities of *N. sativa* defatted cake are produced as by-products and most of it is served as animal feed due to the high bioactive materials and protein content [34]. The *N. sativa* proteins' hydro-methanolic fraction account for about 35%–40% of the total dry weight and it separates into ranges from 10 to 94 kDa on sodium dodecyl sulphate-polyacrylamide gel electrophoresis (SDS-PAGE) [35]. Despite its high pharmacological activity, this fraction has been found to exert effects independent of those exerted by volatile oils, and its effects on human health are receiving increasing attention. Based on research, this extract functions as an effective sedative and has depressant effects on the central nervous system, induces analgesia, prevents progression of pathological changes in the lungs, and decreases blood cytokines in the body [36,37]. In a recent paper by Sabbah et al. [38] the use of proteins from *N. sativa* oilcakes to prepare ecofriendly materials was also investigated [38]. The authors investigated the possibility of preparing hydrocolloid films from proteins obtained from *N. sativa* defatted seed cake (*NS*DSC), when

the latter were modified by means of the enzyme microbial transglutaminase, and they characterized the produced materials from a biological and technological point of view.

Among the most popular fruits by consumers, sweet cherry (*Prunus avium* L.) is known for its high nutritional content and is mostly eaten raw. Several epidemiological studies have recently demonstrated the health-promoting effects related to its content of phytochemicals such as ascorbic acid, anthocyanin, and phenolic compounds [39]. The main characteristics related to the quality of cherry fruits are color, sweetness, sourness, and firmness [40]. Consumer acceptance of sweet cherry depend mainly on the sugar and acid concentrations [41]. Nutritionally, sweet cherries have a higher content of simple sugars (13 g/100 g). Cherries contain water-soluble vitamins (C, B), fat-soluble vitamins (A, E, K), and some carotenoids, in particular beta-carotene. Cherries also contain minerals such as magnesium, calcium, phosphorous, and potassium (10, 14, 20, 200 mg/100 g, respectively). As a result of the high respiration rate and metabolic activity of sweet cherries, they deteriorate rapidly after harvest, causing diminished acidity and phytochemical content, weight loss, and color change [42]. To maintain the good quality of the fruits, it is necessary to work to extend the shelf life of sweet cherries and to maintain the necessary packaging and storage. There are many studies on extending the shelf life of sweet cherries that are gaining great importance. Various techniques such as cold storage, controlled atmosphere storage, modified atmosphere packaging, and edible film coating have been used to maintain the quality and extend the shelf life of sweet cherries after harvest [43–45]. Nowadays, frozen sweet cherries become very popular around the world, and one of the common food quality degradations of frozen food is the freezer burn that occur due to moisture migration in frozen foods. The product appearance becomes glassy due to the evaporating of the ice crystals from the surface area of a products and brownish spots occurring on the food surface that cause the tissue to become dry and tough. The way to help to prevent the freezer burn is by using plastic packaging during the freezing process or to separate the food surfaces from the freezer environment [46].

Grapes (*Vitis vinifera*) is a widely cultivated crop in the world, native to the Mediterranean region and Central Asia. Grapes are non-climacteric fruits for fresh consumption and are botanical groups of true berries. Turkey is an important grape-producing country and is the fifth largest producer of grapes in the world. Since grapes have a very short shelf life, large amounts of grape loss occur due to deterioration. For this reason, grapes must be processed in a form that can be stored for a long time without loss of the nutritional value. Grapes are one of the most widespread fruit crops worldwide and their composition and properties have been extensively studied, with several reports of the presence of large amounts of phenolic compounds [47]. Most of the phenolic compounds in grapes can act as antioxidants [48]. Similarly, wine production residues are also characterized by high contents of phenolic compounds due to their incomplete extraction during wine production [49,50]. By-products obtained after the production of wine, (seeds and pomace) constitute a cheap source for extracting antioxidant compounds, providing important economic advantages [51]. The composition of grapes mainly consists of (*w/w*) 40% fiber, 16% essential oil, 11% protein, and 7% complex phenolic compounds such as tannins, sugars, minerals, and other substances [52]. Grape skin is a source of anthocyanidins and anthocyanins, which are natural pigments with antioxidant properties that act by inhibiting lipid oxidation and also have anti-mutagenic activities [53]. In addition, they are excellent sources of vitamins A, C, K, carotenes, flavonoids, and B-complex vitamins such as pyridoxine, riboflavin, and thiamine.

The main objective of this study was to produce edible films using the protein extracted from *Nigella sativa* defatted seed cakes, functionalized with different concentrations of natural grape juice. The obtained films were evaluated for their mechanical properties as well as for the water content, water uptake, antioxidant activity, and antimicrobial activity. Despite the high biological value of these proteins [54], there are no studies about the shelf-life of foods when protected by *NS*DSC proteins-based materials. Therefore, in this work, the films with the best properties were selected to wrap the sweet cherries and the

quality of unwrapped and wrapped frozen cherries (−18 °C), stored at different times, was evaluated.

2. Materials and Methods

2.1. Materials

The grapes (*Vitis vinifera*) were harvested, washed, had their seeds removed, and their juice extracted with a fruit juicer. The juice was filtrated with cheesecloth to separate the skins and stored at −20 °C until usage. Sweet cherries (*Prunus avium* L., cv Sweetheart) were obtained from a local market in Nablus, Palestine transported, and stored at room temperature until treatment. *Nigella sativa* defatted seed cake (*NS*DSC) was purchased from Alhathnawi General Trade Co. (Jenin, Palestine). All chemicals, BBL™ Mannitol Salt Agar and other solvents used in this study were obtained from Sigma-Aldrich Company (St. Louis, MO, USA). Mueller Hinton Broth Himedia M391 500 g was obtained from HiMedia Leading BioSciences Company (Mumbai, India). Bacterial strains from American Type Culture Collection were *Staphylococcus aureus* (ATCC 25923), *Pseudomonas aeruginosa* (ATCC 27853), *Escherichia coli* (ATCC 25922), *Klebsiella pneumonia* (ATCC 13883), and *Enterococcus faecium* (ATCC 700221), while *Salmonella typhi* were obtained from the microbiology laboratory of An-Najah National University (Nablus, Palestine).

2.2. Methods

2.2.1. Protein Extraction

The proteins were extracted from *NS*DSC by the acid-base extraction method, as previously described [55], with some modifications. After dispersing the dry powder, NSDSC, in distilled water at a ratio of 1:10, w/v, the pH was adjusted to 12.0 by adding 1 N NaOH and stirring at medium speed at room temperature for 2 h. Supernatant was obtained from centrifugation at 4000 rpm for 20 min, and the pH was adjusted at 5.4 with 1 N HCl to precipitate the protein, which was then picked up and dried at 30 °C and 20% relative humidity (RH). The obtained protein concentrate was finely ground by using an electrical miller and stored inside an airtight container at room temperature.

2.2.2. Proximate Analysis

*NS*DSC and *N. sativa* protein concentrate (*NS*PC) was analyzed for its proximate. Moisture content was measured by using infrared moisture analyzer (Sartorius™ MA100C, Sartorius, Goettingen, Germany), the temperature was 105 °C, where applied during analysis, and the measure was stopped automatically when the constant weight was reached. Protein content was determined by Kjeldahl's method [56] using a nitrogen conversion factor of 6.25.

Crude fat is the term used to refer to the crude mixture of fat-soluble material present in a sample. The ANKOM^{XT15} extraction system (ANKOM Technology, Macedon, NY, USA) is a common approach designed to extract crude fat is based on the solubility of lipids in non-polar organic solvents. The analysis is achieved by measuring the loss of mass due to the extraction of fat or oil from the sample encapsulated in a filter bag. Crude fat contained within a food or feed sample can be calculated using the following formula:

$$\text{Crude fat } (\%) = \frac{W2 - W3}{W1} \times 100 \quad (1)$$

where W1—original weight of the sample; W2—weight of pre-dried sample and filter bag; W3—weight of dried sample and filter bag after extraction.

Ash refers to the inorganic residue remaining after either ignition or complete oxidation of organic matter in a foodstuff. Analysis of nutritional evaluation is done by determining the ash content of the food. Ashing is the primary step when preparing a

sample for elemental analysis. The dry ashing method, with a Muffle Furnace, determines the ash content of a variety of food products. The ash content is calculated as follows:

$$\text{Ash } (\%) = \frac{\text{M (ASH)}}{\text{M (DRY)}} \times 100 \quad (2)$$

where M(ASH) and M(DRY) refer to the mass of the ashed sample, and the original masses of the dried samples, respectively.

Carbohydrate was calculated based on the following formula:

$$\text{Total carbohydrat} = 100 - (\text{moisture} + \text{crude fat} + \text{ash} + \text{crude proein}) \quad (3)$$

2.2.3. Film Preparation

The GJ at different concentrations (1%, 2%, 4%, 6%, 8%, 10%, 20%, and 30% v/v) were firstly prepared, then used for dissolving the *NS*PC powder (4 g/100 mL for each GJ concentration) under continuous stirring. The pH value was adjusted to pH 12.0 by using 1 N NaOH. The film-forming solutions were casted onto 15 cm diameter polystyrene Petri dishes and allowed to dry inside the oven dryer at 30 °C for 24 h. Finally, the dried films were peeled off and stored inside desiccator (50%–54% RH $Mg(NO_3)_2$ $6H_2O$) at room temperature for further analysis and use.

2.2.4. Film Characteristics

In order to compare the effects of various treatments to protein films, their mechanical and physical properties have to be determined. For mechanical properties, dry films were peeled off from the casting surface and conditioned at 25 °C and 50% relative humidity for 2 h by placing the film samples into a desiccator over a saturated solution of $Mg(NO_3)_2$ $6H_2O$. Afterwards, their thickness was measured with a micrometer screw gauge (0–25 mm, 0.1 μm), at different positions for each film sample. The mechanical characteristics were measured according to ASTM D882 method [57], using a universal testing instrument (Brookfield CT3 Texture Analyzer, model CT3 50K, Brookfield, Chandler, USA), were described in the relevant literature as follows: (a) Tensile strength (TS), which is the pulling force per film cross-sectional area, required to break the film; (b) The elongation at the break for the degree to which the film can stretch before breaking; (c) Young's modulus, which provides information about a film's resistance to deformation [58]. Film strips (1 cm wide) were mounted between the grips of the texture analyzer and tested with an initial grip separation of 50 mm and a crosshead speed of 0.5 mm/s. Three samples of each film type were tested.

Tensile strength (TS) is calculated by dividing the load at break by the original minimum cross-sectional area. The result is expressed in megapascals (MPa).

$$\text{Tensile strength } = \frac{(\text{Load at break})}{(\text{original width})(\text{original thickness})} \quad (4)$$

Percent elongation (EB) is calculated by dividing the elongation at the moment of rupture by the initial gauge length and multiplying it by 100. The distance between the grips is used as the initial gauge length. The result is expressed in percent.

$$\text{Percent elongation } = \frac{(\text{elongation at rupture}) \times 100}{(\text{initial gage length})} \quad (5)$$

Young's modulus (YM) is calculated by drawing a tangent to the initial linear portion of the stress–strain curve, selecting any point on this tangent, and dividing the tensile stress by the corresponding strain. For the purposes of this calculation, the tensile stress was

calculated by dividing the load by the average original cross-section of the test specimen. The result is expressed in megapascals (MPa).

$$\text{Young's modulus} = \frac{\frac{(\text{load at point on tangent})}{(\text{original width})\ (\text{original thickness})}}{\frac{(\text{elongation at point on tangent})}{(\text{initial gage length})}} \quad (6)$$

The moisture content was measured according to Galus and Lenart [59], determined by the mass loss of 1 g of the film after 24 h of oven drying at 105 °C and was expressed as the percentage of initial film mass loss during drying. The ability of each specimen to absorb moisture was determined by measuring the weight gain of each specimen at 50% RH after 24 h. Three repetitive analyses of each film were made, and the results were expressed as mean value. A total of 3 squares (2 cm × 2 cm) were cut from the films and weighed (W1), then the films were put in the oven (105 °C) for 24 h and then weighed again (W2). Then, the squares were conditioned at 25 °C and 50% RH for 24 h by placing the film samples into a desiccator over a saturated solution of $Mg(NO_3)_2$ $6H_2O$, after which they were weighed (W3).

Water content and uptake were calculated according to the following formulas:

$$\text{Water content } (\%) = \frac{(W1 - W2)}{(W1)} \times 100 \quad (7)$$

$$\text{Water uptake } (\%) = \frac{(W3 - W2)}{(W3)} \times 100 \quad (8)$$

The antioxidant activity of the films and the ability of films and of every single component of the film-casting solution to scavenge DPPH free radicals was assessed using the method described by Siripatrawan and Harte [60], with some modifications. Briefly, the films (20 mg) were dissolved in water (500 mL). Then, sample solutions (100 mL each) were mixed with 900 mL of DPPH methanolic solution (0.05 mg/mL). After 30 min in darkness at room temperature (25 °C), the absorbance was recorded at 517 nm. The percentage of DPPH free radical quenching activity was determined using the following equation:

$$\text{DPPH scavenging effect } (\%) = 100 - \left[\frac{(\text{Abs DPPH} - \text{Abs sample})}{(\text{Abs DPPH})} \times 100\%\right] \quad (9)$$

where Abs DPPH is the absorbance value at 517 nm of the methanolic solution of DPPH and Abs sample is the absorbance value at 517 nm for the samples. Each sample was assayed at least 3 times.

Film antimicrobial activity, the bacterial strains of *Staphylococcus aureus*, *Pseudomonas aeruginosa*, *Escherichia coli*, *Klebsiella pneumonia*, *Enterococcus faecium*, and *Salmonella typhi* were activated twice in a Mueller Hinton broth to reach a cell concentration corresponding to 0.5 turbidities at OD 600. Antimicrobial activity testing of the edible films was carried out using the agar diffusion method, according to Pranoto et al. [61]. The edible films were cut into 5 mm diameter discs and then placed on Mueller Hinton agar plates. These had been previously seeded with 0.2 mL of inoculum containing approximately 10^5–10^6 CFU/mL of tested bacteria. The plates were then incubated at 37 °C for 24 h. Finally, the inhibition zones were observed and evaluated. Experiments were carried out in triplicate.

2.2.5. Sweet Cherry Wrapping

Sweet cherries of uniform size, color, without physical damage, and without fungal infections, were selected, washed with tap water, and dried at room temperature. They were randomly divided into three groups, one was wrapped (W) by sealed *NS*PC bags (10 cm × 10 cm), one in sealed low-density polyethylene (LDPE) bags with the same size of the film, and the control was unwrapped (UW). These samples were placed at −18 °C, the

quality of both wrapped and control samples was evaluated during storage every week for 40 days.

2.2.6. Physicochemical Analyses of Wrapped and Unwrapped Cherries

Samples of 2 cherries from each bag were assessed for color, pH, titratable acidity, and soluble solids. Color ($L^*a^*b^*$ mode) was measured with a Konica Minolta CR-400 Chroma Meter, and expressed as hue angle according to the method of McGuire [62].

The pH values of the juice obtained by hand crushing the cherries in the bags were recorded using a pH meter, then it was titrated with 0.1 N NaOH for titratable acidity (TA) which was expressed as the percentage of malic acid (%).

The total soluble solids concentration (TSS) in the juice was measured with a refractometer (A. KRÜSS Optronic GmbH. DR6100-T, KRÜSS, Hamburg, Germany).

3. Results and Discussion

3.1. Proximate Analysis of Nigella Sativa Seeds and Their Derivatives

Using an acid-base extraction technique, protein concentrates were prepared from the defatted seed meals. Consequently, protein, moisture, fat, carbohydrate, and ash contents of the meal and concentrate protein were determined immediately after drying and then compared with raw *Nigella sativa* seeds (Table 1). The results showed that the protein concentration of raw seeds was 20.3% ± 0.6% and after the extraction of protein, based on the acid base extraction method, it was 43.1% ± 2.5%. Moreover, the fat concentration of raw seeds was 45.4% ± 0.5% while in the *NS*PC was 3.1% ± 0.3% due to the defatted process that proceed to extract the *Nigella sativa* oil before the protein extraction.

Table 1. Proximate analysis of the *Nigella sativa* (*NS*) seeds, *Nigella sativa* defatted seeds cake (*NS*DSC), and *Nigella sativa* protein concentrate (*NS*PC), obtained from defatted seeds cake.

Compositions (%)	*NS* Seed *	*NS*DSC	*NS*PC
Protein	20.3 ± 0.6	34.0 ± 2.7	45.1 ± 2.5
Moisture	7.1 ± 0.2	7.5 ± 0. 1	5.0 ± 0.3
Ash	7.4 ± 0.3	5.5 ± 0.1	3.7 ± 0.7
Fats	45.4 ± 0.5	18.2 ± 0.5	3.1 ± 0.3
Carbohydrate	19.7 ± 0.4	34.8 ± 2.3	43.1 ± 1.4

* Results was according to [63].

3.2. Nigella Sativa Edible Films Obtained in the Presence of Different Concentrations of Grape Juice

Nigella sativa protein concentrate (*NS*PC) powder was dissolved with different concentrations of GJ at pH value 12. The initial experiments showed that the pH value of the film forming solution was critical to obtain very good film appearance and properties, which the *NS*PC films could not obtain at a pH less than 8.0 by using GJ. The *NS*PC–GJ film-forming solutions were casted in a Petri dish and dried for at least 48 h. Figure 1, showed that adding 2%, 4%, 6%, 8%, and 10% was sufficient to obtain handleable films that were homogenized, flexible, and easily to peel off from the Petri dish, without any observed defects cracks or pores. When GJ concentrations were 1%, 20%, and 30%, the film with 1% GJ was rigid, brittle, and easily broken with many cracks—which occurred because the GJ concentration was not enough to plasticize the protein polymers—while, at 20% and 30%, the obtained films were sticky and difficult to separate from Petri dish due to the high concentration of GJ. Therefore, films containing 1%, 20%, and 30% of GJ were excluded. Almost all protein-based films required plasticizing agent to reduce film fragility and obtain certain plastic properties [64,65].

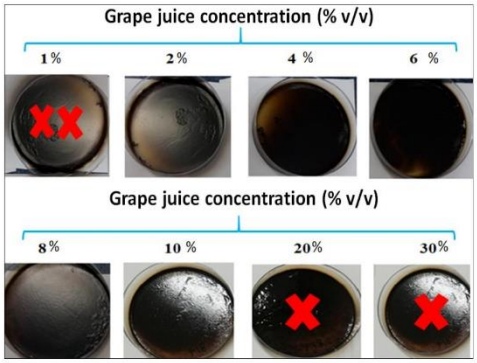

Figure 1. Images of NSDSC protein film containing different concentrations of grape juice (GJ), obtained at pH 12.0. Not-handleable—either brittle (XX) or sticky (X). Further experimental details are given in the text.

Plasticizers are molecules that are able to reduce intermolecular interactions along polymer chains, resulting in increased flexibility, extensibility, and toughness [66]. Plasticizers, on the other hand, decrease films' mechanical resistance and barrier characteristics [67]. The most common use plasticizers are polysaccharides, monosaccharides, disaccharides, or oligosaccharides. Physicochemical properties of edible films produced from whey proteins and plasticized with sucrose have been investigated by several authors, who found that these films are flexible, strong, and extremely glossy, as well as possessing good oxygen barrier qualities [68,69]; therefore, the main reason for the formation of a film based on *NS*DSC protein, with good physicochemical characteristics, without adding glycerol as a plasticizer, is the sugars that presented in GJ that act as plasticizers as in the case of sucrose. Veiga-Santos et al. [70] successfully obtained cassava starch films by using sucrose or invert sugar. Moreover, the pea starch-guar gum also plasticizes with different sugars [71].

The film color was black due to the seed pigmentation represented by phytomelanins, which are high-molecular weight polymers, which formed by the oxidation of phenols [72–74]. The black color of the obtained film will help to protect food products, medicines, or other products from the oxidation that may affect these products.

3.3. Film Characterizations

3.3.1. Film Thickness and Mechanical Properties

Thickness and mechanical properties of edible films are important to ensure that the films have adequate mechanical strength and integrity during transportation, handling, and storage of foods [75]. Figure 2 reports the film thickness and mechanical properties of *NS*DSC protein-based films, prepared with different concentrations of grape juice (2%, 4%, 6%, 8%, and 10% v/v), and casted at pH 12.0.

Results clearly indicated that there is no significant difference in film thickness by increasing the GJ concentration. The film thickness was between 76–72 µm. The different GJ concentrations have significantly affected ($p \leq 0.05$) the *NS*PC films TS, EB, and YM. The obtained results showed that the *NS*CP films TS and YM were reduced significantly when the GJ increased; whereas, film EB increased significantly until 6% GJ, and remained at almost same value at 8% and 10% GJ. Those film mechanical properties were observed by using glycerol, which is recognized as the most used plasticizer to obtain films, even in protein- or polysaccharide-based films [38,76]. Therefore, we recognized that GJ has plasticizing effect for NSPC film, based on the main ingredients of GJ, which are mainly sugars, well known for plasticizing effects. Previous work demonstrated this effect in monosaccharide, especially with glucose produced thinner films, due to the similarity of

its chemical structure to the repeating units of polymers [71]. Veiga-Santos [70] concluded that, by increasing the sucrose or invert sugar as plasticizer to cassava starch, the film EB can be significantly increased.

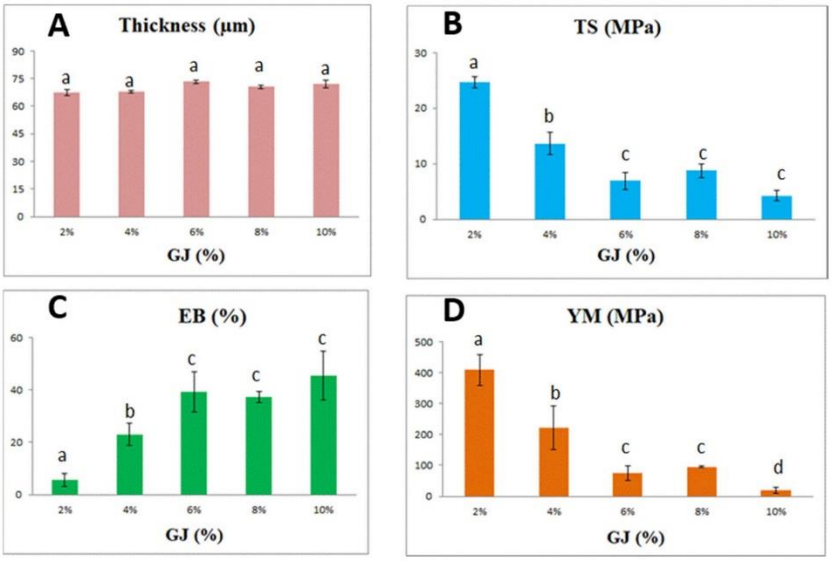

Figure 2. Demonstrates the effect of different concentrations of grape juice (GJ) on the film thickness (**A**) and mechanical properties (TS—tensile strength (**B**); EB—elongation at break (**C**); YM—Young's modulus (**D**) of NSPC edible films obtained at pH 12.0. Different statistical symbols (**a**–**d**) indicate significant difference between treatments ($p < 0.05$).

Table 2 compares the mechanical properties of *NS*DPC films incorporated with 2% and 6% GJ—as well as those of some commercial edible casing called (Viscofan NDX, Tajonar, Spain) that is obtained from gelatin—with plastic high-density polyethylene (HDPE) materials analyzed in previous studies [77]. As shown in Table 2, film prepared with a concentration of 2% of GJ had higher film thickness. Film prepared with 2% GJ almost has similar TS and YM properties as Viscofan (NDX), the commercially available material. Film prepared at 6% GJ had similar YM properties as HDPE, a commercial material.

Table 2. Thickness and mechanical properties of some commercial materials and of *NS*DSC protein films incorporated with 2% and 6% GJ.

Film	Thickness (µm)	TS (MPa)	EB (%)	YM (MPa)
*NS*PC + GJ 2%	67.5 ± 1.5	24.6 ± 1.1	5.6 ± 2.3	409.5 ± 50.0
*NS*PC + GJ 6%	73.3 ± 0.81	6.90 ± 1.5	39.3 ± 7.6	74.5 ± 23.10
Viscofan (NDX) *	30.0 ± 0.4	36.6 ± 8.1	13.1 ± 2.9	356.0 ± 29.0
HDPE *	36.2 ± 1.7	13.1 ± 1.4	501.9 ± 43.3	75.2 ± 2.70

* The results were obtained from previous study [77].

3.3.2. Moisture Content and Uptake

Among the properties of the obtained films that have been evaluated are their water moisture content and uptake, which play important roles in determining the texture and mechanical properties of edible films as coating materials, and are highly essential for potential food packaging applications [78]. Because it is well recognized that high moisture content may allow for increased bacterial and enzymatic activity or mold development

under the available conditions, the use of edible films as a food packing material may be severely limited.

The results indicated no significant change in water content from increasing the GJ concentrations; whereas, the water uptake of the *NS*CP film prepared with 4% GJ has the highest water uptake (11.1% ± 0.3%), which significantly differs from the films prepared with 10% GJ (6.4% ± 1.8%) (Table 3). Plasticizing the NSCP with GJ at 4% showed the maximum water uptake that, due to the higher water-holding capacity inside the film matrixes, then gradually decreased with an increase in GJ concentration. Previous work showed that fructose plasticized cassava starch films absorb less water compared with other films obtained with urea, tri-ethylene glycol, or triethanolamine [79].

Table 3. Water content and uptake of *NS*PC prepared with different concentrations of grape juice (GJ).

Film	Water Content (%)	Water Uptake (%)
*NS*PC + GJ (2%)	12.1 ± 1.4 [a]	7.6 ± 1.1 [a,b]
*NS*PC + GJ (4%)	17.4 ± 1.4 [a]	11.1 ± 0.3 [a]
*NS*PC + GJ (6%)	18.0 ± 0.9 [a]	8.9 ± 0.8 [a,b]
*NS*PC + GJ (8%)	15.5 ± 3.7 [a]	9.8 ± 0.7 [a,b]
*NS*PC + GJ (10%)	16.7 ± 3.4 [a]	6.4 ± 1.8 [b]

[a,b] The values with different letters are significantly different.

There are many studies reporting the moisture content of protein-based edible films under different conditions. Bamdad et al. [80] studied the moisture content of films made from lentil protein concentrate with 50% GLY, which was 23.15% ± 1.6%. Mahmoud and Savello [81] reported that the moisture content in whey protein films ranges from 26.3% to 26.5% when their glycerol content was 1.5% and increased when the concentration of glycerol increased. In a study on peanut protein concentrate film, dried at 70, 80, or 90 °C, the moisture content of peanut protein films prepared at 70 °C was 32.57% higher than for those prepared at 80 °C (23.84%) or 90 °C (14.79%) [82].

3.3.3. Antioxidant Activity of the Film

DPPH scavenging assay was used to indicate the antioxidant activity of the film, when the DPPH solution was mixed with the sample mixture (as a reagent), acting as a hydrogen atom donor, a stable non-radical form of DPPH is obtained with simultaneous change of the violet color to pale yellow, which was determined by using the spectrophotometry method [83]. The results showed that the DPPH scavenging activity of the films significantly increased with an increase in GJ concentration, as shown in comparison with the control films that obtained this with 30% glycerol as plasticizer (Figure 3). The film's scavenging action is connected to the fact that free radicals can react with remaining free amino (NH_2) groups to generate stable macromolecule radicals, and NH_2 groups can form ammonium (NH_3) groups by absorbing a hydrogen ion from the solution [84].

In the films containing GJ, the antioxidant activity increased, due to bioactive components in grapes, which is a good natural source of antioxidants, containing many phytochemicals such as anthocyanin, catechin, epicatechin, resveratrol, and proanthocyanidin, and therefore have strong activity for scavenging free radicals [85]. The expected antioxidant nature of the active film improved as the GJ concentration in the film formulation raised.

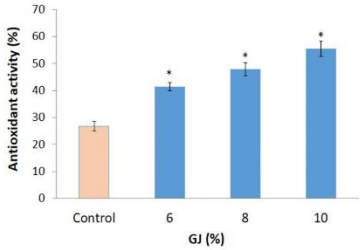

Figure 3. Effects of different concentrations of grape juice (GJ) on the DPPH scavenging activity of obtained *NS*PC edible films, control was the *NS*PC film obtained with 30% glycerol at the same pH value 12. Values with (*) were significantly different compared with the control.

3.3.4. NSDSC Protein Film Antimicrobial Activity

The microbial strains used in this study were of medical importance. They may cause sepsis, pneumonia, and diarrhea infectious diseases, and, more importantly, they may resist conventional antibiotics. The results have shown that there was antimicrobial activity for the films as observed around the film. The inhibition zones, although irregular, increased as the GJ concentration was increased (Figure 4). However, bacterial strains showed different responses with *K. pneumonia*, which was the most affected strain. *K. pneumonia* is a biofilm-forming bacterium that uses extracellular materials to support cell growth. GJ contains active ingredients such as polyphenols that may inhibit or interfere with biofilm formation [86]. Such active ingredients in GJ were also expected to disrupt the cell wall of gram-negative bacteria. Gram-negative bacteria have complex cell walls and are more resistant to antimicrobial agents than gram-positive bacteria [87,88]. Similar work has found that gram-positive bacteria were more susceptible to polyphenols than gram-negative bacteria. This is an advantageous result to promote edible films and increase their functionality. With more attention given to polyphenols as antimicrobial agents, edible films enriched with polyphenols can serve functions for both preserving food and decreasing foodborne diseases. On the other hand, it was documented that polyphenol were not active against probiotics or beneficial microbiota in the gastrointestinal tract [86]. The difference between the results of current studies and other studies, in terms of antimicrobial effects, is mainly due to variations in types of polyphenols, concentrations, method of application, mode of action, and strains of target microorganisms.

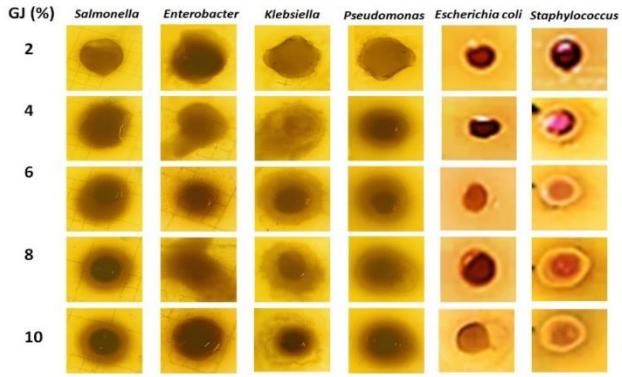

Figure 4. Effects of different concentrations of grape juice (GJ) on the antimicrobial activity of obtained *NS*PC edible films.

3.4. Effect of Wrapping with or without NSPC/GJ Film on Sweet Cherries Quality

Effects of *NS*DPC with 6% GJ films and LDPE on the quality of sweet cherries was shown in (Figures 5–7). The unwrapped sweet cherries and those sweet cherries wrapped with LDPE were the controls in this experiment. The *NS*PC with 6% GJ was selected based on mechanical properties. Figure 5 showed the sweet cherries after removal from freezer where the unwrapped cherries were covered with small ice crystal; whereas, this was not observed in both wrapped cherries when it closed. However, the *NS*PC with GJ films are able to be heat-sealed by a house sealer machine.

Figure 5. Sweet cherries image after removing from freezer: unwrapped (control) and wrapped (W) with LDPE or *NS*PC with 6% GJ.

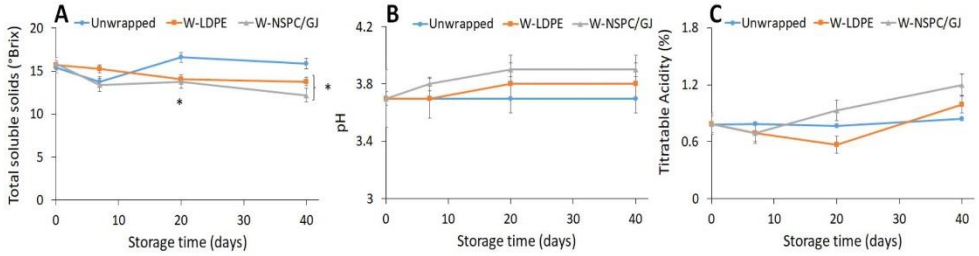

Figure 6. Effect of unwrapped (control) and wrapped (W) with LDPE or *NS*PC plasticized with 6% GJ films on soluble solids content (Brix) (**A**), pH (**B**) and titratable acidity (**C**), of sweet cherries stored at different storage time at −18 °C. Value with (*) is significantly different, compared with the unwrapped sweet cherries.

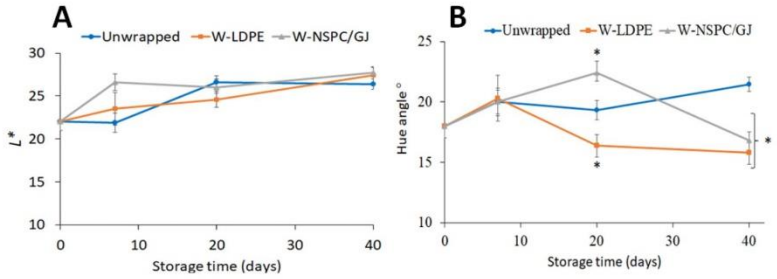

Figure 7. The effects of unwrapped and wrapped (w) with LDPH and *NS*PC plasticized with 6% GJ on optical properties of sweet cherries stored at different storage times at −18 °C. Value with (*) is significantly different compared with the unwrapped sweet cherries. (**A**) *L**; (**B**) Hue angle.

The initial total soluble solids (TSS) were (16.3 ± 1.2 Brix) of fresh cherries, indicated a good maturity as described by Kappel et al. [89]. The results showed that the TSS (Brix)

was significantly lower compared with the control (unwrapped) after 10 days of storage at −18 °C, and no significant effect was observed between the TSS of cherries wrapped with LDPE or *NS*PC films in all storage times (Figure 6). One of the good juice quality indicators is the retention or minimum increase in TSS content of juice during storage [90]. The TSS decrease during storage could attribute to the respiration rate or conversion of sugar, while the increase could be explained by the breakdown of starch to sugar [91]. The results clearly indicated that the TSS concentration was stable until end of the storage period for cherries wrapped with LDPE or *NS*CP–GJ films. However, the titratable acidity and pH value of all cherries, wrapped or not, was not significantly different in any storage times.

The optical result (L^* and hue angle) was analyzed for the sweet cherries, the unwrapped cherries (control), and those wrapped (W) with LDPE or *NS*PC plasticized with 6% GJ, at different storage times, at freezing temperature −18 °C (Figure 7). L^* indicates lightness read from 0 (completely opaque or "black") to 100 (completely transparent or "white") [91]. The results showed that the L^* value was not significant in any of the treatments; whereas, the hue angle results indicated that the sweet cherries wrapped with LDPE were reduced significantly compared with the ones wrapped with *NS*PC plasticized with GJ, or the unwrapped cherries, at 20 days of storage. Moreover, the hue angle value for the sweet cherries wrapped with *NS*PC showed significantly higher values at 20 days compared with the control, and the value decreased at 40 days of storage at −18 °C; additionally, there were no significant differences between the cherries wrapped with LDPE or *NS*PC films after 40 days of storage. Gonçalves et al. [91] and Gutiérrez-Jara et al. [92] concluded that there is a correlation between the hue angle and anthocyanins content, where the lowest value of hue angle is correlated to the cherries with highest anthocyanins content, giving a darker red color. Based on that, the obtained results indicated that the wrapping of sweet cherries is very important during freezing to protect the anthocyanins concentration in the products. However, at 40 days of storage, the unwrapped cherries hue angle value was higher compared to the 0 day hue angle value, due to the loss of the anthocyanins content. Similar results were found by Gutiérrez-Jara et al. [92], where the coated cherries showed the lower hue angle value compared with the uncoated cherries at refrigeration storage control.

4. Conclusions

The use of *NS*CP, plasticized with GJ, represents a stimulating route for creating new food packaging materials. This study indicated that *NS*PC and GJ appear to be interesting raw materials for the formation of functional edible packaging films. The GJ concentrations content was the most important parameter influencing the mechanical properties, as well as the physical properties, due to its plasticizing effects on the biopolymer matrix. The present study revealed, for the first time, that the use of natural GJ in combination with *NS*PC has a positive influence on the physicochemical traits of sweet cherries. The film proved to extend the shelf life of fresh sweet cherries by delaying changes in color, titratable acidity, total soluble solids, and pH during freezing storage. Moreover, the antimicrobial ability of the edible film, together with its antioxidant properties, may act synergistically to preserve food without affecting its properties, in a more environmentally friendly way.

Author Contributions: Conceptualization, M.S. and A.A.-A.; methodology, M.S., D.Y., M.A., C.V.L.G. and M.F.; software, D.Y. and C.V.L.G.; validation, L.M. and M.S.; formal analysis, M.S., M.A., A.A.-A. and M.F.; investigation, D.Y. and A.A-A.; resources, M.S., D.Y., M.A and C.V.L.G.; data curation, M.S. and D.Y.; writing—original draft preparation, M.S. and D.Y.; writing—review and editing, L.M., C.V.L.G., M.A., M.F. and M.S.; visualization, M.S.; supervision, M.S. and L.M.; project administration, M.S. and C.V.L.G.; funding acquisition, C.V.L.G., D.Y. and A.A.-A. All authors have read and agreed to the published version of the manuscript.

Funding: This work was supported by An-Najah National University (Grant No. ANNU-2021-Sc0021).

Institutional Review Board Statement: Not applicable.

Informed Consent Statement: Not applicable.

Data Availability Statement: Original data of this work are available upon reasonable request.

Conflicts of Interest: The authors declare no conflict of interest.

References

1. Thompson, R.C.; Swan, S.H.; Moore, C.J.; vom Saal, F.S. Our plastic age. *Phil. Trans. R. Soc. B* **2009**, *364*, 1973–1976. [CrossRef]
2. Bandoim, L. Can Edible Food Wrappers Solve the Plastic Crisis? Available online: https://sciencing.com/can-edible-food-wrappers-solve-the-plastic-crisis-13717334.html (accessed on 29 February 2020).
3. Verbeek, C.J.R.; Van den Berg, L.E. Extrusion processing and properties of protein-based thermoplastics. *Macromol. Mater. Eng.* **2010**, *295*, 10–21. [CrossRef]
4. Kraśniewska, K.; Gniewosz, M. Substances with antimicrobial activity in edible films. *A review. Pol. J. Food Nutr. Sci.* **2012**, *62*, 199–206. [CrossRef]
5. Muzaffar, H.; Ajesh Kumar, V.; Chirag Maheshwari, S.; Mangraj. Biodegradable and edible film: A counter to plastic pollution. *Int. J. Chem. Stud.* **2020**, *8*, 2242–2245.
6. Shokri, S.; Ehsani, A.; Jasour, M.S. Efficacy of lactoperoxidase system-whey protein coating on shelf-life extension of rainbow trout fillets during cold storage (4 °C). *Food Bioprocess Technol.* **2015**, *8*, 54–62. [CrossRef]
7. Mohareb, E.; Mittal, G.S. Formulation and process conditions for biodegradable/edible soy-based packaging trays. *Packag. Technol. Sci.* **2007**, *20*, 1–15. [CrossRef]
8. Shit, S.C.; Shah, P.M. Edible polymers: Challenges and opportunities. *J. Polym.* **2014**, *2014*, 1–13. [CrossRef]
9. Fangfang, Z.; Xinpeng, B.; Wei, G.; Wang, G.; Shi, Z.; Jun, C. Effects of virgin coconut oil on the physicochemical, morphological and antibacterial properties of potato starch-based biodegradable films. *Int. J. Food Sci. Technol.* **2020**, *55*, 192–200. [CrossRef]
10. Jouki, M.; Yazdi, F.T.; Mortazavi, S.A.; Koocheki, A. Quince seed mucilage films incorporated with oregano essential oil: Physical, thermal, barrier, antioxidant and antibacterial properties. *Food Hydrocoll.* **2014**, *36*, 9–19. [CrossRef]
11. Emiroğlu, Z.K.; Yemiş, G.P.; Coşkun, B.K.; Candoğan, K. Antimicrobial activity of soy edible films incorporated with thyme and oregano essential oils on fresh ground beef patties. *Meat Sci.* **2010**, *86*, 283–288. [CrossRef]
12. Gómez-Estaca, J.; López de Lacey, A.; López-Caballero, M.E.; Gómez-Guillén, M.C.; Montero, P. Biodegradable gelatin–chitosan films incorporated with essential oils as antimicrobial agents for fish preservation. *Food Microbiol.* **2010**, *27*, 889–896. [CrossRef]
13. Moghadam, M.; Salami, M.; Mohammadian, M.; Khodadadi, M.; Emam-Djomeh, Z. Development of antioxidant edible films based on mung bean protein enriched with pomegranate peel. *Food Hyd.* **2020**, *104*, 105735. [CrossRef]
14. Lin, D.; Zhao, Y. Innovations in the development and application of edible coatings for fresh and minimally processed fruits and vegetables. *Compr. Rev. Food Sci. Food Saf.* **2007**, *6*, 60–75. [CrossRef]
15. Dubick, M.A. Historical perspectives on the use of herbal preparations to promote health. *J. Nutr.* **1986**, *116*, 1348–1354. [CrossRef] [PubMed]
16. Ali, B.H.; Blunden, G. Pharmacological and toxicological properties of *Nigella sativa*. *Phytother. Res.* **2003**, *17*, 299–305. [CrossRef]
17. Paarakh, P.M. *Nigella sativa* Linn. A comprehensive review. *Indian J. Nat. Prod. Resour.* **2010**, *1*, 409–429.
18. Salem, M.L. Immunomodulatory and therapeutic properties of the *Nigella sativa* L. seed. *Int. Immunopharmacol.* **2005**, *5*, 1749–1770. [CrossRef]
19. Ramadan, M.F. Nutritional value, functional properties and nutraceutical applications of black cumin (*Nigella sativa* L.): An overview. *Int. J. Food Sci. Technol.* **2007**, *42*, 1208–1218. [CrossRef]
20. Aljabre, S.H.; Alakloby, O.M.; Randhawa, M.A. Dermatological effects of *Nigella sativa*. *J. Dermatol. Dermatol. Surg.* **2015**, *19*, 92–98. [CrossRef]
21. Dubey, P.N.; Singh, B.; Mishra, B.K.; Kant, K.; Solanki, R.K. *Nigella (Nigella sativa)*: A high value seed spice with immense medicinal potential. *Indian J. Agric. Sci.* **2016**, *86*, 967–979.
22. Meddah, B.; Ducroc, R.; Faouzi, M.E.A.; Eto, B.; Mahraoui, L.; Benhaddou-Andaloussi, A.; Martineau, L.; Cherrah, Y.; Haddad, P.S. *Nigella sativa* inhibits intestinal glucose absorption and improves glucose tolerance in rats. *J. Ethnopharmacol.* **2009**, *121*, 419–424. [CrossRef] [PubMed]
23. Tavakkoli, A.; Mahdian, V.; Razavi, B.M.; Hosseinzadeh, H. Review on clinical trials of black seed (*Nigella sativa*) and its active constituent, thymoquinone. *J. Pharmacopuncture.* **2017**, *20*, 179–193. [PubMed]
24. Leong, X.F.; Rais Mustafa, M.; Jaarin, K. *Nigella sativa* and its protective role in oxidative stress and hypertension. *Evid. Based Complementary Altern. Med.* **2013**, *2013*, 1–9.
25. Hosseinzadeh, H.; Parvardeh, S.; Nassiri-Asl, M.; Mansouri, M.T. Intracerebroventricular administration of thymoquinone, the major constituent of *Nigella sativa* seeds, suppresses epileptic seizures in rats. *Med. Sci. Monit.* **2005**, *11*, 106–110.
26. El-Dakhakhny, M.; Barakat, M.; Abd El-Halim, M.; Aly, S.M. Effects of *Nigella sativa* oil on gastric secretion and ethanol induced ulcer in rats. *J. Ethnopharmacol.* **2000**, *72*, 299–304. [CrossRef]
27. Koshak, A.; Wei, L.; Koshak, E.; Wali, S.; Alamoudi, O.; Demerdash, A.; Majdy, Q.; Peter, N.; Heinrich, M. Nigella sativa supplementation improves asthma control and biomarkers: A randomized, double-blind, placebo-controlled trial. *Phytother. Res.* **2017**, *31*, 403–409. [CrossRef] [PubMed]
28. Majdalawieh, A.F.; Fayyad, M.W.; Nasrallah, G.K. Anti-cancer properties and mechanisms of action of thymoquinone, the major active ingredient of *Nigella sativa*. *Food Sci. Nutr.* **2017**, *57*, 3911–3928.

29. Mollazadeh, H.; Afshari, A.R.; Hosseinzadeh, H. Review on the potential therapeutic roles of *Nigella sativa* in the treatment of patients with cancer: Involvement of apoptosis:-black cumin and cancer. *J. Pharmacopunct.* **2017**, *20*, 158–172.
30. Woo, C.C.; Kumar, A.P.; Sethi, G.; Tan, K.H.B. Thymoquinone: Potential cure for inflammatory disorders and cancer. *Biochem. Pharmacol.* **2012**, *83*, 443–451. [CrossRef]
31. Ahmad, A.; Husain, A.; Mujeeb, M.; Khan, S.A.; Najmi, A.K.; Siddique, N.A.; Zoheir, A.D.; Anwar, F. A review on therapeutic potential of *Nigella sativa*: A miracle herb. *Asian Pac. J. Trop. Biomed.* **2013**, *3*, 337–352. [CrossRef]
32. Haseena, S.; Aithal, M.; Das, K.K.; Saheb, S.H. Phytochemical analysis of Nigella sativa and its effect on reproductive system. *J. Pharm. Sci. Res.* **2015**, *7*, 514–517.
33. Yimer, E.M.; Tuem, K.B.; Karim, A.; Ur-Rehman, N.; Anwar, F. *Nigella sativa* L. (black cumin): A promising natural remedy for wide range of illnesses. *Evid. Based Complementary Altern. Med.* **2019**, *2019*, 1–16. [CrossRef]
34. El-Hack, M.E.A.; Alagawany, M.; Saeed, M.; Arif, M.; Arain, M.A.; Bhutto, Z.A.; Fazlani, S.A. Effect of gradual substitution of soyabean meal by *Nigella sativa* meal on growth performance, carcass traits and blood lipid profile of growing Japanese quail. *J. Anim. Feed Sci.* **2016**, *25*, 244–249. [CrossRef]
35. Haq, A.; Lobo, P.I.; Al-Tufail, M.; Rama, N.R.; Al-Sedairy, S.T. Immunomodulatory effect of *Nigella sativa* proteins fractionated by ion exchange chromatography. *Int. J. Immunopharmacol.* **1999**, *21*, 283–295. [CrossRef]
36. Hosseinzadeh, H.; Taiari, S.; Nassiri-Asl, M. Effect of thymoquinone, a constituent of *Nigella sativa* L., on ischemia-reperfusion in rat skeletal muscle. *Naunyn-Schmiedeberg's Arch. Pharmacol.* **2012**, *385*, 503–508. [CrossRef]
37. Farah, I.O.; Begum, R.A. Effect of *Nigella sativa (N. sativa* L.) and oxidative stress on the survival pattern of MCF-7 breast cancer cells. *Biomed. Sci. Instrum.* **2003**, *39*, 359–364.
38. Sabbah, M.; Altamimi, M.; Di Pierro, P.; Schiraldi, C.; Cammarota, M.; Porta, R. Black edible films from protein-containing defatted cake of nigella sativa seeds. *Int. J. Mol. Sci.* **2020**, *21*, 832. [CrossRef] [PubMed]
39. Ferretti, G.; Bacchetti, T.; Belleggia, A.; Neri, D. Cherry antioxidants: From farm to table. *Molecules* **2010**, *15*, 6993–7005. [CrossRef] [PubMed]
40. Esti, M.; Cinquanta, L.; Sinesio, F.; Moneta, E.; Di Matteo, M. Physicochemical and sensory fruit characteristics of two sweet cherry cultivars after cool storage. *Food Chem.* **2002**, *76*, 399–405. [CrossRef]
41. Crisosto, C.H.; Crisosto, G.M.; Metheney, P. Consumer acceptance of "Brooks" and "Bing" cherries is mainly dependent on fruit SSC and visual skin color. *Postharvest Biol. Technol.* **2003**, *28*, 159–167. [CrossRef]
42. Alonso, J.; Alique, R. Influence of edible coating on shelf life and quality of "Picota" sweet cherries. *Eur. Food Res. Technol.* **2004**, *218*, 535–539. [CrossRef]
43. Tian, S.P.; Jiang, A.L.; Xu, Y.; Wang, Y.S. Responses of physiology and quality of sweet cherry fruit to different atmospheres in storage. *Food Chem.* **2004**, *87*, 43–49. [CrossRef]
44. Meheriuk, M.; Girard, B.; Moyls, L.; Beveridge, H.J.T.; McKenzie, D.L.; Harrison, J.; Weintraub, S.E.; Hocking, R. Modified atmosphere packaging of "Lapins" sweet cherry. *Food Res. Int.* **1995**, *28*, 239–244. [CrossRef]
45. Petriccione, M.; De Sanctis, F.; Pasquariello, M.S.; Mastrobuoni, F.; Rega, P.; Scortichini, M.; Mencarelli, F. The effect of chitosan coating on the quality and nutraceutical traits of sweet cherry during postharvest life. *Food Bioprocess Technol.* **2014**, *8*, 394–408. [CrossRef]
46. Pham, Q.T.; Mawson, R.F. Moisture migration and ice recrystallization in frozen foods. *Qual. Frozen Food.* **1997**, 67–91.
47. Rubilar, J.F.; Cruz, R.M.S.; Silva, H.D.; Vicente, A.A.; Khmelinskii, I.; Vieira, M.C. Physico-mechanical properties of chitosan films with carvacrol and grape seed extract. *J. Food Eng.* **2013**, *115*, 466–474. [CrossRef]
48. Priyadarshi, R.; Riahi, Z.; Rhim, J.-W. Antioxidant pectin/pullulan edible coating incorporated with *Vitis vinifera* grape seed extract for extending the shelf life of peanuts. *Postharvest Biol. Technol.* **2022**, *183*, 111740. [CrossRef]
49. Oszmianski, J.; Lee, C.Y. Isolation and HPLC determination of phenolic compounds in red grapes. *Am. J. Enol. Vitic.* **1990**, *39*, 259–262.
50. Somers, T.C.; Ziemelis, G. Spectral evaluation of total phenolic components in Vitis vinifera: Grapes and wines. *J. Sci. Food Agric.* **1985**, *36*, 1275–1284. [CrossRef]
51. Alonso, A.M.; Guillén, D.A.; Barroso, C.G.; Puertas, B.; García, A. Determination of the antioxidant activity of wine byproducts and its correlation with polyphenolic content. *J. Agric. Food Chem.* **2002**, *50*, 5832–5836. [CrossRef] [PubMed]
52. De Campos, L.M.; Leimann, F.V.; Pedrosa, R.C.; Ferreira, S.R. Free radical scavenging of grape pomace extracts from cabernet sauvingnon (*Vitis vinifera*). *Bioresour. Technol.* **2008**, *99*, 8413–8420. [CrossRef]
53. Pedreschi, R.; Cisneros-Zevallos, L. Antimutagenic and antioxidant properties of phenolic fractions from Andean purple corn (*Zea mays* L.). *J. Agric. Food Chem.* **2006**, *54*, 4557–4567. [CrossRef] [PubMed]
54. Mirpoor, S.F.; Giosafatto, C.V.L.; Porta, R. Biorefining of seed oil cakes as industrial co-streams for production of innovative bioplastics. A review. *Trends Food Sci. Technol.* **2021**, *109*, 259–270. [CrossRef]
55. Sabbah, M.; Di Pierro, P.; Giosafatto, C.V.L.; Esposito, M.; Mariniello, L.; Regalado-Gonzales, C.; Porta, R. Plasticizing effects of polyamines in protein-based films. *Int. J. Mol. Sci.* **2017**, *18*, 1026. [CrossRef] [PubMed]
56. American Association of Cereal Chemists (AACC). *Approved Methods of AACC*; The Association: St. Paul, MN, USA, 2003.
57. *ASTM Standard Test Method for Tensile Properties of Thin Plastic Sheeting*; ASTM: West Conshohocken, PA, USA, 1995.
58. Krochta, J.M. Proteins as raw materials for films and coatings: Definitions, current status, and opportunities. *Protein-Based Film. Coat.* **2002**, *1*, 1–40.

59. Galus, S.; Lenart, A. Development and characterization of composite edible films based on sodium alginate and pectin. *J. Food Eng.* **2013**, *115*, 459–465. [CrossRef]
60. Siripatrawan, U.; Harte, B.R. Physical properties and antioxidant activity of an active film from chitosan incorporated with green tea extract. *Food Hydrocoll.* **2010**, *24*, 770–775. [CrossRef]
61. Pranoto, Y.; Salokhe, V.M.; Rakshit, S.K. Physical and antibacterial properties of alginate-based edible film incorporated with garlic oil. *Int. Food Res. J.* **2005**, *38*, 267–272. [CrossRef]
62. McGuire, R.G. Reporting of objective color measurements. *Hort. Sci.* **1992**, *27*, 1254–1255. [CrossRef]
63. Kabir, Y.; Shirakawa, H.; Komai, M. Nutritional composition of the indigenous cultivar of black cumin seeds from Bangladesh. *Prog. Nutr.* **2019**, *21*, 428–434.
64. Dangaran, K.L.; Krochta, J.M. Preventing the loss of tensile, barrier and appearances properties caused by plasticizer crystallization in whey protein films. *Int. J. Food Sci. Technol.* **2007**, *42*, 1094–1100. [CrossRef]
65. Hernandez-Izquierdo, V.M.; Krochta, J.M. Thermoplastic processing of proteins for film formation—A review. *J. Food Sci.* **2008**, *73*, 30–39. [CrossRef] [PubMed]
66. Priyadarshi, R.; Kumar, B.; Negi, Y.S. Chitosan film incorporated with citric acid and glycerol as an active packaging material for extension of green chilli shelf life. *Carbohydr. Polym.* **2018**, *195*, 329–338. [CrossRef] [PubMed]
67. Karbowiak, T.; Hervet, H.; Léger, L.; Champion, D.; Debeaufort, F.; Voilley, A. Effect of plasticizers (water and glycerol) on the diffusion of a small molecule in κcarragennan biopolymer films for edible coating application. *Biomacromolecules* **2006**, *7*, 2011–2019. [CrossRef]
68. Sothornvit, R.; Krochta, J.M. Plasticizer effect on oxygen permeability of betalactoglobulin films. *J. Agric. Food Chem.* **2000**, *48*, 6298–6302. [CrossRef] [PubMed]
69. Dangaran, K.L.; Krochta, J.M. Aqueous whey protein coatings for panned products. *Manuf. Confect.* **2003**, *83*, 61–65.
70. Veiga-Santos, P.; Oliveira, L.M.; Cereda, M.P.; Scamparini, A.R.P. Sucrose and inverted sugar as plasticizer. Effect on cassava starch–gelatin film mechanical properties, hydrophilicity and water activity. *Food Chem.* **2007**, *103*, 255–262. [CrossRef]
71. Saberi, B.; Chockchaisawasdee, S.; Golding, J.B.; Scarlett, C.J.; Stathopoulos, C.E. Physical and mechanical properties of a new edible film made of pea starch and guar gum as affected by glycols, sugars and polyols. *Int. J. Biol. Macromol.* **2007**, *104*, 345–359. [CrossRef]
72. Pandey, A.K.; Dhakal, M.R. Phytomelanin in compositae. *Curr. Sci.* **2001**, *80*, 933–940.
73. Eid, A.M.; Elmarzugi, N.A.; Abu Ayyash, L.M.; Sawafta, M.N.; Daana, H.I. A review on the cosmeceutical and external applications of *Nigella sativa*. *J. Trop. Med.* **2017**, *2017*, 1–6. [CrossRef] [PubMed]
74. Özdemir, Ö.; Keles, Y. Extraction, purification, antioxidant properties and stability conditions of phytomelanin pigment on the sunflower seeds. *Int. J. Second Metab.* **2017**, *5*, 140–148.
75. Ozdemir, M.; Floros, J.D. Optimization of edible whey protein films containing preservatives for mechanical and optical properties. *J. Food Eng.* **2008**, *84*, 116–123. [CrossRef]
76. Hopkins, E.J.; Stone, A.K.; Wang, J.; Korber, D.R.; Nickerson, M.T. Effect of glycerol on the physicochemical properties of films based on legume protein concentrates: A comparative study. *J. Texture Stud.* **2019**, *50*, 539–546. [CrossRef]
77. Porta, R.; Di Pierro, P.; Roviello, V.; Sabbah, M. Tuning the functional properties of bitter vetch (*Vicia ervilia*) protein films grafted with spermidine. *Int. J. Mol. Sci.* **2017**, *18*, 2658. [CrossRef]
78. Vejdan, A.; Mahdi Ojagh, S.; Adeli, A.; Abdollahi, M. Effect of TiO_2 nanoparticles on the physico-mechanical and ultraviolet light barrier properties of fish gelatin/agar bilayer film. *LWT Food Sci. Technol.* **2016**, *71*, 88–95. [CrossRef]
79. Edhirej, A.; Sapuan, S.M.; Jawaid, M.; Zahari, N.I. Effect of various plasticizers and concentration on the physical, thermal, mechanical, and structural properties of cassava-starch-based films. *Starch-Stärke* **2017**, *69*, 1500366. [CrossRef]
80. Bamdad, F.; Goli, A.H.; Kadivar, M. Preparation and characterization of proteinous film from lentils (*Lens culinaris*). *Food Res. Int.* **2006**, *39*, 106–111. [CrossRef]
81. Mahmoud, R.; Savello, P.A. Mechanical properties of and water vapor transferability through whey protein films. *J. Dairy Sci.* **1992**, *75*, 942–946. [CrossRef]
82. Jangchud, A.; Chinnan, M.S. Peanut protein film as affected by drying temperature and ph of film forming solution. *J. Food Sci.* **1990**, *64*, 153–157. [CrossRef]
83. Blois, M.S. Antioxidant determinations by the use of a stable free radical. *Nature* **1958**, *181*, 1199–1200. [CrossRef]
84. Park, P.; Je, J.; Kim, S. Free radical scavenging activities of differently deacetylated chitosans using an ESR spectrometer. *Carbohydr. Polym.* **2004**, *55*, 17–22. [CrossRef]
85. Ramchandani, A.G.; Chettiyar, R.S.; Pakhale, S.S. Evaluation of antioxidant and anti-initiating activities of crude polyphenolic extracts from seedless and seeded Indian grapes. *Food Chem.* **2010**, *119*, 298–305. [CrossRef]
86. Daglia, M. Polyphenols as antimicrobial agents. *Curr. Opin. Biotechnol.* **2012**, *23*, 174–181. [CrossRef]
87. Aires, A.; Marques, E.; Carvalho, R.; Rosa, E.A.; Saavedra, M.J. Evaluation of biological value and appraisal of polyphenols and glucosinolates from organic baby-leaf salads as antioxidants and antimicrobials against important human pathogenic bacteria. *Molecules* **2013**, *18*, 4651–4668. [CrossRef]
88. Taguri, T.; Tanaka, T.; Kouno, I. Antimicrobial activity of 10 different plant polyphenols against bacteria causing food-borne disease. *Biol. Pharm. Bull.* **2004**, *27*, 1965–1969. [CrossRef]

89. Kappel, F.; Toivonen, P.; McKenzie, D.L.; Stan, S. Storage characteristics of new sweet cherry cultivars. *HortScience* **2002**, *37*, 139–143. [CrossRef]
90. Bhardwaj, R.L.; Pandey, S. Juice blends—A way of utilization of under-utilized fruits, vegetables, and spices: A review. *Crit. Rev. Food Sci. Nutr.* **2011**, *51*, 563–570. [CrossRef] [PubMed]
91. Gonçalves, B.; Silva, A.P.; Moutinho-Pereira, J.; Bacelar, E.; Rosa, E.; Meyer, A.S. Effect of ripeness and postharvest storage on the evolution of colour and anthocyanins in cherries (*Prunus avium* L.). *Food Chem.* **2007**, *103*, 976–984. [CrossRef]
92. Gutiérrez-Jara, C.; Bilbao-Sainz, C.; McHugh, T.; Chiou, B.S.; Williams, T.; Villalobos-Carvajal, R. Effect of cross-linked alginate/oil nanoemulsion coating on cracking and quality parameters of sweet cherries. *Foods* **2021**, *10*, 449. [CrossRef]

coatings

MDPI

Article

Production and Characterization of Active Pectin Films with Olive or Guava Leaf Extract Used as Soluble Sachets for Chicken Stock Powder

Mohammed Sabbah [1,*], Asmaa Al-Asmar [2,3], Duaa Younis [1], Fuad Al-Rimawi [4], Michela Famiglietti [5] and Loredana Mariniello [5]

1 Department of Nutrition and Food Technology, An-Najah National University, P.O. Box 7, Nablus P400, Palestine; d.yunis@najah.edu
2 Department of Biology and Biotechnology, Faculty of Science, An-Najah National University, P.O. Box 7, Nablus P400, Palestine; a.alasmar@najah.edu
3 Energy, Water and Food Security Research Center, An-Najah National University, P.O. Box 7, Nablus P400, Palestine
4 Department of Chemistry, Al-Quds University, Abu Dis, Jerusalem P144, Palestine; falrimawi@staff.alquds.edu
5 Department of Chemical Sciences, University of Naples "Federico II", 80126 Naples, Italy; michela.famiglietti@unina.it (M.F.); loredana.mariniello@unina.it (L.M.)
* Correspondence: m.sabbah@najah.edu; Tel.: +790-92345115

Abstract: The goal of this study was to improve the functionality of two pectin (PEC) edible films by incorporating olive leaf extract (OLE) or guava leaf extract (GLE). Different concentrations of OLE or GLE (0.1 and 0.2% *w*/*v*) were used, and 30% glycerol was added as a plasticizer. The obtained films were evaluated for their mechanical properties, antioxidant activity, thickness, color, opacity, permeability to gases and water vapor, moisture content, and moisture uptake. Soluble sachets were then prepared and filled with chicken stock powder. The results indicated that incorporating OLE or GLE into the PEC films significantly increased their opacity, greenness, and antioxidant activity, which increased from 8.5% in the control to 83.9% when 0.2% GLE was added. Additionally, the films had lower water vapor permeability than the control film. The moisture uptake of the films was also significantly increased when GLE was added. Furthermore, the developed sachets were tested in real-life scenarios, mirroring their intended usage in households. After being introduced to boiling water, the sachets rapidly dissolved within seconds. These results suggest that OLE or GLE, as natural additives, can be used to improve the functionality and activity of edible films.

Keywords: functional edible packaging; food preservation; pectin films; food wrapping; olive byproducts; plant leaf; circular economy

check for updates

Citation: Sabbah, M.; Al-Asmar, A.; Younis, D.; Al-Rimawi, F.; Famiglietti, M.; Mariniello, L. Production and Characterization of Active Pectin Films with Olive or Guava Leaf Extract Used as Soluble Sachets for Chicken Stock Powder. *Coatings* **2023**, *13*, 1253. https://doi.org/10.3390/coatings13071253

Academic Editor: Jun Mei, Jing Xie and Biao Zhang

Received: 13 June 2023
Revised: 14 July 2023
Accepted: 14 July 2023
Published: 16 July 2023

Copyright: © 2023 by the authors. Licensee MDPI, Basel, Switzerland. This article is an open access article distributed under the terms and conditions of the Creative Commons Attribution (CC BY) license (https://creativecommons.org/licenses/by/4.0/).

1. Introduction

Today, bioplastics, edible films, and coatings are becoming the most effective ways to reduce food packaging's adverse impact on the environment [1,2]. More than 368 million tons of plastics was used in 2019, and a significant amount of this quantity ended up in landfills and the oceans, polluting our air, water, and soil [3,4]. Several researchers have worked to find the best combination between low-price film-based materials and their activation with different plant extracts or additives that potentially have antioxidant, antimicrobial, and anti-biofilm activities [5], to enhance the food's shelf-life or other functionality for food applications [6–9]. As a result of short shelf-life and inadequate packaging, food waste remains a significant global challenge, emphasizing the need for innovative and sustainable packaging solutions [10–16]. Edible films and coatings are prepared mainly from hydrocolloidal materials (e.g., carbohydrates and proteins, or a combination of both sources). Carbohydrate-material-based films show good mechanical properties, although

they are poor in terms of permeability. Meanwhile, edible films prepared mainly from protein show good barrier properties against gases, although they have poor mechanical properties [15,17–25].

In recent years, the development of edible and coating solutions based on pectin has increased due to several reasons. First, they are classified as food-grade materials and are non-toxic [26]. They can also be obtained from renewable available resources such as citrus peel, apple pomace, and sugar beet [27]. They also have good film formation ability, even without plasticizers [28]. Additionally, they can be used in different food products as stabilizers or thickeners, and they have good water solubility, biocompatibility, and compostability [27].

Commercial pectin is derived from a variety of plant sources, including apple pomace (14%), and citrus peel (85%) [6,29]. Fruit processing industries generate significant quantities of fruit waste that, if not utilized, ends up in landfills, contributing to environmental degradation due to microbial decay and greenhouse gas emissions [30]. However, pectin, which is a complex polysaccharide, represents the highest percentage of plant mass composition (about 35% in dicotyledonous plant cells and approximately 5% in woody tissues [31], whereas in grass plants it is about 2%–10%) [32]. Recently, Chandel et al. [27] reported on pectin obtained from 26 sources, along with the extraction methods that were used to produce commercial pectin for different applications, e.g., food, pharmaceuticals [33], cosmetics, and food packaging [15,17,19,28,34].

Pectin film alone does not possess strong functionality in terms of antimicrobial or antioxidant activity, which may potentially discourage manufacturers from using it for food wrappings or coatings. Lately, many researchers have worked to improve the functionality of pectin film due to its availability and low price, by adding essential oils, functionalized nanoparticles [35], and plant extracts. Adding plant extracts or essential oils such as mint [36], lemon [37], oregano [38], orange [37], clove bud [39], cinnamon [40], or lime peel extract [41] to the edible films proved that pectin-based films can be used as food packaging to extend the shelf-life of food products.

Extracts of plant leaves represent a promising approach that can be incorporated, as they have antioxidant and antimicrobial activity. Therefore, olive (*Olea europaea* L.) leaf extracts (OLEs) have been used for centuries in folk medicine as therapeutic infusions, and they are among the main byproducts generated from the olive oil industry [42]. One of the major phenolic compounds found in olive leaves is oleuropein, a glucoside ester of elenolic acid and hydroxytyrosol. Oleuropein has been reported to have significant health benefits, including antioxidant, cholesterol-lowering, cardioprotective, anti-inflammatory, hypoglycemic, and antimicrobial properties [42]. The wide profile of polyphenols in olive leaves gives OLE great potential as a natural antioxidant. OLE has been incorporated as an antioxidant in several food matrices, such as edible oils, frying oils, table olives, meat, and meat products [43–46]. Moreover, Elsayed et al. [47] utilized an OLE coating incorporated with a zinc/selenium oxide nanocomposite to enhance the postharvest quality of green bean pods; they concluded that by using 3% OLE with zinc, the green bean pods' shelf-life increased to 28 days in cold storage, and all attributes improved compared to the other treatments or controls. In addition, guava (*Psidium guajava* L.) leaf extract (GLE) contains several bioactive compounds, especially phenolic compounds that contribute to antioxidant and anti-inflammatory properties [48,49]. However, quercetin is the most potent antioxidant found in GLE [48,50]. Guava leaves are traditionally used to treat gastrointestinal ailments (e.g., diarrhea, stomach pain, gastroenteritis, indigestion, and dysentery) and dermatological problems (e.g., skin infection, skin aging, and ulcers).

Pectin sachets were prepared from lime peel pectin integrated with coconut water and lime peel extract, and they were used to retard soybean oil's oxidation; the obtained results indicated that the pectin sachets retarded the soybean oil's oxidation for 30 days of storage [41].

Due to the lack of previous works, as well as the potential functionality of OLE and GLE that contribute to the shelf-life and preservation of food, both materials were used in

this study as film functionality materials. The main objective of this project was therefore to utilize OLE and GLE at different concentrations in pectin-based films, and to evaluate their contributions to the obtained films, which were used to prepare soluble sachets that were used in this study as filling sachets for chicken stock powder.

2. Materials and Methods

2.1. Materials

Olive leaves were collected from olive trees in Ramallah/West Bank, Palestine, in October 2021. The leaves were collected, washed with tap water, and then dried for 30 days at room temperature (25–30 °C). The leaves were then ground until a fine powder (0.1 to 0.6 mm) was obtained.

The guava leaf samples used in this study were obtained from guava trees in Qalqilya/West Bank, Palestine. The leaf samples were washed with tap water and dried for 30 days in a dry place at room temperature (25–30 °C). The samples were milled and sieved after drying. Particles ranging from 0.1 to 0.6 mm in size were chosen for the extractions. Prior to the extraction, the samples were placed in plastic bags and stored in a dark, dry area. Food-grade vegetable glycerol (GLY) was purchased from Heartlandvapes LLC., Owasso, OK, USA.

2.2. Preparation of Olive and Guava Leaves Extracts

OLE and GLE were extracted following the methodology outlined by Annegowda et al. [51], with certain modifications. Then, 10 g of leaf powder from each material was combined with 100 mL of ethanol in a beaker. The mixture was subjected to sonication for a duration of 2 h, while maintaining the solvent surface at room temperature. Subsequently, the residues were dissolved in ethanol and subjected to another round of extraction. The resulting extracts were filtered using vacuum filtration and Whatman filter paper, followed by concentration using a rotary evaporator set at 50 °C. After that, the crude extract was dried in a freeze-dryer. Finally, the obtained extract was sieved through a stainless steel sieve (with a mesh size of 425 µm) provided by Octagon Digital Endecotts Limited (Lombard Road, London, UK) until a fine powder was obtained. The extraction yield of OLE was about 9.0%, while that of GLE was 11.0%.

2.3. Film Preparation with Olive and Guava Leaf Extracts

Citrus PEC stock solution (2.0 g) was added to 100 mL of distilled water and completely solubilized. A film-forming solution (FFS) containing 0.1 and 0.2 w/v of OLE or GLE was added and continuously stirred for 30 min at room temperature. Then, GLY (30% w/v relative to PEC) was added to the FFS as a plasticizer. The concentrations of both OLE and GLE were chosen in accordance with the preliminary investigation, wherein varying concentrations of 0%, 0.05%, 0.1%, 0.2%, and 0.4% (w/v) were employed. The obtained film samples were subsequently analyzed for their mechanical properties and color characteristics. After careful evaluation, it was found that the lower concentrations (0.05% w/v) did not show any significant effect on the film properties. However, the higher concentrations (0.4% w/v) had an unwanted effect on the color of the films, which became more greenish, opaque, and rigid. Therefore, the concentrations of 0.1% and 0.2% (w/v) were deemed suitable and selected for further experimentation. The final volume was adjusted to 50 mL using distilled water, and then the FFSs were poured onto 8 cm diameter polystyrene Petri dishes and dried in a drying chamber at 30 °C for 12 h. The dried films were peeled off from the Petri dishes and then placed inside a desiccator (50%–55% RH) containing a saturated solution of $Mg(NO_3)_2 \cdot 6H_2O$ for 2 h before analysis of the properties of the prepared films.

2.4. Film Characterization

The effects of OLE and GLE at two different concentrations (0.1, 0.2% w/v) on the films' mechanical properties—including tensile strength (TS), elongation at break (EB), and

Young's modulus (YM)—were measured using a universal testing instrument (Brookfield CT3 Texture Analyzer, model CT3 50K, Brookfield, Chandler, AZ, USA), as described by [8]. The dry films were used for testing the mechanical properties. The films were cut into strips (10 mm wide) and then loaded between the grips of the CT3 Texture Analyzer and tested, with an initial grip separation of about 50 mm and a speed of 0.5 mm/s. At least six strips from each film were tested, and the experiment was repeated three times at a different intervals.

The thickness of the obtained films was tested using a micrometer screw gauge (0–25 mm), where at least 6 different points from the whole films were measured.

The ability of the films to scavenge DPPH free radicals was tested as described by Famiglietti et al. [43]. Briefly, 20 mg of each film was solubilized in 500 mL of distilled water, and then 100 mL of each solution was mixed with 900 mL of DPPH (0.05 mg/mL methanolic solution). After the samples were kept in the dark for 30 min at 25 °C, the absorbance at 517 nm was measured using a UV–visible Spectrophotometer (SmartSpec 3000 Bio-Rad, Segrate, Milan, Italy), where methanol was used as a blank and a sample with methanol was added to DPPH solution as a control. The antioxidant activity of the films was calculated based on the following equation:

$$\%\text{DPPH scavenging activity} = (A_{control} - A_{sample}/A_{control}) \times 100 \quad (1)$$

where A is the absorbance value of the control and the sample at 517 nm. Each sample was measured in triplicate.

Tonyali et al. [52] and Famiglietti et al. [43] provided insights into measuring the films' opacity. In accordance with their methods, the films were measured six times for each sample. The opacity of the films was then calculated using the following equation:

$$\text{Opacity } (\text{mm}^{-1}) = A600/x \quad (2)$$

where $A600$ is the absorbance of the sample at 600 nm, and x is the film thickness (mm).

The moisture content of the film was determined as described by Galus and Lenart [53], by measuring the mass loss of one gram after 24 h of oven drying at 105 °C and expressing it as a percentage. The weight gain of each specimen after 24 h at 50% RH was used to determine the ability of the specimen to absorb moisture. A total of 3 specimens (2 cm^{-2}) were cut from the films and weighed ($W1$), and then the films were dried in the oven at 105 °C for 24 h before being weighed again ($W2$). Following conditioning at 25 °C and 50% RH for 24 h, the film samples were weighed once more ($W3$) after being placed in a desiccator over a saturated solution of $Mg(NO_3)_2$ $6H_2O$.

Water content and uptake were calculated according to the following formulae:

$$\text{Water content } (\%) = \frac{W1 - W2}{W1} \times 100 \quad (3)$$

$$\text{Water uptake } (\%) = \frac{W3 - W2}{W3} \times 100 \quad (4)$$

The color values of the developed films were measured with a colorimeter (chroma Meter Konica Minolta CR-400, Japan) using the CIE color scale to evaluate the parameters L* (lightness/brightness, which ranges from 0 to 100), a* (redness/greenness), and b* (yellowness/blueness) (the two chromatic components, which range from −120 to 120) [54].

The films' barrier properties against water vapor (WV), O_2, and CO_2 were analyzed by means of a MultiPerm apparatus (ExtraSolution s.r.l, Pisa, Italy). The measurements were performed in duplicate for each film (50% RH, 25 °C) according to ASTM F1249-13 [55], ASTM D3985-05 [56], and ASTM F2476-05 [57]. Before testing, the film specimens were conditioned for 24 h at 50% RH and placed in aluminum masks to reduce the film test area to 2 cm^2.

2.5. Sachet Application Experiment

The obtained films (control, pectin with 0.2% OLE, and pectin with 0.2% GLE), were folded and heat-sealed on two sides using a kitchen sealer machine, and then the sachets were filled to the top with about 18–20 g of chicken stock powder before being heat-sealed. Finally, boiling water was prepared, and the sachets was added to the boiling water and stirred until they completely dissolved.

2.6. Statistical Analysis

The obtained data were statistically analyzed using JMP software (SAS Institute, Cary, NC, USA, version 5.0). The data were subjected to analysis of variance (ANOVA), and the means were compared using the Tukey–Kramer HSD test. Differences were considered to be significant at $p < 0.05$.

3. Results and Discussion

3.1. Effect of Incorporation of OLE and GLE in Pectin-Based Films on Thickness and Opacity

Pectin-based films modified with olive leaf extract (OLE) or guava leaf extract (GLE) were obtained at different concentrations (0.1% and 0.2% w/v) in the presence of 30% glycerol (GLY) as a plasticizer. Figure 1A shows the visual observation of the obtained films compared to the control film containing only pectin (PEC). The addition of GLE or OLE increased the greenish color of the pectin films, with a higher intensity observed in the films containing GLE. Previous research has shown that GLE significantly increased the film color compared to the control [58]. This suggests that the differences in the chemical structure of natural pigments and phenolic compounds between GLE and the control may be responsible for the differences in film color [59,60].

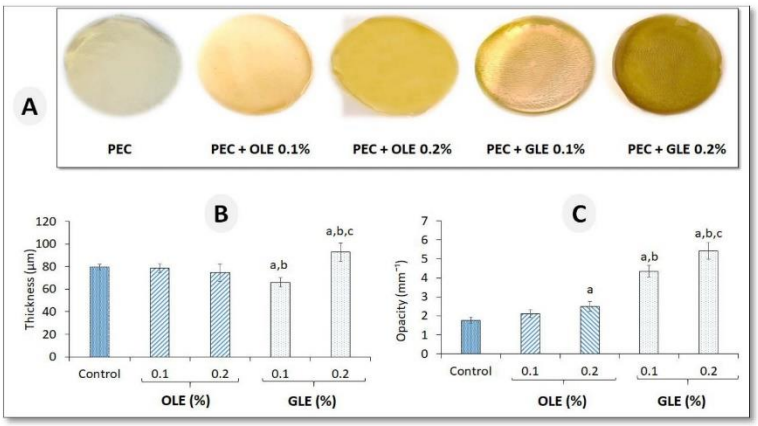

Figure 1. Effects of using OLE and GLE at different concentrations (0.1 w/v and 0.2 w/v) on pectin-based films: observation (**A**), thickness (**B**), and opacity (**C**). The values that are significantly different from the control are indicated by "a" ($p < 0.05$); the values indicated by "b" are significantly different ($p < 0.05$) from films obtained with different materials at the same concentration; the values indicated by "c" are significantly different ($p < 0.05$) from the films obtained with the same material at different concentrations.

Film thickness was also determined, and the results (Figure 1B) indicated that modifying the pectin with OLE did not change the film thickness compared to the control. However, when 0.2% GLE was used, the film thickness significantly increased compared to the control and the films obtained with OLE. This can be explained by the ability of

GLE to increase the intermolecular forces among pectin polymer chains [61]. Moreover, there is no clear explanation for why GLE has different effects on film thickness at different concentrations. In fact, it is thought that the GLE interacts with the pectin molecules differently depending on the concentration. We could hypothesize that when the GLE is present at low concentrations (0.1% w/v), it may be able to penetrate between the pectin molecules and disrupt their interactions. The films would become less thin as a result. At higher concentrations (0.2% w/v), the GLE may not be able to penetrate between the pectin molecules, instead forming a layer on the surface. The films would be thickened as a result.

Additionally, the opacity of the films significantly increased with increasing concentrations of OLE or GLE. Notably, in the films containing 0.2% OLE, the opacity was significantly higher compared to the control film. Similarly, when GLE was used, the results indicated that the film's opacity was twice that of the control film or the films containing OLE (Figure 1C).

3.2. *Films' Mechanical Properties*

The obtained films were also characterized for their mechanical properties, including tensile strength (TS), elongation at break (EB), and Young's modulus (YM). The results, reported in Figure 2, showed that the addition of either OLE or GLE at different concentrations did not significantly affect the TS value. However, the EB result was significantly lower than that of the control films only in the pectin films prepared with 0.1% GLE. The YM of the films significantly decreased in the films prepared with either OLE or GLE compared to the control film containing only PEC. This indicates that increasing the concentration of OLE or GLE led to a significant decrease in YM.

Luo et al. [62] investigated the incorporation of different concentrations of GLE into a sodium-alginate-based material, and they found that adding GLE to sodium alginate significantly increased the TS and significantly decreased the EB compared to the control film obtained using only sodium alginate. This obtained result is consistent with the results obtained recently by Chou et al. [58], where they incorporated GLE into fish skin gelatin. Moreover, according to some studies, excessive proportions of the extracts may result in uneven dispersion in the mixture [62,63]. Plant oils reduce the intermolecular forces between polymer chains, decreasing the films' strength and increasing their flexibility [61].

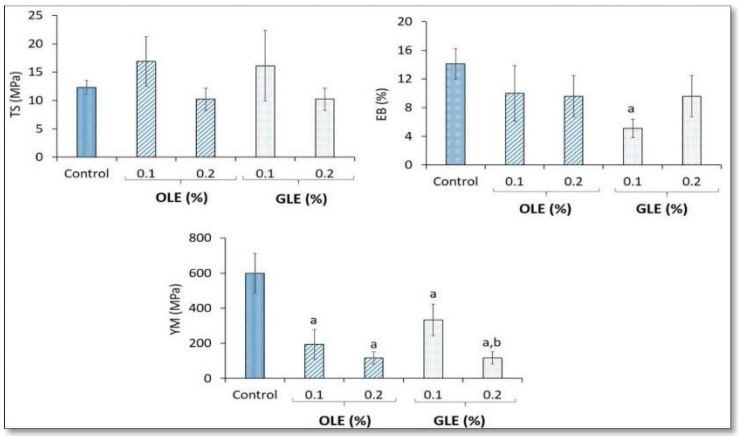

Figure 2. Effect of using OLE and GLE at different concentrations (0.1 w/v and 0.2 w/v) on the mechanical properties (TS, EB, and YM) of pectin-based films. The values that are significantly different from the control are indicated by "a" ($p < 0.05$), while the values indicated by "b" are significantly different ($p < 0.05$) from the films obtained with the same material at a different concentration.

3.3. Antioxidant Activity

The DPPH radical scavenging abilities of the obtained films were evaluated, and the results were compared with the control film that was prepared from only pectin and glycerol. The results are reported in Figure 3. According to many studies, PEC films do not have antioxidant activity naturally; in this context, OLE and GLE have previously been recognized for their antioxidant activity, and they have higher antioxidant activities compared to other materials [42,48,49,62,64]. The pure OLE and GLE were evaluated at two different concentrations (150 and 300 ppm), and the results were 67 ± 1.8% and 76 ± 1.8%, respectively, for OLE, and 61 ± 1.9% and 82 ± 1.2%, respectively, for GLE. The results indicated that when the concentration of pure OLE or GLE increased, the antioxidant activity increased, and GLE at 300 ppm showed the highest activity, reaching 82%, as compared to 76% for OLE. Moreover, the obtained films were evaluated to study the effects of the addition of OLE or GLE to the pectin film-forming solution on the film's antioxidant activity. The obtained results indicated that by increasing the proportion of OLE or GLE from 0.1 to 0.2% w/v, the DPPH radical scavenging abilities of the films were significantly improved compared to the control film. The addition of 0.2% (w/v) OLE to the films showed significantly higher activity compared to the control and to the 0.1% w/v OLE. Moreover, the incorporation of GLE into the films indicated that these films had higher antioxidant activity compared with the OLE at the same concentration. This increased activity may be attributed to the presence of quercetin, which is classified as the most potentially powerful antioxidant compound [48,49]. Similar results were found by Albertos et al. [64] when they evaluated the effects of the addition of different concentrations of OLE to gelatin-based films to enhance the quality of cold smoked salmon, and they reported that increasing the OLE concentrations also increased the antioxidant activity. The addition of OLE and OLE to packaging materials can significantly increase their antioxidant capacity, which can help to protect food from oxidation and deterioration.

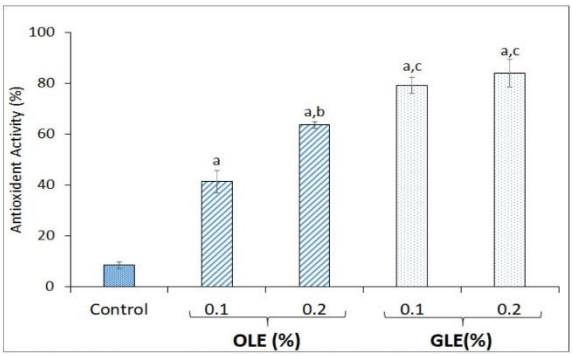

Figure 3. Effects of using OLE and GLE at different concentrations (0.1 w/v and 0.2 w/v) on the antioxidant activity of pectin-based films. The values significantly different from the control are indicated by "a" ($p < 0.05$); the values indicated by "b" are significantly different from the others films obtained with the same material (OLE); the values indicated by "c" are significantly different from the films made of OLE or GLE at a concentration of 0.1% or 0.2% ($p < 0.05$).

3.4. Water Content and Water Uptake

The effects of the incorporation of different concentrations of OLE and GLE on the water content and uptake of pectin-based films were measured, and the results are reported in Figure 4. The results show that OLE and GLE do not have a significant influence on the film's moisture content at any concentration. However, the moisture uptake of the pectin films modified with GLE increased significantly compared to the control film prepared

from pectin alone or the pectin-based films containing OLE. The highest moisture uptake was found in the film that contained 0.2% GLE, reaching 20.20 ± 1.80%, while the control film had about 13.90 ± 0.88% moisture uptake. Luo et al. [62] prepared sodium alginate films incorporating GLE and concluded that films containing GLE tended to have lower moisture content than the control films. Similar results were found by adding grape juice to protein-based films, where the moisture content did not change with increasing grape juice concentration [8].

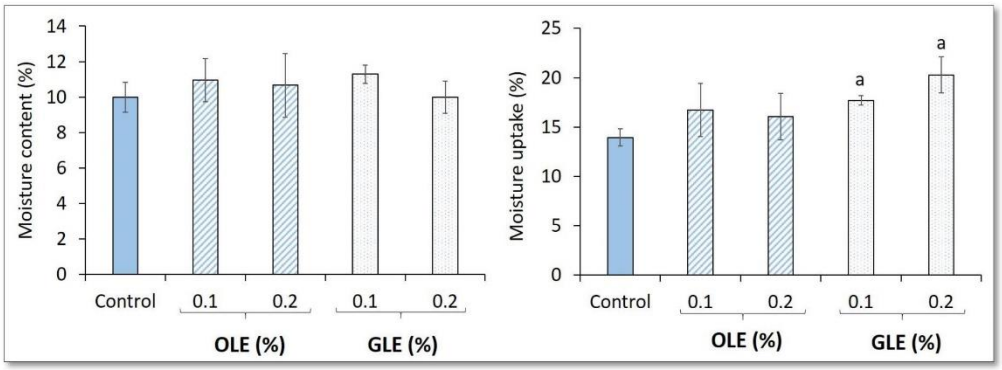

Figure 4. Effects of using OLE and GLE at different concentrations (0.1 *w*/*v* and 0.2 *w*/*v*) on the water content and water uptake of pectin-based films. The values that are significantly different from the control are indicated by "a" ($p < 0.05$).

3.5. Effects of OLE and GLE on the Color of Pectin-Based Films

The effects of adding different concentrations of OLE and GLE on the color of pectin-based films are shown in Table 1. The L* values of the films containing OLE (0.1 and 0.2% *w*/*v*) were significantly increased compared to the control, indicating that the films were lighter. In contrast, the L* values of the films containing GLE decreased significantly compared to the control and the films containing OLE, indicating that these films were darker. The a* value, which indicates greenness, was significantly changed in the films modified with OLE and GLE.

Table 1. Effects of different concentrations of OLE and GLE on pectin-based films' color.

Films	L*	a*	b*
PEC (control)	83.44 ± 0.09	−3.09 ± 0.04	17.41 ± 0.30
PEC + OLE 0.1%	85.02 ± 0.05 ^{A}	−1.50 ± 0.01 ^{A}	11.13 ± 0.17 ^{A}
PEC + OLE 0.2%	86.92 ± 0.14 ^{A,B}	0.72 ± 0.04 ^{A,B}	3.36 ± 0.29 ^{A,B}
PEC + GLE 0.1%	79.83 ± 0.91 ^{A,D}	−2.01 ± 0.03 ^{A,D}	21.76 ± 1.80 ^{A,D}
PEC + GLE 0.2%	74.89 ± 0.38 ^{A,C,D}	−3.08 ± 0.11 ^{C,D}	34.50 ± 0.43 ^{A,C,D}

The values that were significantly different from the controls are indicated by "^{A}" ($p < 0.05$), while the values indicated by "^{B}" were significantly different from the films obtained with OLE ($p < 0.05$), the values indicated by "^{C}" were significantly different from the films obtained with GLE ($p < 0.05$), and the values indicated by "^{D}" were significantly different from the films made of OLE or GLE at a concentration of 0.1% or 0.2% ($p < 0.05$). Further experimental details are given in the text.

The films containing OLE were greener than the control films, and the films containing GLE were even greener. However, the b* value, which indicates yellowness, decreased significantly when the concentration of OLE was increased. This indicates that the films became less yellow. In contrast, the b* value was significantly increased when GLE was incorporated into the pectin films. This indicates that the films became more yellow. In conclusion, the addition of GLE to the films resulted in a darker, more greenish, and more

yellowish color. These findings explain the opacity results reported in Figure 1C. The obtained results are consistent with the results achieved by [62,63].

3.6. Permeability Properties

Table 2 reports the effects of the incorporation of OLE or GLE at different concentrations on the gas (CO_2 and O_2) and water vapor (WV) permeability of the pectin-based films. The permeability of the films that contained either OLE or GLE was higher toward all gases and WV compared to the control film (pectin alone). Gradually, the CO_2 permeability significantly increased when the OLE concentration increased. On the other hand, when increasing the concentration of OLE or GLE, the WV permeability of the films remained almost constant. The obtained results show a lower permeability toward CO_2 compared to Viscofan NDX—the commercial casing material used for processed meat products—and a similar value of O_2 permeability but a higher WV permeability. The WV permeability of films is a function of both the molecular diffusion coefficient and the water solubility of the film material [65]. The obtained results are consistent with those previously obtained by [64], who concluded that the addition of 3.75 and 5.63% OLE to gelatin-based films increased the WV permeability significantly, which they explained as being due to the increasing film thickness and the water solubility factor. However, the obtained results could also be explained by the presence of phenolic compounds that may accumulate in the polymer matrix and form voids, which can lead to higher WV permeability values compared to films that do not contain phenolics [62,66].

Table 2. Gas and water vapor (WV) permeability of 1% PEC films prepared in the presence of different concentrations of OLE or GLE with 30% GLY.

Films	CO_2	O_2	WV
	$cm^3 \cdot mm \cdot m^{-2} \cdot day^{-1} \cdot kPa^{-1}$		$g \cdot mm \cdot m^{-2} \cdot day^{-1} \cdot kPa^{-1}$
PEC *	0.08 ± 0.03	0.01 ± 0.00	0.12 ± 0.01
PEC + OLE 0.1%	0.15 ± 0.02^{A}	0.01 ± 0.00	3.87 ± 0.76^{A}
PEC + OLE 0.2%	$0.35 \pm 0.01^{A,B}$	$0.05 \pm 0.00^{A,B}$	4.64 ± 0.02^{A}
PEC + GLE 0.1%	0.31 ± 0.05^{A}	0.05 ± 0.00^{A}	4.64 ± 0.11^{A}
PEC + GLE 0.2%	$0.37 \pm 0.01^{A,B}$	0.04 ± 0.00^{A}	3.45 ± 0.79^{A}
Viscofan (NDX) **	3.71 ± 0.16	0.03 ± 0.01	0.08 ± 0.01

* Data from Al-Asmar et al. [19]; ** data from Porta et al. [67]. The values that are significantly different from the control are indicated by "^{A}" ($p < 0.05$); the values indicated by "^{B}" are significantly different ($p < 0.05$) from the films obtained with the same material at different concentrations.

3.7. Film Application as a Soluble Sachet for Chicken Stock Powder

One of the important issues related to this type of research is the application of the obtained films that are prepared based on pectin—a well-known material made from citrus peels. OLE and GLE are both natural compounds that have antioxidant and antimicrobial properties. When these extracts are incorporated into pectin films, they improve the film's antioxidant and promising barrier properties, which will potentially extend its shelf-life. This is an active area of research, and more work is needed to understand it fully.

In this study, the obtained materials were kept for up to one year at room temperature, and the films' properties were evaluated the obtained results were extremely promising. Therefore, pectin films that contain OLE or GLE are promising for use as soluble sachets for chicken stock powder. A soluble sachet is a type of packaging that is made from a material that dissolves in water. This allows the food product to be easily poured out of the sachet, without the need for a separate container. Soluble sachets are a convenient and environmentally friendly alternative to traditional packaging materials such as plastic and foil. Pectin films containing OLE or GLE are sustainable and innovative materials that can be used as soluble bags for chicken stock powder (Figure 5). These films have the potential to improve the quality and shelf-life of chicken stock powder while also reducing environmental impacts. As shown in Figure 5, the pectin sachets were prepared and heat-

sealed using the kitchen sealer machine, and chicken stock powder was transferred from commercial plastic foil to our sachets and then added to boiling water to demonstrate their solubility. The sachets were completely dissolved within a few seconds in boiling water, and the chicken stock was ready to use. As a result, pectin films that contain GLE or OLE are promising and warrant further research.

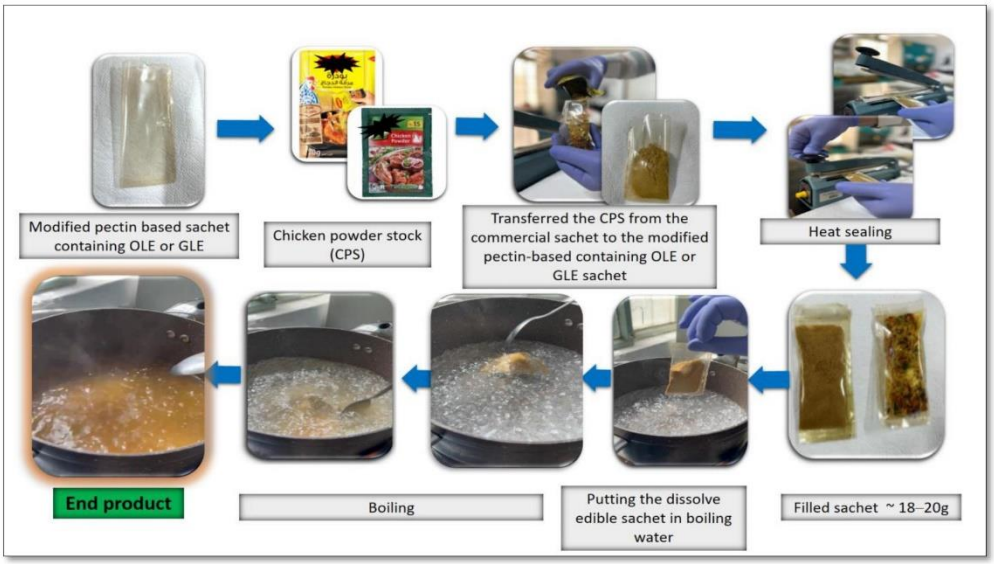

Figure 5. Scheme demonstrating the preparation and use of the pectin sachets containing OLE or GLE filled with chicken stock powder and dissolved in boiling water.

4. Conclusions

In conclusion, natural antioxidants and antimicrobials are becoming increasingly important today due to the worldwide strategy to reduce the use of synthetic additives in our foods. In this work, we successfully functionalized pectin films by incorporating OLE or GLE. The films produced in this study showed lower water vapor permeability than the commercial casing used for processed meat. Additionally, the results indicated a higher antioxidant level compared to the pectin film obtained without OLE or GLE. This helps to reduce the oxidation reactions that can occur during food distribution and storage. This suggests that the obtained films had a significant impact on extending the food's shelf-life. Finally, the films were used to produce soluble sachets filled with chicken stock powder, which was used to prepare soup.

Author Contributions: Conceptualization, M.S., F.A.-R. and A.A.-A.; methodology, F.A.-R., M.F, A.A.-A., and D.Y.; software, M.S.; validation, L.M., M.S. and F.A.-R.; formal analysis, D.Y., A.A.-A. and M.S.; investigation, M.S. and F.A.-R.; resources, F.A.-R., M.S. and L.M.; data curation, M.S. and M.F.; writing—original draft preparation, M.S. and L.M.; writing—review and editing, F.A.-R., A.A.-A., D.Y. and M.F.; visualization, M.S., D.Y., and A.A.-A.; supervision, M.S. and L.M.; project administration, A.A.-A.; funding acquisition, M.S. and L.M. All authors have read and agreed to the published version of the manuscript.

Funding: This research received no external funding.

Institutional Review Board Statement: Not applicable.

Informed Consent Statement: Not applicable.

Data Availability Statement: The original data of this work are available upon reasonable request.

Acknowledgments: We would like to thank the lab instructors at the Faculty of Agriculture and Vet Medicine at An-Najah National University for their help and support.

Conflicts of Interest: The authors declare no conflict of interest.

References

1. Porta, R.; Sabbah, M.; Di Pierro, P. Bio-based materials for packaging. *Int. J. Mol. Sci.* **2022**, *23*, 3611. [CrossRef] [PubMed]
2. Sing, N.; Ogunseitan, O.A.; Wong, M.H.; Tang, Y. Sustainable materials alternative to petrochemical plastics pollution: A review analysis. *Sustain. Horiz.* **2022**, *2*, 100016. [CrossRef]
3. Bauer, F.; Nielsen, T.D.; Nilsson, L.J.; Palm, E.; Ericsson, K.; Frane, A.; Cullen, J. Plastics and climate change—Breaking carbon lock-ins through three mitigation pathways. *One Earth* **2022**, *5*, 361–376. [CrossRef]
4. Plastics Europe. *Plastics—The Facts 2020*; Plastics Europe: Brussels, Belgium, 2020.
5. Dell'Olmo, E.; Gaglione, R.; Sabbah, M.; Schibeci, M.; Cesaro, A.; Di Girolamo, R.; Arciello, A. Host defense peptides identified in human apolipoprotein B as novel food biopreservatives and active coating components. *Food Microbiol.* **2021**, *99*, 103804. [CrossRef] [PubMed]
6. Gerschenson, L.N.; Fissore, E.N.; Rojas, A.M.; Idrovo Encalada, A.M.; Zukowski, E.F.; Higuera Coelho, R.A. Pectins obtained by ultrasound from agroindustrial by-products. *Food Hydrocoll.* **2021**, *118*, 106799. [CrossRef]
7. Rigueto, C.V.T.; Rosseto, M.; Alessandretti, I.; de Oliveira, R.; Wohlmuth, D.A.R.; Menezes, J.F.; Loss, R.A.; Dettmer, A.; Pizzutti, I.R. Gelatin films from wastes: A review of production, characterization, and application trends in food preservation and agriculture. *Food Res. Int.* **2022**, *162*, 112114. [CrossRef]
8. Yaseen, D.; Sabbah, M.; Al-Asmar, A.; Altamimi, M.; Famiglietti, M.; Giosafatto, C.V.L.; Mariniello, L. Functionality of films from *Nigella sativa* defatted seed cake proteins plasticized with grape juice: Use in wrapping sweet cherries. *Coatings* **2021**, *11*, 1383. [CrossRef]
9. Villanueva, V.; Valdés, F.; Zúñiga, R.N.; Villamizar-Sarmiento, M.G.; Soto-Bustamante, E.; Romero-Hasler, P.; Riveros, A.L.; Tapia, J.; Lisoni, J.; Oyarzun-Ampuero, F.; et al. Development of biodegradable and vermicompostable films based on alginate and waste eggshells. *Food Hydrocoll.* **2023**, *142*, 108813. [CrossRef]
10. Lahiri, A.; Daniel, S.; Kanthapazham, R.; Vanaraj, R.; Thambidurai, A.; Peter, L.S. A critical review on food waste management for the production of materials and biofuel. *J. Hazard. Mater. Adv.* **2023**, *10*, 100266. [CrossRef]
11. Gerna, S.; D'Incecco, P.; Limbo, S.; Sindaco, M.; Pellegrino, L. Strategies for Exploiting Milk Protein Properties in Making Films and Coatings for Food Packaging: A Review. *Foods* **2023**, *12*, 1271. [CrossRef]
12. Righetti, G.I.C.; Nasti, R.; Beretta, G.; Levi, M.; Turri, S.; Suriano, R. Unveiling the hidden properties of tomato peels: Cutin ester derivatives as bio-based plasticizers for polylactic acid. *Polymers* **2023**, *15*, 1848. [CrossRef]
13. Cai, Z.; Haque, A.N.M.A.; Dhandapani, R.; Naebe, M. Sustainable Cotton Gin Waste/Polycaprolactone Bio-Plastic with Adjustable Biodegradation Rate: Scale-Up Production through Compression Moulding. *Polymers* **2023**, *15*, 1992. [CrossRef] [PubMed]
14. Restaino, O.F.; Hejazi, S.; Zannini, D.; Giosafatto, C.V.L.; Di Pierro, P.; Cassese, E.; D'ambrosio, S.; Santagata, G.; Schiraldi, C.; Porta, R. Exploiting Potential Biotechnological Applications of Poly-γ-glutamic Acid Low Molecular Weight Fractions Obtained by Membrane-Based Ultra-Filtration. *Polymers* **2022**, *14*, 1190. [CrossRef]
15. Avila, L.B.; Schnorr, C.; Silva, L.F.O.; Morais, M.M.; Moraes, C.C.; da Rosa, G.S.; Dotto, G.L.; Lima, É.C.; Naushad, M. Trends in Bioactive Multilayer Films: Perspectives in the Use of Polysaccharides, Proteins, and Carbohydrates with Natural Additives for Application in Food Packaging. *Foods* **2023**, *12*, 1692. [CrossRef] [PubMed]
16. Restaino, O.F.; Giosafatto, C.V.L.; Mirpoor, S.F.; Cammarota, M.; Hejazi, S.; Mariniello, L.; Schiraldi, C.; Porta, R. Sustainable exploitation of posidonia oceanica sea Balls (*Egagropili*): A Review. *Int. J. Mol. Sci.* **2023**, *24*, 7301. [CrossRef]
17. Al-Asmar, A.; Giosafatto, C.V.L.; Sabbah, M.; Mariniello, L. Hydrocolloid-based coatings with nanoparticles and transglutaminase crosslinker as innovative strategy to produce healthier fried kobbah. *Foods* **2020**, *9*, 698. [CrossRef] [PubMed]
18. Giosafatto, C.V.L.; Fusco, A.; Al-Asmar, A.; Mariniello, L. Microbial Transglutaminase as a tool to improve the features of hydrocolloid-based bioplastics. *Int. J. Mol. Sci.* **2020**, *21*, 3656. [CrossRef]
19. Al-Asmar, A.; Giosafatto, C.V.L.; Sabbah, M.; Sanchez, A.; Villalonga Santana, R.; Mariniello, L. Effect of mesoporous silica nanoparticles on the physicochemical properties of pectin packaging material for strawberry wrapping. *Nanomaterials* **2020**, *10*, 52. [CrossRef]
20. Góral, D.; Góral-Kowalczyk, M. Application of metal nanoparticles for production of self-sterilizing coatings. *Coatings* **2022**, *12*, 480. [CrossRef]
21. Krivorotova, T.; Cirkovas, A.; Maciulyte, S.; Staneviciene, R.; Budriene, S.; Serviene, E.; Sereikaite, J. Nisin-loaded pectin nanoparticles for food preservation. *Food Hydrocoll.* **2016**, *54*, 49–56. [CrossRef]
22. Valdés, A.; Burgos, N.; Jiménez, A.; Garrigós, M.C. Natural pectin polysaccharides as edible coatings. *Coatings* **2015**, *5*, 865–886. [CrossRef]

23. Sabbah, M.; Di Pierro, P.; Cammarota, M.; Dell'Olmo, E.; Arciello, A.; Porta, R. Development and properties of new chitosan-based films plasticized with spermidine and/or glycerol. *Food Hydrocoll.* **2019**, *87*, 245–252. [CrossRef]
24. Porta, R.; Di Pierro, P.; Sabbah, M.; Regalado-Gonzales, C.; Mariniello, L.; Kadivar, M.; Arabestani, A. Blend films of pectin and bitter vetch (*Vicia ervilia*) proteins: Properties and effect of transglutaminase. *Innov. Food Sci. Emerg. Technol.* **2016**, *36*, 245–251. [CrossRef]
25. Sabbah, M.; Di Pierro, P.; Giosafatto, C.V.L.; Esposito, M.; Mariniello, L.; Regalado-Gonzales, C.; Porta, R. Plasticizing effects of polyamines in protein-based films. *Int. J. Mol. Sci.* **2017**, *18*, 1026. [CrossRef]
26. Mierczyńska, J.; Cybulska, J.; Pieczywek, P.; Zdunek, A. Effect of storage on rheology of water-soluble, chelate-soluble and diluted alkali-soluble pectin in carrot cell walls. *Food Bioprocess Technol.* **2015**, *8*, 171–180. [CrossRef]
27. Chandel, V.; Biswas, D.; Roy, S.; Vaidya, D.; Verma, A.; Gupta, A. Current advancements in pectin: Extraction, properties and multifunctional applications. *Foods* **2022**, *11*, 2683. [CrossRef] [PubMed]
28. Giosafatto, C.V.L.; Sabbah, M.; Al-Asmar, A.; Esposito, M.; Sanchez, A.; Villalonga Santana, R.; Cammarota, M.; Mariniello, L.; Di Pierro, P.; Porta, R. Effect of mesoporous silica nanoparticles on glycerol-plasticized anionic and cationic polysaccharide edible films. *Coatings* **2019**, *9*, 172. [CrossRef]
29. Sengar, A.S.; Rawson, A.; Muthiah, M.; Kumar Kalakandan, S. Comparison of different ultrasound assisted extraction techniques for pectin from tomato processing waste. *Ultrason. Sonochem.* **2019**, *61*, 104812. [CrossRef]
30. Torres-León, C.; Ramírez, N.; Londoño, L.; Martinez, G.A.; Díaz, R.; Navarro, V.; Alvarez-Pérez, O.B.; Picazo, B.; Villarreal, M.; Ascacio, J.; et al. Food Waste and Byproducts: An Opportunity to Minimize Malnutrition and Hunger in Developing Countries. *Front. Sustain. Food Syst.* **2018**, *2*, 52. [CrossRef]
31. Voragen, A.G.J.; Coenen, G.J.; Verhoef, R.P.; Schols, H.A. Pectin, a versatile polysaccharide present in plant cell walls. *Struct. Chem.* **2009**, *20*, 263. [CrossRef]
32. Tanhatan Naseri, A.; Thibault, J.-F.; Ralet-Renard, M.-C.; Tanhatan Nasseri, A.; Ralet, M.-C. Citrus Pectin: Structure and Application in Acid Dairy Drinks. In *Tree and Forestry Science and Biotechnology*; Global Science Books: Carrollton, GA, USA, 2008.
33. Brouns, F.; Theuwissen, E.; Adam, A.; Bell, M.; Berger, A.; Mensink, R.P. Cholesterol-lowering properties of different pectin types in mildly hyper-cholesterolemic men and women. *Eur. J. Clin. Nutr.* **2012**, *66*, 591–599. [CrossRef]
34. Nastasi, J.R.; Kontogiorgos, V.; Daygon, V.D.; Fitzgerald, M.A. Pectin-based films and coatings with plant extracts as natural preservatives: A systematic review. *Trends Food Sci. Technol.* **2022**, *120*, 193–211. [CrossRef]
35. Wu, W.; Wu, Y.; Lin, Y.; Shao, P. Facile fabrication of multifunctional citrus pectin aerogel fortified with cellulose nanofiber as controlled packaging of edible fungi. *Food Chem.* **2022**, *374*, 131763. [CrossRef] [PubMed]
36. Moradi, L.T.; Sharifan, A.; Larijani, K. The Effect of multilayered chitosan–pectin–mentha piperita and lemon essential oil on oxidation effects and quality of rainbow trout fillet (*Oncorhynchus Mykiss*) during refrigeration at 4 ± 1 °C storage. *Iran. J. Fish. Sci.* **2020**, *19*, 2544–2559.
37. Sumonsiri, N.; Danpongprasert, W.; Thaidech, K. Comparison of sweet orange (*Citrus sinensis*) and lemon (*Citrus limonum*) essential oils on qualities of fresh-cut apples during storage. *Chem. Chem. Eng. Biotechnol. Food Ind.* **2020**, *21*, 47–57.
38. Xiong, Y.; Li, S.; Warner, R.D.; Fang, Z. Effect of oregano essential oil and resveratrol nanoemulsion loaded pectin edible coating on the preservation of pork loin in modified atmosphere packaging. *Food Control.* **2020**, *114*, 107226. [CrossRef]
39. Nisar, T.; Wang, Z.; Yang, X.; Tian, Y.; Iqbal, M.; Guo, Y. Characterization of citrus pectin films integrated with clove bud essential oil: Physical, thermal, barrier, antioxidant and antibacterial properties. *Int. J. Biol. Macromol.* **2018**, *106*, 670–680. [CrossRef] [PubMed]
40. Liu, H.; Li, J.; Zhu, D.; Wang, Y.; Zhao, Y.; Li, J. Preparation of Soy Protein Isolate (SPI)-Pectin Complex Film Containing Cinnamon Oil and Its Effects on Microbial Growth of Dehydrated Soybean Curd (Dry Tofu). *J. Food Process. Preserv.* **2014**, *38*, 1371–1376. [CrossRef]
41. Rodsamran, P.; Sothornvit, R. Lime peel pectin integrated with coconut water and lime peel extract as a new bioactive film sachet to retard soybean oil oxidation. *Food Hydrocoll.* **2019**, *97*, 105173. [CrossRef]
42. Şahin, S.; Bilgin, M. Olive tree (*Olea europaea L.*) leaf as a waste by-product of table olive and olive oil industry: A review. *J. Sci. Food Agric.* **2018**, *98*, 1271–1279. [CrossRef]
43. Famiglietti, M.; Savastano, A.; Gaglione, R.; Arciello, A.; Naviglio, D.; Mariniello, L. Edible films made of dried olive leaf extract and chitosan: Characterization and applications. *Foods* **2022**, *11*, 2078. [CrossRef]
44. Hayes, J.E.; Stepanyan, V.; Allen, P.; O'Grady, M.N.; Kerry, J.P. Evaluation of the effects of selected phytochemicals on quality indices and sensorial properties of raw and cooked pork stored in different packaging systems. *Meat Sci.* **2010**, *85*, 289–296. [CrossRef]
45. Hayes, J.E.; Stepanyan, V.; Allen, P.; O'Grady, M.N.; Kerry, J.P. Evaluation of the effects of selected plant-derived nutraceuticals on the quality and shelf-life stability of raw and cooked pork sausages. *Meat Sci.* **2011**, *44*, 164–172. [CrossRef]
46. Nunes, M.A.; Pimentel, F.B.; Costa, A.S.; Alves, R.C.; Oliveira, M.B.P. Olive by-products for functional and food applications: Challenging opportunities to face environmental constraints. *Innov. Food Sci. Emerg. Technol.* **2016**, *35*, 139–148. [CrossRef]
47. Elsayed, N.; Hasanin, M.S.; Abdelraof, M. Utilization of olive leaves extract coating incorporated with zinc/selenium oxide nanocomposite to improve the postharvest quality of green beans pods. *Bioact. Carbohydr. Diet. Fibre* **2022**, *28*, 100333. [CrossRef]
48. Naseer, S.; Hussain, S.; Naeem, N.; Pervaiz, M.; Rahman, M. The phytochemistry and medicinal value of *Psidium guajava* (guava). *Clin. Phytosci.* **2018**, *4*, 32. [CrossRef]

49. Ruksiriwanich, W.; Khantham, C.; Muangsanguan, A.; Phimolsiripol, Y.; Barba, F.J.; Sringarm, K.; Rachtanapun, P.; Jantanasakulwong, K.; Jantrawut, P.; Chittasupho, C.; et al. Guava (*Psidium guajava L.*) leaf extract as bioactive substances for anti-androgen and antioxidant Activities. *Plants* **2022**, *11*, 3514. [CrossRef] [PubMed]
50. Nantitanon, W.; Yotsawimonwat, S.; Okonogi, S. Factors influencing antioxidant activities and total phenolic content of guava leaf extract. *LWT Food Sci. Technol.* **2010**, *43*, 1095–1103. [CrossRef]
51. Annegowda, H.V.; Anwar, L.N.; Mordi, M.N.; Ramanathan, S.; Mansor, S.M. Influence of sonication on the phenolic content and antioxidant activity of *Terminalia catappa L.* leaves. *Pharm. Res.* **2010**, *2*, 368–373. [CrossRef]
52. Tonyali, B.; Cikrikci, S.; Oztop, M.H. Physicochemical and microstructural characterization of gum tragacanth added whey protein based films. *Food Res. Int.* **2018**, *105*, 1–9. [CrossRef] [PubMed]
53. Galus, S.; Lenart, A. Development and characterization of composite edible films based on sodium alginate and pectin. *J. Food Eng.* **2013**, *115*, 459–465. [CrossRef]
54. Papadakis, S.E.; Abdul-Malek, S.; Kamdem, R.E.; Yam, K.L. A versatile and inexpensive technique for measuring colour of foods. *Food Technol.* **2000**, *54*, 48–51.
55. *ASTM F1249-13*; Standard Test Method for Water Vapor Transmission Rate through Plastic Film and Sheeting Using a Modulated Infrared Sensor. ASTM International: West Conshohocken, PA, USA, 2013.
56. *ASTM D3985-05*; Standard Test Method for Oxygen Gas Transmission Rate through Plastic Film and Sheeting Using a Colorimetric Sensor. ASTM International: West Conshohocken, PA, USA, 2010.
57. *ASTM F2476-05*; Standard Test Method for Carbon Dioxide Gas Transmission Rate through Barrier Materials Using an Infrared Detector. ASTM International: West Conshohocken, PA, USA, 2005.
58. Chou, M.; Osako, K.; Lee, T.; Wang, M.; Lu, W.; Wu, W.; Huang, P.; Li, P.; Ho, J. Characterization and antibacterial properties of fish skin gelatin/guava leaf extract bio-composited films incorporated with catechin. *LWT Food Sci. Technol.* **2023**, *178*, 114568. [CrossRef]
59. Du, H.; Liu, C.; Unsalan, O.; Altunayar-Unsalan, C.; Xiong, S.; Manyande, A.; Chen, H. Development and characterization of fish myofibrillar protein/chitosan/ rosemary extract composite edible films and the improvement of lipid oxidation stability during the grass carp fillets storage. *Int. J. Biol. Macromol.* **2021**, *184*, 463–475. [CrossRef]
60. Mondal, K.; Bhattacharjee, S.K.; Mudenur, C.; Ghosh, T.; Goud, V.V.; Katiyar, V. Development of antioxidant-rich edible active films and coatings incorporated with de-oiled ethanolic green algae extract: A candidate for prolonging the shelf life of fresh produce. *RSC Adv.* **2022**, *12*, 13295–13313. [CrossRef] [PubMed]
61. Tongnuanchan, P.; Benjakul, S.; Prodpran, T. Properties and antioxidant activity of fish skin gelatin film incorporated with citrus essential oils. *Food Chem.* **2012**, *134*, 1571–1579. [CrossRef]
62. Luo, Y.; Liu, H.; Yang, S.; Zeng, J.; Wu, Z. Sodium alginate-based green packaging films functionalized by guava leaf extracts and their bioactivities. *Materials* **2019**, *12*, 2923. [CrossRef] [PubMed]
63. Dou, L.; Li, B.; Zhang, K.; Chu, X.; Hou, H. Physical properties and antioxidant activity of gelatin-sodium alginate edible films with tea polyphenols. *Int. J. Biol. Macromol.* **2018**, *118*, 1377–1383. [CrossRef]
64. Albertos, I.; Avena-Bustillos, R.J.; Martín-Diana, A.B.; Du, W.; Rico, D.; McHugh, T.H. Antimicrobial olive leaf gelatin films for enhancing the quality of cold-smoked Salmon. *Food Packag. Shelf Life* **2017**, *13*, 49–55. [CrossRef]
65. McHugh, T.H.; Avena-Bustillos, R.J.; Krochta, J.M. Hydrophilic edible films: Modified procedure for water vapor permeability and explanation of thickness effects. *J. Food Sci.* **1993**, *58*, 899–903. [CrossRef]
66. Wu, H.; Lei, Y.; Zhu, R.; Zhao, M.; Lu, J.; Xiao, D.; Jiao, C.; Zhang, Z.; Shen, G.; Li, S. Preparation and characterization of bioactive edible packaging films based on pomelo peel flours incorporating tea polyphenol. *Food Hydrocoll.* **2019**, *90*, 41–49. [CrossRef]
67. Porta, R.; Di Pierro, P.; Roviello, V.; Sabbah, M. Tuning the functional properties of bitter vetch (*Vicia ervilia*) protein films grafted with spermidine. *Int. J. Mol. Sci.* **2017**, *18*, 2658. [CrossRef] [PubMed]

Disclaimer/Publisher's Note: The statements, opinions and data contained in all publications are solely those of the individual author(s) and contributor(s) and not of MDPI and/or the editor(s). MDPI and/or the editor(s) disclaim responsibility for any injury to people or property resulting from any ideas, methods, instructions or products referred to in the content.

Food Packaging and Shelf Life 31 (2022) 100779

Contents lists available at ScienceDirect

Food Packaging and Shelf Life

journal homepage: www.elsevier.com/locate/fpsl

Hemp (*Cannabis sativa*) seed oilcake as a promising by-product for developing protein-based films: Effect of transglutaminase-induced crosslinking

Seyedeh Fatemeh Mirpoor, C. Valeria L. Giosafatto *, Rocco Di Girolamo, Michela Famiglietti, Raffaele Porta

Department of Chemical Sciences, University of Naples "Federico II", Monte Sant'Angelo Campus, Via Cintia 4, 80126 Naples, Italy

ARTICLE INFO

Keywords:
Seed oilcake
hemp proteins
microbial transglutaminase
film properties

ABSTRACT

Protein concentrates were obtained from hemp seed oilcakes (OCs) and investigated as potential waste-derived source of biodegradable films at different protein and glycerol concentrations and at different pH values. These studies indicated that hemp protein (HP) film forming solutions gave rise to higher performance films when cast at pH 12 in the presence of 50% glycerol (w/w protein) used as plasticizer. Since HPs were demonstrated to act as both acyl donor and acceptor substrates of microbial transglutaminase (mTGase), they have been used as raw material to obtain films also after enzyme treatment. Film morphological characterization demonstrated that mTGase treatment was effective to produce more homogeneous and smoother films, influencing in turn positively their properties. In fact, mTGase-crosslinked films were shown to be more resistant, still flexible and exhibited a higher heat-sealing strength. In addition, the enzymatic treatment of HPs originated bio-plastics with a higher gas permeability and a greater hydrophobicity. These findings suggest the possibility to exploit the mTGase-crosslinked proteins derived from hemp OC as a promising source to produce bio-based materials useful as packaging systems for protecting food products from physical contamination and, thus, for extending their shelf-life.

1. Introduction

The use of petroleum-based plastics in different fields, such as food and pharmaceutical sectors, has increased significantly in the last years, being the durability of the plastic materials, as well as their outstanding features, the main reason of their success. However, their worldwide applications led to huge waste-disposal problems and, as a consequence, to a dramatic environmental pollution. Every year 300 million tons of plastic wastes are generated and only less than 10% of them are recycled. The remaining part of plastic materials are disposed off in landfills and oceans releasing small and toxic petro-polymers, which are swallowed by marine animals killing more than 100,000 of them each year (Porta, 2019; Geyer, Jambeck, & Law, 2017). Therefore, the replacement of fossil-based packaging materials with the ones based on renewable and biodegradable polymeric sources are on the rise (Letcher, 2020; Jiang et al., 2020). Among these biopolymers, several researchers are being focused on developing bio-plastics from residual protein sources since they are cheap, biodegradable, abundant and possess promising film forming capacities (Wittaya, 2012; Jiménez-Rosado, Bouroudian, Perez-Puyana, Guerrero & Romero, 2020; González, Gastelú, Barrera, Ribotta & Igarzabal, 2019; Kaewprachu, Osako, Benjakul, Tongdeesoontorn & Rawdkuen, 2016; Sorde & Ananthanarayan, 2019; Kaewprachu, Osako, Tongdeesoontorn & Rawdkuen, 2017). In this context, plant proteins obtained from wastes of vegetable origin are potential candidates for producing biodegradable/edible plastics and, in particular, several attempts have been done for developing bio-plastics from proteins contained in different seed OCs, such those derived from soybean, rapeseed, cottonseed, sunflower, groundnut, sesame, bitter vetch and black cumin (Karimian, Tabatabaee Bafroee, & Sharifan, 2019; Fetzer, Hintermayr, Schmid, Stäbler & Eisner,2020; de Oliveira Filho et al., 2019; Rouilly & Vaca-Garcia, 2013; Riveros, Martin, Aguirre & Grosso, 2018; Fathi, Almasi, & Pirouzifard, 2019; Sabbah, Altamimi, Di Pierro, Schiraldi, Cammarota & Porta, 2020; Porta, Di Pierro, Rossi-Marquez, Mariniello, Kadivar & Arabestani, 2015).

Among the various oilseed plants, special attention should be given to the hemp (*Cannabis sativa L.*), a multipurpose, sustainable, and low

* Corresponding author.
E-mail address: giosafat@unina.it (C.V.L. Giosafatto).

https://doi.org/10.1016/j.fpsl.2021.100779
Received 1 March 2021; Received in revised form 23 June 2021; Accepted 16 November 2021
Available online 3 December 2021
2214-2894/© 2021 Elsevier Ltd. All rights reserved.

environmental impact crop belonging to the Cannabaceae family and containing low levels of Δ9-tetrahydrocannabinol (THC, <0.1–1%), that is cultivated for producing textiles, food, paper, biofuel, medicine and hygiene products (Fike, 2016; Kitrytė, Bagdonaitė, & Venskutonis, 2018). Due to its ability to grow under a wide range of conditions, *Cannabis sativa* L. can be found at different latitudes (Zhao, Xu, Wang, Griffin, Roozeboom & Wang, 2020). The world production of hemp seeds was around 110×10^3 tons/year in the last 25 years and France was the country with the highest production (about 65×10^3 tons per year) followed by China (about 35×10^3 tons/year) (FAOSTAT, 2020). The yield of hempseed oil extracted from 1 kg of seeds can reach up to 300 mL and, being not widespread on the market, it is considered a niche product characterized by a high content of polyunsaturated fatty acids. In particular, hemp seeds contain oil (25–35%) with important nutritional and functional properties. Hemp seed oil is indeed a rich source of polyunsaturated fatty acids including linoleic acid (18:2 ω-6) and α-linolenic acid (18:3 ω − 3), with a favorable balance ratio of ω-6 to ω-3 that makes it a potential candidate to be used in food and cosmetics (Crescente, Piccolella, Esposito, Scognamiglio, Fiorentino & Pacifico, 2018; Callaway, 2004; Pojić et al., 2014). Differently from most of the oilseeds, hemp seeds contain also low concentrations of antinutritional compounds, such as phytic acid, condensed tannins and trypsin inhibitors (Russo & Reggiani, 2015). In addition to lipids, hemp seeds contain proteins (20–30%), carbohydrates (10–15%) and insoluble fibers, vitamins and different minerals, such as phosphorus, potassium, magnesium, sulfur, calcium, iron, and zinc (Callaway, 2004; House, Neufeld, & Leson, 2010). The main protein content of hemp seeds consists of albumin and edestin, polypeptides with high amounts of arginine, glutamic acid, as well as of sulfur-containing amino acids, which makes their amino acid profiles comparable with those of soybean, egg and meat proteins (Tang, Ten, Wang & Yang, 2006; Dapčević-Hadnađev, Dizdar, Pojić, Krstonošić, Zychowski & Hadnađev, 2019; Callaway, 2004).

However, protein-based films generally exhibit poor mechanical and water vapor barrier properties, so that their application in food packaging sector is still quite limited. Therefore, in order to improve the protein-based film properties, different preliminary treatments of the protein sources, such as gamma-irradiation, heating or crosslinking, have been often performed, as well as the protein blending with other biopolymers or additives (Xu, Liu, Yang, Liu, Jia & Chen, 2012; Amadori, Torricelli, Rubini, Fini, Panzavolta & Bigi, 2015; Haghighi et al., 2020; Jiménez-Rosado et al., 2020; Wihodo and Moraru, 2013). Among these procedures, enzymatic crosslinking has received an increasing attention, due to its nontoxicity and the higher level of acceptance by consumers (Gaspar & Góes-Favoni, 2015; Kaewprachu et al., 2017). The most extensively used tool to reinforce protein-based films is represented by microbial transglutaminase (mTGase; EC.2.3.2.13), enzyme responsible for catalysing the formation of intermolecular ε-(γ-glutamyl)-lysine crosslinks into proteins via an acyl transfer reaction (Giosafatto, Fusco, Al-Asmar & Mariniello, 2020; Zink, Wyrobnik, Prinz & Schmid, 2016).

Despite the numerous researches carried out on developing protein-based films, information about hemp protein (HP)-derived films is still very scarce. Therefore, the present study was carried out to investigate the possibility to use hemp seed oilcakes (OCs) as an effective source to obtain bio-plastics. In addition, the ability of HPs to act as mTGase substrates was also tested with the aim to reinforce HP-based films and improve their properties.

2. Experimental section

2.1. Materials

Hemp OCs purchased from Consorzio Goji Italia (Andria, Italy) were a generous gift of prof. Daniele Naviglio; mTGase (Activa WM, containing 1% of mTGase and 99% of maltodextrins), obtained from the culture of *Streptoverticillium* sp., was supplied by Prodotti Gianni SpA (Milano, Italy). Chemical reagents used for electrophoresis were from Bio-Rad (Segrate, Milano, Italy). Sodium hydroxide, hydrochloric acid and glycerol (GLY) were purchased from Sigma Chemical Co (USA). All other chemicals and reagents utilized in this study were of analytical grade.

2.2. Extraction of hemp proteins (HPs)

HPs were extracted from the hemp OC according to acid precipitation method as described previously with some slight modification (Arabestani, Kadivar, Shahedi, Goli & Porta, 2013; Dapčević-Hadnađev et al., 2019; Hadnađev et al., 2018). Hemp OC flour (150 g) was added to 1.5 L of distilled water adjusted to pH 11 by 1 N NaOH, and the mixture stirred for 1 h at room temperature. The supernatant was collected after centrifugation at 5000 rpm for 15 min and the proteins were precipitated at pH 5.4 by adding 1 N HCl, and the suspension was then centrifuged at 5000 rpm for 15 min. The obtained pellet was finally dried in a plastic plate at 25 °C and 45% relative humidity (RH). The obtained protein concentrate was grinded in a Knife Mill Grindomix GM 200 (Grindomix GM200, Retsch GmbH, Haan, Germany) at a speed of 1000 rpm for 3 min. The protein content of the derived final HP concentrate was determined by the Kjeldahl's method (AACC, 2003), using a nitrogen conversion factor of 6.25.

2.3. Determination of zeta potential and particle size

HP concentrate was dissolved in distilled water (0.1 mg/mL) under constant stirring and the pH was then adjusted to 12.0 by using 0.1 N NaOH. Zeta potential and particle size values of HP solution were measured by titration from pH 12.0 to pH 2.0, adding 1.0, 0.1, and 0.01 N HCL under constant stirring at 25 °C (Gómez-Estaca, Gavara, Catalá & Hernández-Muñoz, 2016; Sabbah et al., 2017), with a Zetasizer Nano-ZSP (Malvern®, Worcestershire, UK) in the wavelength of 633 nm using a helium-neon laser of 4 mW output power. Zeta potential was calculated by the instrument software programmer trough the electrophoretic mobility at a voltage of 200 mV using the Henry equation, and all the results were reported as mean ± standard deviation. Zeta potential and particle size measurements were performed at each pH in triplicate. The effect of different concentrations of mTGase on zeta potential and particle size of the HP containing Film Forming Solutions (FFSs) at pH 12 was also studied. To this aim, each FFS (1.0 mL) containing 50% GLY and 16 mg HPs was previously incubated for 2 h at 37 °C and pH 7.5 in the absence or presence of different amounts of mTGase. At the end of incubation the pH of the FFSs was brought at 12 and, then, the samples were introduced in the measurement vessel. Each analysis took approximately 10 min.

2.4. Two-dimensional polyacrylamide gel electrophoresis (2D-PAGE)

2D-PAGE was carried out by analyzing 100 μg of HPs onto 7-cm IPG strips (pH 3–10) previously dissolved in 125 μL of sample rehydration buffer (Bio-Rad). 2 mL of mineral oil were added to each strip in order to prevent the evaporation during the 24 h protein separation. In the second step, protein separation according to molecular mass has been carried out by placing the gel horizontally into the precast SDS-PAGE gel (12%, Mini-protein gels, Bio-Rad) and performed at a current of 220 V for 40 min. The gel was finally stained with Coomassie Brilliant Blue R250 (Bio-Rad, Segrate, Milan, Italy).

2.5. Sodium dodecyl sulfate polyacrylamide gel electrophoresis (SDS-PAGE)

HPs (100 μg) were incubated at 37 °C in the presence of 80 mM Tris-HCl buffer, pH 7.5, and different concentration of mTGase (0, 5, 10, 20, 40 U/g protein) for two hours, as well as for different times (5, 10, 20,

40, 60 min and 2, 4 and 24 h) in the presence of 40 U/g of enzyme (100 μL final volume). 25 μL of sample buffer (62.5 mM Tris-HCl, pH 6.8, containing 4% (w/v) SDS, 30% (v/v) GLY, 10% (v/v) β-mercaptoethanol, and 0.05% (w/v) bromophenol blue) were added to the reaction mixtures at the end of incubation, then the samples were heated for 5 min in a boiling water bath and, finally, 25 μL of each sample finally analyzed by 12% SDS-PAGE as described by Laemmli (Laemmli, 1970). Bio-Rad Precision Protein Standards were run as molecular weight markers.

2.6. Preparation and casting of FFSs

HP stock solution (2g in 100 mL) was prepared by dissolving the HP concentrate in distilled water and by adding 1 N NaOH, under constant stirring at room temperature, until the pH of the solution was brought at 12. To find out the best conditions for developing HPs-based films, different FFSs (25 mL), containing 200, 300 and 400 mg of HPs and different concentrations of GLY (10-50%, w/w protein) used as plasticizer, were prepared at two different pH values (pH 7 and 12). Further FFSs were also prepared after incubation of HPs (400 mg) for 2 h, at 37 °C and pH 7.5, in the absence or presence of different amounts of mTGase (5, 10, 20, 40 U/g HPs). At the end of incubation, the pH was adjusted to 12 by 1 N NaOH addition and the mTGase-treated HP samples were heated at 80 °C in a water bath for 20 min to deactivate the enzyme. After cooling of the samples at room temperature, GLY was added to obtain FFSs containing a concentration of plasticizer of 50% (w/w protein). All the prepared FFSs were cast onto 8 cm diameter polycarbonate Petri dishes and allowed to dry in an environmental chamber at 25 °C and 45% RH for 24 h. The dried films were peeled intact from the casting surface and analyzed after their conditioning at 50% RH and 25 °C by placing them in a desiccator over a saturated solution of $Mg(NO_3)_2.6\ H_2O$ for 24 h.

2.7. Film properties

2.7.1. Opacity

The opacity values of the HP-based films were recorded by measuring the absorbance of the films, at a wavelength of 600 nm, divided by the film thickness (mm), using a UV/visible Spectrophotometer (SmartSpec 3000 Bio-Rad, Segrate, Milan, Italy), according to the method described previously by Jahed, Khaledabad, Bari, and Almasi (2017). Four strips of each film were cut (1 cm × 4 cm) and put in a spectrophotometer quartz cuvette; air was considered as a blank reference.

2.7.2. Density

Film density (ρ_s) was calculated according to the following equation. (Zahedi, Fathi-Achachlouei, & Yousefi, 2018; Cruz-Diaz, Cobos, Fernández-Valle, Díaz & Cambero, 2019):

$$\rho_s = (m/A \times \delta) \quad (1)$$

where m is the film dry mass after conditioning (g), A is the film area ($2 \times 2\ cm^2$), δ is the film thickness (cm) and ρ_s is the density of the film (gcm^{-3}). Three specimens of different points of each film were randomly selected.

2.7.3. Morphology

The surface microstructure and cross-sections of the films were studied by scanning electron microscopy (SEM) (Nova NanoSem 450-FEI-Thermo Fisher, Scientific, Waltham, MA, USA). The samples were coated with thin layers of gold and platinum using a sputter coater at a current of 20 mA for 90 s and then the images were taken at an accelerating voltage of 3 kV, (4.4–5.2) mm working.

2.7.4. Moisture content, swelling ratio and solubility

Film moisture content was analyzed according to the method described by Zahedi, Fathi-Achachlouei, & Yousefi, (2018) with some modifications. The film specimens ($3 \times 3\ cm^2$) were placed in the aluminum plates and dried at 105 °C in an oven for 24 h. Moisture content was evaluated by calculating the difference between their initial and final weight, before and after drying, using the following equation:

$$\text{Moisture content} = [(W_i - W_d)/W_i] \times 100 \quad (2)$$

Where, W_i and W_d represent the weights of the initial and dried film, respectively.

Film swelling ratio was examined using a gravimetric method as reported by Roy, Rhim, & Jaiswal (2019). Each film sample ($3 \times 3\ cm^2$) was pre-weighed (W_i) and then immersed in 30 mL of distilled water at 25 °C for 1 h. After film surface drying by an absorbent paper, the films were finally weighed again (W_s). The swelling ratio was calculated using the following equation:

$$\text{Swelling ratio} = [(W_s - W_i)/W_i] \times 100 \quad (3)$$

For the determination of film solubility in water, the dried film samples were weighed (W_i), immersed in 30 mL distilled water and then shaken for 24 h at 25 °C. The undissolved film residues were collected and dried in the oven at 105 °C to calculate their final dry weight (W_f). Film solubility was determined as the percentage of total weight by using the following equation (Roy and Rhim, 2020):

$$\text{Solubility}(\%) = \left[\left(W_i - W_f\right)/W_i\right] \times 100 \quad (4)$$

All the experiments were repeated three times.

2.7.5. Contact angle

Measurements of contact angle between water and HP-based films were carried out by using a homemade contact angle goniometer. Five droplets (10 μL) of distilled water were deposited on both sides of each film at different points and the photo was captured at the moment that the drop was in contact with the film surface. The mean value of contact angle was acquired with ImageJ software (González et al., 2019).

2.7.6. Thickness and mechanical properties

Film thickness was determined randomly in five different locations by using a micrometer (IP65 Alpa exacto) with a precision of 0.001 mm. Film tensile strength (TS), elongation at break (EB) and Young's modulus (YM) were determined by a dynamometer (Instron universal testing instrument model no. 5543 A, Instron Engineering Corp., Norwood, MA, USA). The conditioned films were cut into strips with a width of 10 mm and a length of 60 mm and five specimens of each film (1 kN load and 5 mm/min speed) were then tested as previously described according to the.

Film seal strength, evaluated according to (Amadori et al., 2015; Arabestani, Kadivar, Shahedi, Goli, & Porta, 2013; ASTM E88-07a, 2007a; AACC, 2003), was determined by reducing each film into strips of 5 × 2.5 cm, and placing each strip onto another one of the same sample. All the samples were previously conditioned at 25 °C and 50% RH for 24 h and, then, the two overlapped strips were placed into an automatic heat sealer (MagicVac®Axolute Mod: P0608ED, Italy). The seal strength (N/m), quantified by means of the above mentioned dynamometer, was calculated by dividing the maximum peak force to the film width.

2.7.7. Water vapor and gas permeability

HP-based film water vapor (WV) and gas (CO_2 and O_2) permeabilities were investigated and compared to the values obtained by analyzing two commercial materials, *i.e* low density polyethylene (LDPE), an oil-based plastic, and Mater-Bi, a starch-based bio-plastic, both purchased from a local supermarket. The measurements were performed in duplicate for each film (50% RH, 25°C and 101 kPa for gas

permeability; 90% RH, 38°C and 6 kPa for WV permeability) by using a Total Perm apparatus (ExtraSolution s.r.l., Pisa, Italy) according to the Standard Methods (ASTM D3985–05, 2010; ASTM F-2476-13, 2013). The measurements were carried out after conditioning the film specimens for 24h at 50% RH and placing them in the aluminum masks to reduce the film test area to 2 cm^2. The gas transmission rate was the actual measured volume converted into its value at standard temperature and pressure (STP) conditions.

2.8. Statistical analysis

SPSS19 (Version 19, SPSS Inc., Chicago, IL, USA) software was used for all statistical analyses. One-way analysis of variance (ANOVA) and Duncan's multiple range tests ($p < 0.05$) were used to determine the significant difference among the samples. All treatments were analyzed in triplicate.

3. Results and discussion

3.1. HP solution stability

Zeta potential values of a protein solution is affected by different factors, such as its pH and ionic strength, as well as the nature and composition of the solvent and the concentration of the dispersed particles (Bhattacharjee, 2016). It is an indicator of the colloidal stability of the solution, since values higher than ± 25 mV (in absolute value) indicate that the solution is relatively stable (Bhattacharjee, 2016). Thus, zeta potential of the aqueous solution of HP concentrate (72% HPs) obtained from hemp OCs was monitored at different pH values (2−12) in order to detect the best experimental conditions for preparing stable FFSs of HPs (Giosafatto, Al-Asmar, D'Angelo, Roviello, Esposito & Mariniello, 2018).

Panel A of Fig. 1 indicates that HP solution was quite stable between pH 8.0 and 12.0 and as demonstrated by the slight decrease in the zeta potential value from − 31 mV to − 24 mV. By further lowering the pH, the zeta potential values were observed to markedly decrease up to − 17 mV and − 4 mV at pH 6.0 and 5.0, respectively. Moreover, panel A of Fig. 1 also shows that, during the titration, the diameter (d.) of particle size values of the proteins were about 400–500 nm in the range of pH between 12.0 and 8.0, whereas they sharply increased over 1000 nm under pH 7.0. It is worthy to note that HP solution lost stability and began to flocculate around pH 6.0, as shown by the marked increase in the Z-average size of the protein particles, because this pH value is close to the isoelectric point (pI) of the majority of HPs as demonstrated by 2D-PAGE profile reported in the panel B of Fig. 1.

3.2. HP-based films

(ASTM E88–07a, 2007) the protein concentrate obtained from the hemp OCs was used as possible biopolymer source to produce biodegradable films at different pH values in the absence or presence of different concentrations of GLY used as plasticizer (Basiak, E., Lenart, A., & Debeaufort, F., 2018).

3.3. HPs as mTGase substrates

Panel A of Fig. 2 shows the HP SDS-PAGE profile following protein incubation with increasing amounts of mTGase. It is possible to note that HPs act as both acyl donor and acyl acceptor substrates of the enzyme as demonstrated by the decrease in intensity of the low molecular mass protein bands and the concomitant appearance of high molecular mass polymer(s), some of them unable to enter the stacking gel. Conversely, HP samples incubated in the absence of enzyme (lane 1) exhibited only three major bands with molecular masses of ~35 kDa, ~19 kDa, and ~16 kDa, identified as the main proteins occurring in the HP concentrate.

It is worthy to point out that the HP polymerization rate increased with the increase of mTGase concentration and that the most prominent disappearance of the HP bands was observed in lane 4 and lane 5 where the highest concentration of mTGase was used. These results are consistent with those reported by Giosafatto et al. (2018), Porta et al. (2015), Zhong et al. (2017) and Sabbah et al. (2020), who demonstrated that proteins extracted from several other seeds are able to act as mTGase substrates. Further experiments were carried out by incubating HPs at different times in the presence of the same amount of mTGase (40 U/g) (Fig. 2, **panel B**). In this case it was possible to observe that HPs started being polymerized by the enzyme after only 10 min and that the highest degree of polymerization was achieved after 2 h. Therefore, all the subsequent experiments were performed by incubating HPs for 2 h in the presence of different mTGase amounts.

3.4. Characterization of HP containing FFS treated with mTGase

Mean particle size and zeta potential of HPs, previously incubated at pH 7.5 for 2 h either in the absence or presence of different amounts of mTGase, were measured after GLY addition under alkaline conditions

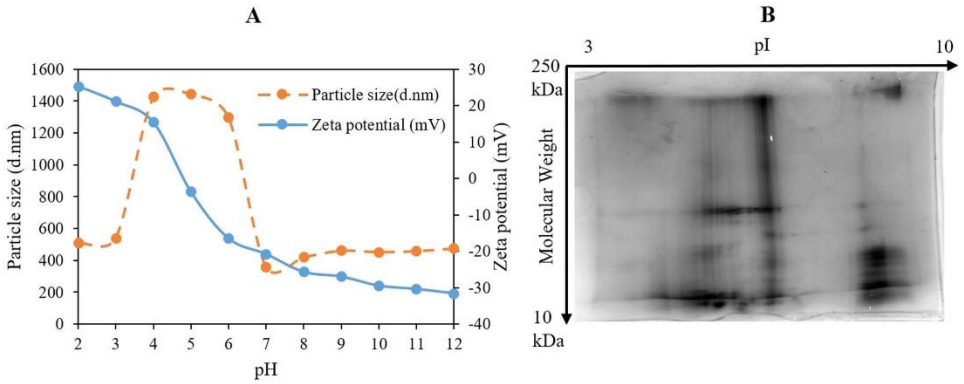

Fig. 1. Hemp protein zeta potential and particle size measurements at different pH values (A) and hemp protein 2D-PAGE (12%) profile (B). Further experimental details are given in the text.

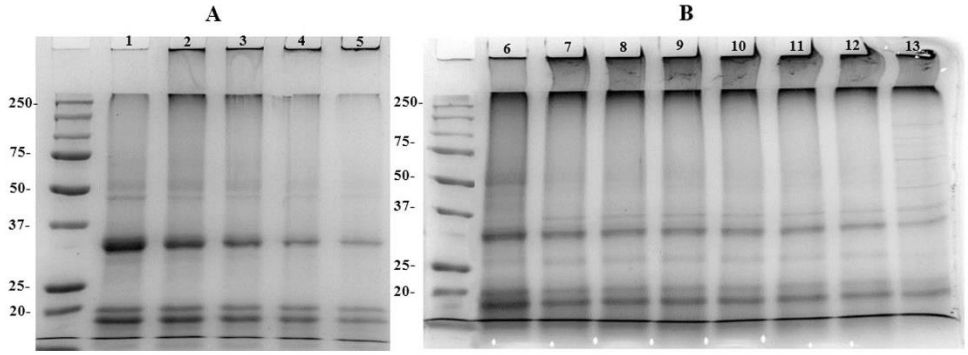

Fig. 2. SDS-PAGE analysis of hemp proteins (100 mg) incubated for 2 h in the absence (A1) or presence of different concentrations of microbial transglutaminase (A2, 5 U/g; A3, 10 U/g; A4, 20 U/g; A5, 40 U/g), or in the presence of 40 U/g of enzyme at different incubation times (B6, time 0; lane B7, 10 min; B8; 20 min; B9, 40 min; B10, 1 h; B11, 2 h; B12, 4 h; B13, 24 h). Further experimental details are given in the text.

(pH 12).

The results reported in Table 1 show that the negative zeta potential values of the FFSs slightly and progressively decreased with the increasing amounts of mTGase. However, all FFSs were quite stable exhibiting zeta potential values between − 30.3 and − 26.9 mV. Conversely, the mean particle size was observed to significantly increase by increasing mTGase concentration. This result seems to confirm the formation of HP polymers, already observed by SDS-PAGE (Fig. 2), and justify the observed linear increase of polydispersity index (PDI) value, that is an indicator of the relative variance in particle size distribution in the different FFS samples. Similar results have been recently reported by Liu et al. (2019), who investigated the particle size of mTGase-crosslinked whey proteins, and by Giosafatto et al. (2018) who studied the effect of the enzyme on the grass pea protein particle size.

3.5. mTGase-crosslinked HP-based films

Previous characterization of the FFSs containing HPs crosslinked by mTGase suggested the best experimental conditions to produce HP-based films following protein treatment with the crosslinking enzyme. It is worth to point out that, also in this case, it was necessary to add GLY (at least 30%) as plasticizer to the FFSs containing crosslinked HPs in order to obtain handleable films. Therefore, to compare the results obtained with the crosslinked HPs to the ones previously obtained with unmodified HPs, 50% GLY concentration was added to each FFS after enzyme treatment, as well as the FFS pH value was adjusted to pH 12 before casting. After drying, the films were peeled off intact from the plates and, after equilibration in a saturated solution of Mg $(NO_3)_2$.6 H_2O, their properties were investigated.

Table 1
Mean particle size, zeta potential and polydispersity index (PDI) of hemp protein film forming solutions incubated for 2 h in the presence of different amounts of microbial transglutaminase (mTGase)*.

mTGase (U/g of protein)	Mean particle size (nm)	Zeta potential (mV)	PDI (%)
0	368.33 ± 8.45^{d}	-30.30 ± 0.46^{d}	0.45 ± 0.03^{d}
5	432.27 ± 12.60^{c}	-29.63 ± 1.10^{cd}	0.53 ± 0.02^{c}
10	460.20 ± 12.40^{c}	-28.80 ± 0.46^{bc}	0.56 ± 0.03^{c}
20	533.16 ± 6.48^{b}	-27.73 ± 0.50^{ab}	0.67 ± 0.03^{b}
40	652.17 ± 37.54^{a}	-26.86 ± 0.35^{a}	0.76 ± 0.12^{a}

* Different small letters (a-d) indicate significant differences among the values reported in each column ($p < 0.05$). Further experimental details are given in text.

3.5.1. Thickness, opacity, density and morphology

Table 2 shows the values of thickness, opacity and density of the films produced with HPs previously incubated in the absence or presence of increasing mTGase concentrations. The thickness of crosslinked HP-based films was found to enhance as a function of mTGase amount used, ranging from about 97 μm for the uncrossliked films to 133 μm for the films derived from FFSs containing the maximal concentration of enzyme (40 U/g). Similar results have been previously reported by Porta et al. (2015) for bitter vetch protein-based films and by Giosafatto et al. (2018) for grass pea-based films.

The optical properties of the prepared films were also investigated because it is known that the appearance of the packaged products may influence the consumer acceptance of them (Shojaee-Aliabadi et al., 2014; Hosseini, Rezaei, Zandi & Ghavi, 2013). As reported in Table 2, the transparency of the mTGase-crosslinked films significantly decreased with the increase of the amount of enzyme used to modify HPs. The observed opacity enhancement is most probably due to the formation of protein aggregation consequent to the covalent crosslinks produced among the HP chains causing an hamperement to the light transmission through the film and changing of the refractive index (Ortega-Toro, Jiménez, Talens & Chiralt, 2014). Similar results were previously reported by Yilmaz, Turhan, Saricaoglu, and Tural (2020) for anchovy by-product protein films and by Rostamzad, Paighambari, Shabanpour, Ojagh, and Mousavi (2016) for fish protein-based films.

These data were also confirmed by the increase of film density of the films produced with crosslinked HPs that indicates the existence of a more compact film matrix network. Same results were obtained by Fathi, Almasi, & Pirouzifard, (2018) who reported that the density of sesame protein isolate films increased after crosslink formation due to

Table 2
Thickness, density and opacity of films containing 50% glycerol and prepared at pH 12 with hemp proteins previously incubated for 2 h in the absence or presence of different amounts of microbial transglutaminase (mTGase)*.

mTGase (U/g of protein)	Thickness (μm)	Density (g/cm^3)	Opacity (mm^{-1})
0	97.63 ± 7.09^{d}	1.31 ± 0.03^{d}	2.39 ± 0.27^{c}
5	106.00 ± 5.57 ^{cd}	1.45 ± 0.03^{c}	2.60 ± 0.21^{bc}
10	108.00 ± 6.25^{c}	1.50 ± 0.02^{b}	2.87 ± 0.19^{bc}
20	122.33 ± 2.08^{b}	1.61 ± 0.02^{a}	3.00 ± 0.30^{b}
40	133.33 ± 1.15^{a}	1.63 ± 0.03^{a}	3.77 ± 0.38^{a}

* Different small letters (a-d) indicate significant differences among the values reported in each column ($p < 0.05$). Values are given as mean ± standard deviation from triplicate determinations. Further experimental details are given in the text.

UV exposure.

Although the visual inspection of crosslinked HP-films (Fig. 3, A2–5) indicated that they were macroscopically similar to the ones produced with unmodified HPs (Fig. 3, **A1**) with a brownish color, SEM analyses of film cross-sections and surfaces showed significant differences. As far as the cross-section analyses, the films appeared more porous when manufactured with unmodified HPs (Fig. 3, **B1**) with respect to the films prepared with crosslinked HPs (Fig. 3, B2–5), as well as their surface resulted quite rough (Fig. 3, **C1**) in comparison with the smoother and more homogeneous surface observed in the films obtained with mTGase-crosslinked HPs (Fig. 3, C2–5), even though by using 20 U/g of mTGase the surface structure of the materials seems even more compact, thus influencing the film mechanical properties (Fig. 3, **C4**). Similar results have been previously reported by Porta et al. (2015), who observed a more compact microstructure of the films made with bitter vetch proteins when these proteins had been pretreated with mTGase.

3.5.2. Mechanical properties

As it is illustrated in Fig. 4, mechanical properties were significantly affected by the presence in the film matrix of isopeptide bonds produced by mTGase. TS of HP-based films was higher when enzymatically crosslinked proteins were used, reaching a value more than double, with respect to control films, by using 20 U/g of mTGase in the protein pretreatment. A similar trend was observed in the film YM change, thus indicating a more resistant and rigid feature of the material obtained following the treatment of HPs with mTGase (Sorde & Ananthanarayan, 2019; Kaewprachu et al., 2017; Yilmaz et al., 2020; Yayli, Turhan, & Saricaoglu, 2017). Conversely, and unexpectedly, only a slight decrease of the EB of the film produced by using crosslinked HPs was detected, indicating that the mobility of the protein chains and, consequently, the film flexibility were only slightly reduced following the enzyme catalyzed protein crosslinking.

Finally, HP-based films were also examined to determine their heat sealing ability, as this feature is fundamental for their potential

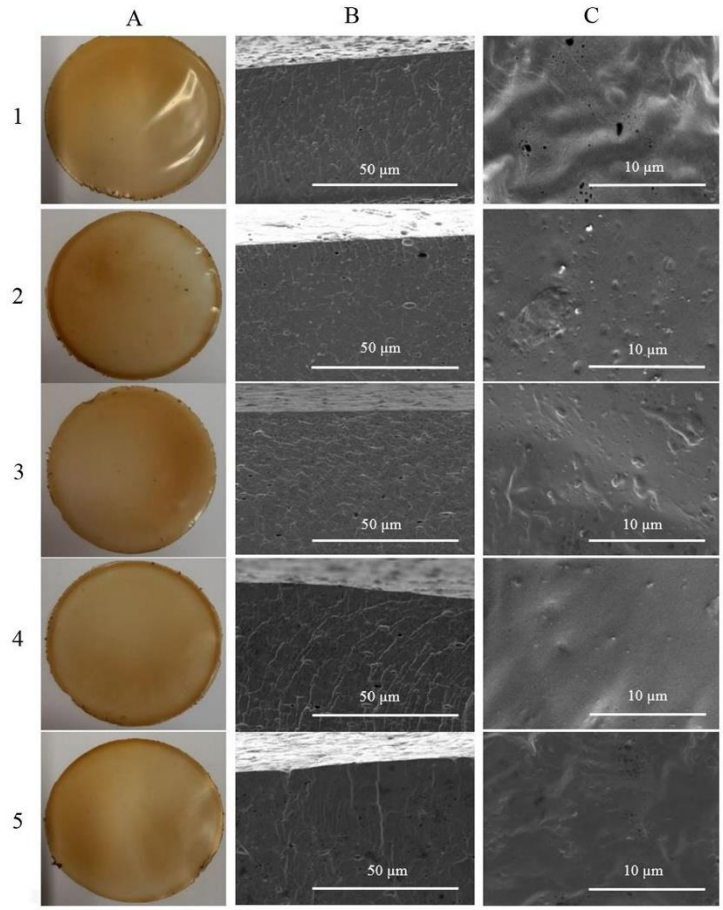

Fig. 3. Images of films (A), and of their SEM cross sections (B, magnification 2000 ×) and surfaces (C, magnification 8000 ×), containing 50% glycerol and prepared at pH 12 with hemp proteins previously incubated for 2 h in the absence (1) or presence of 5 (2), 10 (3) 20 (4), and 40 (5) U/g of microbial transglutaminase (mTGase).

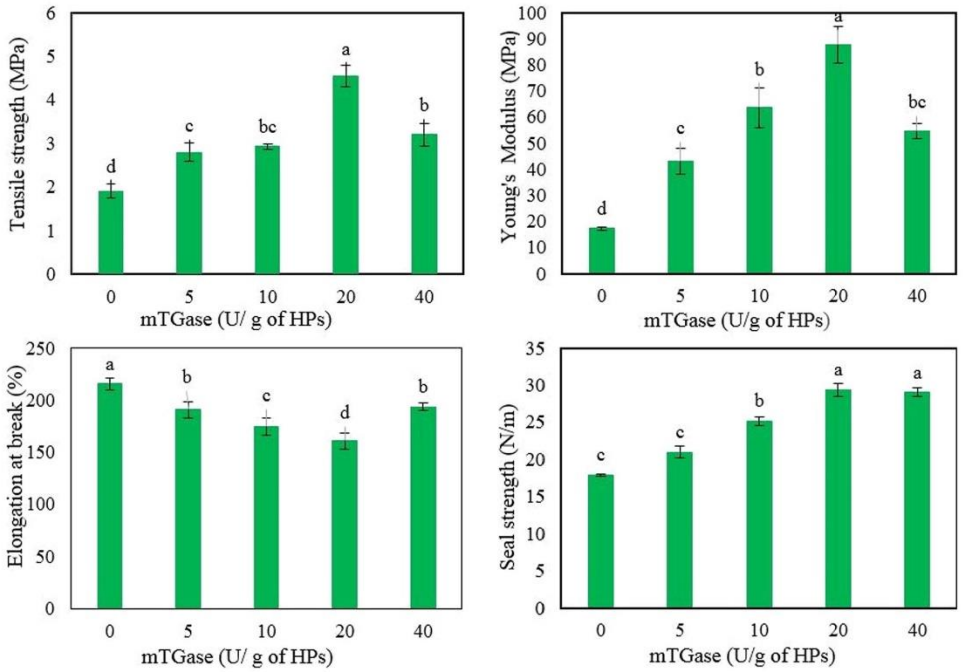

Fig. 4. Mechanical properties of films containing 50% glycerol and prepared at pH 12 with hemp proteins previously incubated for 2 h in the absence or presence of different amounts of microbial transglutaminase (mTGase). Different small letters (a-d) indicate significant differences among the values reported in each bar ($p < 0.05$).

industrial applications as food wrapping system. The analyses have shown that all the films were able to be heat-sealed and that the presence of mTGase-catalysed isopeptide bonds in HP matrix markedly increased the heat-sealing strength of the produced films, that almost doubled reaching a value of 30 N/m by using 20 U/g of enzyme (Fig. 4). This effect was probably due to the more compact structure of the films obtained with mTGase-crosslinked HPs and to the consequent increase of film hydrophobicity.

3.5.3. Moisture content, water solubility, swelling ratio and contact angle

Further investigations were carried out to determine moisture content, solubility, swelling ratio, as well as contact angle, of the films prepared with both unmodified and crosslinked HPs. Fig. 5 shows that the moisture content of HP films was higher and that it gradually decreased with the increase of mTGase concentration from 0 to 20 U/g (Fig. 5). This result could be explained with the reduction of the free ε-amino groups of HP lysines following the isopeptide bond formation catalyzed by mTGase (Tang, Jiang, Wen & Yang, 2005; Kaewprachu et al., 2017; Masamba et al., 2016). Similar results were obtained by analyzing the film water solubility, indicating that also this reduction was dependent on the formation of a stronger structure in the film network due to the enzyme-catalyzed crosslinks. Nevetherless, it is worthy to point out that, by visual observation, all the films appeared still intact even after 1 h immersion in water. Also the swelling ratio of the developed films revealed the same lowering trend (Fig. 5), confirming previous results (Schmid, Sängerlaub, Wege & Stäbler, 2014; Kaewprachu et al., 2017) reporting a reduction in swelling ratio of films made with mTGase-modified whey proteins and fish myofibrillar proteins, respectively. Therefore, all these findings could be attributed to the high degree of crosslinking in the film matrix (Schmid et al., 2014). Finally, the increase in film hydrophobicity was also assessed by measuring film contact angle which was double when HPs were previously treated with 20 U/g of enzyme. In conclusion, all the measured parameters reported in Fig. 5 clearly indicate a decrease in film hydrophylicity with a maximal effect observed when 20 U/g of mTGase were used. In fact, the treatment with higher enzyme amounts (40 U/g) did not give rise to a further decrease of film hydrophylicity, suggesting that, although the further increase in isopeptide bonds formed significantly modified film mechanical properties, it did not influence at all moisture content, water solubility and swelling ratio of the films, reverting slightly the observed increase of their contact angle values. This latter result might be explained from the SEM experiments illustrated in Fig. 3, since the surface of mTGase-crosslinked films appeared more compact by using 20 U/g of mTGase than that observed in the analysis of films prepared with lower or higher enzyme concentrations.

3.5.4. Water vapor and gas permeability

WV permeability is an important parameter for food packaging being a well known drawback of most hydrocolloid films. It is generally affected by several factors such as the material crystallinity and porosity, the type and amount of plasticizer added, as well as the matrix crosslinking and density (Han & Scanlon, 2005; Jasse, Seuvre and Mathlouthi, 1994; Miller & Krochta, 1997). Reduced WV permeability was evidenced in the films made with HPs previously treated with concentrations of mTGase up to 20 U/g (80% decrease), whereas an opposite trend was observed by analyzing the barrier effect of the crosslinked HPs films toward O_2 and CO_2 (Table 3). In fact, the O_2 and CO_2 transfer rate was found to significantly increase with increasing concentrations of

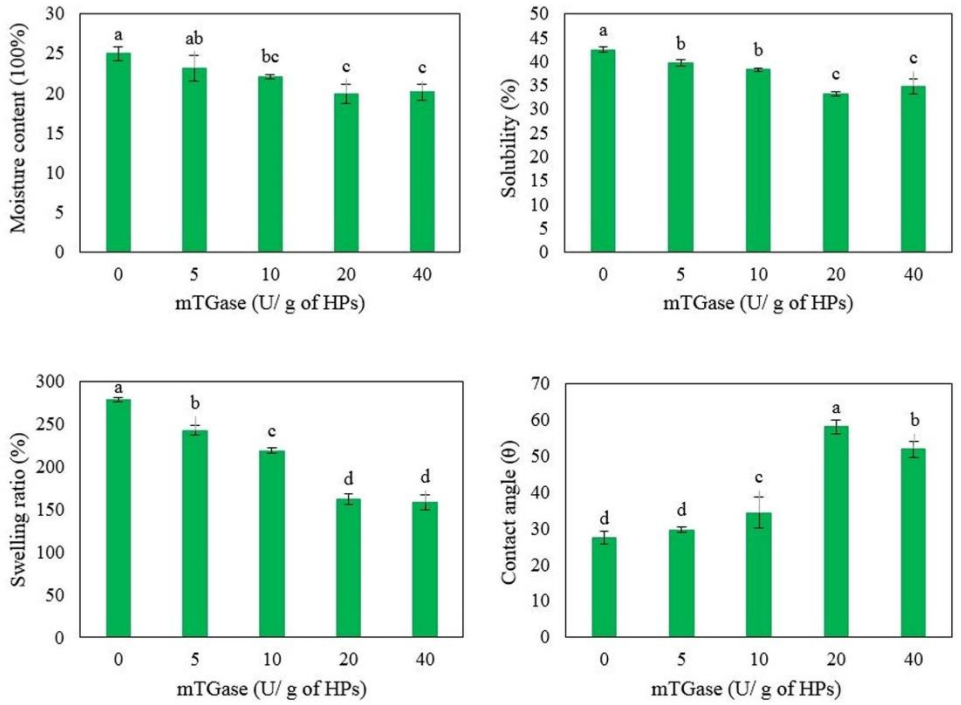

Fig. 5. Moisture content, solubility, swelling ratio and contact angle of films containing 50% glycerol and prepared at pH 12 with hemp proteins previously incubated for 2 h in the absence or presence of different amounts of microbial transglutaminase (mTGase). Different small letters (a-d) indicate significant differences among the values reported in each bar ($p < 0.05$).

Table 3
Water vapor (WV) and gas permeability of films containing 50% glycerol and prepared at pH 12 with hemp proteins previously incubated for 2 h in the absence or presence of different amounts of microbial transglutaminase (mTGase).*

mTGase (U/g of protein)	WV g mm m^{-2} d^{-1} kPa^{-1}	O_2 cm^3_{STP} mm m^{-2} d^{-1} kPa^{-1}	CO_2
0	19.53 ± 1.81^a	1.52 ± 0.01^a	0.86 ± 0.01^a
5	13.65 ± 1.62^b	1.61 ± 0.02^b	0.99 ± 0.01^b
10	11.72 ± 1.61^b	1.66 ± 0.04^b	1.02 ± 0.01^b
20	3.91 ± 1.51^c	2.22 ± 0.01^c	2.04 ± 0.04^c
40	7.81 ± 1.80^b	2.44 ± 0.01^d	2.34 ± 0.01^d

* Different small letters (a-e) indicate significant differences among the values reported in each column ($p < 0.05$). Values are given as mean ± standard deviation from triplicate determinations. Further experimental details are given in the text.

mTGase, in agreement with recent results obtained analyzing films manufactured with crosslinked proteins obtained from a different oilseed industrial byproduct, such as black cumin OC (Sabbah et al., 2020). The observed WV permeability reduction could be due to the decrease of the available free polar groups of HPs following the formation of isopeptide bonds catalysed by mTGase that, on the contrary, might allow the less polar CO_2 and O_2 molecules to pass more easily through the films. By comparing the films prepared by previously treating HPs with 20 U/g of mTGase to some commercial packaging materials, it is worthy to note that HP-based films showed a barrier property towards WV (3.91 g mm m^{-2} d^{-1} kPa^{-1}) higher than that exhibited by the starch-based bio-plastics commercialized under the trade name Mater-Bi (9.8 g mm m^{-2} d^{-1} kPa^{-1}), but much lower than that of LDPE (0.075 g mm m^{-2} d^{-1} kPa^{-1}). As far as CO_2, the two commercial materials were more permeable than the HP-based films crosslinked by mTGase, showing Mater-Bi a value of 4.76 cm^3_{STP} mm m^{-2} d^{-1} kPa^{-1} and LDPE a value of 12.82 cm^3_{STP} mm m^{-2} d^{-1} kPa^{-1} *vs* a value of 2.04 cm^3_{STP} mm m^{-2} d^{-1} kPa^{-1} exhibited by the HP-based films. Conversely, the O_2 barrier properties of Mater-Bi and LDPE were found higher (0.64 cm^3_{STP} mm m^{-2} d^{-1} kPa^{-1}) and slightly lower (3.48 cm^3_{STP} mm m^{-2} d^{-1} kPa^{-1}), respectively, than that of the crosslinked HP-based material (2.22 cm^3_{STP} mm m^{-2} d^{-1} kPa^{-1}).

3.5.5. Comparison of the properties of films obtained with different proteins crosslinked by mTGase

It was previously demonstrated that different proteins, of both plant and animal origin, are able to act as mTGase substrates giving rise to edible films with modified properties. It should be emphasized that the enzymatically produced crosslinks might have variable effects on the film performances depending both on the experimental conditions, such as the enzyme concentration used, and on the specific structural features of the single proteins tested. In fact, Weng and Zheng (2015) reported that the protein treatment with higher amounts of mTGase weakened the mechanical properties of the gelatin-based films due to an excess of crosslinks formed that limit the mobility of the protein chains. More in detail, the authors found that, after protein treatment with mTGase, TS and EB of the derived films decreased from 65.7 MPa and 32.9% to

42.7 MPa and 12.1%, respectively, and these values were further reduced by increasing the enzyme concentration. Similar findings were obtained by Yayli et al. (2017), who reported that TS increased in films made with deboned chicken meat proteins treated with low concentrations (3%) of mTGase (increase from 2.4 MPa to 4.0 MPa), whereas the same parameter was observed to decrease (2.3 MPa) when the proteins were pretreated with higher amounts (4%) of enzyme. Moreover, Kaewprachu et al. (2017) reported that TS of myofibrillar protein films treated with mTGase increased when enzyme content was increased from 0% to 4%. Anchovy by-product protein films showed the highest TS and lowest EB when proteins were pretreated with 5% mTGase, that was the highest concentration of enzyme used in that study (Yilmaz et al., 2020), whereas their EB decreased. These results may be due to the formation of covalent crosslinks between protein chains, catalyzed by mTGase, and the consequent formation of high molecular weight polymers leading to an increase of the resistance of the derived films and to a decrease of their extensibility (Kaewprachu et al., 2017; Yilmaz et al., 2020; Yayli et al., 2017). However, although opposite effects on film EB, YM and WV permeability were often observed, the main measured parameters indicated that, most of the time, an increase in both film resistance and hydrophobicity was detected when comparison was carried out between the films prepared with mTGase-treated proteins with respect to the untreated counterparts (Table S1).

4. Conclusions

HPs were isolated from the hemp OC and demonstrated to effectively act *in vitro* as acyl donors and acceptors for mTGase, as well as to produce handleable films in the presence of plasticizer. Moreover, the enzymatically crosslinked HPs were showed to be able to give rise to bioplastics with improved performances. The scale up of these new materials on industrial scale might open new horizons to produce one time or short-term use items suitable for food packaging. For example, as the obtained bio-plastics are endowed with low water vapor permeability, they could be useful to protect and extend the shelf-life of fresh fruits, as apricots and persimmons, in order to allow their respiration. In this respect, the brownish appearance of the proposed packaging material should not negatively influence the customer acceptance, being of the same colour of that of mentioned food products and for the possible food protection from photooxidation by amber coloured films (Intawiwat et al., 2010). More in general, these findings encourage further investigations since hemp OC seems a potential renewable bio-source capable to partially substitute the highly pollutant petroleum-derived polymers, the production of which is continuing to exponentially increase. In fact, from an environmental and economic point of view, it is worthy to note that petroleum is becoming significantly expensive and a progressively limited resource expected to decline over the next few decades. Therefore, an early transition to renewable sources, such as that represented by hemp OCs, might be a valuable milestone at least for some specific sectors of food packaging industry.

CRediT authorship contribution statement

S.F.M., R.D.G., C.V.L.G., R.P.: Conceptualization; S.F.M., R.D.G., C.V.L.G.: Data curation; F S.F.M., C.V.L.G., R.P.: Investigation; S.F.M., R.D.G., M.F.: Methodology; C.V.L.G., R.P.: Supervision; C.V.L.G., S.F.M.: Writing-original draft; S.F.M., C.V.L.G., R.P.: Writing - review & editing; R.P.: Funding acquisition.

Acknowledgments

This research was funded by the grant PRIN: Progetti di Ricerca di Interesse Nazionale –Bando 2017– "CARDoon valorisation by InteGrAted biorefiNery (CARDIGAN)" of Italian Ministero dell'Università e della Ricerca (COD. 2017KBTK93), Italy.

Author contributions

Seyedeh Fateneh Mirpoor: Investigation; Methodology; Formal analysis; Writing-original draft. C. Valeria L. Giosafatto: Supervision; Conceptualization; Writing review and editing. Rocco Di Girolamo: Methodology; Investigation. Michela Famiglietti: Methodology; Raffaele Porta: Supervision; Conceptualization; Writing review and editing,; Supervision.

Appendix A. Supporting information

Supplementary data associated with this article can be found in the online version at doi:10.1016/j.fpsl.2021.100779.

References

Amadori, S., Torricelli, P., Rubini, K., Fini, M., Panzavolta, S., & Bigi, A. (2015). Effect of sterilization and crosslinking on gelatin films. *Journal of Materials Science: Materials in Medicine, 26*(2), 69.

AACC (2003). Approved Methods of AACC.; The Association: St. Paul, MN, USA. Available at: ⟨https://methods.aaccnet.org/default.aspx⟩.

Arabestani, A., Kadivar, M., Shahedi, M., Goli, S. A. H., & Porta, R. (2013). Properties of a new protein film from bitter vetch (*Vicia ervilia*) and effect of $CaCl_2$ on its hydrophobicity. *International Journal of Biological Macromolecules, 57*, 118–123.

ASTM E88-07a. (2007). Standard test method for seal strength of flexible barrier materials. F88-07. *Annual book of American standard testing method*, 768–777.

ASTM D3985–05 (2010). Standard test method for oxygen gas transmission rate through plastic film and sheeting using a colorimetric sensor; West Conshohocken, PA, USA.

ASTM F2476–13 (2013). Standard test method for the determination of carbon dioxide gas transmission rate through barrier materials using an infrared detector; West Conshohocken, PA, USA.

Basiak, E., Lenart, A., & Debeaufort, F.. (2018). How glycerol and water contents affect the structural and functional properties of starch-based edible films.. *Polymers, 10 (4)*, 412.

Bhattacharjee, S. (2016). DLS and zeta potential–what they are and what they are not? *Journal of Controlled Release, 235*, 337–351.

Callaway, J. C. (2004). Hempseed as a nutritional resource: An overview. *Euphytica, 140*, 65–72.

Crescente, G., Piccolella, S., Esposito, A., Scognamiglio, M., Fiorentino, A., & Pacifico, S. (2018). Chemical composition and nutraceutical properties of hempseed: an ancient food with actual functional value. *Phytochemistry Reviews, 17*, 733–749.

Cruz Diaz, K., Cobos, Á., Fernández Valle, M. E., Díaz, O., & Cambero, M. I. (2019). Characterization of edible films from whey proteins treated with heat, ultrasounds and/or transglutaminase. Application in cheese slices packaging. *Food Packaging and Shelf Life, 22*, Article 100397.

Dapčević-Hadnađev, T., Dizdar, M., Pojić, M., Krstonošić, V., Zychowski, L. M., & Hadnađev, M. (2019). Emulsifying properties of hemp proteins: Effect of isolation technique. *Food Hydrocolloids, 89*, 912–920.

de Oliveira Filho, J. G., Rodrigues, J. M., Valadares, A. C. F., de Almeida, A. B., de Lima, T. M., Takeuchi, K. P., … Dyszy, F. H. (2019). Active food packaging: alginate films with cottonseed protein hydrolysates. *Food Hydrocolloids, 92*, 267–275.

FAOSTAT (2020). Food and agriculture organization of the united Nations. Countries by commodity ⟨http://www.fao.org/faostat/en/#rankings/countries_by_commodity⟩. Accessed on 16 June 2021.

Fathi, N., Almasi, H., & Pirouzifard, M. K. (2018). Effect of ultraviolet radiation on morphological and physicochemical properties of sesame protein isolate based edible films. *Food Hydrocolloids, 85*, 136–143.

Fathi, N., Almasi, H., & Pirouzifard, M. K. (2019). Sesame protein isolate based bionanocomposite films incorporated with TiO_2 nanoparticles: study on morphological, physical and photocatalytic properties (doi.org/) *Polymer Testing, 77*, Article 105919. https://doi.org/10.1016/j.polymertesting.2019.105919.

Fetzer, A., Hintermayr, C., Schmid, M., Stäbler, A., & Eisner, P. (2020). Effect of acylation of rapeseed proteins with lauroyl and oleoyl chloride on solubility and film-forming properties (doi.org/) *Waste and Biomass Valorization*. https://doi.org/10.1007/s12649-020-01012-6.

Fike, J. (2016). Industrial hemp: renewed opportunities for an ancient crop. *Critical Reviews in Plant Sciences, 35*, 406–424.

Gaspar, A. L. C., & Góes-Favoni, S. P. D. (2015). Action of microbial transglutaminase (MTGase) in the modification of food proteins: A review. *Food Chemistry, 171*, 315–322.

Geyer, R., Jambeck, J. R., & Law, K. L. (2017). Production, use, and fate of all plastics ever made. *Science Advances, 3*(7), Article e1700782.

Giosafatto, C. V. L., Al-Asmar, A., D'Angelo, A., Roviello, V., Esposito, M., & Mariniello, L. (2018). Preparation and characterization of bioplastics from grass pea flour cast in the presence of microbial transglutaminase. *Coatings, 8*(12), 435.

Giosafatto, C. V. L., Fusco, A., Al-Asmar, A., & Mariniello, L. (2020). Microbial transglutaminase as a tool to improve the features of hydrocolloid-based bioplastics. *International Journal of Molecular Sciences, 21*(10), 3656.

Gómez-Estaca, J., Gavara, R., Catalá, R., & Hernández-Muñoz, P. (2016). The potential of proteins for producing food packaging materials: A review. *Packaging Technology and Science, 29*(4–5), 203–224.

González, A., Gastelú, G., Barrera, G. N., Ribotta, P. D., & Igarzabal, C. I.Á. (2019). Preparation and characterization of soy protein films reinforced with cellulose nanofibers obtained from soybean by-products. *Food Hydrocolloids, 89*, 758–764.

Hadnadev, M., Dapčević Hadnadev, T., Lazaridou, A., Moschakis, T., Michaelidou, A. M., Popović, S., & Biliaderis, C. G. (2018). Hempseed meal protein isolates prepared by different isolation techniques. Part I. physicochemical properties. *Food Hydrocolloids, 79*, 526–533.

Haghighi, H., Leugoue, S. K., Pfeifer, F., Siesler, H. W., Licciardello, F., Fava, P., & Pulvirenti, A. (2020). Development of antimicrobial films based on chitosan–polyvinyl alcohol blend enriched with ethyl lauroyl arginate (LAE) for food packaging applications. *Food Hydrocolloids, 100*, Article 105419.

Han, J. H., & Scanlon, M. G. (2005). Mass transfer of gas and solute through packaging materials. In J. H. Han (Ed.), *In Innovations in Food Packaging. Oxford* (pp. 12–23). Oxford: Elsevier Science & Technology.

Hosseini, S. F., Rezaei, M., Zandi, M., & Ghavi, F. F. (2013). Preparation and functional properties of fish gelatin–chitosan blend edible films. *Food Chemistry, 136*, 1490–1495.

House, J. D., Neufeld, J., & Leson, G. (2010). Evaluating the quality of protein from hemp seed (*Cannabis sativa* L.) products through the use of the protein digestibility-corrected amino acid score method. *Journal of Agricultural and Food Chemistry, 58*, 11801–11807.

Intawiwat, N., Pettersen, M. K., Rukke, E. O., Meier, M. A., Vogt, G., Dahl, A. V., … Wold, J. P. (2010). Effect of different colored filters on photooxidation in pasteurized milk. *J. Dairy Sci., 93*, 1372–1382.

Jahed, E., Khaledabad, M. A., Bari, M. R., & Almasi, H. (2017). Effect of cellulose and lignocellulose nanofibers on the properties of *Origanum vulgare* ssp. gracile essential oil loaded chitosan films. *Reactive and Functional Polymers, 117*, 70–80.

Jasse, B., Scuvre, A. M., & Mathlouthi, M. (1994). Permeability and structure in polymeric packaging materials. In M. Mathlouthr (Ed.), *Food Packaging and Preservation* (pp. 1–22). Blackie.

Jiang, S., Zou, L., Hou, Y., Qian, F., Tuo, Y., Wu, X., … Mu, G. (2020). The influence of the addition of transglutaminase at different phase on the film and film forming characteristics of whey protein concentrate-carboxymethyl chitosan composite films. *Food Packaging and Shelf Life, 25*, Article 100546.

Jiménez Rosado, M., Bouroudian, E., Perez Puyana, V., Guerrero, A., & Romero, A. (2020). Evaluation of different strengthening methods in the mechanical and functional properties of soy protein-based bioplastics. *Journal of Cleaner Production, 262*, Article 121517.

Kaewprachu, P., Osako, K., Benjakul, S., Tongdeesoontorn, W., & Rawdkuen, S. (2016). Biodegradable protein-based films and their properties: a comparative study. *Packaging Technology and Science, 29*(2), 77–90.

Kaewprachu, P., Osako, K., Tongdeesoontorn, W., & Rawdkuen, S. (2017). The effects of microbial transglutaminase on the properties of fish myofibrillar protein film. *Food Packaging and Shelf life, 12*, 91–99.

Karimian, Z., Tabatabaee Bafroee, A. S., & Sharifan, A. (2019). Physico-mechanical and antimicrobial properties of isolated soy protein film incorporated with peppermint essential oil on raw hamburger. *Journal of Agricultural Science and Technology, 21*, 1145–1159.

Kitrytė, V., Bagdonaitė, D., & Venskutonis, P. R. (2018). Biorefining of industrial hemp (*Cannabis sativa* L.) threshing residues into cannabinoid and antioxidant fractions by supercritical carbon dioxide, pressurized liquid and enzyme assisted extractions. *Food Chemistry, 267*, 420–429.

Laemmli, U. K. (1970). Cleavage of structural proteins during the assembly of the head of bacteriophage T4. *Nature, 227*(5259), 680–685.

Plastic Waste and Recycling: Environmental Impact. In Letcher, T. M. (Ed.), *Societal Issues*, (pp. 1–664). (2020) (pp. 1–664). Academic Press. https://doi.org/10.1016/B978 0 12 817880 5.00004 9.

Liu, Y., Liu, Y., Xu, Z., Shan, M., Ge, X., Zhang, Y., … Lu, F. (2019). Effects of *Bacillus subtilis* transglutaminase treatment on the functional properties of whey protein. *LWT Food Science and Technology, 116*, Article 108559.

Masamba, K., Li, Y., Hategekimana, J., Zeladi, M., Ma, J., & Zhong, F. (2016). Evaluation of mechanical and water barrier properties of transglutaminase cross linked zein films incorporated with oleic acid. *International Journal of Food Science & Technology, 51*(5), 1159–1167.

Miller, K. S., & Krochta, J. M. (1997). Oxygen and aroma barrier properties of edible films: A review. *Trends in Food Science & Technology, 8*(7), 228–237.

Ortega-Toro, R., Jiménez, A., Talens, P., & Chiralt, A. (2014). Properties of starch–hydroxypropyl methylcellulose based films obtained by compression molding. *Carbohydrate Polymers, 109*, 155–165.

Pojić, M., Mišan, A., Sakač, M., Dapčević Hadnađev, T., Šarić, B., Milovanovič, I., & Hadnađev, M. (2014). Characterization of byproducts originating from hemp oil processing. *Journal of Agricultural and Food Chemistry, 62*(51), 12436–12442.

Porta, R. (2019). The plastics sunset and the bio plastics sunrise. *Coatings, 9*, 526. https://doi.org/10.3390/coatings9080526

Porta, R., Di Pierro, P., Rossi-Marquez, G., Mariniello, L., Kadivar, M., & Arabestani, A. (2015). Microstructure and properties of bitter vetch (*Vicia ervilia*) protein films reinforced by microbial transglutaminase. *Food Hydrocolloids, 50*, 102–107.

Riveros, C. G., Martin, M. P., Aguirre, A., & Grosso, N. R. (2018). Film preparation with high protein defatted peanut flour: characterization and potential use as food packaging. *International Journal of Food Science & Technology, 53*, 969–975.

Rostamzad, H., Paighambari, S. Y., Shabanpour, B., Ojagh, S. M., & Mousavi, S. M. (2016). Improvement of fish protein film with nanoclay and transglutaminase for food packaging. *Food Packaging and Shelf Life, 7*, 1–7.

Rouilly, A., & Vaca-Garcia, C. (2013). Industrial use of oil cakes for material applications. In A. Kazmi, & P. Shuttleworth (Eds.), *The Economic Utilization of Food Co-Products* (pp. 185–213). Royal Society of Chemistry Publ. https://doi.org/10.1039/9781849737326.

Roy, S., & Rhim, J. W. (2020). Preparation of carbohydrate-based functional composite films incorporated with curcumin. *Food Hydrocolloids, 98*, Article 105302.

Roy, S., Rhim, J. W., & Jaiswal, L. (2019). Bioactive agar-based functional composite film incorporated with copper sulfide nanoparticles. *Food Hydrocolloids, 93*, 156–166.

Russo, R., & Reggiani, R. (2015). Evaluation of protein concentration, amino acid profile and antinutritional compounds in hempseed meal from dioecious and monoecious varieties. *American Journal of Plant Sciences, 6*(01), 14.

Sabbah, M., Di Pierro, P., Giosafatto, C. V. L., Esposito, M., Mariniello, L., Regalado-Gonzales, C., & Porta, R. (2017). Plasticizing effects of polyamines in protein-based films. *International Journal of Molecular Sciences, 18*(5), 1026.

Sabbah, M., Altamimi, M., Di Pierro, P., Schiraldi, C., Cammarota, M., & Porta, R. (2020). Black edible films from protein-containing defatted cake of *Nigella sativa* seeds. *International Journal of Molecular Sciences, 21*, 832. https://doi.org/10.3390/ijms21030832

Schmid, M., Sängerlaub, S., Wege, L., & Stäbler, A. (2014). Properties of transglutaminase crosslinked whey protein isolate coatings and cast films. *Packaging Technology and Science, 27*(10), 799–817.

Shojaee-Aliabadi, S., Hosseini, H., Mohammadifar, M. A., Mohammadi, A., Ghasemlou, M., Hosseini, S. M., & Khaksar, R. (2014). Characterization of κ-carrageenan films incorporated plant essential oils with improved antimicrobial activity. *Carbohydrate Polymers, 101*, 582–591.

Sorde, K. L., & Ananthanarayan, L. (2019). Effect of transglutaminase treatment on properties of coconut protein-guar gum composite film. *LWT Food Science and Technology, 115*, Article 108422.

Tang, C. H., Jiang, Y., Wen, Q. B., & Yang, X. Q. (2005). Effect of transglutaminase treatment on the properties of cast films of soy protein isolates. *Journal of Biotechnology, 120*(3), 296–307.

Tang, C. H., Ten, Z., Wang, X. S., & Yang, X. Q. (2006). Physicochemical and functional properties of hemp (*Cannabis sativa* L.) protein isolate. *Journal of Agricultural and Food Chemistry, 54*(23), 8945–8950.

Weng, W., & Zheng, H. (2015). Effect of transglutaminase on properties of tilapia scale gelatin films incorporated with soy protein isolate. *Food Chemistry, 169*, 255–260.

Wihodo, M., & Moraru, C. I. (2013). Physical and chemical methods used to enhance the structure and mechanical properties of protein films: A review. *Journal of Food Engineering, 114*, 292–302.

Wittaya, T. (2012). Protein-based edible films: Characteristics and improvement of properties (doi.org/) *Structure and Function of Food Engineering*, 43–70. https://doi.org/10.5772/48167.

Xu, W., Liu, B., Yang, H., Liu, K., Jia, S., & Chen, F. (2012). Effect of γ irradiation on the physicochemical properties of mixed soy protein isolate/starch material. *African Journal of Biotechnology, 11*(28), 7238–7246.

Yayli, D., Turhan, S., & Saricaoglu, F. T. (2017). Edible packaging film derived from mechanically deboned chicken meat proteins: Effect of transglutaminase on physicochemical properties. *Korean Journal for Food Science of Animal Resources, 37*(5), 635.

Yilmaz, K., Turhan, S., Saricaoglu, F. T., & Tural, S. (2020). Improvement of physicochemical, mechanical, thermal and surface properties of anchovy by-product protein films by addition of transglutaminase, and the correlation between secondary structure and mechanical properties. *Food Packaging and Shelf Life, 24*, Article 100483.

Zahedi, Y., Fathi-Achachlouei, B., & Yousefi, A. R. (2018). Physical and mechanical properties of hybrid montmorillonite/zinc oxide reinforced carboxymethyl cellulose nanocomposites. *International Journal of Biological Macromolecules, 108*, 863–873.

Zhao, J., Xu, Y., Wang, W., Griffin, J., Roozeboom, K., & Wang, D. (2020). Bioconversion of industrial hemp biomass for bioethanol production: A review. *Fuel, 281*, 118725–118733.

Zhong, T., Liang, Y., Jiang, S., Yang, L., Shi, Y., Guo, S., & Zhang, C. (2017). Physical, antioxidant and antimicrobial properties of modified peanut protein isolate based films incorporating thymol. *RSC Advances, 7*, 41610–41618.

Zink, J., Wyrobnik, T., Prinz, T., & Schmid, M. (2016). Physical, chemical and biochemical modifications of protein based films and coatings: An extensive review. *International Journal of Molecular Sciences, 17*(9), 1376.

coatings

MDPI

Article

A Comparison of Cellulose Nanocrystals and Nanofibers as Reinforcements to Amylose-Based Composite Bioplastics

Marwa Faisal [1,†], Marija Žmirić [1,†], Ngoc Quynh Nhu Kim [1], Sander Bruun [1], Loredana Mariniello [2], Michela Famiglietti [2], Heloisa N. Bordallo [3], Jacob Judas Kain Kirkensgaard [3,4], Bodil Jørgensen [1], Peter Ulvskov [1], Kim Henrik Hebelstrup [5] and Andreas Blennow [1,*]

[1] Department of Plant and Environmental Sciences, Faculty of Science, University of Copenhagen, 1871 København, Denmark; marwa@plen.ku.dk (M.F.); marijazmiric2@gmail.com (M.Ž.); qkn.nhu@gmail.com (N.Q.N.K.); sab@plen.ku.dk (S.B.); boj@plen.ku.dk (B.J.); ulvskov@plen.ku.dk (P.U.)
[2] Department of Chemical Sciences, Monte Sant'Angelo Campus, University of Naples "Federico II", Via Cinthia 4, 80126 Naples, Italy; loredana.mariniello@unina.it (L.M.); michela.famiglietti@unina.it (M.F.)
[3] Niels Bohr Institute, Faculty of Science, University of Copenhagen, 2100 København, Denmark; bordallo@nbi.ku.dk (H.N.B.); jjkk@food.ku.dk (J.J.K.K.)
[4] Department of Food Science, University of Copenhagen, DK-1958 Frederiksberg C, 1871 København, Denmark
[5] Department of Agroecology, Aarhus University, 4200 Slagelse, Denmark; kim.hebelstrup@agro.au.dk
* Correspondence: abl@plen.ku.dk
† These authors contributed equally to this work.

Abstract: Starch-based bioplastics offer a promising alternative to conventional plastics. However, they exhibit certain limitations, notably in terms of mechanical strength and barrier properties. These challenges could potentially be addressed through the incorporation of nanocellulose as a reinforcing agent. In this study, we fabricated bioplastic films using a casting and blending approach, employing highly linear pure amylose (AM) in combination with cellulose nanofibers (CNF) or cellulose nanocrystals (CNC) at various ratios. This allowed for a direct comparison of CNF and CNC functionality within the AM matrix. We systematically assessed mechanical properties and water barrier characteristics, encompassing parameters such as water permeability, moisture content, swelling, solubility, crystallinity, thermal stability, transmittance, and opacity. Additionally, we investigated water vapor and oxygen permeability. Furthermore, we delved into distinctions between CNC and CNF biocomposites. Incorporation of either type of nanocellulose yielded enhancements in film properties, with CNF exerting a more pronounced positive influence compared to CNC. Particularly noteworthy were the mechanical properties, wherein CNF composite films demonstrated markedly higher tensile strength and Young's modulus compared to their CNC counterparts. For instance, the inclusion of 1% CNF led to a substantial increase in AM tensile strength from 66.1 MPa to 144.8 MPa. Conversely, water vapor permeability exhibited a converse behavior, as the addition of 1% CNF resulted in a significant reduction of water barrier properties from 8.7 to 1.32 g mm m^{-2} 24 $h^{-1}kPa^{-1}$. Intriguingly, CNC films displayed greater elongation at the point of rupture in comparison to CNF films. This can be attributed to the larger surface area of the CNC and the favorable interfacial interaction between AM and CNC. Notably, the introduction of nanocellulose led to reduced film opacity and improved thermal stability. In summary, nanocellulose interacted synergistically with the AM matrix, establishing a robust hydrogen-bonded network that greatly enhanced the performance of the biocomposite films.

Keywords: biocomposites; amylose; nanocellulose; nanocellulose crystal; nanocellulose fibers; bioplastics; food packaging; novel material

check for updates

Citation: Faisal, M.; Žmirić, M.; Kim, N.Q.N.; Bruun, S.; Mariniello, L.; Famiglietti, M.; Bordallo, H.N.; Kirkensgaard, J.J.K.; Jørgensen, B.; Ulvskov, P.; et al. A Comparison of Cellulose Nanocrystals and Nanofibers as Reinforcements to Amylose-Based Composite Bioplastics. *Coatings* **2023**, *13*, 1573. https://doi.org/10.3390/coatings13091573

Academic Editor: Levente Csoka

Received: 30 June 2023
Revised: 31 August 2023
Accepted: 5 September 2023
Published: 9 September 2023

Copyright: © 2023 by the authors. Licensee MDPI, Basel, Switzerland. This article is an open access article distributed under the terms and conditions of the Creative Commons Attribution (CC BY) license (https://creativecommons.org/licenses/by/4.0/).

1. Introduction

Bio-composites exhibit significant potential as environmentally friendly alternatives in the realms of both food and medicine, presenting renewable and sustainable options [1].

Their versatile applications have spurred extensive research and integration across various industries. Recently, the advancement of nanocomposite technology has addressed challenges associated with biopolymer packaging materials. Nanocomposites surpass plain polymers and traditional composites, demonstrating enhanced barrier properties, increased strength, and heightened heat resistance. The concept of biocomposites is undergoing evolution to encompass nanostructured hybrid materials. Key biopolymer constituents, such as starch, cellulose, chitin/chitosan, and silk, are derived from polysaccharides linked by glycosidic bonds [2,3]

Starch represents an abundant raw material with the potential to yield robust and biodegradable bioplastics characterized by both high-value and versatile bulk properties [4]. It consists of two primary polysaccharide types: amylopectin (AP) and amylose (AM). Amylopectin is composed of short α (1–4) bonded chain segments, comprising 10–16 glucose units forming parallel double helices that are α (1–6) linked to longer linear backbone chains [5]. In contrast, AM is chiefly a linear α (1 → 4) linked polymer capable of forming both single and double helices, which align in ordered structures, offering a strong structural foundation for biocomposites. The proportions of AM and AP in starch generally fall between 28% and 75%, with only one documented instance of producing a high-yield AM-only starch type [6,7].

Starch-based films possess crucial attributes for food packaging materials, including transparency, odor neutrality, lack of taste interference, and non-toxicity. However, they still contend with limitations such as brittleness, hydrophilicity, suboptimal barrier properties, and inadequate cohesiveness [6]. Augmenting the cohesiveness of starch films can be achieved through either blending them with appropriate polymers to create an interconnected matrix with starch or by crosslinking starch with a flexible polymer. The inclusion of plasticizers such as glycerol or water addresses brittleness and augments film flexibility by diminishing intra- and intermolecular hydrogen bonding. This, in turn, enhances the mobility of starch chains.

Cellulose, a linear homo-polysaccharide comprised of numerous β-(1 → 4)-D-glucopyranose residues, stands out as a superb option for reinforcement [7]. Of particular interest is nanocellulose, lauded for its advantageous physical and chemical properties. Characterized by chemical inertness, remarkable stiffness, high strength, low density, dimensional stability, and a minimal coefficient of thermal expansion, nanocellulose draws attention. Its surface chemistry is amenable to alteration. Cellulose nanocrystals (CNCs), in particular, exhibit versatile surface chemistry due to the heightened reactivity of their available hydroxyl groups. This facilitates diverse modifications, including the introduction of charged or hydrophobic components, modulation of water interactions, and the promotion of integration within polymer matrices. Surface modifications can occur during isolation/purification or via other treatments, encompassing covalent bonds or physical absorption.

The most prevalent approach for CNC production involves acidic hydrolysis, which eliminates amorphous segments in cellulose microfibrils while preserving crystalline regions. Acid-catalyzed hydrolysis with sulfuric acid yields sulfate esters with varying degrees of sulfonation, resulting in a negatively charged surface that stabilizes nanocrystal suspensions for a multitude of applications. Alternatively, hydrochloric acid usage leads to hydroxylated surfaces with lower charge density and reduced water dispersibility. Less conventional methods involving phosphoric and hydrobromic acids have also been explored [8].

Acid hydrolysis finds widespread use in the top-down production of cellulose nanocrystals (CNCs) [9]. These CNCs are generated by ending hydrolysis at the leveling off degree of polymerization (LODP) stage where hydrolysis comes to a near halt, leaving behind only highly resilient crystalline segments. These individual cellulose crystals are subsequently gathered and refined through processes involving centrifugation and dialysis, and loss is minimal [10].

Employing HCl vapor leads to swift hydrolysis of cellulose fibers derived from cotton. These fibers are consistently coated by a thin layer of water in ambient conditions (5).

In these experiments, the equilibrium between HCl vapor and aqueous HCl solutions is utilized. The study shows that HCl vapor proves highly effective in breaking down cellulose within a cotton-based filter paper at room temperature. This process rapidly reduces the degree of polymerization (DP) to the level of LODP, approximately 170. The resultant nanocrystals have dimensions akin to those obtained from conventional liquid/solid acid hydrolysis of cotton, measuring around 7–8 nm in width and 100–300 nm in length with high yield [11,12].

Using TEMPO (2,2,6,6-tetramethylpiperidine-1-yl)oxyl radical as an oxidation catalyst enables the creation of stable suspensions of cellulosic particles with a high surface charge density [13,14]. These particles, derived from microgranular cellulose, exhibit characteristics across three length scales simultaneously: nanocrystals, micron-sized longitudinal particles, and larger particles up to tens of microns.

Presently, cellulose nanofibers (CNF) and cellulose nanocrystals (CNC) have garnered significant attention as reinforcement agents. The influence of CNF and CNC on starch properties diverges due to differences in size and preparation methods. Various studies suggest that CNF extracted from renewable sources, such as agro-wastes, bolster the crystallinity, barrier characteristics, mechanical strength, and thermal stability of starch while preserving its biodegradability.

CNF features an intricate structure comprising elongated, interwoven cellulose fibers with a notable aspect ratio. This network of fibers resembles a larger-scale fibrous matrix compared to the rod-like crystalline nanoparticles constituting CNC. Conversely, CNC exhibits a higher degree of crystallinity and comprises crystalline nanoparticles with a distinct rod-like shape. It boasts a larger surface area and an elevated density of surface hydroxyl groups, rendering it more reactive and conducive to diverse chemical modifications and functionalizations.

Manufacturing CNF/CNC films can be achieved through bottom-up assembly methods such as solvent casting, vacuum filtration, or layer-by-layer assembly. However, these approaches present certain limitations, including time-consuming processes and challenges associated with scaling up to bulk materials.

To address these limitations, a recent study [15] introduced a novel top-down recombination method for producing large-scale cellulosic structural materials. This method capitalizes on the inherent alignment of nanocellulose structures. Through the induction of hydrogen bonding with water molecules, the study developed a straightforward and versatile technique for generating robust and resilient structural materials. The investigation employed Finite Element Analysis (FEA) to examine the influence of water-induced hydrogen bonding on cellulose nanofibers. Dynamic mechanical properties were assessed using FEA, revealing that increased moisture levels led to improvements in tensile strength and toughness. Water molecules played a pivotal role by plasticizing cellulose nanofibrils and facilitating the establishment of hydrogen bonds, culminating in the creation of sturdy materials [15].

Another noteworthy study [16] introduced an efficient method for extracting micro and nano holocellulose fibers (HCNFs) from the natural stem of the manau rattan. This process encompassed three steps: pulping, bleaching, and TEMPO oxidation. Through this method, a high-haze yet transparent HCNF film was successfully fabricated using vacuum filtration, solvent exchange, and ambient drying techniques. The resulting HCNF film exhibited an impressive tensile strength of 84.8 MPa, attributed to the compact microstructure formed via self-association through hydrogen bonding among cellulose nanofibrils. Furthermore, the HCNF film showed exceptional optical properties, boasting high light transmittance (93.7%) at a wavelength of 550 nm. These remarkable traits stemmed from the dense, wrinkle-shaped microstructure that enabled visible light to penetrate and diffuse across the film surface. It was anticipated that this distinctive film, combining robustness with distinctive optical qualities, will find practical applications in industries such as optical devices and aerospace materials.

Numerous studies have consistently shown that incorporating CNF or CNC into the starch matrix enhances the mechanical, thermal, and barrier properties of resulting nanocomposites [17]. These enhancements are particularly significant for packaging applications. The specific properties required for these films vary depending on the intended application and the type of food being preserved [18]. Given that CNC and CNF exert distinct effects on starch films due to variations in size and preparation methods, the selection of nanocellulose can be customized to precisely match the specific demands of food packaging.

In our preceding investigation [19], we successfully produced nanocomposite films using AM sourced from transgenic barley, possessing a remarkable 99% AM content in the grain starch. We combined this with cellulose nanofibers (CNFs) obtained from sugar beet pulp. The AM matrix was reinforced with 25% and 50% CNF. Rigorous analyses were conducted to assess the mechanical, thermal, and water permeability properties of the AM/CNF composites, both in the presence and absence of glycerol.

The results from the composite films cast with AM-CNF showed increased crystallinity and improved mechanical properties. Additionally, these films exhibited decreased water contact angles, reduced water vapor permeability, and lower oxygen permeability, particularly evident at 50% CNF loading. A noteworthy observation was the emergence of an anti-plasticizing effect in the AM film at a glycerol content of 15%. However, the presence of 25% CNF reversed this effect. The inclusion of 50% CNF in the composite yielded surfaces with rougher textures, featuring fiber-like structures and heightened wettability.

This research introduces reinforced composite films comprising pure AM and two types of nanocellulose: CNC and CNF. Our study represents the first endeavor to blend pure AM with CNC and subsequently compare it to CNF while accounting for differences in size and preparation methods. The central aim of this study is to evaluate the influence exerted by CNF and CNC on the AM matrix. The outcomes of this investigation are expected to identify an alternative starch source for environmentally friendly packaging and establish a theoretical foundation for incorporating nanocellulose in starch-based films.

While CNCs and CNFs have been explored as reinforcement agents for starch-based films and have demonstrated property enhancement, a direct comparison between these two components in the context of pure AM remains absent. This paper directly compares and evaluates the performance and enhancement effects of CNCs and CNFs to discern their distinctions and identify the more suitable option for integration into 99% AM films.

We created casted films using various combinations of raw polysaccharides, plasticized with glycerol. This study aimed to comprehensively characterize the nanocomposite films in terms of their physical, mechanical, opacity, thermal, and barrier properties. The morphological features were examined using scanning electron microscopy (SEM) and X-ray diffraction (XRD). As a control, an AM-only film was utilized. Nanocomposites composed of AM, CNC, and CNF were fabricated in the range of 0.5%–17% of CNF or CNC. Our investigation revealed that the introduction of CNC or CNF led to a reduction in water barrier properties, accompanied by improvements in mechanical and thermal film characteristics. Notably, CNF exhibited superior results in several of these properties. We anticipate that our findings will streamline the search for an alternative starch source for biodegradable packaging and contribute to establishing a foundational framework for the utilization of nanocellulose in starch films.

2. Materials and Methods

2.1. Materials

AM, NCF, and CNC were the main components of the films. AM was produced from a genetically modified barley line that was previously generated [7]. CNCs were extracted from woody biomass provided by Nanografi Nano Technology Germany. The CNCs were 10–20 nm wide and 300–900 nm long. CNF was extracted from sugar beet pulp [20] provided by Nordic Sugar A/S Denmark. Glycerol and Milli-Q water were used as plasticizers for the films.

2.2. Extracting Amylose (AM) from Barley

Barley grains were ground into a fine powder using the Komo Fidibus 21 Grain Mill. Next, 500 mL of 0.075 M NaOH and 100 g of barley flour were mixed into a 1000 mL beaker and stirred for 3 h. The suspension was screened using a 100-micron mesh sieve, and the leftovers containing bran and pericarp were discarded. The filtrate was centrifuged at 4000× *g* for 10 min. The supernatant was discarded, and the AM granules were washed twice with distilled water and pH checked to secure neutral conditions. The AM was collected and washed with ethanol (96%), pelleted, and left to air dry overnight with occasional stirring to secure the complete dryness of the powder [21].

2.3. Extracting Nanocellulose Fibers from Sugar Beet Pulp

CNF was prepared following the procedures outlined in [12,14,20,22] with slight modifications. Briefly, 15 g (dry weight) of sugar beet pulp was washed with 5000 mL of dH_2O using a 38 µm sieve, followed by suspension in 500 mL of 0.5 M NaOH. This mixture was stirred at 80 °C for 2 h and washed to neutrality with dH_2O. The NaOH-treated pulp was then immersed in a 500 mL bleach solution (1% $NaClO_2$, pH 5.0) and stirred at 70 °C for 2 h. After this, further washing with dH_2O eliminated lignin and tannins. The remaining cellulose fiber suspension's dry weight was measured post-drying and diluted to 1.00% (*w/w*) in dH_2O. A 200 mL portion of the obtained fiber suspension was subjected to circulation in a high-shear homogenizer (microfluidizer materials processor M110-P, Newton, MA, USA) with 200 and 400 µm orifices under 500 bar pressure for 18 min, resulting in the production of nanocellulose fibers. The CNFs were stored at 4 °C in the refrigerator for subsequent use [20]. The CNF width ranged from 5 nm for the thinnest fibers to 16–55 nm for the thickest (Figure S1).

2.4. Creating the Biocomposite Films

Different nanocomposite formulations were prepared by blending AM with either CNC or CNF, along with glycerol as a plasticizer. For composite film creation, 1 g of AM was suspended in 100 mL of MilliQ water and mixed with 30% (*w/w*) glycerol. Various percentages of CNF or CNC (0.5%, 1%, 3%, 6%, 9%, and 17% wt% of AM) were subsequently added to the suspension. A control film comprising pure AM (1%) and 30% glycerol was also prepared. The components were introduced into a high-pressure glass reactor and heated in an oil bath at 140 °C with continuous stirring. Afterward, the reactor and solutions were cooled to 70 °C, followed by casting in Teflon-coated Petri dishes. Films were incubated at 50 °C for 8 h or until fully dry. To equalize moisture content and prevent film shrinkage, all films were stored in a sealed desiccator with potassium chloride at 90% relative humidity at room temperature before analysis [19].

2.5. Fourier Transform Infrared (FTIR) Spectroscopy

Infrared spectroscopy was conducted using a Bruker Alpha FTIR spectrometer (Bruker Optik GmbH, Ettlingen, Germany). The measurements employed an attenuated total reflectance (ATR) single reflectance cell equipped with a diamond crystal. The samples underwent 32 scans over the range of 4000–400 cm^{-1} at a resolution of 4 cm^{-1}, with air as the background.

2.6. Thickness and Moisture Content

Film thickness was gauged at 8 randomly selected points per film using a micrometer device (148–121 Zhongtian Experimental Instrument Co., Ltd., Shanghai, China). The average of these 8 measurements was computed to establish the overall thickness for each film. Each film's thickness was based on 8 replicates [23]. Moisture content was assessed by taking triplicate 2 × 2 cm squares from each film, which were then dried at 105 °C until a constant weight was achieved [24]. The moisture content was determined using the

following equation, where *Mi* represents the initial weight and *Mt* denotes the final weight of the sample (Equation (1)):

$$\mathrm{MC}(\%) = \frac{(Mi - Mt)}{Mi} \times 100\% \quad (1)$$

2.7. Swelling Index (SI) and Water Solubility (WS)

The swelling index (SI) and water solubility (WS) were determined by weight using three different masses. Square-shaped 2 × 2 cm samples were prepared, and the tests were conducted in triplicate. The first mass (*M*1) was measured after the samples were equilibrated in an oven at 70 °C for 24 h to attain a constant weight. Subsequently, each sample was immersed in 20 mL of deionized water and stirred for 24 h at 30 °C to obtain *M*2 (wet weight). After drying the samples with filter paper, they were weighed to obtain *M*3, following another 24-h drying at 70 °C. Sample measurements were performed in triplicate simultaneously to ensure consistency. The swelling index (SI) and water solubility (WS%) were calculated using Equations (2) and (3) [25].

$$\mathrm{SI}(\%) = \frac{(M2 - M1)}{M1} \times 100\% \quad (2)$$

$$\mathrm{WS}(\%) = \frac{(M1 - M3)}{M1} \times 100\% \quad (3)$$

2.8. Mechanical Properties

Rectangular strips measuring 1 cm in width and 10 cm in length were cut from the films. Tensile properties were determined using an Instron machine model 5569 (MTS, Eden Prairie, MN, USA), equipped with a 5 kN tensile load cell, following ASTM D882 standard [26]. The distance between clamps was set at 60 mm, and the crosshead speed was maintained at 10 mm/min. For each film, 8 samples were tested and averaged. Film thickness was measured using a micrometer screw gauge. The results were derived from 6–8 replicates per film.

2.9. Scanning Electron Microscopy (SEM)

SEM images were captured using a Quanta 3D FEG (FEI Company, Eindhoven The Netherlands, The Netherlands), depicting both film surfaces and cross sections. Small film pieces were affixed to a metal plate and coated with a 2 nm colloidal gold layer prior to analysis. To examine the dispersion of CNF and CNC within the AM matrix, samples were cryogenically fractured in liquid nitrogen and subsequently gold-sputtered [19].

2.10. Light Transmittance and Opacity

Light transmittance was measured on small round pieces of the films. The film pieces were scanned on a Lambda 35 UV–vis spectrophotometer (PerkinElmer Inc., Waltham, MA, USA) from 200 to 800 nm, and the opacity was calculated [6]:

$$Opacity = \frac{A}{x} \quad (4)$$

where A is the absorbance of the film at 600 nm and x the film thickness (mm) [27].

2.11. Thermogravimetric Analysis (TGA)

TGA coupled with Fourier Transform Infrared Spectroscopy (FTIR) was utilized to characterize the thermal stability of the diverse films. All samples were analyzed using the TG 209 F1 Libra PERSEUS from NETZSCH coupled to an FTIR instrument from Bruker Optics. Experimental conditions were as follows: N2 atmosphere (20 mL/min), heating rate of 10 K/min. Measurements were conducted between 28 °C and 600 °C in a standard Al_2O_3 crucible, employing an automatic sample changer. An empty crucible was used

for instrument correction. Data processing was conducted using NETZSCH-provided software. FTIR spectra of the evolved gases were recorded every 3 °C throughout the measurement. A selection of spectra at temperatures of interest, guided by TGA data, were further analyzed from the collected FTIR data.

2.12. Wide Angle X-ray Scattering(WAXS)

XRD analysis of the films was performed using a Nano-inXider instrument from Xenocs (Grenoble, France), employing a Cu Kα source with a wavelength of 1.54 Å and a 2D Pilatus detector (Dectris Ltd., Baden, Switzerland). Samples were loaded between mica windows, and background contributions were subtracted from the recorded spectra. The total relative crystallinity was calculated as the ratio of the crystalline peak area to the overall diffraction area, utilizing Peak Fit software (Version 4.0, Systat Software Inc., San Jose, CA, USA).

2.13. Permeability

The barrier properties of the films against water vapor (WV) and O_2 were assessed using a MultiPerm instrument (ExtraSolution s.r.l, Pisa, Italy). Duplicate tests were conducted for each film at 50% RH and 25 °C, following ASTM F1249-13 (2013) and ASTM D3985-05 (2010) standards [1,2]. Prior to testing, film specimens were conditioned for 24 h at 50% RH and were enclosed in aluminum masks, reducing the film test area to 2 cm^2.

2.14. Degradation Studies

For degradation studies, square pieces (3 cm × 3 cm) of pure films containing 1% AM, 1% CNF, 1% CNC, and composite films of AM with 17% CNF and 17% CNC were prepared. A 100 mL flask with a blue cap was filled with 25 g of soil, and each film was positioned on the soil surface and covered with another 25 g of soil. To achieve 80% of the water holding capacity (WHC), 500 µg of ionized water was added, maintaining constant water content (WC) during composting. The flasks were incubated at 25 °C ± 3 °C in a dark incubator with ensured air supply to prevent anaerobic conditions, sealed with rubber plugs, and equipped with syringes for sampling [28].

Gas concentrations (CO_2, CH_4, N_2O) in collected samples were measured using a gas chromatograph (Bruker 450-GC 2011, Billerica, MA, USA) with appropriate detectors. Calibration was performed using standards encompassing all gases at the beginning and end of each sample run.

Fourier transform-infrared spectroscopy (FT-IR) was applied for analyzing samples before and after degradation, using an attenuated total reflectance (ATR) single reflectance cell with a diamond crystal. Scans were conducted 32 times over the 4000–400 cm^{-1} range at a 4 cm^{-1} resolution against an air background. A Bruker Alpha FTIR spectrometer (Bruker Optik GmbH, Ettlingen, Germany) was utilized for sample analysis.

2.15. Statistical Analysis

One-way analysis of variance (ANOVA) was utilized for data analysis, and means were compared using Tukey's test at a significance level of 5% ($p < 0.05$). In the bar chart plot, different letters above the error bars denote significant differences between means. Thickness and mechanical properties were measured with 8 replicates, while moisture content, swelling, and water solubility were assessed in triplicates. Principal component analysis (PCA) was conducted to summarize and visually represent the data. Statistical analyses were carried out using IBM® SPSS® Statistics 27 software and Origin 2020.

3. Results and Discussions

3.1. FTIR

The AM spectra revealed distinctive peaks: the band at 3280 cm^{-1} corresponded to the stretching vibration of -OH groups in AM. The band at 2921 cm^{-1} indicated C-H single

bond stretching, while the peak at 1648 cm^{-1} was associated with water molecules in AM. Peaks at 1156 and 989 cm^{-1} were assigned to C-O-H and C-O-C stretching, respectively.

In the AM nanocomposite films, spectra of AM, CNF (Figure 1a), and CNC films (Figure 1b) exhibited a broad band at 3600–3000 cm^{-1} attributed to O-H stretching. This was due to extensive hydrogen bonding among cellulose, AM, and glycerol hydroxyl groups [19], with variation in peak intensities across samples. The strongest signals were in 6% CNF and 17% CNC films, indicating increased H-bonding and adhesion. Hygroscopic behavior of polysaccharides led to an adsorption band at 1648 cm^{-1}, attributed to absorbed water, with reduced intensity in 3% CNF and 3% CNC films due to interactions among AM, CNF/CNC, and glycerol that decreased hydroxyl group-water binding.

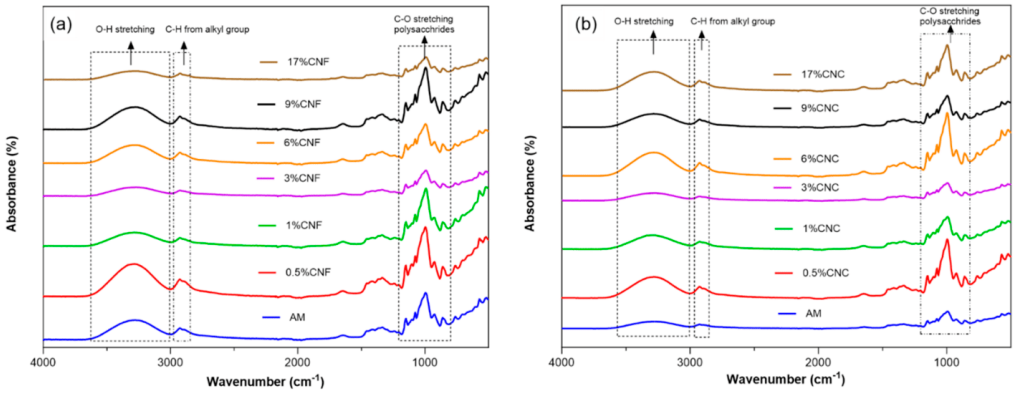

Figure 1. FT-IR of composite films, (**a**) AM/CNF composite films, (**b**) AM/CNC composite films.

In conclusion, CNC, CNF, and AM spectra were similar due to their similar chemical nature, complicating peak distinction [20]. Yet, absorbance's at certain wavenumbers in CNC and CNF films exceeded those in the AM film, likely due to extensive bonding among AM, glycerol, and nanocellulose [29].

3.2. Thickness and Moisture

Film thickness is a crucial parameter affecting properties like gas permeability and opacity. The measured thickness for both AM and nanocomposites ranged around 0.06–0.08 mm. There was no significant difference observed before and after incorporating CNC or CNF into the AM matrix ($p > 0.05$) (Figure 2a). This consistency can be attributed to precise control over the dry mass content per unit area during the casting process [30].

Moisture content in the composite films was generally lower than in pure AM films, except for the lowest nanofiber concentrations (0.5% CNF and 1.0% CNC). This reduction can be attributed to the interaction between CNF/CNC and AM, leading to decreased water absorption (Figure 2b). No significant difference was observed between the CNC and CNF composite films ($p > 0.05$) (Figure 2b). In AM/CNF composite films, higher CNF concentrations led to slightly lower moisture content compared to CNC films, attributed to the entanglement and confinement behavior of CNF. This finding suggests that CNF exhibited stronger bonding compared to CNC due to its flexibility and length, which is reflected in the subsequent mechanical analysis results below.

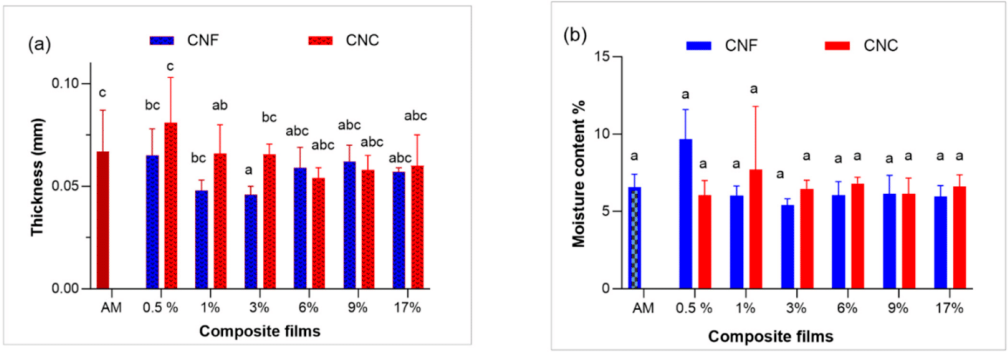

Figure 2. (**a**) Thickness and (**b**) moisture content of the AM, AM/CNF, and AM/CNC composite films. Different letters represent statistical differences ($p \leq 0.05$) n = 3.

3.3. Swelling Index (SI) and Water Solubility(SW)

AM demonstrated a lower swelling index compared to both CNF and CNC composites, which may limit its application in the food industry. However, the incorporation of CNC and CNF led to an increase in the swelling index (Figure 3a). This behavior can be attributed to the interaction of nanocellulose with water, resulting in the observed swelling index increment. Remarkably, CNF films displayed a progressive rise in the swelling index with increasing CNF concentration, highlighting its unique ability compared to CNC in restricting the free volume within the AM matrix, consequently impeding water diffusion into the film.

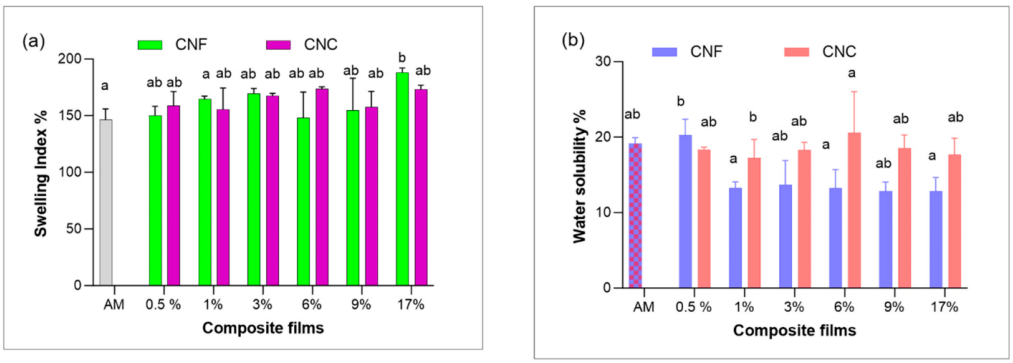

Figure 3. (**a**) SI of CNF and CNC composite films; (**b**) WS of the composite films. Different letters represent statistical differences ($p \leq 0.05$) n = 3.

As anticipated, owing to the lower water affinity of nanocellulose compared to AM, the water solubility of the films decreased upon the addition of CNC and CNF (Figure 3b). Remarkably, the CNF composite films displayed even lower values compared to CNC. This effect might be attributed to the agglomeration of CNC within the AM matrix.

3.4. Mechanical Properties

Mechanical assessments revealed that the incorporation of nanocellulose generally enhanced the strength and stiffness of the films (Figure 4a–c). Particularly, CNF had a pronounced influence on stress at break (TS) and Young's modulus (YM), leading to

significant enhancements (Figure 4b,c). Consequently, a noticeable disparity emerged between CNF- and CNC-containing films. The introduction of CNC moderately raised these properties. However, films containing 0.5% CNC or CNF, as well as 1% CNC, exhibited lower YM and TS values. The original TS of AM was 66 MPa, while in the presence of CNF, it increased to 128 MPa at a 3% CNF concentration and to 145 MPa with the addition of 1% CNF. The diminished YM and TS values at higher CNC concentrations are likely attributable to reduced crystal dispersion and agglomeration (Figure 4a) [31].

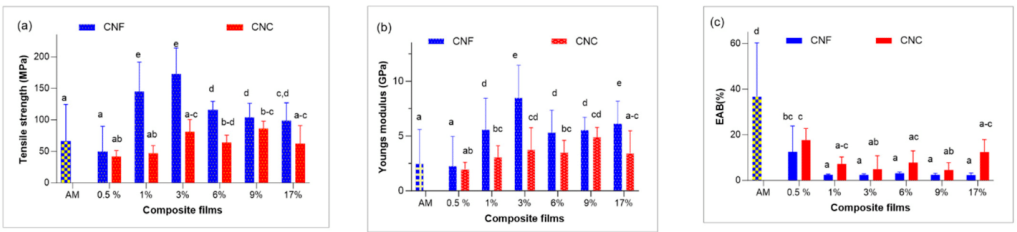

Figure 4. (**a**) TS; (**b**) YM of the films; and (**c**) EAB. Different letters represent statistical differences ($p \leq 0.05$), n = 8.

Including either CNC or CNF in the films reduced the elongation at break (EAB), especially for the CNF-containing films (Figure 4c). The significantly lower values observed for the elongation of the CNFs could be attributed to strong and stable bonds and interactions between the nanofibers and the AM matrix, as well as an effective stress transfer from the matrix to the fibers [25]. This effect is likely due to the inherent rigidity of nanofibers and the homogeneous dispersion of their crystalline and amorphous phases [32]. On the other hand, the lower values of TS and higher values of EAB in CNC films as compared to the CNF films suggest that CNCs form less dense structures, allowing for higher polymeric mobility under stress. In contrast, CNF films created highly compacted polymeric networks that resisted the applied stress.

3.5. SEM

SEM analysis of the film surfaces revealed distinctive effects of different concentrations of CNC and CNF on film topography and cross-sections (Figure 5). The AM film exhibited a uniformly smooth surface, free from cracks or voids. At very low concentrations of 0.5% CNC and 0.5% CNF, the surfaces appeared even smoother and continuous, indicating compatibility between CNF/CNC and AM (Figure 5b,c). This smoother topography can be attributed to the hydrogen bonding effect of plasticizing glycerol within the AM phase, which hinders aggregate formation. Similarly, CNC can promote the development of a homogeneous structure due to the chemical affinity between nanocellulose and AM, creating strong bonding between them [33]. However, some films exhibited topographic cracks. Films such as 1% CNC and 1% CNF displayed smaller and more frequent cracks on their surfaces, while 3% CNC showed larger fractures (Figure 5d,e). Despite occasional cracks and variations, all films presented relatively smooth surfaces devoid of pores, remaining robust, flexible, and maintaining commendable mechanical and barrier properties [34].

Among the films, AM exhibited the most rugged cross-section fracture, contrasting with the smoother fracture surfaces seen in the presence of CNC or CNF (Figure S2a–m). Irrespective of the percentage, the inclusion of CNC or CNF yielded smoother fracture surfaces. Notably, films containing 0.5% CNF and 1% CNF displayed the smoothest cross-section fractures (Figure S2b,c). However, higher concentrations, starting from 3% CNF, revealed less uniform fractures, suggesting reduced adhesion between nanocellulose structures and the AM matrix. Certain films, like 6% CNF and 3% CNC, showed coherent layers of crystals and fibers in their cross-section structures [19]. The cross-sections also exhibited micro cavities, potentially originating from the imprint of nanocrystal aggregates

left after the detachment of the AM matrix and the nanocellulose particles [35]. Furthermore, the SEM data align with the lower solubility observed in the CNC compared to the CNF composites (Figure 4b), attributed to CNC agglomeration within the AM matrix. To mitigate cracks and ensure homogeneity in composite films, optimization of nanocellulose particle dispersion is crucial; this can be achieved by combining homogenization techniques with the stirring process before suspension heating.

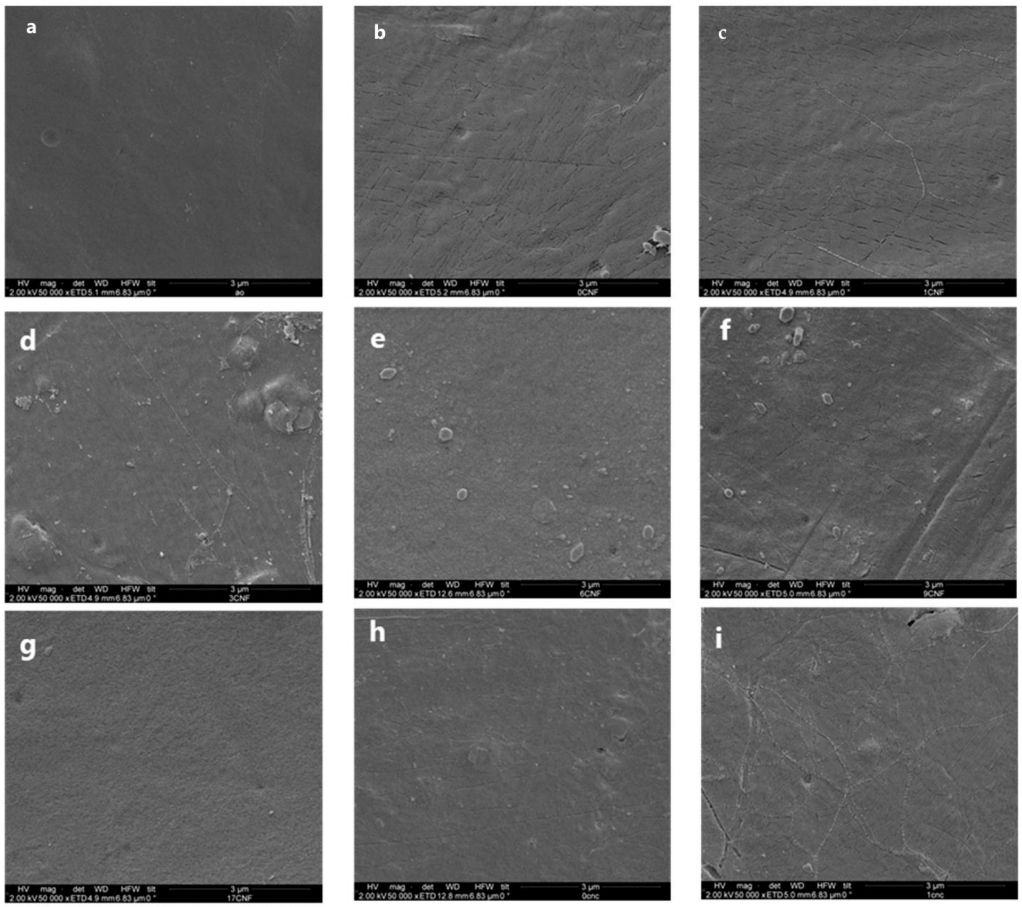

Figure 5. *Cont.*

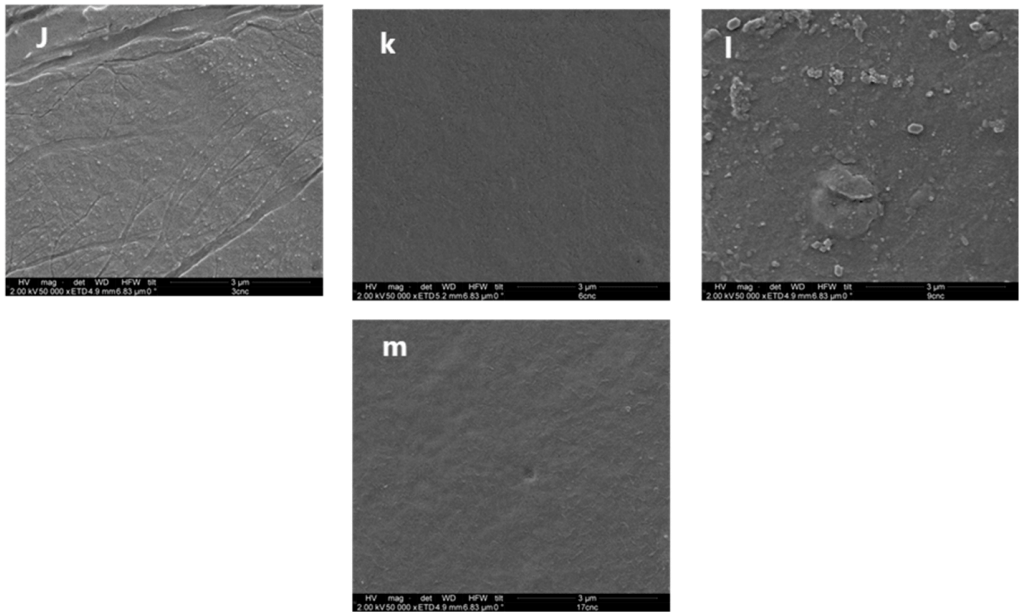

Figure 5. Micrographs of surface of (**a**) AM and composite films of (**b**) 0.5% CNF, (**c**) 1% CNF, (**d**) 3% CNF, (**e**) 6% CNF, (**f**) 9% CNF, (**g**) 17% CNF, (**h**) 0.5% CNC, (**i**) 1% CNC, (**j**) 3% CNC, (**k**) 6% CNC, (**l**) 9% CNC, (**m**) 17% CNC.

3.6. Light Transmittance and Opacity

The transparency of a film holds significance in assessing its compatibility with polymer blends. For various food packaging applications, achieving high visibility in the visible spectrum is essential for presenting the food product appealingly to consumers [36]. Hence, the opacities of the films were evaluated based on their visible spectra. Within the film set, the AM film displayed the lowest transparency (Table 1). However, upon incorporating CNF or CNC, the composite films exhibited increased transparency, thus enhancing the visual representation of the enclosed product for consumers [35]. In comparison to the AM film, all films demonstrated improved light transmittance, with the 9% CNC film achieving the highest transparency while the 9% CNF film exhibited the lowest. This phenomenon could be attributed to the strong interactions between nanocellulose fillers and the AM matrix, effectively restraining retrogradation and recrystallization of gelatinized AM during the air-drying process [37].

Table 1. The opacity and transmittance values of the films, n = 3.

Composition	Opacity	Transmittance
AM	6.4 ± 1.0^{d}	41 ± 15^{a}
0.5% CNC	2.7 ± 1^{abc}	60 ± 19^{ab}
1% CNC	2.3 ± 1^{a}	69 ± 7^{ab}
3% CNC	3 ± 0.0^{abc}	67 ± 8^{ab}
6% CNC	4 ± 0.0^{c}	70 ± 2^{ab}
9% CNC	3.1 ± 1.0^{abc}	79 ± 1^{b}
17% CNC	3 ± 0.0^{abc}	71 ± 3^{ab}
0.5% CNF	2.5 ± 1.0^{ab}	74 ± 1^{b}
1% CNF	3.8 ± 0.0^{bc}	71 ± 4^{ab}
3% CNF	3.8^{nd}	76 ± 12^{b}
6% CNF	3.4 ± 0.0^{abc}	66 ± 1^{ab}
9% CNF	3.2 ± 0.0^{abc}	66 ± 5^{ab}
17% CNF	3.7 ± 0.0^{abc}	68 ± 14^{ab}

Different letters represent statistical differences ($p \leq 0.05$).

3.7. Water Vapor (WV) and Gas Permeability

WV and gas permeability constitute crucial attributes in packaging materials. The WV characteristics of thermoplastic films are contingent upon film matrix crystallinity, compactness, hydrophilic groups, and thickness. Elevation of both CNC and CNF concentrations led to diminished barrier performance against water vapor transmission (WV) (Figure 6). Notably, the WV permeability of AM films was quantified at 8.7 ± 0.4 g mm m^{-2} 24 $h^{-1}kPa^{-1}$ [38].

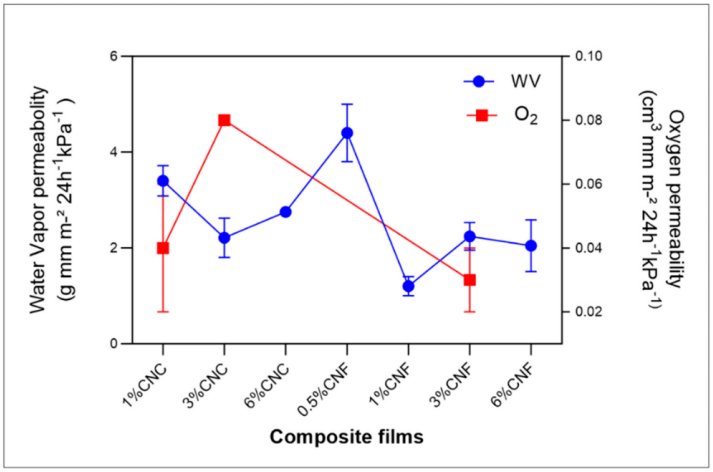

Figure 6. WV and O_2 permeability of composite films.

The augmented diffusion of WV can be attributed to hindered permeation stemming from intricate pathways formed within the films. Specifically, the inclusion of 1% CNF in AM film exhibited a more pronounced hindrance to water diffusion ($p < 0.05$) than 1% CNC, likely attributed to CNC aggregation in the AM matrix [39]. However, a trend was discernible—albeit statistically non-significant ($p > 0.05$)—indicating a propensity to reduce WV permeability upon exceeding this concentration (Table S1).

Concerning oxygen permeability, subtle distinctions emerged between bioplastic films containing CNC or CNF. Specifically, the 3% CNC films demonstrated elevated oxygen permeability, while the 3% CNF films exhibited enhanced gas barrier properties. These phenomena align with the compact network structure achieved through CNF, as corroborated by SEM analysis [19].

Importantly, the WV and oxygen (O_2) permeability values of all composite films outperformed the majority of petroleum-based materials [40]. Notably, the composite films' water vapor permeability exceeded that of LDPE, measuring 0.07 ± 0.01 (cm^3 mm m^{-2} 24 $h^{-1}kPa^{-1}$). Additionally, the barrier efficacy of the composite films yielded higher oxygen permeability compared to LDPE, registering at 3.79 ± 0.80 (cm^3 mm m^{-2} 24 h^{-1} kPa^{-1}) [41].

3.8. Wide Angle X-ray Scattering (WAXS)

X-ray diffraction analysis revealed well-defined crystalline structures within the biocomposite films. Differences in intensities were apparent between the CNF and CNC films, arising from the repeated β-(1 → 4)-D-glucopyranose units constituting parallel glucan chains [42].

The AM film featured a V-type polymorph, primarily characterized by single helices around 17°, 19.8°, 23°, and 25°—hallmarks of high AM starch (Figure 7a,b) [19]. CNF exhibited discernible diffraction peaks at 2θ values of 16.2° and 22.3°, indicative of a type-I cellulosic crystalline structure (Figure 7a) [19].

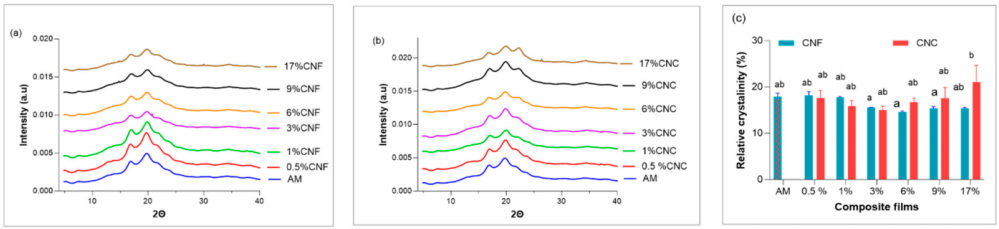

Figure 7. (**a**) WAXS of AM/CNF composite films; (**b**) WAXS of AM/CNC composite films; (**c**) relative crystallinity of all the films. Different letters represent statistical differences ($p \leq 0.05$), n = 2.

Of interest, the characteristic XRD peaks associated with CNC and CNF vanished in the nanocomposite films. This outcome signifies the successful integration of CNF and CNC into the AM matrix, except for the 17% CNC film, where the peak at 2θ = 22° grew in intensity due to its higher film content (Figure 7b). Notably, no new peaks or shifts in diffraction angles surfaced (Figure 7a,b). The relative crystallinity of the composite films remained largely unchanged ($p > 0.05$) upon filler addition, with the exception of the 17% CNC film (Figure 7c). Analogous behavior was documented in plasticized starch films reinforced with CNF, suggesting that favorable interfacial crystallization arises when the starch matrix is plasticized with glycerol and due to effective filler dispersion in the matrix [31].

Consequently, it is apparent that the diffractograms of the films encompassed a coexistence of the two film components (AM/CNF) and (AM/CNC). The addition of CNF or CNC did not precipitate any alteration in the crystal structure of AM.

3.9. Thermogravimetric Analysis (TGA)

The thermal degradation of the films was assessed using TGA (Table 2). Figure 8a,b show TG and derivative thermogravimetric (DTG) curves for both AM and the composite films. The degradation profiles of AM, both with and without fillers, unveiled a three-stage degradation process. The first stage, within the 40–120 °C range, was attributed to water loss. The second stage, spanning 135–190 °C, marked the decomposition of the glycerol-rich phase. The third degradation stage, taking place between 290 and 350 °C, led to the formation of carbon black (Figure 8a,b).

Table 2. The initial temperature at which the degradation starts (T_i), derivative thermogravimetric at T_{max} (DTG), and the % of mass residue at the DTG peak, n = 2.

Composition	T_i (°C)	DTG at T_{max}(°C)	Mass Residue (%)
AM	38 ± 7^{ab}	305 ± 2^{abc}	43 ± 1^{ab}
0.5% CNC	47 ± 6^{b}	307 ± 0^{bc}	60^{nd}
1% CNC	28 ± 2^{a}	301 ± 0^{ab}	38 ± 4^{a}
3% CNC	44 ± 2^{b}	299 ± 0^{abc}	46 ± 1^{ab}
6% CNC	50 ± 2^{b}	302 ± 1^{a}	45 ± 3^{ab}
9% CNC	47 ± 0^{b}	299 ± 2^{abc}	46 ± 1^{ab}
17% CNC	47 ± 4^{b}	301 ± 1^{a}	52 ± 1^{a}
0.5% CNF	35^{ND}	307^{ND}	53^{ND}
1% CNF	47 ± 3^{b}	301 ± 0^{abc}	37 ± 11^{a}
3%CNF	45 ± 3^{b}	305 ± 3^{abc}	57 ± 2^{b}
6%CNF	49 ± 0^{b}	303 ± 1^{abc}	50 ± 1^{ab}
9% CNF	37 ± 4^{ab}	308 ± 0.1^{c}	45 ± 6^{ab}
17% CNF	48 ± 4^{b}	308 ± 4^{c}	51^{ab}

Different letters represent statistical differences ($p \leq 0.05$). ND: not determined.

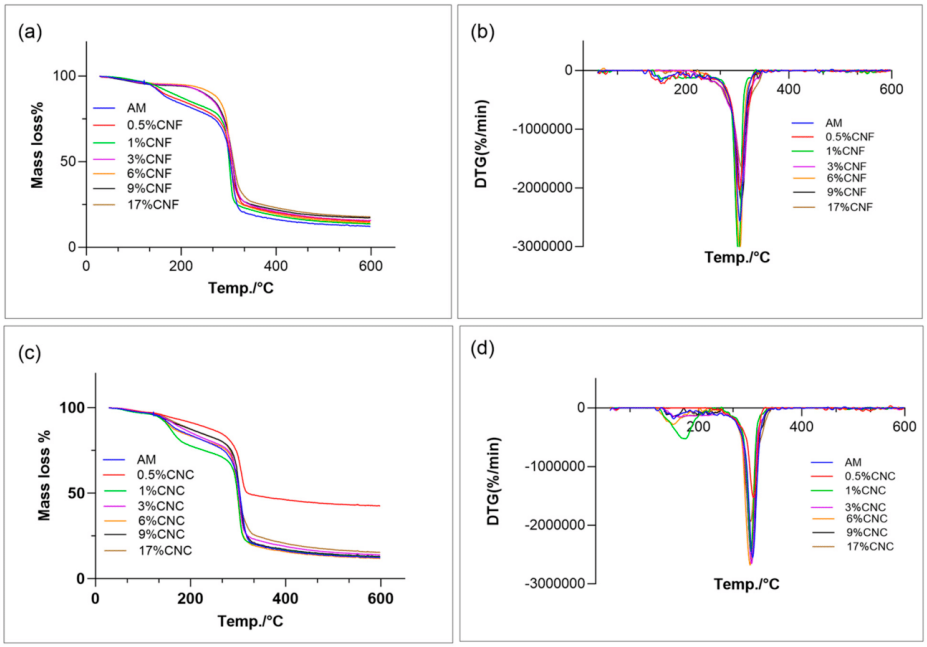

Figure 8. TG and DTG curves of AM and AM nanocomposite films, (**a**,**b**) AM/CNF composite films, (**c**,**d**) AM/CNC composite films.

For the CNF-filled nanocomposite films, degradation commenced at higher temperatures compared to the AM film, particularly at higher ratios of 9% and 17% CNF (Figure 8a). Conversely, the CNC-filled nanocomposite films exhibited reduced degradation as CNC content increased, likely due to agglomeration at higher concentrations (Figure 8b). These findings suggest that CNF possesses higher thermal stability than CNC. This insight is supported by XRD and SEM results, as CNF exhibited larger size and lower crystallinity. Therefore, the heightened thermal stability of AM/CNF can likely be attributed to CNF's larger size and network structure.

Notably, similar observations were reported in previous studies involving pumpkin starch composite films reinforced with CNF, showing increased thermal stability compared to CNC-reinforced films [43].

3.10. Compost Biodegradation

In the soil burial test, three films of each sample underwent degradation over a 56-day period [44,45]. Notably, in the case of pure films, the AM-only film exhibited the most pronounced changes post-degradation, in contrast to CNF and CNC films (Figure S3). This suggests that biodegradation had initiated, with α-, β-, and γ-amylases hydrolyzing the α-(1 → 4)-glycosidic bonds of AM. At higher nanocellulose concentrations, fewer changes were observed, particularly in the 17% CNF film, suggesting that the 56-day degradation duration might not be sufficient for cellulases to degrade the cellulose structure.

Throughout flask incubation, the anticipated CO_2 evolution occurred (Figure 9a). After 56 days, CNC exhibited the highest CO_2 accumulation, reaching 1.4 mg. Initial CO_2 production was minimal and nearly negligible [19]. Following a 16-day lag phase, CO_2 evolution began increasing for all films, marking the commencement of assimilation and mineralization and entering the biodegradation phase. The steepest segments on the

graphs indicated the most active phase of mineralization. All films displayed ongoing accumulation after 56 days of degradation, except for AM-only, which plateaued. The AM-only film reached the plateau, signifying the conclusion of assimilation and mineralization during biodegradation. The gases CH_4 and N_2O were only present in trace amounts, indicating the conducive, oxygen-rich conditions within the blue cap flasks remained optimal for degradation.

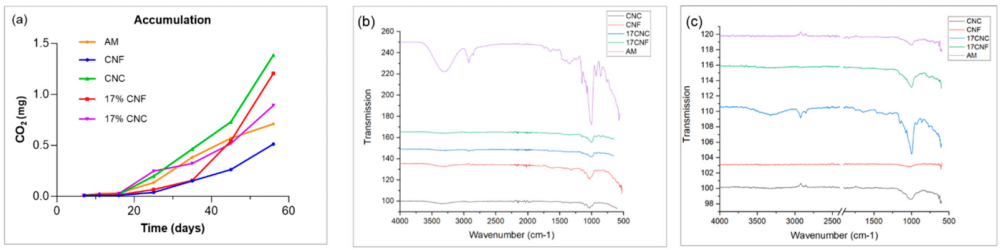

Figure 9. (**a**) CO_2 accumulation during the degradation process of the films; (**b**)FTIR spectra of the films before degradation; (**c**) FTIR spectra of the films after the degradation.

Samples were subjected to FTIR analysis before and after degradation to ascertain shifts in spectral intensities of the films' functional groups (Figure 9b,c). Pre-degradation, all pure films (AM, CNF, and CNC), as well as AM composite films with 17% CNF and 17% CNC, exhibited prominent characteristic peaks at 3330 cm^{-1} (O–H stretching), 2902 cm^{-1} (C–H stretching), 1650 cm^{-1} (C–O stretching), and 1316 cm^{-1} (–CH_2 bending). Additionally, absorption bands at 1159 cm^{-1} (anti-symmetric stretching of the C–O–C bridge) and 1028 cm^{-1} (skeletal vibrations involving C–O stretching) indicated a saccharide structure. Notably, no discernible differences were observed before and after the addition of CNF or CNC (Figure 9b).

Post-degradation, significant variations in absorption intensities were evident across all films. Notably, two characteristic bands within the 3650–3150 cm^{-1} range and at 2900 cm^{-1}, corresponding to the O-H bond and C-H stretching in α-glucans and β-glucans, were absent in the degraded samples. An exception was the 17% CNC composite film, where they were reduced (Figure 9c) [19]. These findings suggest rapid degradation of CNF and CNC films within this timeframe, while the 17% CNC film exhibited slower degradation.

3.11. Principal Component Analysis

To illustrate the impact of CNF and CNC on the properties of the AM matrix, a Principal Component Analysis (PCA) was conducted (Figure 10). The primary component, PC1, accounted for 47.91% of the total variance and reflected the influence of CNF and CNC on the AM film. Notably, AM appeared as a distinct outlier among the samples due to its distinct characteristics, particularly high elasticity (EOB). PC1 effectively differentiated the data points corresponding to CNF and CNC. Young's modulus (YM), tensile strength (TS), and opacity clustered closely with 1%, 3%, 6%, and 9% CNF samples. Transmittance and swelling index (SI) exhibited proximity with 17% CNF and 9% CNC. On the other hand, relative crystallinity, moisture content (MC), water solubility (WS), elongation at break (EB), and thickness were more characteristic of most CNC films and the 0.5% CNF film, specifically in terms of crystallinity and MC. This analysis serves to synthesize the previously elaborated findings, emphasizing the efficacy of CNF and CNC as reinforcing agents within the AM matrix.

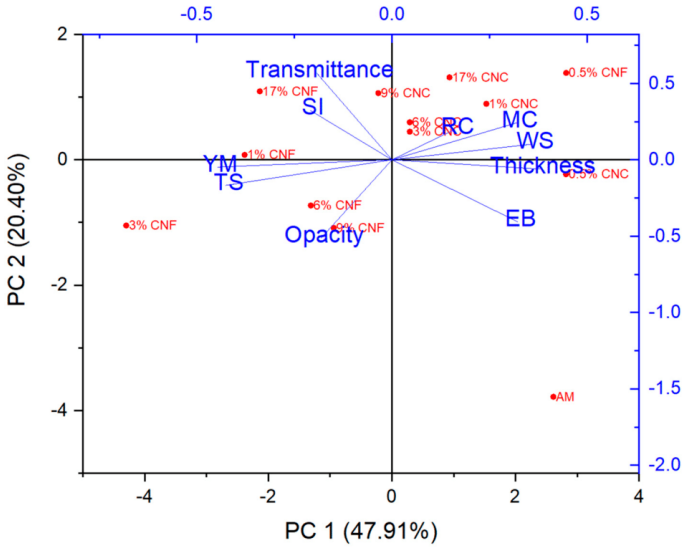

Figure 10. (PCA) reveals the main variations within the composite systems by considering all the available data. The vectors indicate the direction and strength of loadings for the characterization variables.

4. Conclusions

The addition of NC fillers to the AM matrix in casted film systems had a substantial impact on all the measured properties, revealing discernible differences between CNC and CNF. AM-CNF composites notably exhibited significantly elevated tensile strength (TS) and Young's modulus (YM), with the 3% CNF composite displaying the highest values, followed by 1% and 6% CNF. This underscores the remarkable potential of even a small NC proportion to greatly enhance a film's tensile strength. Conversely, the CNC composites demonstrated relatively lower TS and higher elongation at break (EB), implying the formation of less dense structures that allow for greater polymer mobility under stress. Overall, CNF exerted a more pronounced influence compared to CNC. Consequently, these films possess the versatility for diverse food applications owing to their distinct advantages, offering sustainable alternatives to petroleum-based packaging. Their potential benefits encompass improved shelf life, augmented barrier properties, and reduced environmental impact. However, further research is imperative to optimize protocols for commercial utilization, with emphasis on mechanical properties, biodegradability, and the scalability of production methods.

Supplementary Materials: The following supporting information can be downloaded at: https://www.mdpi.com/article/10.3390/coatings13091573/s1. Figure S1: SEM images of cellulose nanofibers produced from sugar beet using chemical treatment (CNF). The arrows highlight one thin and one thick nanofiber in each sample. The magnification of nanofibers is 100,000× and the scale bar represents 1 µm; Figure S2: Micrographs of cross section of (a) AM, and and composite films of (b) 0.5% CNF, (c) 1% CNF, (d) 3% CNF, (e) 6% CNF, (f) 9% CNF, (g) 17% CNF, (h) 0.5% CNC, (i) 1% CNC, (j) 3% CNC, (k) 6% CNC, (l) 9% CNC, (m) 17% CNC; Table S1. Water vapor (WV) and O2 permeability; Figure S3: Biodegradation images of pure films of AM, CNF, CNC and composite films 17% CNF and 17% CNC before and after 5 days.

Author Contributions: Conceptualization, M.F. (Marwa Faisaland), M.Ž., P.U., B.J. and A.B; methodology, M.F. (Marwa Faisaland), L.M., S.B., M.F. (Marwa Faisaland), H.N.B., K.H.H. and J.J.K.K.; software, M.F. (Marwa Faisaland) and M.Ž.; validation, M.F. (Marwa Faisaland), M.Ž., P.U. and A.B.; formal analysis, M.F. (Marwa Faisaland), M.Ž., P.U. and A.B.; investigation, M.F. (Marwa Faisaland), M.Ž., N.Q.N.K., M.F. (Michela Famiglietti), and J.J.K.K.; resources, A.B. and P.U.; data curation, M.F. (Marwa Faisaland), A.B. and L.M.; writing—original draft preparation, M.F. (Marwa Faisaland), M.Ž. and L.M.; writing—review and editing, A.B., M.F. (Marwa Faisaland), M.Ž., L.M., H.N.B., B.J., P.U. and K.H.H.; visualization, M.F. (Marwa Faisaland), M.Ž., N.Q.N.K. and J.J.K.K.; supervision, A.B., L.M. and P.U.; project administration, A.B.; funding acquisition, A.B., P.U., H.N.B. and J.J.K.K. All authors have read and agreed to the published version of the manuscript.

Funding: This study was mainly supported by the Danish Council for Independent Research (grant number 8022-00095B) and the Innomission 4 Program of Innovation Fund Denmark. The thermoanalysis instrument was financed by Carlsberg Fondet (grants 2013_01_0589, CF14-0230, and CF20-0130). XRD data were generated via a research infrastructure at the University of Copenhagen, partly funded by FOODHAY (Food and Health Open Innovation Laboratory, Danish Roadmap for Research Infrastructure). Plant Carb ApS is acknowledged for providing amylose to the project.

Institutional Review Board Statement: Not applicable.

Informed Consent Statement: Not applicable.

Data Availability Statement: Not applicable.

Conflicts of Interest: The authors declare no conflict of interest. The funders had no role in the design of the study, in the collection, analyses, or interpretation of data, in the writing of the manuscript, or in the decision to publish the results.

References

1. Mousa, M.H.; Dong, Y.; Davies, I.J. Recent advances in bionanocomposites Preparation, Properties, and Applications. *Int. J. Polym. Mater. Polym. Biomater.* **2016**, *65*, 225–254. [CrossRef]
2. Karki, S.; Gohain, M.B.; Yadav, D.; Ingole, P.G. Nanocomposite and Bio-Nanocomposite Polymeric Materials/Membranes Development in Energy and Medical Sector: A Review. *Int. J. Biol. Macromol.* **2021**, *193*, 2121–2139. [CrossRef] [PubMed]
3. Noreen, A.; Sultana, S.; Sultana, T.; Tabasum, S.; Zia, K.M.; Muzammil, Z.; Sultana, S. Chapter 3-Natural polymers as constituents of bionanocomposites. In *Bionanocomposites*; Elsevier: Amsterdam, The Netherlands, 2020; pp. 55–85.
4. Sagnelli, D.; Hebelstrup, K.H.; Leroy, E.; Rolland-Sabaté, A.; Guilois, S.; Kirkensgaard, J.J.K.; Mortensen, K.; Lourdin, D.; Blennow, A. Plant-Crafted Starches for Bioplastics Production. *Carbohydr. Polym.* **2016**, *152*, 398–408. [CrossRef]
5. Tetlow, I.J.; Bertoft, E. A Review of Starch Biosynthesis in Relation to the Building Block-Backbone Model. *Int. J. Mol. Sci.* **2020**, *21*, 7011. [CrossRef] [PubMed]
6. Abe, M.M.; Martins, J.R.; Sanvezzo, P.B.; Macedo, J.V.; Branciforti, M.C.; Halley, P.; Botaro, V.R.; Brienzo, M. Advantages and Disadvantages of Bioplastics Production from Starch and Lignocellulosic Components. *Polymers* **2021**, *13*, 2484. [CrossRef]
7. Carciofi, M.; Blennow, A.; Nielsen, M.M.; Holm, P.B.; Hebelstrup, K.H. Barley Callus: A Model System for Bioengineering of Starch in Cereals. *Plant Methods* **2012**, *8*, 36. [CrossRef]
8. Frost, B.A.; Johan Foster, E. Isolation of Thermally Stable Cellulose Nanocrystals from Spent Coffee Grounds via Phosphoric Acid Hydrolysis. *J. Renew. Mater.* **2020**, *8*, 187–203. [CrossRef]
9. Rinaldi, R.; Schüth, F. Acid Hydrolysis of Cellulose as the Entry Point into Biorefinery Schemes. *ChemSusChem* **2009**, *2*, 1096–1107. [CrossRef]
10. Funahashi, R.; Ono, Y.; Tanaka, R.; Yokoi, M.; Daido, K.; Inamochi, T.; Saito, T.; Horikawa, Y.; Isogai, A. Changes in the Degree of Polymerization of Wood Celluloses during Dilute Acid Hydrolysis and TEMPO-Mediated Oxidation: Formation Mechanism of Disordered Regions along Each Cellulose Microfibril. *Int. J. Biol. Macromol.* **2018**, *109*, 914–920. [CrossRef]
11. Kontturi, E.; Meriluoto, A.; Penttilä, P.A.; Baccile, N.; Malho, J.M.; Potthast, A.; Rosenau, T.; Ruokolainen, J.; Serimaa, R.; Laine, J.; et al. Degradation and Crystallization of Cellulose in Hydrogen Chloride Vapor for High-Yield Isolation of Cellulose Nanocrystals. *Angew. Chemie-Int. Ed.* **2016**, *55*, 14455–14458. [CrossRef]
12. Spiliopoulos, P.; Spirk, S.; PPaakkonen, T.; Viljanen, M.; Svedstrom, K.; Pitkanen, L.; Awais, M.; Kontturi, E. Visualizing Degradation of Cellulose Nanofibers by Acid Hydrolysis. *Biomacromolecules* **2021**, *22*, 1399–1405. [CrossRef] [PubMed]
13. Isogai, A.; Saito, T.; Fukuzumi, H. TEMPO-Oxidized Cellulose Nanofibers. *Nanoscale* **2011**, *3*, 71–85. [CrossRef]
14. Peyre, J.; Pääkkönen, T.; Reza, M.; Kontturi, E. Simultaneous Preparation of Cellulose Nanocrystals and Micron-Sized Porous Colloidal Particles of Cellulose by TEMPO-Mediated Oxidation. *Green Chem.* **2015**, *17*, 808–811. [CrossRef]
15. Han, X.; Wang, J.; Wang, X.; Tian, W.; Dong, Y.; Jiang, S. Finite Element Analysis of Strengthening Mechanism of Ultrastrong and Tough Cellulosic Materials. *Polymers* **2022**, *14*, 4490. [CrossRef]

16. Han, X.; Wang, J.; Wang, J.; Ding, L.; Zhang, K.; Han, J.; Jiang, S. Micro- and Nano-Fibrils of Manau Rattan and Solvent-Exchange-Induced High-Haze Transparent Holocellulose Nanofibril Film. *Carbohydr. Polym.* **2022**, *298*, 120075. [CrossRef] [PubMed]
17. Babaee, M.; Jonoobi, M.; Hamzeh, Y.; Ashori, A. Biodegradability and Mechanical Properties of Reinforced Starch Nanocomposites Using Cellulose Nanofibers. *Carbohydr. Polym.* **2015**, *132*, 1–8. [CrossRef] [PubMed]
18. Otoni, C.G.; Avena-Bustillos, R.J.; Azeredo, H.M.C.; Lorevice, M.V.; Moura, M.R.; Mattoso, L.H.C.; McHugh, T.H. Recent Advances on Edible Films Based on Fruits and Vegetables—A Review. *Compr. Rev. Food Sci. Food Saf.* **2017**, *16*, 1151–1169. [CrossRef]
19. Xu, J.; Sagnelli, D.; Faisal, M.; Perzon, A.; Taresco, V.; Mais, M.; Giosafatto, C.V.L.; Hebelstrup, K.H.; Ulvskov, P.; Jørgensen, B.; et al. Amylose/Cellulose Nanofiber Composites for All-Natural, Fully Biodegradable and Flexible Bioplastics. *Carbohydr. Polym.* **2021**, *253*, 117277. [CrossRef]
20. Perzon, A.; Jørgensen, B.; Ulvskov, P. Sustainable Production of Cellulose Nanofiber Gels and Paper from Sugar Beet Waste Using Enzymatic Pre-Treatment. *Carbohydr. Polym.* **2020**, *230*, 115581. [CrossRef]
21. Matsunaga, K.; Kawasaki, S.; Takeda, Y. Influence of Physicochemical Properties of Starch on Crispness of Tempura Fried Batter. *Cereal Chem.* **2003**, *80*, 339–345. [CrossRef]
22. Holland, C.; Perzon, A.; Cassland, P.R.C.; Jensen, J.P.; Langebeck, B.; Sørensen, O.B.; Whale, E.; Hepworth, D.; Plaice-Inglis, R.; Moestrup, Ø.; et al. Nanofibers Produced from Agro-Industrial Plant Waste Using Entirely Enzymatic Pretreatments. *Biomacromolecules* **2019**, *20*, 443–453. [CrossRef] [PubMed]
23. Teixeira, C.E.F.; de Almeida Rebechi, I.; Fontaneli, R.S. Digital Micrometer Used in Thickness Measurement of Plastic Film Compared to Standardized Instrument. *Mater. Sci. Appl.* **2017**, *8*, 577–583. [CrossRef]
24. Faisal, M.; Bevilacqua, M.; Bro, R.; Bordallo, H.N.; Judas, J.; Kirkensgaard, K.; Hebelstrup, K.H.; Blennow, A. International Journal of Biological Macromolecules Colorimetric PH Indicators Based on Well-Defined Amylose and Amylopectin Matrices Enriched with Anthocyanins from Red Cabbage. *Int. J. Biol. Macromol.* **2023**, *250*, 126250. [CrossRef] [PubMed]
25. Taherkhani, E.; Moradi, M.; Tajik, H.; Molaei, R.; Ezati, P. Preparation of On-Package Halochromic Freshness/Spoilage Nanocellulose Label for the Visual Shelf Life Estimation of Meat. *Int. J. Biol. Macromol.* **2020**, *164*, 2632–2640. [CrossRef] [PubMed]
26. *ASTM D 882-02*; Standard Test Method for Tensile Properties of Thin Plastic Sheeting. ASTM International: West Conshohocken, PA, USA, 2002.
27. Qin, Y.; Liu, Y.; Yong, H.; Liu, J.; Zhang, X.; Liu, J. Preparation and Characterization of Active and Intelligent Packaging Films Based on Cassava Starch and Anthocyanins from Lycium Ruthenicum Murr. *Int. J. Biol. Macromol.* **2019**, *134*, 80–90. [CrossRef]
28. Harrison, J.P.; Boardman, C.; O'Callaghan, K.; Delort, A.M.; Song, J. Biodegradability Standards for Carrier Bags and Plastic Films in Aquatic Environments: A Critical Review. *R. Soc. Open Sci.* **2018**, *5*, 171792. [CrossRef]
29. Razzaq, W.; Javaid, A. Synthesis & Characterization of Cotton Fiber Reinforced Starch/PVA Biodegradable Composite Films. *J. Fac. Eng. Technol.* **2015**, *22*, 27–35.
30. de Almeida, V.S.; Barretti, B.R.V.; Ito, V.C.; Malucelli, L.; da Silva Carvalho Filho, M.A.; Demiate, I.M.; Pinheiro, L.A.; Lacerda, L.G. Thermal, Morphological, and Mechanical Properties of Regular and Waxy Maize Starch Films Reinforced with Cellulose Nanofibers (CNF). *Mater. Res.* **2020**, *23*. [CrossRef]
31. Nasri-Nasrabadi, B.; Behzad, T.; Bagheri, R. Preparation and Characterization of Cellulose Nanofiber Reinforced Thermoplastic Starch Composites. *Fibers Polym.* **2014**, *15*, 347–354. [CrossRef]
32. Meneguin, A.B.; Ferreira Cury, B.S.; dos Santos, A.M.; Franco, D.F.; Barud, H.S.; da Silva Filho, E.C. Resistant Starch/Pectin Free-Standing Films Reinforced with Nanocellulose Intended for Colonic Methotrexate Release. *Carbohydr. Polym.* **2017**, *157*, 1013–1023. [CrossRef]
33. Bangar, S.P.; Whiteside, W.S. Nano-Cellulose Reinforced Starch Bio Composite Films—A Review on Green Composites. *Int. J. Biol. Macromol.* **2021**, *185*, 849–860. [CrossRef] [PubMed]
34. Fonseca, L.M.; Henkes, A.K.; Bruni, G.P.; Viana, L.A.N.; de Moura, C.M.; Flores, W.H.; Galio, A.F. Fabrication and Characterization of Native and Oxidized Potato Starch Biodegradable Films. *Food Biophys.* **2018**, *13*, 163–174. [CrossRef]
35. Csiszár, E.; Kun, D.; Fekete, E. The Role of Structure and Interactions in Thermoplastic Starch–Nanocellulose Composites. *Polymers* **2021**, *13*, 3186. [CrossRef] [PubMed]
36. Oleyaei, S.A.; Almasi, H.; Ghanbarzadeh, B.; Moayedi, A.A. Synergistic Reinforcing Effect of TiO_2 and Montmorillonite on Potato Starch Nanocomposite Films: Thermal, Mechanical and Barrier Properties. *Carbohydr. Polym.* **2016**, *152*, 253–262. [CrossRef] [PubMed]
37. Cheng, G.; Zhou, M.; Wei, Y.J.; Cheng, F.; Zhu, P.X. Comparison of Mechanical Reinforcement Effects of Cellulose Nanocrystal, Cellulose Nanofiber, and Microfibrillated Cellulose in Starch Composites. *Polym. Compos.* **2019**, *40*, E365–E372. [CrossRef]
38. Famiglietti, M.; Zannini, D.; Turco, R.; Mariniello, L. Mechanical, Barrier and Thermal Properties of Amylose-Argan Proteins-Based Bioplastics in the Presence of Transglutaminase. *Int. J. Mol. Sci.* **2023**, *24*, 3405. [CrossRef]
39. Arifin, H.R.; Djali, M.; Nurhadi, B.; Hasim, S.A.; Hilmi, A.; Puspitasari, A.V. Improved Properties of Corn Starch-Based Bio-Nanocomposite Film with Different Types of Plasticizers Reinforced by Nanocrystalline Cellulose. *Int. J. Food Prop.* **2022**, *25*, 509–521. [CrossRef]
40. Ferrer, A.; Pal, L.; Hubbe, M. Nanocellulose in Packaging: Advances in Barrier Layer Technologies. *Ind. Crops Prod.* **2017**, *95*, 574–582. [CrossRef]

41. Mirpoor, S.F.; Giosafatto, C.V.L.; Mariniello, L.; D'Agostino, A.; D'Agostino, M.; Cammarota, M.; Schiraldi, C.; Porta, R. Argan (*Argania spinosa* L.) Seed Oil Cake as a Potential Source of Protein-Based Film Matrix for Pharmaco-Cosmetic Applications. *Int. J. Mol. Sci.* **2022**, *23*, 8478. [CrossRef]
42. Klemm, D.; Cranston, E.D.; Fischer, D.; Gama, M.; Kedzior, S.A.; Kralisch, D.; Kramer, F.; Kondo, T.; Lindström, T.; Nietzsche, S.; et al. Nanocellulose as a Natural Source for Groundbreaking Applications in Materials Science: Today's State. *Mater. Today* **2018**, *21*, 720–748. [CrossRef]
43. Zhang, L.; Zhao, J.; Zhang, Y.; Li, F.; Jiao, X.; Li, Q. The Effects of Cellulose Nanocrystal and Cellulose Nanofiber on the Properties of Pumpkin Starch-Based Composite Films. *Int. J. Biol. Macromol.* **2021**, *192*, 444–451. [CrossRef] [PubMed]
44. Tan, Z.; Yi, Y.; Wang, H.; Zhou, W.; Yang, Y.; Wang, C. Physical and Degradable Properties of Mulching Films Prepared from Natural Fibers and Biodegradable Polymers. *Appl. Sci.* **2016**, *6*, 147. [CrossRef]
45. Kijchavengkul, T.; Auras, R.; Rubino, M.; Ngouajio, M.; Fernandez, R.T. Assessment of Aliphatic-Aromatic Copolyester Biodegradable Mulch Films. Part I: Field Study. *Chemosphere* **2008**, *71*, 942–953. [CrossRef] [PubMed]

Disclaimer/Publisher's Note: The statements, opinions and data contained in all publications are solely those of the individual author(s) and contributor(s) and not of MDPI and/or the editor(s). MDPI and/or the editor(s) disclaim responsibility for any injury to people or property resulting from any ideas, methods, instructions or products referred to in the content.

7.2 COMMUNICATIONS

- **61° SIB 2021 Congress**
  Virtual Edition, 23-24 September 2021

CHITOSAN-BASED EDIBLE FILMS CONTAINING DRIED OLIVE LEAF EXTRACT

Michela Famiglietti, Alessandro Savastano, Daniele Naviglio, and Loredana Mariniello

Department of Chemical Sciences, University of Naples "Federico II"

e-mail: michela.famiglietti@unina.it

Chitosan derives chemically from chitin and it is the second most abundant polymer on the earth obtained from renewable sources[1]. Because of its biodegradability, biocompatibility, good film forming capacity and again because of its antibacterial and antifungal activity, it is a very interesting polymer for applications in pharmaceutical and food industry as well as in biomaterials production. Chitosan is a weak base insoluble in water and organic solvents but the presence of amino groups makes it soluble under acidic conditions. It was reported that chitosan is effectively soluble in several organic and inorganic acids such as acetic, lactic, hydrochloric[2].

Here we investigate, the solubility of chitosan in citric acid in order to use this polymer as matrix for delivering antioxidant compounds present in dried olive leaf extracts. It is known that olive tree cultivation and olive processing industry produce every year a huge amount of byproducts and wastes. It was estimated that annually worldwide the amount of olive leave accumulated may reach 1 million tonnes. The olive leaf byproducts are made up by leave and branches obtained from olive tree pruning and from olive harvesting. The amount of this waste is about 10% of weight of harvested olives and it is generally used as animal feed or simply burned[3]. Recently, many studies focused on the valorisation of this unexpensive raw material because of its high potential in different applicative fields. In this study we propose a way to recover this waste and use it to produce a high-added value product destinated to nutraceutical industry.

Phenolic compounds, present in olives leave, are already studied for their several beneficial effects on human health. In fact, it was confirmed in different researchers the high antioxidant activity of these polyphenols and their effects as antihypertensive, cholesterol-lowering, cardio-protective, anti-inflammatory, antibacterial molecules and as coadjutant in the obesity treatment[4]. Considering all these positive functions our objective was investigating the polyphenols content of Dried Olive Leaf Extract (DOLE), obtained by Naviglio extractor[5] and the antioxidant activity of this extract entrapped in chitosan-based edible films. Naviglio extractor is an innovative technology that allows to extract quickly, from a solid material, extractable compounds, in organic and inorganic solvents[5].

By means of the Folin-Ciocâlteu method, we studied the amount of polyphenolic compounds in DOLE at different time of extraction in order to establish the best ratio time/yield for this kind of raw material. After that, an evaluation of chitosan solubility in citric acid was carried out and a solution of 3 % w/v of citric acid was chosen to prepare the film forming solutions. Edible films were prepared with different volumes of DOLE using glycerol as plasticizer. The stability of film-forming solutions with different volumes of DOLE was evaluated determining Zeta potential. Finally, the antioxidant activity of these films was investigated by DPPH assay, during one month, taking in account the conditions of storage of dried films. Thus, our results are promising for the development of thin edible films conveying DOLE to enrich the diet of consumers.

[1]. Shukla, S. K., Mishra, A. K., Arotiba, O. A. & Mamba, B. B. Chitosan-based nanomaterials: A state-of-the-art review. *Int. J. Biol. Macromol.* **59**, 46–58 (2013).

[2]. Melro E., Antunes F. E., da Silva G. J., Cruz Ines, Ramos P. E., Carvalho F., A. L. Changing Acidic Dissolution Conditions. 1–12 (2021).

[3]. Özcan, M. M. & Matthäus, B. A review: benefit and bioactive properties of olive (Olea europaea L.) leaves. *Eur. Food Res. Technol.* **243**, 89–99 (2017).

[4]. Sabry, O. M. M. Review : Beneficial Health Effects of Olive Leaves Extracts. *J. Nat. Sci. Res.* **4**, 1–9 (2014).

[5]. Naviglio D. Naviglio's Principle and Presentation of an Innovative Solid-Liquid Extraction Technology: Extractor Naviglio. *Anal. Lett.* **36**, 1647–1659 (2003).

- **7th CUCS Conference | Naples, 21st - 23rd April 2022**
  UNIVERSITY COOPERATION IN THE NEW CHALLENGES FOR SUSTAINABLE DEVELOPMENT

VII Congresso CUCS
LA COOPERAZIONE UNIVERSITARIA NELLE NUOVE SFIDE
PER LO SVILUPPO SOSTENIBILE
Capacity-building, Science Diplomacy e Open Science nei rapporti tra Nord e Sud del mondo nel nuovo contesto globale
Napoli, 21-23 aprile 2022

ARGAN SEEDS PROTEINS VALORISATION TO OBTAIN AMYLOSE-CONTAINING BLENDED BIOPLASTICS

Michela Famiglietti and Loredana Mariniello

Department of Chemical Sciences, University of Naples Federico II, Via Cinthia 80126, Naples, Italy

Argan, *Argania spinosa*, is a plant typically widespread in arid and semiarid regions of Northern Africa useful for protecting soil from desertification and erosion. Until now, argan was mainly used to obtain a biologically active oil extracted from its seeds producing oilcake, a by-product rich in proteins, generally used as animal feed. Recently argan oilcakes have been attracting attention as a waste to be recovered to obtain high-add value products for different applications. This work aimed to investigate the possibility to produce novel bioplastics, made up of argan proteins extracted from oilcakes and amylose obtained from barley by RNA interference technique. Amylose is an optimal raw material for bioplastic purposes because of its linear molecular structure and it was already demonstrated that it is provided with better performances compared to starch. Moreover, we studied the effect of the enzyme transglutaminase as reticulating agent for the argan protein component to influence the mechanical properties and gas barrier properties of these novel blended bioplastics. Our results confirmed the possibility to valorise a by-product using it as new raw material, thus contributing to the development of new sustainable processes of production.

SESSION: NET3-ORBIS

□ Oral
□ Poster

Parole chiave/ Keywords

1. Argan
2. Bioplastics
3. Transglutaminase
4. Amylose

- **Trends in Biotechnology: the SIB group perspectives Naples 23-24 June 2022**

Trends in Biotechnology: the SIB group perspectives

Naples 23-24 June 2022

Antioxidant and antimicrobial activity of edible films made of Dried Olive Leaf Extract and Chitosan

Michela Famiglietti*, Alessandro Savastano, Rosa Gaglione, Angela Arciello, Daniele Naviglio, Loredana Mariniello

Department of Chemical Sciences, University of Naples "Federico II", 80126 Naples, Italy

*Corresponding author e-mail: michela.famiglietti@unina.it

Keywords: Olive by-products; Chitosan; Food Active Packaging; Circular Economy

Topic 1: Industrial Biochemistry, integrated biotechnological processes from renewable resources to added-value products

Packaging is an effective means of protecting food products from external contaminants and can prevent chemical, physical, and biological changes during storage or even during the preparation of products. A possible strategy in food preservation consists of the use of active and functional packaging to improve safety and ensure high-quality products. Because of its antibacterial and antifungal activity[1], chitosan is a very interesting polymer for applications in food preservation.

In this work, we developed chitosan-based films containing Dried Olive Leaf Extract (DOLE), obtained by Naviglio extractor, with the aim to investigate the polyphenols yield and the antioxidant activity of this extract in chitosan-based-edible films. Olive tree cultivation and the olive processing industry produce every year a huge amount of by-products and residues that usually are used as animal feed or simply burned. Phenolic compounds, the main high-added-value fraction of extractives present in olives leaves, are already studied for their several beneficial effects on human health. Some studies reported that phenolic compounds isolated from olive leaves have been shown to inhibit the growth of different strains of microorganisms[2]. Thus, we tested *in vitro* the antimicrobial effect of DOLE-containing films against bacterial strains (*Salmonella typhimurium* ATCC® 14028, *Salmonella enteritidis* RIVM 706, and *Enterococcus faecalis* ATCC 29212).

Films DOLE component is effective in inhibiting all the bacteria tested in a dose-dependent manner. Taking advantage of these results, we have demonstrated the capability of DOLE-containing films as active bioplastics, able to control bacterial spoilage of meat hamburgers over the time up to 20 days in comparison to baking (parchment) paper normally used.

Preparation and characterization of argan-amylose-based novel bioplastics

Michela Famiglietti and Loredana Mariniello

Department of Chemical Sciences, University of Naples Federico II, Via Cinthia 80126, Naples, Italy

This work aimed to investigate the possibility to produce novel bioplastics, made up of argan proteins extracted from oilcakes, and amylose obtained from barley by RNA interference technique.
Argan, *Argania spinosa*, is a plant typically widespread in arid and semiarid regions of Northern Africa useful for protecting soil from desertification and erosion. Until now, argan was mainly used to obtain a biologically active oil extracted from its seeds producing oilcake, a by-product rich in proteins, generally used as animal feed. Recently argan oilcakes have been attracting attention as a waste to be recovered to obtain high-add value products for different applications.
Amylose is an optimal raw material for bioplastic purposes because of its linear molecular structure and its high thermal stability. It was already demonstrated that amylose-based films provided better properties compared to normal starch-based films[1].
We investigated the performance of these novel blended bioplastics in terms of mechanical and barrier properties, and we also studied the effect of the enzyme microbial transglutaminase (mTGase) as reticulating agent for the argan protein component. Finally, we verified that both films, prepared respectively with unmodified and mTGase-modified argan proteins, are completely digested during oral and gastric digestion. In fact, amylose is digested by amylase in the simulated oral digestion process and the remaining proteins are digested by simulated gastric digestion because of the presence of pepsin. Our results confirmed the possibility to valorize a by-product, as argan proteins, using it as new raw material possibly destined to different applications in several industrial sectors, thus contributing to the development of new sustainable processes of production.

1Xu, J. *et al.* Amylose/cellulose nanofiber composites for all-natural, fully biodegradable and flexible bioplastics. *Carbohydr. Polym.* **253**, (2021).

- **XVI FISV Congress 3R: Research, Resilience, Reprise Portici (Naples); 14-16 SEPTEMBER 2022**

Mechanical, thermal, and barrier properties of amylose-based bioplastics

L. Mariniello, Michela Famiglietti

Department of Chemical Sciences, University of Naples "Federico II", Italy

Looking for new sources to produce energy and materials and valorizing by-products, that otherwise would get wasted, are the aims of the circular economy. In this work, amylose, obtained by RNA interference technique from barley plants, and proteins, derived from argan oil cake, were exploited to produce novel blended bioplastics. Amylose provides added-value functionalities to the normal starch reducing or eliminating the need for subsequent chemical modification or blending with synthetic polymers.

Argania spinosa is a plant typically widespread in arid regions of Northern Africa, which plays a fundamental ecological role. Recently argan oilcakes have been attracting attention as a waste to be recovered to obtain high-added value products for different applications.

This work aimed to investigate the possibility to produce novel hydrocolloid bioplastics, improving the performance of amylose-based films and argan proteins-based films in terms of mechanical, barrier, and thermal properties. The effect of the enzyme microbial transglutaminase as reticulating agent for the argan protein component blended with amylose was also studied.

- **Meeting Sezione SIB Campania Napoli, 26 ottobre 2022**

Biotecnologie Biochimiche ed Enzimologia

Hydrocolloid-based Bioplastics from Argan Oilcake and Amylose

Michela Famiglietti, Domenico Zannini, Rosa Turco, Loredana Mariniello
Department of Chemical Sciences, University of Naples Federico II, Italy

BACKGROUND

Amylose (AM) is an optimal raw material for bioplastic purposes because of its linear molecular structure. AM chains longer than approximately 1000 glucose units form a gel consisting of crosslinked AM chains[1]. Oilseed processing of argan, *Argania spinosa*, produces a large amount of waste. It contains ~ 46% (w/w) of proteins[2] (APs) that have been proven to be a substrate of the enzyme microbial transglutaminase (mTGase).

METHODS

Production of blended films by casting method using different ratios AM/APs in the absence and the presence of mTGase, as a tool to reinforce the matrix

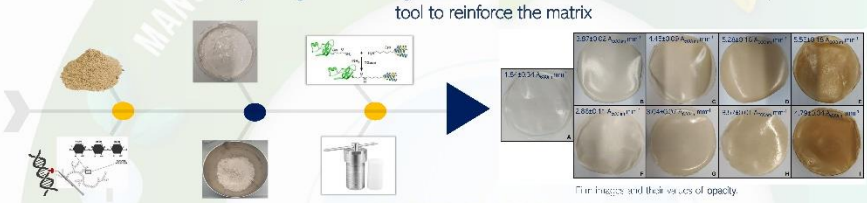

RESULTS

Mechanical properties

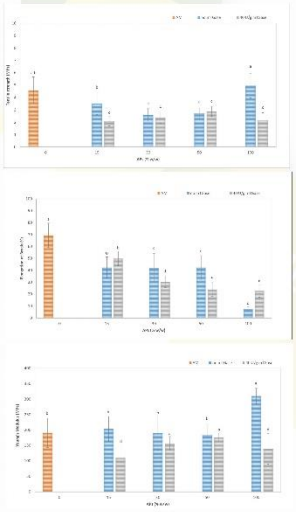

Barrier properties

APs-AM ratio	WVP (g*mm*m⁻²*d⁻¹*kPa⁻¹)	CO_2P (cm³*mm*m⁻²*d⁻¹*kPa⁻¹)
0-100	8.68±0.16[a]	0.42±0.04[a]
15-85	6.16±0.10[c]	0.42±0.06[a]
30-70	3.56±0.57[e]	0.25±0.02[bc]
50-50	3.27±1.31[e]	0.24±0.06[c]
100-0	2.89±1.18[e]	0.30±0.05[bc]

APs-AM ratio - mTGase (40U/g)	WVP (g*mm*m⁻²*d⁻¹*kPa⁻¹)	CO_2P (cm³*mm*m⁻²*d⁻¹*kPa⁻¹)
15-85	3.01±0.03[e]	0.35±0.02[c]
30-70	2.74±1.42[e]	0.12±0.02[d]
50-50	2.53±0.97[e]	0.16±0.04[d]
100-0	1.87±0.78[e]	0.45±0.07[a]

Moisture content, Swelling ratio, Solubility

APs-AM ratio	Moisture content (%)	Swelling ratio (%)	Solubility (%)
0-100	33.78±0.63[a]	86.25±2.75[a]	15.14±1.21[d]
30-50	22.30±0.11[b]	252.73±4.60[b]	27.32±2.10[c]
100-0	17.30±3.39[b]	410.70±32.68[a]	31.12±1.80[b]

APs-AM ratio-mTGase (40U/g)	Moisture content (%)	Swelling ratio (%)	Solubility (%)
50-50	21.08±0.30[bc]	205.00±28.76[b]	27.68±0.08[bc]
100-0	16.34±1.48[b]	367.75±174.94[a]	32.66±0.34[c]

Thermal properties

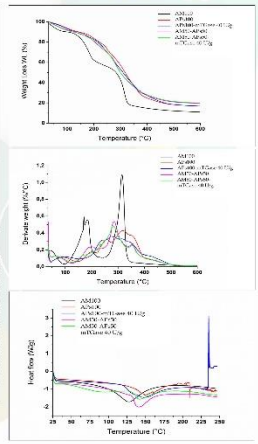

CONCLUSIONS

- Pure AM-based films show better mechanical properties than pure APs-based films;
- Pure APs-based films result in a higher barrier to Water Vapor than pure AM-based films;
- Blended films show reduced CO_2 permeability than pure AM and APs-based films;
- mTGase does not seem to improve film mechanical properties but improves their barrier properties;
- Pure APs-based films show a higher melting temperature than pure AM-based films.

References:
1. Xu J. *et al. Carbohyd. Polym.* 253 (2021).
2. Mirpoor S.F. et al. *Int.J.Biol.Sci.* 25, (2022).

- **BIOPROSYS JOINT MEETING From basic understanding of cell networks to their modulation and engineering for health and industrial applications 18-19 MAY 2023**

ARGAN PROTEINS-BASED BIOMATERIALS AS PROMISING COSMECEUTICALS AND MEDICAL DEVICES

FATEMEH SEYEDEH MIRPOOR[1], MICHELA FAMIGLIETTI[1], CONCETTA VALERIA GIOSAFATTO[1], ANTONELLA D'AGOSTINO[2], MARIA D'AGOSTINO[2], MARCELLA CAMMAROTA[2], CHIARA SCHIRALDI[2], RAFFAELE PORTA, LOREDANA MARINIELLO[1]*

[1] DEPARTMENT OF CHEMICAL SCIENCES, MONTE SANT'ANGELO CAMPUS, UNIVERSITY "FEDERICO II", NAPLES, ITALY
[2] DEPARTMENT OF EXPERIMENTAL MEDICINE, SECTION OF BIOTECHNOLOGY AND MOLECULAR BIOLOGY, UNIVERSITY OF CAMPANIA "LUIGI VANVITELLI", NAPLES, ITALY
*CORRESPONDING AUTHOR: loredana.mariniello@unina.it

Argan *(Argania spinosa)* is an endemic plant of Northern African regions used to obtain a biologically active oil from its seeds. Oil extraction produces a byproduct, called oilcake and rich in proteins, so far used as animal feed. Recently, argan oilcake has been attracting attention as a waste to be recovered to obtain high-added value products.
In this work, proteins were extracted from argan oilcake and used to produce films by casting method adding glycerol as a plasticizer. Argan proteins-based films (APs films) were characterized for their mechanical, barrier, and thermal properties as well as for their morphology and hydrophilicity.
It is worthy of note that the produced biomaterials showed values of tensile strength and Young's modulus very similar to those observed for the petrochemical-based film LDPE, analyzed under the same conditions, even though the value of elongation at break is quite far from that of LDPE. Moreover, a markedly higher barrier property to CO_2 and O_2 of APs films than that exhibited by the LDPE was also observed.
Due to the presence of residual argan oil in the matrix, as observed by SEM, films potential application in the pharma-cosmetic sector has been further studied. A cytotoxicity assay was performed with different concentrations of APs films and the results showed that 0.1 mg/mL of the film promotes the viability of fibroblasts (HDF-hTERT) over control samples. In addition, 0.1 mg/mL APs-based films showed the fastest wound healing rate. These results suggest that the APs films have potential applications in cosmeceuticals and perhaps even in medical devices for skin repair.

Preferred sections

First choice: Exploiting biological functions for biotechnology (and beyond)
Second choice: Advanced biological model for "bio-health"

Submitted for: Only poster

REFERENCES:
1.Mirpoor et al., *Int.J.Mol.Sci*, (2022), 23, 8478
2.Famiglietti et al., *Int.J.Mol.Sci,* (2023), 24, 3405

- **EUROPEAN CONGRESS ON BIOPOLYMERS AND BIOPLASTICS 16-17 NOVEMBER, ROME**

Presentation title - NOVEL AMYLOSE-ARGAN PROTEINS-BASED BIOPLASTICS: PRODUCTION AND CHARACTERIZATION

Corresponding Author name: Ms. Michela Famiglietti

Affiliation: Department of Chemical Sciences, University of Naples "Federico II"

Ph. No: +39 3494745477

Email ID's: michela.famiglietti@unina.it

WhatsApp No: +39 3494745477

Other Authors if any: Seyedeh Fatemeh Mirpoor, Andreas Blennow, Loredana Mariniello

Presentation type: (Oral presentation)

Abstract (250-300 words):

Bioeconomy has the challenging aims to look for new sources for materials production and valorize unused byproducts.
This work exploited amylose, obtained by RNA interference technique from barley plants, and proteins, extracted from argan oil cake, to produce novel blended bioplastics. Amylose is a biopolymer that provides added-value functionalities to the normal starch for bioplastics production, reducing the need for subsequent chemical modification or blending with synthetic polymers. Argan oilcake is a byproduct of argan oil extraction that until now was used for animal feeding or disposed of. Here it was recovered to obtain high-added value products such as proteins. This work aimed to investigate the production of novel hydrocolloid-based bioplastics, blending amylose and argan proteins, and characterize them for their mechanical, barrier, and thermal properties. Moreover, it was verified that the films were completely digested during *in vitro* oral and gastric digestion to use them as edible films for food packaging applications. Amylose is digested by amylase in a simulated oral digestion process and the proteins are digested by simulated gastric digestion in the presence of pepsin. Finally, the biodegradability of the films was studied by the burial test method using soils deriving from three different local areas. The films showed suitable performance for application in the bioplastic industry.

KEYWORDS: amylose; argan seeds proteins; biopolymers; biodegradability

Biography (150-200 words):

Ms. Michela Famiglietti is currently a PhD Student in Biotechnology with a project titled "Production and Characterization of novel active polysaccharides/proteins blended

bioplastics". She is working on her research in the group of Biochemical Biotechnologies and Enzymology coordinated by Professor Loredana Mariniello at the Department of Chemical Sciences of the University of Naples "Federico II". The research line of the group focuses on the exploitation of natural polymers, such as proteins extracted from wastes and byproducts or polysaccharides like starch, cellulose, and chitosan to produce edible films destinated mainly to food packaging. The long and relevant expertise of the group in enzymology allowed them to exploit the enzyme microbial transglutaminase as a tool to modify and improve the performance of proteins-based bioplastics. In this context, Ms. Michela Famiglietti is working specifically on the production of hydrocolloid-based bioplastics made up of polysaccharides, such as amylose and chitosan, and proteins extracted from argan oil cake. This field of research is in line with her background: the master's degree in Industrial and Environmental Biotechnology at the University of Rome Sapienza, and the specialization in Green Chemistry and Production of Materials from Biomasses at the Polytechnic of Milan.

7.3 EXPERIENCES IN FOREIGN LABORATORIES

- **01/06/2023-31/10/2023** Visiting period at Nanosensors and Nanomachines group at the Faculty of Chemistry, Department of Analytical Chemistry, Complutense University of Madrid under the supervision of Professor Reynaldo Villalonga

Ciudad Universitaria
28040 - Madrid
Telefono – 913944331
Fax - 913934329

UNIVERSIDAD COMPLUTENSE DE MADRID
FACULDAD DE CIENCIAS QUIMICAS

DEPARTAMENTO DE QUIMICA ANALITICA

CERTIFICATE

I, the undersigned Prof. Reynaldo Villalonga, head of the Nanosensors & Nanomachines Group at the Faculty of Chemistry, Department of Analytical Chemistry, Complutense University of Madrid in Spain, hereby certify that Ms. Michela Famiglietti, Ph.D. student from the Università degli Studi di Napoli Federico II in Italy, has performed a research internship at our group, under my supervision in collaboration with Prof. Alfredo Sánchez, in the period from 01/06/2023 to 31/10/2023.

In this period, Ms. Michela Famiglietti carried out experiments related to the preparation and characterization of several nanomaterials and nanomaterials-enriched films related to her Ph.D. research. To do this, the student used advanced techniques such as Scanning Electron Microscopy DSC/TG and Fourier-transform infrared spectroscopy.

Yours sincerely,

Prof. Reynaldo Villalonga
Nanosensors & Nanomachines Research Group
Department of Analytical Chemistry
Faculty of Chemistry, Complutense University of Madrid
28040 – Madrid, Spain
Phone: +34 617597866 - Fax: +34 91 3934329
E-mail: rvillalonga@quim.ucm.es

November 07th, 2023
Madrid, Spain

7.4 HONOURS AND AWARDS

- **Meeting Sezione SIB Campania Napoli, 26 ottobre**
  Novel hydrocolloid-based bioplastics from argan oilcake and amylose
  Michela Famiglietti, Domenico Zannini, Rosa Turco, Loredana Mariniello
  Premio Best Poster Award

- **01/06/2023 - 31/10/2023**
  Grant from the ITALIAN SOCIETY OF BIOCHEMISTRY AND MOLECULAR BIOLOGY (SIB) for research staying abroad as financial support for short periods